ID Cover Page

Summary of WP Student Team

Economic Sustainability Models for Land Uses on Rural Territory

Group constitution:

Lucas Mendes de Almeida	Business Analytics	Economic Sustainability Models for Land Uses on Rural Territory – The Case of Solar Panels
Margarida Sobral de Matos Cardoso Pinto	Business Analytics	Economic Sustainability Models for Land Uses on Rural Territory - The Case of Olive Tree
Maria Catarina Mendes da Silveira Antunes Pereira	Business Analytics	Economic Sustainability Models for Land Uses on Rural Territory – The Case of Maritime Pine
Mariana Cabral Godinho	Business Analytics	Economic Sustainability Models for Land Uses on Rural Territory - The Case of Eucalyptus
Nuno Artur Moreira Marques Baptista	Business Analytics	Economic Sustainability Models for Land Uses on Rural Territory - The Case of Cork Oak

Work project carried out under the supervision of:

Advisor: João Moura Pires

Co-advisor: Margarida Tomé, Rui Ferreira Santos

Reading observations for jury:

Note: this template is a support document for the jury members before the defense, only.

A Work Project, presented as part of the requirements for the Award of a Master's degree in Business Analytics from the Nova School of Business and Economics.

Economic Sustainability Models for Land Uses on Rural Territory

Lucas Mendes de Almeida

Margarida Sobral de Matos Cardoso Pinto

Maria Catarina Mendes da Silveira Antunes Pereira

Mariana Cabral Godinho

Nuno Artur Moreira Marques Baptista

Work project carried out under the supervision of:

João Moura Pires

Margarida Tomé

Rui Ferreira Santos

23/01/2025

Abstract

This thesis evaluates the economic viability of five land-use systems - maritime pine, eucalyptus, cork oak, olive groves, and solar panels - through growth, financial, and geospatial modelling. For forestry cultures, APIs linked to StandsSIM and SUBER 5.0 simulators were used to simulate and assess profitability of Mação's management approach and provide recommendations. Olive groves were assessed across three cultivation systems to balance profitability and sustainability. Solar farms were evaluated using GIS and financial models, identifying optimal sites based on socio-environmental, location and climate. Findings highlight strategies for sustainable resource use, improved land-use practices, and renewable energy development in Mação.

Keywords

Business Analytics, Territory Sustainability, Economic Models, Forest, Wildfires

Acknowledgements

We would like to express our gratitude to our advisor, Professor João Moura Pires, for his guidance and availability. Additionally, we would like to thank Professor Margarida Tomé for all the help with the forest species. Our sincere thanks also go to António Louro and Álvaro Rodrigues for their valuable contributions and insights. Finally, we would like to extend our thanks to Márcia Matias for all the feedback and support throughout the project.

This work used infrastructure and resources funded by Fundação para a Ciência e a Tecnologia (UID/ECO/00124/2013, UID/ECO/00124/2019 and Social Sciences DataLab, Project 22209), POR Lisboa (LISBOA-01-0145-FEDER-007722 and Social Sciences DataLab, Project 22209) and POR Norte (Social Sciences DataLab, Project 22209).

TABLE OF CONTENTS

ABSTRACT **1**

1. INTRODUCTION **4**

1.1 MOTIVATION AND CONTEXT 4
1.2 OBJECTIVES AND APPROACH 6
1.3 DOCUMENT STRUCTURE 7

2. MAÇÃO **8**

2.1 MAÇÃO'S LOCATION AND TERRITORY CHARACTERISTICS 8
2.2 MAÇÃO'S AIGPS 9
2.3 POSA AND POSP: CURRENT AND PROPOSED LANDSCAPE DESIGN 10

3. LAND IT PLATFORM **11**

4. SIMFLOR PLATFORM **11**

4.1 STANDSSIM 12
4.2 SUBER 17

5. THE CASE OF MARITIME PINE **21**

5.1 MARITIME PINE IN PORTUGAL 21
5.2 MARITIME PINE CHARACTERISTICS 21
5.3 GROWING CYCLE 22
5.4 RELATED WORK AND STATE OF THE ART 23
5.5 METHODOLOGY AND APPROACH 25
5.6 DEVELOPED MODELS 27
5.7 RESULTS' ANALYSIS 29
5.8 SENSITIVITY ANALYSIS 33
5.9 CONCLUSION - RECOMMENDATIONS 39
5.10 LIMITATIONS 40
5.11 FUTURE WORK 41

6. THE CASE OF EUCALYPTUS **42**

6.1 EUCALYPTUS IN PORTUGAL 42
6.2 EUCALYPTUS CHARACTERISTICS 42
6.3 GROWING CYCLE 43
6.4 RELATED WORK AND STATE OF ART 44
6.5 METHODOLOGY AND APPROACH 47
6.6 DEVELOPED MODELS 49
6.7 RESULTS' ANALYSIS 51
6.8 SENSITIVITY ANALYSIS 54
6.9 CONCLUSION - RECOMMENDATIONS 60
6.10 LIMITATIONS 61
6.11 FUTURE WORK 62

7. THE CASE OF CORK OAK **63**

7.1 CORK OAK IN PORTUGAL 63
7.2 CORK OAK CHARACTERISTICS 64
7.3 GROWING CYCLE 65
7.4 RELATED WORK AND STATE OF THE ART 66
7.5 METHODOLOGY AND APPROACH 70
7.6 INTEGRATION AND APPLICATION OF THE SUBER 71
7.7 RESULTS 73

7.8 Conclusion - Recommendation ... 81
7.9 Limitations ... 82
7.10 Future Work ... 82

8. THE CASE OF THE OLIVE TREE ... 83

8.1 Olive Tree in Portugal and Mação ... 83
8.2 Olive Growing Systems ... 86
8.3 Related Work and State of the Art ... 88
8.4 Methodology ... 90
8.5 Developed Model ... 91
8.6 Sensitivity Analysis ... 96
8.7 Conclusion - Recommendations ... 102
8.8 Limitations ... 103
8.9 Future Work ... 103

9. THE CASE OF SOLAR PANELS ... 104

9.1 Introduction ... 104
9.2 Fundamental Concepts ... 104
9.3 Related Work and State of the Art ... 109
9.4 Methodology and Approach ... 113
9.5 Limitations ... 125
9.6 Conclusion - Recommendations and Future Work ... 125

REFERENCES ... 126

APPENDIX ... 146

Appendix II - Mação ... 146
Appendix IV – StandsSIM ... 150
Appendix V – The case of Maritime Pine ... 151
Appendix VI – The case of Eucalyptus ... 167
Appendix VII - The Case of Cork Oak ... 178
Appendix VIII – The Case of Olive Tree ... 190
Appendix IX – The Case of Solar Panels ... 191

1. Introduction

This first chapter introduces the document and is divided into three sections. The first section describes the origin of the project, the context in which it is situated, and the motivation for its development. The second one presents the problem addressed and summarizes the approach used to resolve it. Finally, the third and last section discusses the organization of this document.

1.1 Motivation and Context

Historically, in the 1950s and 1960s, the agro-silvo-pastoral systems that characterized rural areas maintained a multifunctional landscape from both economic and ecological perspectives. However, with significant population exodus, most of the territory was abandoned and left unmanaged, leading to the widespread accumulation of vegetation, serving as fuel for wildfires.

Mação, a Portuguese region located in the district of Santarém, is a living example of these challenges. This Portuguese territory covers 41,000 hectares and is divided into 80,000 properties owned by 20,000 individuals, averaging 0.7 hectares (Médio Tejo 2019). Since most property owners left their land unmanaged, the territory has become highly vulnerable to fires.

Over the past 30 years, Mação's municipality has seen its territory being devastated by wildfires. Between 1991 and 2019, large wildfires burned a significant proportion of the territory, the most severe ones being those that took place in 2003, 2017, and 2019 (Fernandes et al. 2020). In 2017 (ICNF 2017), 27,000 hectares were affected by wildfires, corresponding to 67% of the territory's area. In 2019, although the burned area was smaller compared to 2017, the wildfires affected the areas that had not burned in the previous wildfire, leaving a total of 90% of the territory affected (ICNF 2019). These numbers show the necessity of changing the current design of the rural landscape to reduce the fire vulnerability of this Portuguese territory.

Currently, in response to these challenges, Mação has developed 9 Integrated Landscape Management Areas (AIGP) (Câmara Municipal de Mação 2021). These areas are designed with the objective of promoting sustainable landscape management through collective agroforestry exploitation, especially in areas with a high risk of wildfires. Each AIGP includes the development of Integrated Landscape Management Operations (OIGP), consisting of strategies for landscape transformation, territorial enhancement, and revitalization. They also address practical aspects including financing, management, and monitoring ensuring long-term success.

These operations are detailed through two key maps: the POSA (Current Land Use Map) and the POSP (Proposed Land Use Map). The POSA documents the existing land use, while the POSP outlines the planned changes, focused on reducing wildfire risks, improving ecosystems, and revitalizing the local economy. It follows a transformation strategy based on the natural characteristics of the territory and land suitability, following preventive forestry laws and territorial programs. The POSP includes the proposed land use units (based on the COS 2018 nomenclature, a land occupation map that provides a structural view of the territory), the ecological and resilience structures and the structural elements, such as notable landmarks, hedges, walls, terraces, and infrastructure necessary for landscape transformation and management. The landscape transformation matrix compares the POSA with the POSP, providing a summary table showing the variation of values across different land use categories.

In total, AIGPs cover 20,209 hectares which corresponds to around 50% of the municipality's total area (Matias 2023). Within these areas, conditions will be created for the development of OIGPs, executed by a collective management model overseen by a managing entity. The OIGPs are supported by a long-term, multi-fund program that provides financial backing for initial investments and ongoing management activities (Câmara Municipal de Mação 2021).

To design and implement these AIGPs it is essential to assess the medium and long-term economic sustainability of the proposed landscape models. This project's objective is to address this challenge by studying, implementing, and evaluating the most efficient models available in the literature for the AIGPs. These will be integrated into the LAND IT system (Computer-Aided System for the Design of Integrated Territory Management), currently being developed in a partnership between NOVA School of Science and Technology and AZR - Gestão Territorial, S.A., a company established in Mação that manages the AIGP of Mação and is responsible for developing its Integrated Landscape Management Operation (OIGP). A more detailed explanation on the LAND IT platform can be found in Section 3.

1.2 Objectives and Approach

This thesis integrates various approaches to model and analyze the economic and environmental performance of five selected land use systems: maritime pine, eucalyptus, cork oak, olive groves, and solar panels. The order of analysis reflects the temporal scale, progressing from long term forestry crops (maritime pine, eucalyptus, and cork oak) to a one-year agricultural system (olive groves), and finally to solar panels. Forestry systems prioritize sustainability and profitability over extended timelines, while agricultural systems aim to optimize yields, and solar panels focus on site feasibility and financial modelling to maximize energy production.

I. Forest Species – Maritime Pine, Eucalyptus and Cork Oak

The StandsSIM simulator served as the foundation for the development of a growth and economic model for both eucalyptus and maritime pine, while cork oak modelling was based on SUBER 5.0. To enhance usability, APIs were created for each species, to integrate these models into the LAND IT platform. The APIs enable users to customize simulations by inputting parameters such as tree density and planning horizon, generating tailored outputs like cash flow projections and operational costs. To provide practical guidance for sustainable forest management, both univariate and multivariate sensitivity analyzes were conducted so that optimal management strategies could be identified.

Group Part

II. Olive Tree

The analysis of olive tree cultivation focuses on three distinct systems: traditional, potted, and hedge. The model is built on practical inputs, including annual maintenance costs, installation expenses, olive oil market price and yield dynamics, that are going to vary according to the age of the olive grove. The main goal of the developed model is to provide actionable recommendations that balance profitability with sustainability practices in olive production.

III. Solar Panels

The feasibility of utility-scale solar farms was assessed through a combination of geospatial and financial modelling. Using Geographic Information Systems (GIS), 16 polygons from the OIGP database were evaluated based on criteria such as slope, solar radiation, and proximity to substations. This analysis shortlisted four viable sites, which were further analyzed. Financial models integrated investment costs and operational expenses with the objective of identifying the most economically viable options for renewable energy development.

1.3 Document Structure

This thesis is structured into nine sections, each addressing specific parts of the research. The first section introduces the motivation, context, and objectives of the study, highlighting the challenges addressed, and the methodologies applied to achieve the thesis' main objectives. It concludes with this overview of the document structure. The second section focuses on Mação's geography and territorial characteristics, as well as the relevance of the AIGPs. The third and fourth introduce and give key insights regarding both LAND IT and sIMfLOR, respectively. From the fifth to seventh section the maritime pine, eucalyptus, and cork oak are analyzed, respectively. These sections present the development of an API, sensitivity analyzes, and recommendations for sustainable management practices. Section eight analyzes olive trees, and its different cultivation systems to evaluate their economic and operational performance in

Mação, while the ninth section evaluates the feasibility of solar farms, incorporating geospatial and financial modelling to optimize site selection and assess economic viability.

2. Mação

This chapter provides a detailed analysis of Mação, focusing on its location, territorial characteristics, and implementation of AIGPs (Integrated Landscape Management Areas).

2.1 Mação's Location and Territory Characteristics

Mação, located in the district of Santarém, lies at the geometric center of Portugal, and spans approximately 41,000 hectares. Figures 2.1 and 2.2 show the most recent land use cartography, COS 2018, and that the predominant land use is forestry, marked in green in Figure 2.1, with maritime pine and eucalyptus dominating the landscape with 48.6% and 27.7%, respectively. On the other hand, agricultural lands, including olive groves occupy smaller areas, accounting for 4.89%, represented in orange, while buildings and roads are represented by red polygons.

Additionally, Mação is divided into six parishes: Amêndoa, Cardigos, Carvoeiro, Envendos, Mação, Penhascoso, Aboboreira, and Ortiga. These geographic features define a diverse landscape but with challenges related to land management and environmental sustainability.

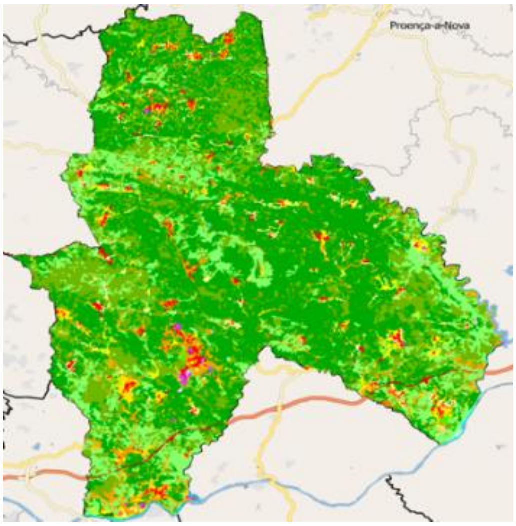

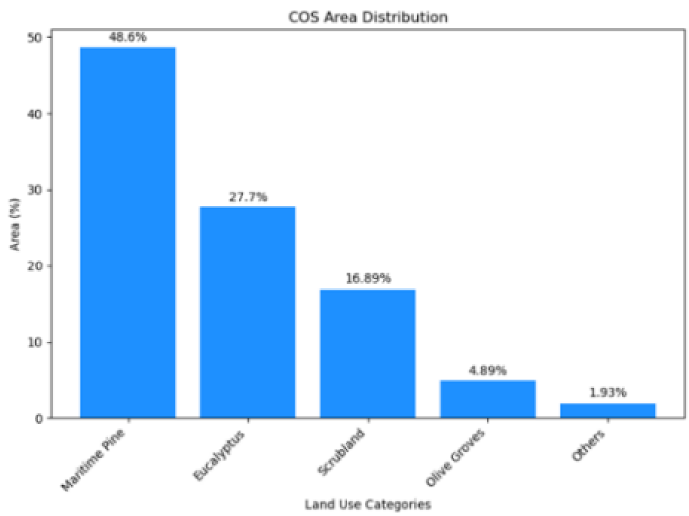

Figure 2.1: COS Map | Source: Matias 2023

Figure 2.2: COS Area distribution

The topography of Mação is highly varied with more than 55% of the terrain exhibiting slopes between 5º and 15º, which makes the area prone to erosion and increases the risk of wildfire propagation, especially in steeper regions. Also, the hypsometry further highlights its varied land with 50% of the area situated 250–350 meters above sea level (Figures 2.3 and 2.4).

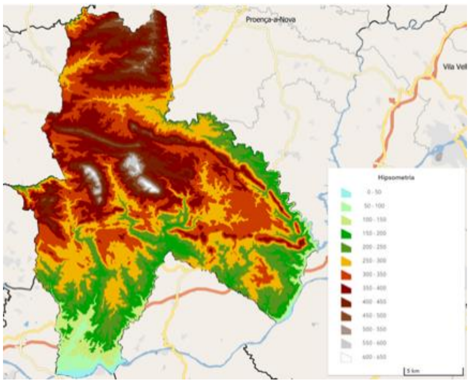

Figure 2.3: Hypsometry in Mação

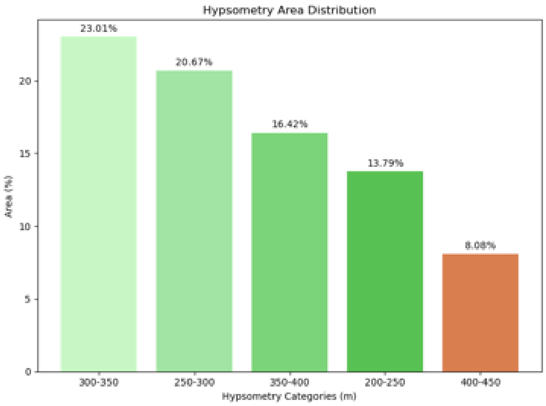

Figure 2.4: Map Hypsometry in Mação | Source: Matias 2023

These physical characteristics, combined with abandoned properties, biomass accumulation, and high summer temperatures exacerbated by climate change, make Mação one of Portugal's most wildfire-prone zones. Figures 2.5 and 2.6 show that 60% of its territory is classified as high or very high fire risk.

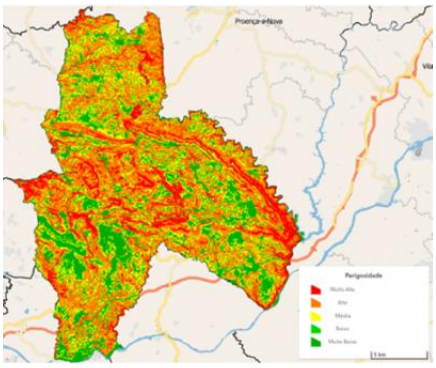

Figure 2.5: COS Hypsometry in Mação

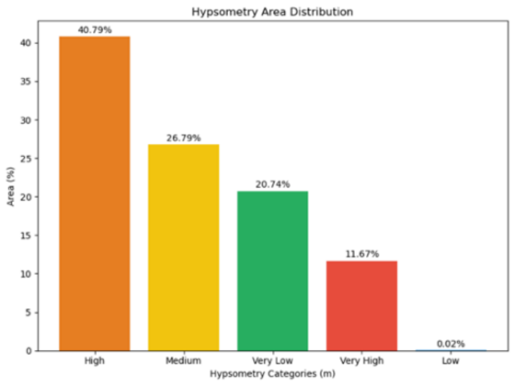

Figure 2.6: COS Map Mação | Source: Matias 2023

2.2 Mação's AIGPs

Mação has established nine AIGPs: Aboboreira, Amêndoa, Cardigos, Carvoeiro, Castelo, Envendos, Mação, Ortiga, and Penhascoso, which cover approximately 20,209 hectares or about 50% of the municipality's total territory. These AIGPs are a response to the critical need to reduce wildfire vulnerability while aiming to promote environmental, social and economic sustainability. This project focuses on analyzing four AIGPs: Amêndoa, Ortiga, Castelo, and Carvoeiro, which were selected by the Municipality of Mação for their strategic importance.

2.3 POSA and POSP: Current and Proposed Landscape Design

Mação's strategy for landscape management relies on two essential tools: the Current Land Use Map (POSA) and the Proposed Land Use Map (POSP). POSA provides a detailed overview of the current land use, revealing the dominance of maritime pine and eucalyptus forests, while agricultural areas, such as olive groves are presented in a smaller portion. This distribution reflects historical land management patterns, heavily focused on forestry, which has contributed to the region's economic activities. However, this increases vulnerability to wildfires, given the high flammability of these species. Figure 2.7 shows the areas occupied by the cultures under study in each AIGP. The POSP presented in Figure 2.8, shows the proposed changes to Mação's landscape, aiming to address the fire hazards and ecological imbalances identified in the POSA. A key change is the reduction of maritime pine and eucalyptus forests in favor of fire-resistant vegetation, such as cork oak forests and agroforestry systems. These adjustments aim to diversify land use, integrating sustainable agricultural practices and increasing the coverage of olive groves and cork oak forests, which offer greater ecological resilience and economic value. Additionally, the POSP introduces innovative land uses, such as renewable energy projects of solar farms to enhance economic productivity while reducing dependence on common forestry.

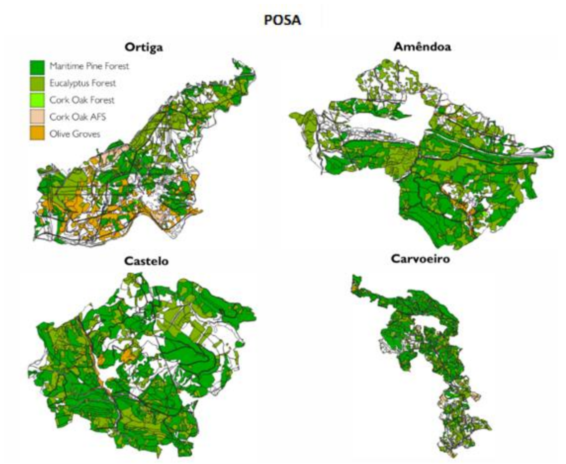

Figure 2.7: Current Land Use Map in four specific AIGPS

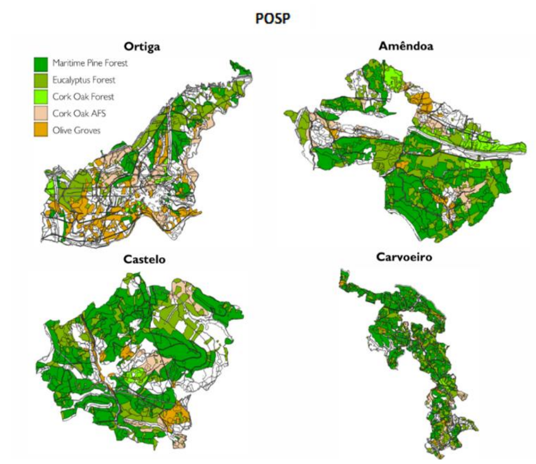

Figure 2.8: Proposed Land Use Map in four specific AIGPs

3. LAND IT Platform

The creation of an OIGP is a highly detailed and iterative process that was designed to address challenges in land-use planning in territories identified as vulnerable in the AIGP (DGT 2023). LAND IT creation emerged to solve the inefficiencies associated with OIGPs creation. It consists of a Decision Support System that integrates advanced geospatial tools and data-driven decision-making capabilities, in order to save time and reduce errors when developing an OIGP.

LAND IT platform is very useful when it comes to automate and enhance the OIGP creation, however, one of its limitations consists in the integration of economic models. Although some models are already integrated within the platform, some are still missing, which restricts the specialists from fully understanding the economic viability of their proposed projects.

Economic models are an essential part to understand the feasibility of the land use proposals (Direção Geral do Território 2023), since they provide the ability to evaluate if a given scenario will generate the income necessary to surpass the initial investment to reorganize a determined area. The values returned by the economic models integrated will give the necessary insights to guide decisions that balance both economic and ecological resilience of the projects developed.

Therefore, this study aims to address this gap in the platform. Models for key land uses such as maritime pine, Eucalyptus, Cork Oak and Olive Trees will be incorporated, as well as a study for Solar Panels' installation. These models will provide detailed information regarding the Net Present Value, Equivalent Annual Annuity, Total Costs and Total Profit, helping them to be more informed when analyzing the viability of their developed projects.

4. sIMfLOR Platform

This chapter introduces sIMfLOR, that integrates diverse simulators for the principal forestry species in Portugal and aims to facilitate the use of growth models by its users. It allows to manage data inputs, running and visualizing outputs. This chapter is divided into two sections, providing a detailed description of the StandsSIM and the SUBER simulators.

4.1 StandsSIM

In the following subsections the StandsSIM simulator will be introduced. The first section will give an overview, while the subsequent ones will describe both the inputs and outputs given. Finally, the last section describes some improvements made to the simulator during this study.

4.1.1 StandsSIM Overview

The StandsSIM is a Management Driven Forest simulator developed to model and predict forest growth dynamics for Portugal's primary wood-producing species: eucalyptus (Eucalyptus globulus) and maritime pine (Pinus pinaster Aiton.). Designed to address challenges like deforestation, reduced wood production, and compromised carbon sequestration exacerbated by climate change and wildfires in the Mediterranean region, StandsSIM provides a long-term simulation framework tailored to Portuguese forest landscapes (Barreiro et al. 2016); Simflor Platform 2024). Its advanced growth models allow for simulations at both the individual-tree and stand levels, offering flexibility for even-aged and uneven-aged stands. By incorporating theoretical models and customizable silvicultural operations — such as harvesting, thinning, and planting — StandsSIM ensures adaptability for diverse forest management scenarios.

StandsSIM's unique advantage lies in its integration of climate dynamics, wildfires risks, and economic variables into forest simulations, filling the gaps left by earlier simulators. Users can tailor parameters like basal area targets, thinning intensity, and planting densities to meet specific goals while evaluating financial metrics, such as operation costs and production receipts (Barreiro et al. 2016). These features empower landowners and forest managers to make informed decisions. By combining cutting-edge models, StandsSIM is an indispensable resource for addressing the evolving challenges of forest management in Portugal.

4.1.2 Inputs

The StandsSIM requires a variety of inputs related to the forest management approaches, costs of operations, prices and site characteristics. Moreover, data on the climate of a specific country, region or even management unit is integrated, tailoring the predictions to each specific land.

Firstly, data on the stands' characteristics is received for new and existing stands. For both, information on the species – if the simulation is for maritime pine or eucalyptus –, age of the stand in years, number of trees planted per hectare, if the stand is even- or uneven-aged, and the time horizon planning, is gathered. For the specific case of existing stands simulations, there is a need for additional data related to tree measurements, such as height and diameter. At this stage, the user can also specify the beat-up rate, representing the percentage of trees planted that are expected to die, making it possible for the simulator to account for the mortality rate.

Moreover, data on silvicultural operations is gathered. This accounts for all silvicultural practices taking place in the culture's lifetime. There is a wide variety of operations for the user to choose, from land preparation, planting, cleaning, thinning, final harvesting, debarking and shoot selection. Thinning operations involve selectively cutting individual trees of a stand while the final harvesting is the last cut when trees reach commercial maturity (Mendes et al. 2017), where fully-grown trees are collected. Both operations generate income (Centro *Pinus* 2016). Although thinning occurs more than once in the life cycle of maritime pine, it generates less revenue compared to the final cut, as trees are smaller. Moreover, the simulator operates under the constraint that shoot selection must take place in the same ordinary year across all rotations. For the eucalyptus, information on the duration of each rotation cycle is also necessary.

Furthermore, growth conditions are mandatory inputs for the simulator to predict the trees' growth over time. To measure the productivity capacity of a specific site, the simulator receives the site index. This forestry measurement is expressed as the expected height of dominant trees, based on previous plantations in that land, and at a specific reference age that depends on the species and region (ICNF 2021). The height of the tallest or most vigorous trees reflects the quality of the growing conditions, making the predictions for the tree growth more accurate.

For accurate financial predictions, it is important to gather economic inputs, such as costs and revenues. The costs of each silvicultural operation and corresponding unit –tree, kilometer or hectare –, costs on wages and products such as seeds, pesticides, and fertilizers are necessary to calculate total cash outflows. For the revenue's calculation, it is necessary to input wood and biomass prices. Lastly, climate data such as number of rainy days per year, precipitation, average temperature and frost days is gathered to simulate the growth pattern of each species.

By integrating all this information, the simulator generates highly accurate and customized predictions for each forest management unit. This high volume of inputs ensures a realistic simulation, providing a robust tool for informed decision-making in forestry planning.

4.1.3 Outputs

With the inputs presented in Section 4.1.2, the simulator generates some outputs, in the form of comma separated files, with the growth and financial predictions for each site index inputted.

The first output file provides information about the number of trees alive throughout the species' lifespan and their corresponding diameters. As such, for each site index and year, the simulator predicts the number of alive trees and distributes them across different diameter ranges. An overview of this file is presented in the Appendix IV Section, in Figure IV.2.

Moreover, the simulator creates another output file with financial predictions. For each site index, the simulator calculates the Net Present Value (NPV) and Equivalent Annual Annuity (EAA) for discount rates of 3%, 4% and 5%, allowing users to select the rate that aligns with their desired rate of return. The NPV assesses the project's profitability by calculating the present value of future cash flows and comparing them to the initial investment (Brealey et al.

2020). The EAA translates the NPV value into a constant annual cash flow, helping to access the evaluation of projects with different time horizons (Brealey et al. 2020). A visual of this file is depicted in Figure IV.3 present in the Appendix IV Section.

Lastly, the final output file combines all calculations from the simulator. For each year and site index, the simulator computes over 50 indicators. Starting with the final cut, thinning and debarking operations, the file marks the year in which these were performed. This is of extreme importance because, maritime pine is subject to Wilson Factor criteria.

Wilson's Factor consists of a relative measure of stand density, which evaluates the appropriate number of trees per hectare in a stand, as a function of the dominant tree height, being a key measure in guiding thinning operations. The logic behind the Wilson Factor is that larger trees (with greater heights or diameters) require more space, resulting in fewer trees per hectare for the same stand density. In contrast, smaller trees can support a higher density.

Thinning is an operation performed to optimize growth conditions. If the number of trees per hectare in a stand is already below the threshold determined by the chosen Wilson Factor, no thinning is applied, ensuring that the stand is not under the deserved number of trees per hectare. The site index has a certain influence, as trees in higher site indexes achieve greater heights and diameters than those at lower site indexes, at a faster rate. This rapid growth means that trees occupy more space earlier in their development, reaching thresholds of competition and crowding sooner, therefore requiring thinning operations to occur sooner. Conversely, trees that grow in less productive soils achieve smaller height and diameter, taking longer to reach the thresholds associated with competition. This leads to the delay of thinning operations.

For the maritime pine case, the simulator works under these explanations. Even if a thinning operation is prescribed by the user, the simulator will only execute it if the conditions mentioned above are fulfilled. Specifically, for thinning operations, the simulator checks if the tree density is sufficient, given the site index conditions applied, to proceed with the operation. As such, if a thinning operation is scheduled for a year when the stand density falls below the required threshold, the operation is skipped and a 0 is recorded for that year in the output file. This distinction is very important since it ensures the simulation is realistic and intelligent, avoiding operations that violate the imposed requirements.

Additionally, the file also provides the expected tree's dominant height for each year, along with the number of trees that are expected to be alive or dead. Other calculated indicators include the basal area, wood volume with and without bark, total wood volume produced and cut, and biomass volume – distinguishing between branches, leaves, resin and more. Lastly, the file also includes financial data, detailing the inflows from wood and biomass sale, and outflows related to management schedules, assortments and labor costs. The revenues generated by biomass are also recorded, allowing the simulator to calculate the Net Present Value (NPV) for each year, its cumulative, and the Equivalent Annual Annuity (EAA) of the project.

This final output file is the most important to analyze, as it consolidates all information in one place, shown by Figure IV.4 in the Appendix IV Section. As such, for further evaluations, it should be the main focus, as it can reveal essential insights and trends.

4.1.4 StandsSIM Improvements

The StandsSIM simulator requires a significant amount of information. As a result, consulting forestry specialists in Mação became critical to determine fixed parameters applicable across the region. For example, it was clarified that Mação only sells wood in eucalyptus plantations, while biomass is also sold for maritime pine stands. Additionally, the costs associated with land preparation, plantation, maintenance and harvesting are uniform across all AIGPs. This allowed these parameters to be treated as fixed inputs for the model. To obtain these values, consultations with experts such as Margarida Tomé, professor at *Instituto Superior de*

Agronomia, and António Louro, president of AZR and Aflomação, were conducted. By these, practiced prices in the municipality, the typical planning horizons for maritime pine and eucalyptus stands, and other critical metrics were gathered. These values and operations are explained in Sections 5.7.1 and 6.7.1 of the maritime pine and eucalyptus chapters, respectively.

One of the most important inputs for the simulator is the site index, as previously mentioned. Unfortunately, no specific data was available regarding site indexes for maritime pine and eucalyptus lands in Mação. To address this issue, data from the Inventário Florestal Nacional was used, covering parcels in Mação and nearby municipalities (Proença-a-Nova, Sertã, Vila de Rei, Sardoal, Abrantes, Gavião, Nisa, and Vila-Velha de Ródão). Based on this information, three possible site index scenarios were calculated: low (*Mação 5*), medium (*Mação med*), and high (*Mação 95*). These site indexes - 15.44, 20.69, and 25.86 for low, medium, and high productivity levels, respectively - enabled simulations to be evaluated under different growth scenarios. Since the productivity of maritime pine and eucalyptus soils is similar in Mação, the same site indexes were applied for both species in the simulations.

However, working with the StandsSIM simulator posed significant challenges during this thesis. The simulator had to be replaced, updated and improved eight times due to errors and inconsistencies identified throughout the research process. These repeated changes required constant adaptation and recalibration of the models, which added complexity to the analysis. Despite these difficulties, the iterative process led to more accurate simulations and a deeper understanding of the proposed landscape management strategies.

4.2 SUBER

This section introduces SUBER, its inputs, simulation process and outputs.

4.2.1 SUBER Overview

The SUBER simulator was specifically developed for the management of cork oak stands in Portugal. By providing simulations for cork oak plantations, it enables analysis of cork production, stand growth and economic viability along the tree's lifecycle.

This simulator has various improved versions, the most recent one the SUBER 5.0. This can calculate cork production independently of the tree's age, allowing more flexible simulations for different management scenarios. Additionally, SUBER 5.0 integrates a site quality index that considers the management practices, soil and climatic variables. The index assesses the productivity potential of a stand to plan the strategies that will maximize the cork production and economic returns. Another distinctive feature of SUBER 5.0 is its classification as an individual-tree and distance-independent model. This approach simplifies calculations by excluding spatial competition indices, making it applicable across various management scenarios while maintaining robust predictions for tree growth, cork production, and stand dynamics. This version also simulates new cork oak stands without requiring prior forest data, expanding the model's usability to areas where historical data is unavailable.

To improve its utility, the model incorporates a graphical user interface within the sIMfLOR platform, enabling visualization of simulation results. Overall, SUBER 5.0 represents a comprehensive tool that allows the simulation of long-term cork oak stands and its evolution, allowing to better understand the impact of the management practices.

4.2.2 Inputs

SUBER 5.0 requires a detailed and structured set of inputs to guarantee accurate predictions. These inputs are the foundations for predicting growth and economic parameters over time and can be distinguished between inventory and economic data. The inventory data contains variables such as tree identification, height, cork thickness, and harvesting height collected during forest inventories. The model also incorporates specific parameters for cork harvesting, including the minimum age for the first stripping, coefficients for cork removal, and whether subsequent harvests will increase the harvesting height. This data must follow strict validation rules on cork age, harvesting height and the number of cork layers removed, ensuring it aligns with structural and legal requirements of cork oak management. This validation is important as it helps to avoid errors that could compromise the accuracy of the simulations.

Regarding the economic inputs, it includes information on labor costs, machinery, consumables and management operations, as well as revenues derived from cork and wood products. To calculate revenue, cork and wood, prices are necessary and can be differentiated by cork type, such as virgin or "amadia" cork. Cork price ranges can also be defined by five caliber classes (e.g., <18mm, 18–23mm, 23–27mm, 27–41mm, 41–90mm) and three quality levels (e.g., grades 3, 4, and 5), creating up to 15 combinations that reflect real market conditions. The discount rate used to calculate the NPV and EAA is 5% by default but can also be adjusted.

Lastly, the stand's operational plan is received as input. Users can specify operations for regular or irregular stands, reflecting the diverse realities of cork oak stands. Finalizing input configuration process, users can save the inputs in formats compatible with sIMfLOR's platform, enabling seamless integration and its future reuse for multiple simulations.

4.2.3 Simulation

There are two types of simulations: one for newly established stands and another for existing forests, allowing users to simulate different scenarios, depending on available data.

For new established stands, as there are no measurements, the model uses data collected from forest inventory plots, allowing for a precise analysis of growth. Users can choose between simulating each plot individually, enabling highly specific projections, or aggregating data to represent a larger stand, used when data is not available or when the objective is a general overview of forest dynamics. For the specific case of already existing forest, users must add information on the number of branches, total height, cork caliber, and cork quality. If tree measurements are not available, the model estimates them from existing data.

Regardless of the approach, the simulations executed and its results are accessible, enabling the analysis of outputs such as production trends, biomass growth, and cork quality over time.

4.2.4 Outputs

Outputs are tailored to provide insights into tree and stand level. At the individual tree level, the model analyzes variables like height, basal area, and diameter growth.

At stand level, the outputs analyze general trends of the stand, such as the basal area with and without cork, the density of trees per hectare, and canopy coverage. This perspective provides a better understanding of the stand's overall growth trajectory. Cumulative to that, the data on biomass components, including wood, branches, leaves and roots, show the total productive capacity of the stand. The metrics on the weight and quality of the cork harvested (virgin and "amadia") provide insights into economic outputs over multiple harvest cycles.

The outputs also record the metrics before and after interventions, such as cork harvesting or thinning, and help to understand the changes in growth dynamics and the impact of the interventions. The diameter class evolution and carbon stock are other metrics present in the outputs. The diameter class evolution demonstrates how trees progress through various size categories, while the carbon stock reflects the stand's role in carbon sequestration.

The SUBER simulator also integrates visualization tools. The generated graphics and charts allow for easier interpretation of complex datasets and aim to help strategic decision-making. By analyzing detailed quantitative data with environmental and operational considerations, the outputs allow forest managers, researchers, and policymakers to make informed decisions that balance economic returns with ecological awareness on the cork oak.

5. The case of Maritime Pine

5.1 Maritime Pine in Portugal

In Portugal, the pine forests have historically played an important role in the country's forest sector. However, these ecosystems have experienced significant reductions in area due to factors like wildfires, pest infestations and diseases. Between 1995 and 2015, the area of maritime pine forest has shown a decrease of around 264,000 hectares, although, the rate of reduction slowed significantly between 2010 and 2015 (ICNF 2019). Nowadays, maritime pine is the third most common forest species in Portugal, covering around 22% of the country's total forest area, which corresponds to around 1 million hectares (ICNF 2019).

This species has been in Portugal for over 33,000 years (Figueiral 1995) and is distributed across the Northern and Central regions, covering areas from Tejo and Sado basins up to Minho. Additionally, it is found in inland areas of the Center and South, specifically in Penamacor, Idanha-a-Nova, Serra Mamede and Santo Aleixo da Restauração (Autoridade Florestal Nacional 2012), at hypsometric levels ranging from 700 and 900 meters (Oliveira et al. 2000).

5.2 Maritime Pine characteristics

Maritime pine is very adaptable, resistant to prolonged dry periods, cold and moderate climate conditions, managing to grow and develop in unfavorable environments. However, this forest species is light-demanding, unable to tolerate shade due to its leaf structure (Oliveira 1999). This tree shows preference for siliceous and sandy soils, with depths up to 30 to 60 cm (Florestas 2023), where its roots can grow freely. *Pinus Pinaster Aiton.* has a better development in areas where the medium temperatures round the 11ºC and 15ºC (Centro *Pinus* 2016), with annual precipitation between 550 mm and 1200 mm (Centro *Pinus* 2016). However, due to its resilient characteristics, it was widely used for the afforestation of coastal dunes and mountainous wastelands. It played a key role in early reforestation initiatives in Continental Portugal, as well as in the autonomous regions, as it allowed to plant forests on steep terrain, serving as protection against erosion and floods (Florestas 2023).

This species lives for 200 years in optimal conditions, however, signs of crown weakening and reddening of the bark indicate aging, and it starts around 80 to 90 years (Centro *Pinus* 2015).

Maritime pine has a big relevance to Portugal when it comes to economy, since practically all the tree's parts can be commercialized. Although the main product is wood, resin is a product that generates annual revenue, as well as biomass that consists of various components of this forest species (Gonçalves et al. 2020), such as its bark, needles, branches and leaves.

5.3 Growing Cycle

The typical growing model of maritime pine consists of plantation, cleaning, and maintenance activities, and different phases of growth. The plantation involves a recommended density of 1,250 to 1,670 trees per hectare and a minimum distance of 3 meters between rows is required (Oliveira et al. 2000). According to Centro *Pinus*, *Pinus Pinaster Aiton.* growth is divided into 5 different phases: Nascedio – Seedling Stage, Novedio – Young Growth Stage, Bastio – Thicket Stage, Fustadio – Pole Stage, and Alto Fuste – Mature Tree Stage. These stages of growth characterize the tree based on its dimensions, as presented in Table 5.1 (Centro *Pinus* 2018), where hdom/ddom represent the average heights and diameters of dominant trees.

	nascedio	novedio	bastio	fustadio	alto fuste
ddom(cm)	-	0-10	10-20	20-30	30-50
hdom(m)	0,3-1,3	1,3-8	8-15	15-18	18-20

Table 5.1: Diameter and height variations in maritime pine (Matias, 2023)

The planting period, Nascedio, varies between areas. For areas with prolonged summer, such as Minho or Douro, planting should occur from November to May, and, in more Central and Southern regions, planting should take place from November to March (Oliveira et al. 2000).

When it comes to cleaning, it consists of removing the lowest quality, dead and diseased, or non-dominant trees and is recommended that, by the age of 10, the stands' density reduces to 1000 or 1200 trees per hectare (Oliveira et al. 2000). Thinning should occur first around 15 to 20 years after planting, and with intervals of 5 to 10 years. In this process, 20% to 30% of the stand's trees should be removed (Oliveira et al. 2000), with exception to the first, that should be denser than the others, where 20% to 40% of the trees are cut (Matias 2023).

The final cut is the last process that occurs in a stand of maritime pine and usually 300 to 500 trees are removed from the stand (Oliveira et al. 2000). An image that illustrates the growing cycle of maritime pine can be found in the Appendix V.1 Section.

5.4 Related Work and State of the Art

Maritime pine is a resinous species highly valued for its fire resistance. According to Fernandes et al. (2005), this species has evolutionary features that result from adaptations to fire: resistance, evidenced by its thick bark, that protects the tree from low-intensity fires, and evasion, through thermally induced cone dehiscence, enabling the tree to reproduce after exposure to high-severity fires. These characteristics made maritime pine a key species for reforestation in vulnerable regions, including Mação, one of the most affected areas in Portugal.

Several projects have been developed to study the ecological resilience and economic viability of maritime pine. Research by Gómez-García et al. (2015) highlighted the importance of using height-diameter models to enhance forest management practices, since accurate tree height predictions combined with diameter, and other specific stand variables, have proven essential for monitoring forest growth and optimizing yield projections.

Moreover, Alegria's (2004) study emphasized the importance of growth and production models to forest management, since these allow to predict future production and explore different forest intervention options. PBIRROL, which consist of growth and yield models tailored to the irregular stands of maritime pine in the Oleiros region developed by Alegria (2004), can be applied to similar forest systems, like Mação's region. This helps to predict the future productivity of future replanted forests, since individual growth of the trees can be studied.

The work of Alegria (2007) and Tomé et al. (2007) also contributes to this by providing equations for estimating total and mercantile wood volume to commercialize. While Alegria's (2007) equations are more specific to regions like Castelo Branco, Tomé et al.'s (2007) ones can be used across the country, making them more useful for predicting the volume of wood available for commercialization in Mação. These equations are crucial when it comes to calculating potential economic returns from the reordering of territory with maritime pine.

In addition, Ogana et al. (2020) presented a new height-diameter model that has been developed to both *Pinus Pinaster* and *Pinus radiata* (Monterey Pine) in Spain. This model consists of a nonlinear mixed-effects technique that provides predictions of tree's height from diameter measurements, yielding a Root Mean Square Error (RMSE) of 0.906 for *Pinus Pinaster*.

A similar study in Northeast Portugal by Msaouak (2016) also shows the potential of using mixed models when it comes to improving the predictive performance. Applying height-diameter equations can help estimate tree volume, competition indices and assessing the stand dynamics in general, crucial to optimize wood production, and, consequently, the potential economic return that Mação can have. Msaouak (2016) thesis also mentions that this resinous can thrive in fire-affected areas, emphasizing its ideal characteristics for reordering forests. Combining the potential of maritime pine to thrive after wildfires and by using the mixed models mentioned, it is possible to assess the long-term potential of this species. This way, wood production can be maximized, offering some financial return to Mação's municipality.

StandsSIM, a forest simulator developed by Barreiro et al. (2016), incorporates up-to-date models sensitive to climate change scenarios, and allows users to project forest growth, considering a range of management prescriptions. The analysis made by this existing simulator helps to analyze the economic viability of reordering territory in areas affected by fires with maritime pine. The usage of this simulator can help users understand which management approach can yield a higher Net Present Value as well as higher wood production over time, while keeping the production costs affordable for the municipality. Also, it helps in understanding which species is more economically feasible compared to others.

The studies and models presented in this section represent some fundamental tools to evaluate the ecological and financial viability of reordering Mação's forest. From height-diameter models to advanced growth simulators, like StandsSIM, these tools enable accurate predictions of growth, yield, and financial returns. Bridging these models in the LAND IT platform, this thesis aims to create a comprehensive decision-making framework to support sustainable and economically viable reforestation projects in fire-affected areas.

5.5 Methodology and Approach

In this part, the objective was to build a growth and economic model for maritime pine that can be integrated into the LAND IT platform. The model aimed to calculate the expected profit from wood, resin and biomass, over the entire life cycle of the species, using users' information about their maritime pine stands. Before developing the model, it was necessary to review relevant literature to incorporate the most accurate growth functions into the model.

Unlike species treated collectively as a stand, maritime pine trees are modeled individually, with the calculations performed on a tree-by-tree basis. This approach allows for more detailed predictions, as it accounts for individual variations in tree height, diameter, and growth patterns.

In this first approach, the decision was to start designing a model that calculates wood, biomass, and resin's volume as well as the associated profit for each tree, based on its specific attributes of height and diameter. These individual calculations would then be aggregated to estimate these values for the entire stand. Recognizing that users may only have information regarding their stand's age, it became essential to either develop or find functions capable of estimating tree height and diameter as a function of the maritime pine's stand' age.

One challenge encountered was the lack of reliable data that links height, diameter and age, crucial for building a predictive model. In scenarios where users may only have information on the age of their stand, the inexistence of equations that relate these variables made the accurate estimation challenging. Height-Diameter models, such as the ones mentioned by Gómez-García et al. (2015) or developed by Alegria (2004) to estimate *Pinus Pinaster Aiton*. growth and production, although useful and widely applied in Portugal, were not age dependent. Instead, they rely on other variables, such as basal area – cross-sectional area of tree trunks at 1.3 meters above ground – and dominant height – height of the 100 tallest trees per hectare in a stand – which are, similarly, very difficult to estimate in the absence of specific data.

Despite extensive research, no models were found that estimated tree height and diameter based on age or other variables that could be estimated. Without equations that module the evolution of the tree's height and diameter over time, it becomes difficult to perform reliable calculations. Users would need to know their stand's average height and diameter in each process – thinning, final harvesting, resin and biomass extraction – to calculate the net value precisely. Even with this information, the results of the predictive model would likely remain inaccurate, since the calculations would have to be performed in a collective approach, while stands of this species are managed on an individual-tree basis in practice.

After careful evaluation and consulting with forestry experts, it became clear that continuing with the development of the growth and economic model was not feasible, especially, given the existence of well-established simulators such as StandsSIM. As a result, instead of duplicating their functionality, it was opted to integrate these simulators into our system.

The focus began to build an API that integrates an established simulator, StandsSIM. This change allowed the project to use StandsSIM existing empirical models and larger database, more suitable for generating accurate predictions without requiring extensive additional data.

To pursue the API development, some data regarding fixed values and management approaches that were commonly applied in Mação was gathered. Once all the data was collected, the API development started. The management of the stand and the horizon planning were set as input variables, allowing the model to adapt to changing management strategies over time. The biomass and wood prices were, as well, left as input variables due to their dynamic nature.

After the API was developed, testing was conducted using the data that was gathered from Mação. The results were analyzed in terms of economic viability for new maritime pine stands, and sensitivity analysis was performed to assess whether the current management strategies used in the region are optimized for maximizing profitability.

5.6 Developed Models

The literature presented in Section 5.4 enabled the creation of a growth and economic model in Python. This model aimed to simulate the lifecycle revenue generated from wood, resin and biomass, using user-provided data. The details of this design, as well as the equations used to perform it, are presented in the Appendix V.2 Section.

Due to the already mentioned reasons in Section 5.5, the approach changed, so, this section will focus on the integration of StandsSIM simulator into LAND IT platform. The development of the API followed three main stages: inputs, simulations and outputs.

5.6.1 Inputs

The first stage focused on structuring the necessary user inputs for the simulation. To structure and analyze the parameters provided by the users, a class was created, ensuring that all values provided followed the data type restrictions implemented.

The main input variables included final cut age, which defines the planning horizon of the simulation, number of hectares, management schedule and wood and biomass price. The management schedule accounts for key information to run the simulator, such as the periodicity of harvesting operations, the beat-up percentage and the number of trees planted per hectare. Also, two different wood prices were required since Mação makes a distinction between the selling value of wood that is collected for chipping actions and to sawmilling actions.

5.6.2 Simulation

Once the input structure was developed, it was necessary to implement functions that automatically modify and update the input files, inherent to StandsSIM, with information provided by the user. A group of functions was developed to customize the management schedule - based on a list of predefined operations, specifically mentioned by Mação's forest experts - the timing for key operations like harvesting and thinning, the wood and biomass practiced prices and total number of hectares being simulated.

5.6.3 Outputs

The outputs that are being given to the user include total costs and receipts, Net Present Value (NPV), Equivalent Annual Annuity (EAA), total wood and biomass revenues.

In addition, a visualization interface was integrated into the outputs, so that users could analyze the evolution of some parameters over time. The created visualizations available include the changes over the simulation years for dominant height, number of trees, basal area, wood volume, biomass weight, quadratic mean diameter, NPV and EAA.

5.7 Results' Analysis

5.7.1 Assessing the profitability of the proposed management approach of Mação

To evaluate the profitability of the proposed management approach of Mação, a simulation was conducted based on the information provided. Using data from the ICNF's 22 document, it was possible to understand that the region has a horizon plan of 46 years, with harvest operations occurring at regular intervals of 10 years, starting in year 17. Since the simulator needs a threshold on the Wilson Factor metric, a value of 0.25 was indicated.

In addition, maintenance operations – such as regular vegetation control, plantation, soil preparation and fertilization – are routinely performed in the territory. Since plantation operations are conducted, Mação added the information that 1,470 trees are planted per hectare, and that it is expected that beat-up percentage has a value of around 15%. By combining this information with details about the commonly practiced prices applied in Mação, it was possible to create a schedule of operations and input accurate pricing data for the simulation.

5.7.2 Output and analysis of the results

Table 5.2 presents the results obtained for the three productivity scenarios.

Scenario	Site Index	Total Cash Inflows (€)	Total Cash Outflows (€)	NPV (€)	EAA (€)	Total Wood Revenues (€)	Total Biomass Revenues (€)
Mação 5	15.44	15354.5	1605.4	1181.0	56.5	14461.5	893.0
Mação med	20.69	28359.7	1605.4	4123.2	197.4	27693.5	666.2
Mação 95	25.86	43884.5	1605.4	8449.1	404.6	43188.9	695.6

Table 5.2: Simulation Results for Maçãos' management approach for three site indexes

As expected, higher site indexes result in higher cash inflows, wood revenues and greater NPV and EAA, showing the influence of land productivity levels on the overall financial outcomes. Notably, total costs have remained unchanged in all scenarios, with a value of €1,605.4, indicating that operational costs do not depend on productivity levels.

An observation from Table 5.2 is the decrease in biomass revenues with the increasing site index. Contrary to wood revenues, biomass revenues decline as productivity increases. In lower productivity scenarios, like *Mação 5*, trees often do not reach heights or diameters required for viable wood commercialization, resulting in higher biomass revenues, explaining the €893 obtained. Intermediate productivity scenario yields the lowest biomass revenue, €666.2, as more trees meet wood standards. High productivity scenarios, like *Mação 95*, balance faster growth with increased residue collection throughout the time horizon planning, reflecting the €695.6 revenues.

Wood revenues increase with productivity. In *Mação 5*, lower tree density and delayed thinning operations limit wood revenue, justifying the lowest value of €14,461.5, since revenues from wood are solely obtained in years 37 and 46 (year in which the final cut is performed). The medium scenario includes an additional thinning operation, in year 27, reflecting higher wood revenues. Finally, *Mação 95* generates the highest wood revenues, €43,188.9, due to the execution of all scheduled thinning operations.

Consequently, *Mação 95* scenario achieves the highest NPV (€43,884.5) and EAA (€404.6), while *Mação 5* shows the lowest values since fewer income operations are performed. These results reinforce the importance of selecting high-quality sites to plant maritime pine stands, as well as the imprudence of performing three thinning operations in soils with site indexes similar to *Mação 5* and *Mação med*. For a better understanding of changes that occur throughout the stands' lifecycle, some of the most relevant charts will be introduced.

The dominant height gives important information on site productivity, as dominant trees are the least affected by competition and reflect the quality of the growing environment. Figure 5.1 shows the behavior of this parameter through the 46 years of the stand. It is easy to see that higher site indexes achieve faster growth rates and higher maximum heights. *Mação 95* has the highest growth rate and maximum height, while *Mação 5* has the lowest in both.

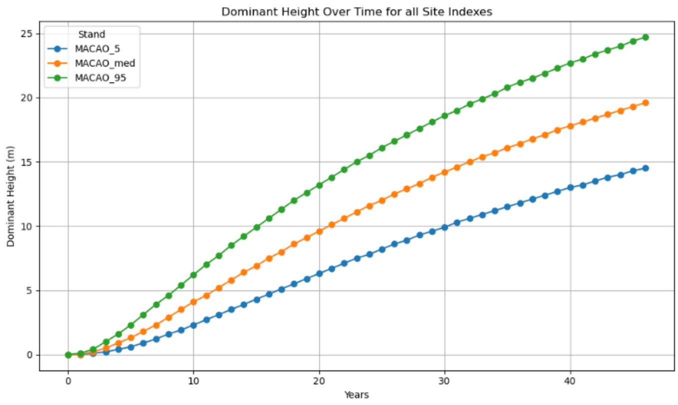

Figure 5.1: Dominant Height over time for three site indexes

Figures 5.2, 5.3 and 5.4 show the evolution of tree density over time. In *Mação 5*, only one thinning occurs, – visible by the only decrease in the chart – leading to minimal reductions in tree density. Figure 5.3, representing the medium scenario, two decreases are shown, in years 27 and 37, where thinning occurs, and, finally, Figure 5.4, the highest and only productivity scenario that had the required number of trees to perform the three thinning scheduled, resulting in a lower density of trees. This is a result of the principal objective being the production of high-quality wood coming from trees with larger diameters. In higher productivity stands, the wood has higher economic value, and is therefore harvested and sold more extensively, whereas this is not the case in lower productivity stands.

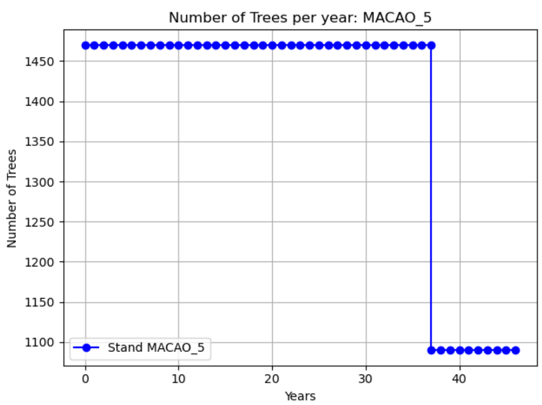

Figure 5.2: Number of trees over time for Mação 5

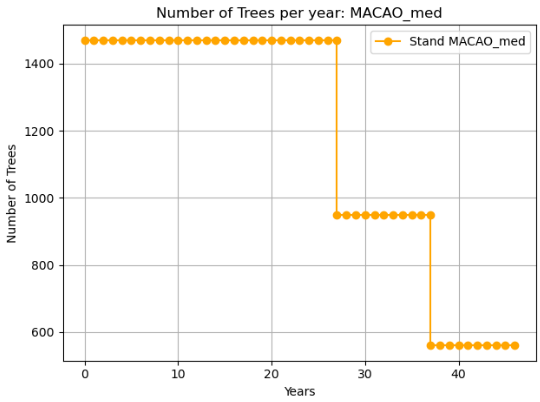

Figure 5.3: Number of trees over time for Mação med

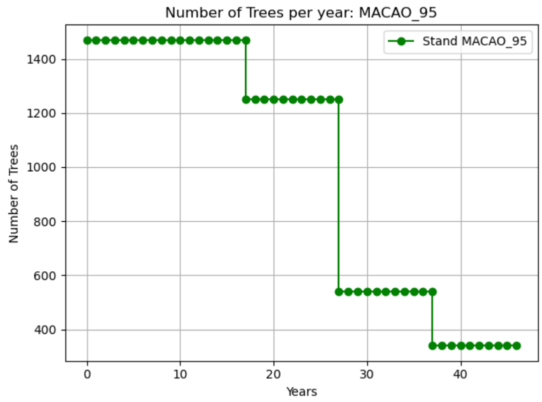

Figure 5.4: Number of trees over time for Mação 95

Graphs of wood volume and basal area evolution can be seen in the Appendix V.3 Section.

Lastly, Figure 5.5 shows the trends in cumulative NPV across site indexes. *Mação 5*'s cumulative NPV remains negative for most of the planning period, only reaching positive values at the final cut age – the last point of the chart. *Mação med* achieves positive values at the second thinning, at year 37. *Mação 95*, turns positive earlier, at the second thinning in year 27, explained by both the number of harvesting operations performed, and the economically viable wood that is collected in each scenario. Since both NPV and EAA follow the same trends of cumulative NPV, a deeper analysis will be done regarding only this plot, others can be seen in the Appendix V.3 Section.

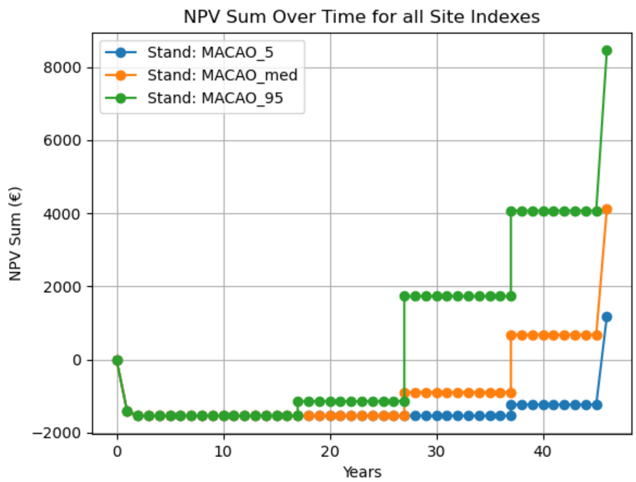

Figure 5.5: Cumulative NPV over time for three site indexes

5.8 Sensitivity Analysis

To assess the impact of the input parameters and highlight opportunities for maximizing profit, it is crucial to perform a sensitivity analysis, so that users can identify which factors have the greatest potential to be improved. To provide Mação with the best and most informed advice regarding their management approach, both univariate and multivariate analysis were conducted to change the following parameters: Number of trees per hectare, Beat-up percentage, Final cut age, First harvesting operation year and regularity.

5.8.1 Univariate Analysis

In this analysis, each parameter that seemed probable of influencing the profit outcome was isolated. Between the selected parameters, a range of acceptable values was tested to determine their individual impact on the NPV. The outputs that resulted from each analysis were compared to Mação's base values, enabling the identification of the ones that may be able to enhance profitability. The charts used to perform this analysis were designed in Tableau Desktop.

5.8.1.1 Tree Density per hectare

An analysis, performed to assess the ideal tree density to maximize profit was conducted, using a range of values among 1,250 and 1,670, incremented by 10, as recommended by Centro *Pinus*.

A bar chart was designed for each productivity scenario. In Figure 5.6 we can observe that *Mação 5* shows the lowest NPV values, while *Mação 95* has the highest ones. The NPV for 1,470 trees per hectare, representing the current number used in Mação, is marked in each chart.

The maximum NPV is highlighted as well and, in the case of *Mação 5*, the highest NPV, €1,252, occurs with 1,590 trees per hectare. In *Mação med* and *Mação 95* the highest NPVs were €4,502 and €8,952, with 1,670 and 1,660 trees per hectare, respectively.

As noticed, in none of the scenarios, the current tree density aligns with the value that maximizes the NPV, however, and as visible, the variation between bar sizes, is minimal across all scenarios. This indicates that, although the NPV increases, the rise in question may not be significant to justify the change in the current practice. Percentage differences between the NPV of the current and optimal tree densities can be seen in Table V.1 of the Appendix V.4 Section.

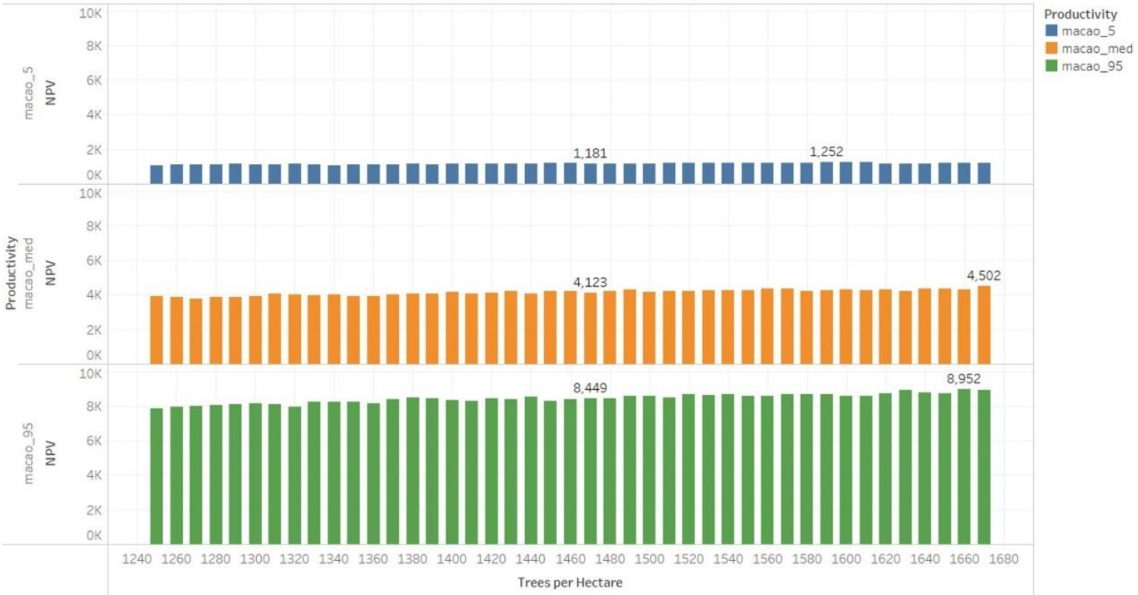

Figure 5.6: Sensitivity Analysis of NPV of different Trees per hectare, for all three scenarios

5.8.1.2 Beat-up Percentage

The beat-up percentage refers to the proportion of the stand that requires replanting due to tree mortality (Produtores Florestais 2024). Since this process involves replacing trees that died, it is logical to aim for the lowest percentage possible, so additional costs associated are minimal. A sensitivity analysis, ranging from 5% to 25 %, with 5% increments, is shown in Figure 5.7.

It is visible in Figure 5.7 that, across all productivity scenarios, when the beat-up percentage increases, the NPV tends to decrease, implying that a negative correlation between these variables exists. For instance, in *Mação 5* scenario, the NPV decreases significantly by 23.97% as the beat-up percentage rises from 5% to 25%. A smaller decline is seen in *Mação med* and

Mação 95, that only diminish 7.51% and 3.74%, respectively. More details regarding these differences in NPV can be seen in Table V.2, in the Appendix V.4 Section.

These results show the importance of maintaining high-quality soil, especially in lower productivity areas, to minimize the beat-up percentage and enhance profitability.

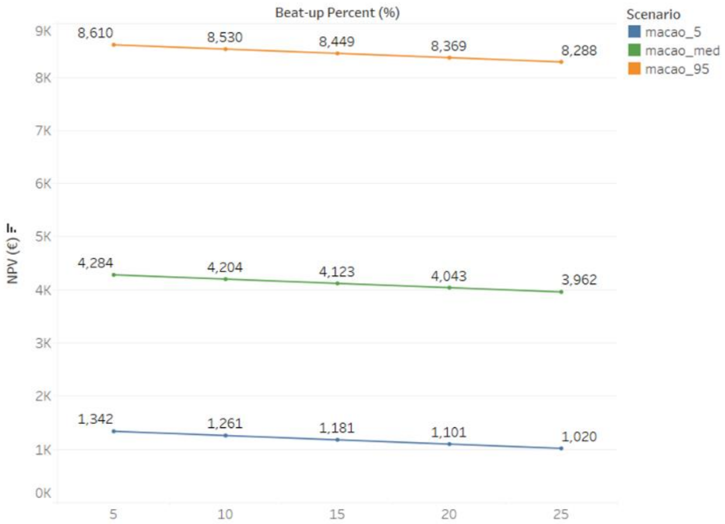

Figure 5.7: Sensitivity Analysis of NPV with different Beat-up percentages

5.8.1.3 Final Cut Age

In regions regularly affected by fires, trees are usually harvested earlier, at 35 years, as a strategy to diminish fire risk. However, under optimal conditions, the ideal age is 50 years. A sensitivity analysis was conducted using EAA instead of NPV, given the varying project time horizons. The results in Figure 5.8 show that the final cut age applied by Mação, set at 46 years, is already optimal for the schedule implemented, suggesting no necessary adjustments in this input.

Moreover, by analyzing Figure 5.8, it is possible to assess the impact of cutting stands earlier than scheduled, a practiced implemented by many Portuguese regions. In the case of lower productive soils, this approach can result in negative annual profits, as trees are not able to reach their maximum potential height and diameter.

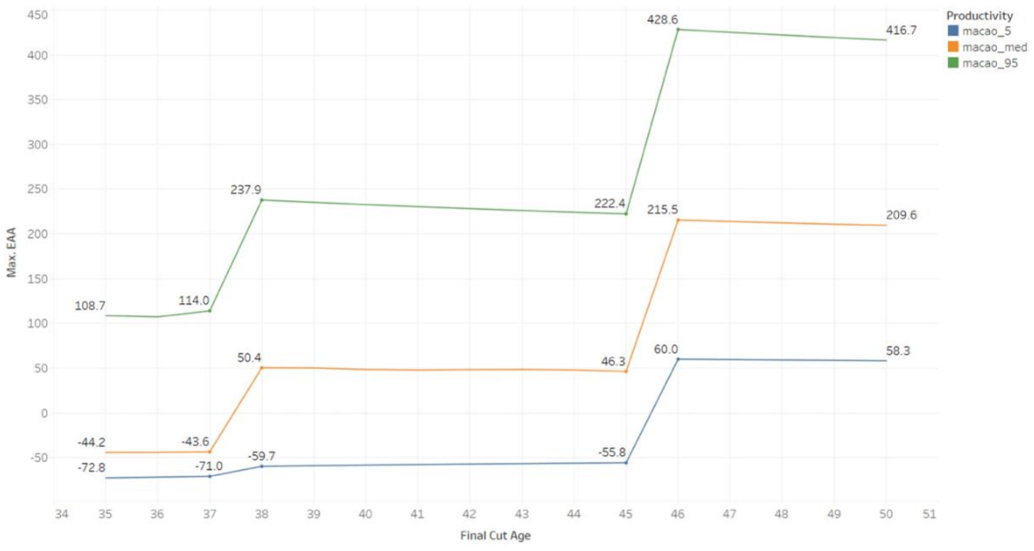

Figure 5.8: Sensitivity Analysis of the EAA with different Final cut ages

5.8.1.4 First harvesting process and regularity

The first harvesting operation typically occurs between the first 15 to 20 years of the stand, with subsequent intervals of 5 to 10 years (Centro Pinus 2015). Currently, the management approach of Mação includes three harvesting processes, the first at year 17, followed by two additional operations with intervals of 10 years. A sensitivity analysis was conducted with ranges of 15 to 20 years for the first operations and 5 to 10 years for intervals. A sorted heatmap, for each scenario, be seen in Figures 5.9, 5.10 and 5.11.

In each figure, the darker color marks the most profitable combination, while the lighter one marks the lowest NPV obtained. In all scenarios, the combinations that are marked with a darker color have intervals of 8 years. For *Mação 5* and *Mação 95* scenarios, this begins at year 16, while, for *Mação med* it is at year 15. However, due to the Wilson Factor criteria, the simulator only allows thinning in certain years. In *Mação 5*, thinning begins at year 32, so only two of the four operations scheduled are made. In *Mação med*, thinning starts at year 23, so, three out of four operations are made. In *Mação 95*, all scheduled thinning occurs, starting at year 16.

After assessing the actual performing thinning years, it is concluded that one additional operation is being done compared to Mação's baseline. Since thinning directly contributes to wood and biomass receipts, one additional operation will impact positively the NPV.

By observing the NPV labeled in each figure, significant differences in the NPV yield are only seen on the lowest productivity scenario, while, on the other two, the differences are only of 7.58% and 1.3%. Given these findings, adjusting schedules may be most beneficial if in the presence of a lower productivity soil. Table V.3 summarizes the results found and can be seen in the Appendix V.4 Section.

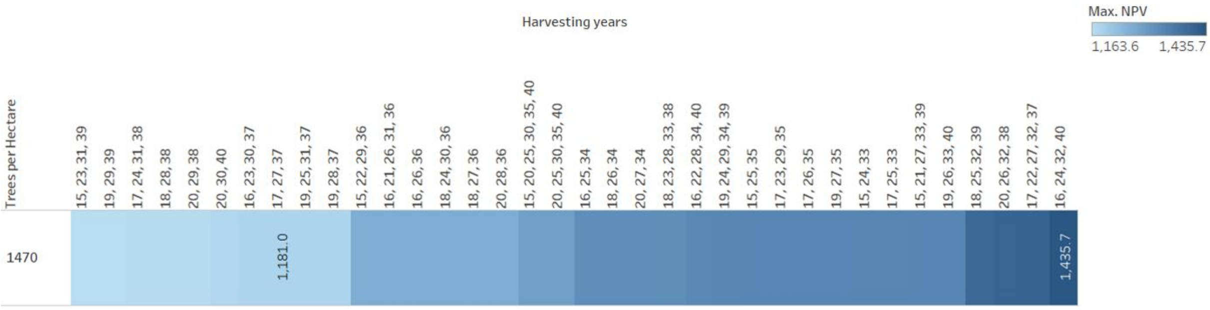

Figure 5.9: Sensitivity Analysis of the NPV with different Schedules, Mação 5

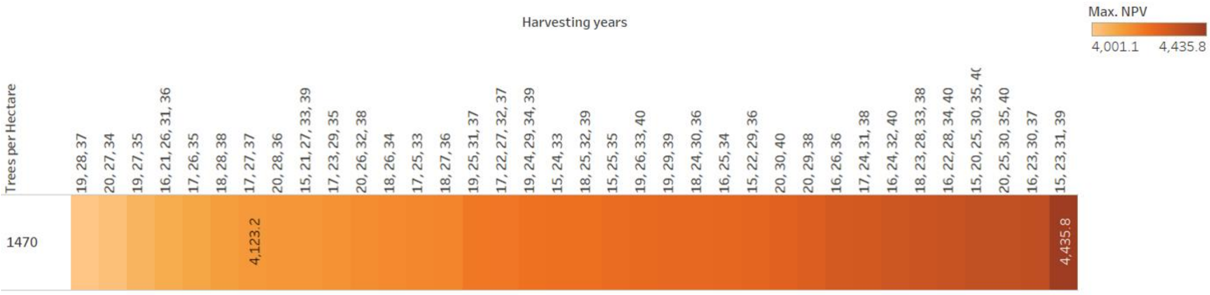

Figure 5.10: Sensitivity Analysis of the NPV with different Schedules, Mação med

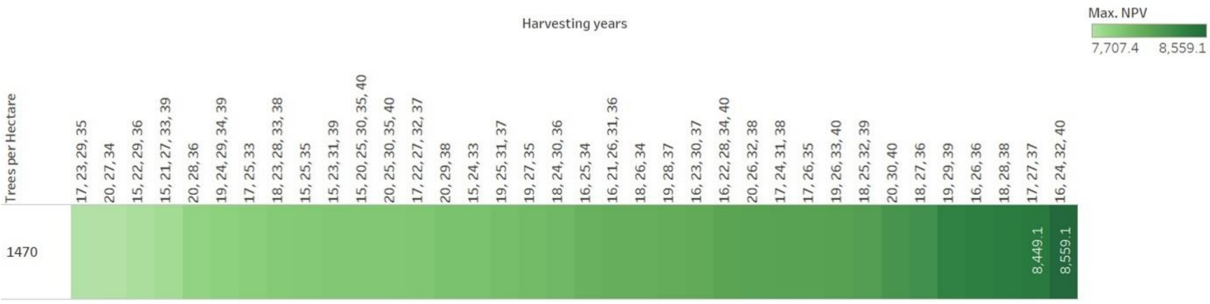

Figure 5.11: Sensitivity Analysis of the NPV with different Schedules, Mação 95

5.8.2 Multivariate Analysis

In the multivariate analysis, the main objective was to search for the optimal combination of parameters evaluated the univariate analysis. However, since the beat-up percentage is a complex parameter, and Mação provided information indicating that it is consistently around 15%, the results in this chapter are based on this fixed value.

The results obtained are shown in Table 5.3 and demonstrate that independently of the productivity scenario, the best planning horizon is 46 years. *Mação 5* continues to be the scenario that most benefits from parameter adjustments, with a 28% NPV increase, achieved by increasing the number of trees by 110 and the scheduling thinning to start at year 16 with 8-year intervals. Also, by revising some of the results obtained in Section 5.8.1, we can see that by combining the optimal schedule with a tree density of 1,580, 10 less than the value obtained in the univariate analysis, the NPV increased.

For *Mação med*, the optimal tree density and schedule obtained in the univariate analysis remained the same, resulting in an increase of €721.8, 17.5%, when combined.

In *Mação 95*'s scenario, while the optimal tree density remained the same, 1,660, the thinning schedule changed to starting at year 15 with intervals of 8 years. If Mação decides to increase the number of trees planted for 1,660, applying the schedule obtained in this analysis, can enhance the NPV. Charts regarding this analysis can be found in the Appendix V.4 Section.

Scenario	Type	Trees per Hectare	Beat-up Percent (%)	Schedule	Actual Performing Thinning years	Final Cut Age	NPV (€)	Difference (%)
Mação 5	Practiced	1470	15	(17, 27, 37)	(37)	46	1181.0	-
Mação 5	Max NPV	1580	15	(16, 24, 32, 40)	(32, 40)	46	1511.6	27.99
Mação med	Practiced	1470	15	(17, 27, 37)	(27, 37)	46	4123.2	-
Mação med	Max NPV	1670	15	(15, 23, 31, 39)	(23, 31, 39)	46	4845.0	17.5
Mação 95	Practiced	1470	15	(17, 27, 37)	(17, 27, 37)	46	8449.1	-
Mação 95	Max NPV	1660	15	(15, 23, 31, 39)	(15, 23, 31, 39)	46	9216.4	9.08

Table 5.3: Summary of Multivariate Sensitivity Analysis

5.9 Conclusion - Recommendations

After conducting both univariate and multivariate sensitivity analysis, recommendations on the best values to use in each parameter will be given so that Mação's overall returns are optimized.

5.9.1 Management schedule

In *Mação med*, the optimal schedule, regardless of other parameters' variation, remained the same, starting at year 15 with intervals of 8 between harvesting, making it the recommended schedule for medium site indexes. The same was observed for *Mação 5*, either with a lower or a higher number of trees per hectare, – 1,470 or 1,590, respectively – starting at year 16, with intervals of 8, might be beneficial, since the wood collected and available for selling is higher than with the base schedule.

In *Mação 95*, the management schedule differs between the multivariate and univariate sensitivity analysis. With 1,470 trees, the best schedule starts at year 16 with intervals of 8, while, with 1,660 trees, starting at year 15 with intervals of 8 marks the optimal point. Although, the NPV yield was higher when both a higher tree density and optimal schedule were combined, given Mação's characteristics, following the findings of the univariate might be more prudent.

5.9.2 Tree Density

In every productivity scenario, the analysis showed that planting more than 1,500 trees increases the NPV. However, Mação is a territory very affected by wildfires, meaning that planting the base 1,470 trees might be more prudent. By planting a lower tree density of trees, the territory is able to reduce the impact of a high intensity fire, and, at the same time, increase spacing between trees, lowering the competition between and enhancing their overall healthy growth.

5.9.3 Planning Horizon

As previously referred, Mação is territory highly vulnerable to fires, so, given its conditions, the life cycle of trees should be reduced to protect the municipality. Although it is usual to cut the stand at age 50, Mação usually harvests earlier, at the age of 46. As it was possible to see in the sensitivity analysis, the age of 46 is the most profitable for Mação, leading to the conclusion that that age might be the most appropriate to apply.

5.9.4 Beat-up Percentage

Lower beat-up percentages result in higher yields of the NPV. This fact shows the importance of making efforts to lower this percentage. Applying adequate soil preparation, planting techniques and preventive measures to reduce the impact of climate changes can directly impact the performance of the management approach followed.

5.9.5 Proposed Management Strategy

Considering Mação's characteristics and the results of sensitivity analysis, the following management approach is recommended to maximize returns while protecting from wildfires:

- Harvesting operations should have increments of 8, regardless of the productivity of the land. In the case of low and high-site indexes, the first harvest should be at year 16 and, in the case of a medium, it should start at year 15.
- Implement measures that lower the beat-up rate as much as possible, while maintaining both the 1,470 trees per hectare and the 46 years as the time horizon planning.

5.10 Limitations

The API design presented several limitations, mostly regarding the unavailability of site index data. Given this fact, the simulation could not accurately tell what to expect regarding the NPV. However, by using estimated site indexes, it was possible to address this challenge. Conversely, the same did not happen with prices, since the simulations relied on static prices provided by

Mação, which do not reflect market fluctuations or variations caused by land slope, as these operational cost differences were not considered.

StandsSIM, assumes a linear relationship between NPV, productivity, and the number of hectares, meaning that the simulations are conducted for one hectare only and the output values are multiplied by the number of hectares introduced by the user. In reality, variations such as tree spacing, competition or resource distribution can affect productivity differently in smaller or larger stands, differing from this linear assumption.

Lastly, the sensitivity analysis was very complete, accounting for the variation of all parameters, individually and collectively. Nevertheless, it was limited in exploring alternative management schedules besides harvesting years. Other operations, such as vegetation control timing, were not tested due to the lack of alternative management plans for maritime pine.

5.11 Future Work

Currently, the API only supports non-existent and even-aged stands. However, extending its functionalities to include more complex scenarios could significantly benefit users. Since StandsSIM already possesses these capabilities, incorporating them into the API would enhance its utility for LAND IT platform and, consequently, for its users. By offering a wider range of options and increasing the flexibility of allowed stand types for simulation, the API could extend its functionalities to a broader range of use cases and provide greater value.

Moreover, one limitation encountered was the fact that data necessary to perform an economic feasibility analysis of already existing maritime pine stands' in Mação, was not able to obtain in time duration of this thesis. However, it is of great importance that this data is collected and analyzed, to enable the integration of existing plantations into the API. This enhancement would allow LAND IT users to simulate not only new plantations but also existing ones.

6. The Case of Eucalyptus

6.1 Eucalyptus in Portugal

By the end of the 20th century, Portugal was home to 250 species of eucalyptus, with the *Eucalyptus globulus Labill* being the dominant one (Cabral 2019, 27). According to the *Inventário Florestal Nacional*, the area covered by eucalyptus expanded rapidly, totaling 647,000 hectares in 2005-2006, which represented 19% of the country's forested area (Alves et al. 2007), as presented in Table 6.1. Since then, eucalyptus plantations kept growing. The most recent inventory, IFN6, covering the period of 2015 to 2020, shows that eucalyptus now accounts for 26% of the country's forest, which translates to 850,000 hectares (ICNF 2021).

Ano	1928	1956	1963/66	1968/80	1980/89	1990/92	1995/98	2005/06
Área (10^3 ha)	8	58	99	214	386	529	672	647

Table 6.1: Evolution of eucalyptus plantations in Portugal | Source: Alves, Pereira, e Silva 2007

It is still one of the most widespread species in Portugal nowadays, bringing several ecological benefits, such as capturing carbon dioxide that reduces greenhouse gases (Produtores Florestais 2023). For each hectare, approximately 11.3 tons of carbon dioxide is captured annually, the equivalent of a car's emissions traveling 109 kilometers (Produtores Florestais 2023).

6.2 Eucalyptus Characteristics

Eucalyptus plantations can be managed through coppice or high-stem regimes. Coppice is the most common in Portugal, where the trees are periodically cut at ground level. This approach takes advantage of the eucalyptus' ability to regenerate quickly, allowing for 2 to 3 harvest cycles, each with a duration of 10 to 15 years. With one of the fastest growths among all tree species, the eucalyptus is particularly valuable for pulp and paper production industries (Caldas et al. 2022), as it allows for multiple harvests within short periods of time. In contrast, the high-stem regime allows the trees to grow to a desired height, involving fewer growth cycles. The trees are harvested exclusively for high-quality wood after 25 to 30 years (Marques et al. 2012).

Moreover, eucalyptus trees are highly adaptable to diverse environmental conditions, including suboptimal soil types where other species might struggle. The trees have a robust root system that enables them to access deep water reserves, which is essential to survive in drier regions. However, eucalyptus generally performs best in humid climates, which is why plantations are most concentrated along Portugal's coastline, where conditions are conducive to optimal growth (Alves, Pereira, and Silva 2007; ICNF 2021) as can be seen in Figures 6.1 and 6.2.

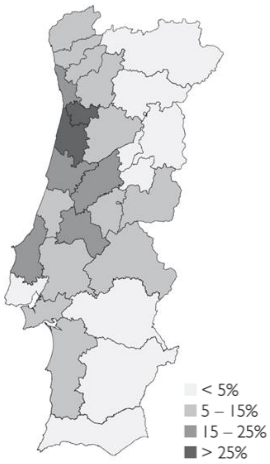

Figure 6.1 – Distribution of eucalyptus plantation in Portugal 2005-2006 | Source: Alves, Pereira, e Silva 2007

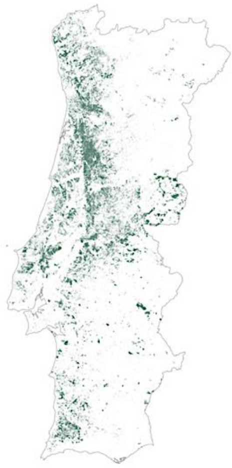

Figure 6.2 – Distribution of eucalyptus plantations in Portugal 2018 | Source: Direção-Geral de Território

6.3 Growing Cycle

As coppice is the most common regime, this study will focus on that specifically. The growing cycle begins with land preparation – soil loosening and weed control –, planting and fertilization. This initial step is crucial for root development and tree growth, once it enhances aeration, infiltration, water retention and nutrient availability in the soil, which are essential conditions for a healthy growth. During planting, it is important to space the trees 3.5 meters apart between rows and 2 meters apart between each tree, always respecting the maximum density of 1,400 trees per hectare (Caldas et al. 2022). A post-planting assessment occurs during the first year, allowing for the replanting of trees that died during the planting process. This assessment ensures adherence to the initial forestry plan. Between the second and sixth year of growth, cleaning and controlling the unwanted vegetation around the eucalyptus takes place and is crucial for maintaining low biomass density and preventing fire hazards. Additionally, fertilization is applied during this period. Lastly, when the trees reach approximately 10 to 15 years of age, they are harvested and the cycle starts all over again (Biond, "Rearboreação").

This cycle is repeated for the second and third rotations, with shoot selection taking place shortly after each harvest. Shoot selection is the process of selecting and retaining the best shoots that grow after each harvest while removing the others. This ensures that the remaining shoots have optimal conditions to grow, promoting high-quality for future harvests.

6.4 Related Work and State of Art

The sustainable management of eucalyptus plantations has gained importance due to the species' significance in fire prevention, ecological benefits, and economic impact. Representing 5% of Portugal's exports (The Navigator Company 2020, 5) and being one of the most efficient species for carbon sequestration (Behera et al. 2020, 79), eucalyptus has prompted extensive studies to model its growth. These models enable more accurate forecasts of forest productivity, support the optimization of management strategies, and maximize economic returns.

In general, forest species exhibit a logistic S-shaped growth curve (Figure 6.3) characterized by a rapid initial phase with convex growth, followed by a linear phase with a constant yearly growth rate, and concluding with a slower concave phase as the species mature (Goes 2012, 8).

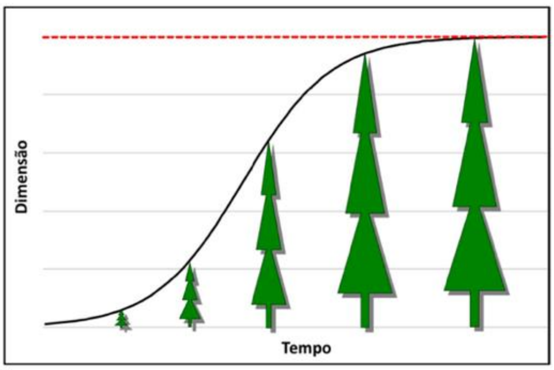

Figure 6.3 – Logistic Growth Function | Source: Goes, 2012

This growth pattern has been found to fit eucalyptus well (Mhamdi et al. 2022), but other models have also been proposed. G. A. Chapman and R. A. Richards have developed the Chapman-Richards nonlinear growth function that describes the biological growth patterns of various species, one of which the eucalyptus (Zhao-gang and Feng-ri 2003). This function models height and diameter forecasts, demonstrating strong predictive performance for these variables (Carvalho et al. 2020). Other theoretical models have been created to predict height growth, such as the Smalian, Gompertz, Lundqvist-Korf, and Weber functions, as well as the logistic, Lundqvist-Korf and Gompertz functions for diameter growth (Mhamdi et al. 2022).

To analyze the performance of all these growth models, some studies have taken place to evaluate their accuracy. A study in Tunisia examined growth models for seven eucalyptus species, concluding that the Gompertz function was effective for modeling the diameter growth while the Chapman-Richard was suitable for height evolution forecasts (Mhamdi et al. 2022). Apart from this, a study in India explored how these models behaved in eucalyptus predictions and concluded that the logistic growth model was suited for the eucalyptus growth estimations especially at harvesting periods (Malik et al. 2003). Finally, research on individual trees' growth models was undertaken in Brazil, finding that the Lundqvist-Korf model provided the most accurate estimate for both the diameter and height growth (Martins et al. 2014).

As can be seen by these studies, there is no agreement on the best model to use, which can be justified by the different types of eucalyptus species being studied and the contrasting atmospheric characteristics of the forests they are in. As such, and for the purpose of this study, the function that presents the best results for both diameter and height should be considered. According to the book *Modeling Forest Trees and Stands*, the Chapman-Richard growth function presented the best results and will be used for this study (Burkhart and Tomé 2012). There is however a disadvantage on the use of this equation, which is the mandatory knowledge of the stands' age. This can become a problem as there are regular- and irregular-aged stands.

Regular-aged stands are characterized by a group of trees of the same age, with features so similar among themselves that stand models are preferred in comparison to tree models (Peng 1999). On the other hand, the irregular-aged stands are composed of different aged trees with different values for diameter and height, making it more difficult to apply these equations. This added complexity level of irregular-aged stands makes it difficult to predict height and diameter, as there is no age or station quality index to assign to the stand (Kiernan et al., 2008).

To overcome this problem, as the Chapman-Richard function is dependent on the stands' age, Portuguese professors of *Instituto Superior de Agronomia* proposed a growth model that is independent of the stand's age, as can be seen in Table 6.2 (Tomé et al. 2006).

Função	Forma integral dependente da idade	Forma integral independente da idade
Hossfeld IV	$Y_i = \frac{At_i^m}{k + t_i^m}$	$Y_{i+a} = A\frac{\left(\left(\frac{Y_i k}{A - Y_i}\right)^{\frac{1}{m}} + a\right)^m}{k + \left(\left(\frac{Y_i k}{A - Y_i}\right)^{\frac{1}{m}} + a\right)^m}$ (Burkhart & Tomé, 2012)
Richards	$Y_i = A(1 - e^{-kt_i})^{\frac{1}{1-m}}$	$Y_{i+a} = A\left(1 - e^{-ka}\left(1 - \left(Y_i/A\right)^{1-m}\right)\right)^{\frac{1}{1-m}}$ (Tomé *et al.*, 2006)
Lundqvist–Korf	$Y_i = Ae^{\frac{-k}{t_i^m}}$	$Y_{i+a} = Ae^{\frac{-k}{\left(\left(\frac{-k}{\ln(Y_i/A)}\right)^{\frac{1}{m}+a}\right)^m}}$ (Tomé *et al.*, 2006)

Table 6.2 - Dependent and independent growth functions | Source: Goes, 2012

The main association representing the pulp and paper industry in Portugal, known as Biond (Biond), prefers independent age models for both regular and irregular eucalyptus stands (Goes 2012, 19). This preference is justified by the presence of irregular stands on 262,000 hectares in Portugal, a figure that has been increasing in recent years due to the impact of wildfires.

Nevertheless, some data needed to be studied to estimate the equation's parameters. Francisco's thesis gathered data on eucalyptus in Portugal from the *Inventário Florestal do Eucalipto* (IFE) conducted by Biond, the *Direção Geral dos Recursos Florestais*, and *Altri Florestal*. With this data, it was possible to predict the equation's parameters and apply the growth model (Goes 2012). Calculating wood volume is now straightforward with height and diameter predictions.

It is also important to calculate the eucalyptus biomass. For that, some equations developed by forestry experts are available, to calculate wood, bark, branches and leaves (Tomé et al. 2007).

The combination of growth and financial models result in an enhanced accuracy, as the growth model feeds the financial model, presenting tailored optimizing management strategies (Cunha and Fontes 2004). The StandsSIM simulator, developed by researchers at the *Instituto Superior de Agronomia*, represents the practical integration of these models (Simflor Platform 2024). This combination enables users to model growth patterns and evaluate financial outcomes simultaneously, with sensitivity to climate variables, costs, and silvicultural practices. Thus, the simulator can be tailored to reflect the specific characteristics of Mação. Its wise use can efficiently aid in organizing forest lands to prevent wildfires while also allowing for a comparison of the Net Present Value (NPV) for different management strategies in eucalyptus.

6.5 Methodology and Approach

The objective of this section is to develop a growth and economic model for even-aged eucalyptus plantations that can be integrated into LAND IT's platform, introduced in Section 3. With information users have about their plantations, the model aims to calculate the expected profit from wood and biomass over the tree's lifetime.

As the eucalyptus trees are treated collectively as a stand, the model can calculate the volume and profit for one tree and multiply by the total number of trees, which is called a stand model. This model does not describe individual trees but the whole stand, requiring less information to predict the stand's growth (Peng 2000). The stands models are advantageous because they rely solely on stand parameters, such as the dominant height – average height of the tallest trees in a stand – and basal area – area of the trunk at 1.3 meters above the ground. Additionally, as the models provide little information about individual trees within the stand, they are of great utility in pure plantations, where only eucalyptus are planted (Vanclay 1994).

Given that users will likely only have information of the current age of their plantation, it was important to include predictive models for the tree's height and diameter at that specific age. This is because both height and diameter are mandatory to calculate wood volume and, consequently, estimating profit. As such, two models were developed – an age-dependent, for users that only have information on the stand's age, and an age-independent model, for those that have the current height and diameter of the stand. While the age-dependent model receives harvest age and returns the expected height and diameter, the age-independent model receives the current height and diameter and predicts those values through yearly increments.

Both models were first introduced by Frank J. Richards, and since the functions are generic for all forest species, they contain several parameters to be estimated, ideally using data from the location in which the model is applied (Richards 1959). Moreover, it would be valuable to have data from different site indexes to predict growth across different productivity soils in Mação.

Given the lack of data specific to Mação, an alternative solution was found in the estimates provided by Francisco Goes (Goes 2012), who calculated these parameters using data from Portuguese companies, such as Biond and Altri. Although this approach is not ideal, since it does not use data directly from Mação, it was the only available data source. While this decision addressed the data limitations, it also reduced the model's accuracy when applied specifically to Mação, as the utilized data does not fully reflect the municipality's unique characteristics.

As such, upon careful consideration, conversations with forestry specialists, and the recognition of already established simulators for eucalyptus, such as StandsSIM and Globulus that have been developed with data and expertise, it became clear that replicating their capabilities was not necessary for this project. By integrating these robust simulators, their existing functionalities could be leveraged without the need for further duplication of efforts. As a result, it was decided to pursue an alternative approach that offers more potential for positive outcomes that was the integration of the StandsSIM simulator (Simflor Platform 2024) into LAND IT. This shift in focus allowed users to benefit from its capabilities in a user-friendly environment. Several meetings with the creators of StandsSIM simulator were conducted to understand the rationale behind the model and how it could be translated into an API. Section 4.1 presents an extensive explanation of the simulator and the outcomes of several meetings with their creators.

As the simulator requires a significant amount of information, explained in Section 4.1.2, which was not to be directly received from LAND IT users, consulting forestry specialists in Mação became critical. They were able to provide insights into which values were fixed across all lands in the region. For instance, it became clear that Mação only sells wood, and the costs associated with land preparation, plantation, maintenance, harvesting, and sale are uniform across their AIGPs, making these parameters fixed information for the model. With all the required data collected, the creation of a dynamic API began, leaving the duration of all three rotations, number of hectares, management schedule, number of trees per hectare, and wood selling price, as changeable parameters. The API development is further explained in Section 6.6.

With the API developed, further consultation with forestry specialists provided valuable insights on Mação's management schedule. Testing the model using this information led to predictions of financial parameters and an evaluation of the project's economic viability. Lastly, sensitivity analysis was performed to compare the current management schedule with the optimal strategy, culminating in recommendations for maximizing returns.

6.6 Developed Models

With all the literature present in Section 6.4, it was possible to program a model in Python, that predicted both tree growth and profit. Two growth models were considered, with age-dependent and -independent equations. The detail of these models, including equations selected and rationale is in the Appendix VI.1. As such, this section will only focus on the integration of StandsSIM into LAND IT through an API. Its development was divided into processing user inputs, running the simulation, and analyzing and presenting the outputs.

6.6.1 Inputs

The first stage was to create a mechanism to handle user inputs, enumerated in Section 4.1.2. For that, a class was created to structure and validate the input data. This class was responsible for ensuring that all input variables had the correct data type and were properly formatted to be integrated into the simulator. The input variables are wood price, management schedule, number of trees, number of hectares and duration of each of the three rotation cycles.

6.6.2 Simulation

The second stage was to automate the API to update the necessary input files for the StandsSIM simulator with the user's data. A set of functions was created, each one to modify a specific input file, automating the process of inserting user data into the simulation's framework. These functions handle the management schedule – chosen by users based on a predefined list customized to the practices Mação's forestry experts perform –, the duration of each rotation cycle and its sum to update the final cut age, the wood selling price and total number of hectares.

6.6.3 Outputs

To program the outputs of the API, meeting with forestry experts to understand the key metrics valued was essential. These specialists emphasized the importance of financial indicators, such as total inflows and outflows of money, the Net Present Value (NPV) and Equivalent Annual Annuity (EAA) of the project. Although Mação does not currently sell eucalyptus biomass, the output was programmed to also display revenues from both wood and biomass. For now, wood revenues represent the total cash inflows, as they only sell wood, while biomass revenues are zero. However, if Mação begins selling biomass, the API is prepared to handle those values. The combined wood and biomass revenues would then correspond to the total cash inflows. They also requested graphical outputs showing changes over time for parameters such as the dominant height, number of trees, basal area, wood volume and its increment, biomass, EAA, and NPV. These outputs provide users with the most relevant information for decision-making.

6.7 Results' Analysis

6.7.1 Assessing the profitability of the proposed management approach of Mação

With the API developed, the NPV and EAA can be accurately predicted for the low, average and top soil productivities, represented by *Mação 5*, *Mação Med* and *Mação 95*. The outputs of each of these site indexes can be approximated to those expected in Mação's plantations. So, the NPV of a land in Mação with a site index close to that of *Mação 95* (dominant height of 25,86) is expected to be similar to the predicted values of *Mação 95*.

Eucalyptus plantations in Mação operate on three-rotation cycles with durations of 13, 11, and 11 years for each rotation, respectively. Additionally, they are certified eucalyptus producers, increasing wood selling price to €34. The planting density is 1,250 trees per hectare, with a management schedule of land preparation and beat-up in the first year, regular fertilization and vegetation control, and shoot selection in the second year of each rotation.

6.7.2 Output and analysis of the results

Using the information presented above as input, the API calculates the predefined output variables for three different site index scenarios: low (*Mação 5*), average (*Mação med*), and high (*Mação 95*). The results are summarized in Table 6.3.

Scenario	Site Index	Hectares	Total Cash Inflows (€)	Total Cash Outflows (€)	NPV (€)	EAA (€)
Mação 5	15.44	1	5446.5	4390.6	-743.6	-39.8
Mação médio	20.69	1	10605.9	4390.6	1576.0	84.4
Mação 95	25.86	1	18731.6	4390.6	5184.3	277.8

Table 6.3 – Simulator results for three base site indexes

As anticipated, higher site indexes lead to greater wood volume and, consequently, Net Present Value and Equivalent Annual Annuity. Moreover, total cash outflows are constant among all site indexes as the price of the performed operations does not depend on land productivity. This relationship highlights the crucial role of land quality in eucalyptus profitability.

In this specific simulation performed with the management schedule used by Mação, lands with low productivity have a negative NPV and EAA. This means that lands expected to grow stands with dominant height of 15.44 meters, should not plant eucalyptus. The initial investment and costs incurred during the tree's lifespan are not outweighed by wood revenues.

This does not apply for the other site indexes, as they have positive a NPV and EAA. For average site indexes, denoted by *Mação med*, the NPV is €1,576 and EAA €84.4. So, for stands expected to reach a dominant height of 20.69 meters, the project is expected to be lucrative. As for high productive soils represented by *Mação 95*, the NPV is €5,184.3 and the EAA is €277.8.

As expected, planting in more productive lands is more profitable, as more wood is produced. For instance, wood revenue is expected to generate €5,446.5, €10,605.9 and €18,731.6 for each site index respectively, representing an increase of 95% from *Mação 5* to *Mação med*, and 77% from *Mação med* to *Mação 95*. This shows the importance of selecting optimal plantation sites.

Moreover, the API was also programmed to present charts that illustrate the timely variation of several output variables. This is advantageous because it provides users with a clear visual representation of trends and changes over time, helping in their decision-making process.

As the eucalyptus is harvested twice before the final cut, the stands' dominant height, number of trees, basal area, and wood volume reach zero in these years. This is shown in Figures 6.4 and 6.5 where the parameters reach zero at ages 13 and 24, the end of each rotation.

The growth dynamics of the dominant height provides valuable insights into site productivity. Figure 6.4 shows the almost sigmoid growth behavior of this parameter, indicating that higher site indexes achieve faster growth rates and higher dominant heights. This clearly reflects the influence of site quality on tree growth. Overall, the conclusion taken is that the dominant height does not decrease over time or with tree cuts and increases with diminishing returns.

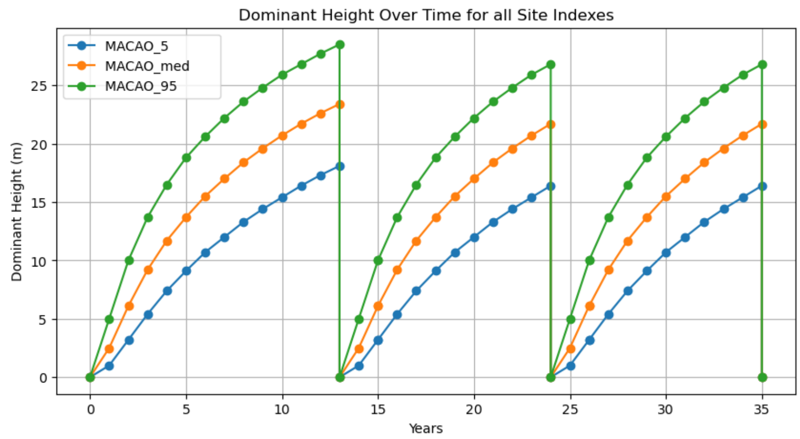

Figure 6.4 – Dominant Height over time for all site indexes

Additionally, a graph on the number of trees and basal area over the years was created. As the site index only influences the productivity (wood volume produced) rather than tree density, the number of trees is the same for all site indexes. As time goes by, the number of trees decreases, as the simulation accounts for a mortality rate of 15%. For the basal area, high productive lands grow trees faster and with higher dimensions, which increases the basal area of a stand. A more visual and in-depth explanation is present in the Appendix VI.2.

Moreover, a graph on wood volume over time was plotted (Figure 6.5). As expected, the decrease in number of trees during the second and third rotations leads to lower wood volumes. Also, higher site indexes result in faster wood production and greater total quantities. Once more, harvest years 13 and 24 null the wood volume.

Lastly, charts for financial parameters – EAA and NPV – were plotted to compare the three site indexes. Figure 6.6 shows the cumulative NPV behavior over time. As most costs occur in the first years due to land preparation, planting, and fertilization, the NPV is negative during these years. Moreover, as the total costs are the same across all site indexes (Table 6.3), the NPV until the first harvest at year 13 is the same for all site indexes. As the cycle progresses, the NPV rises further during the second and final cut, reaching the final value presented in Table 6.3. Overall, as higher site indexes generate more wood volume and at a faster rate (Figure 6.5), the NPV is greater for *Mação 95*, whereas it remains negative for *Mação 5*. This behavior is the same for the yearly NPV and EAA that can be analyzed in the Appendix VI.2.

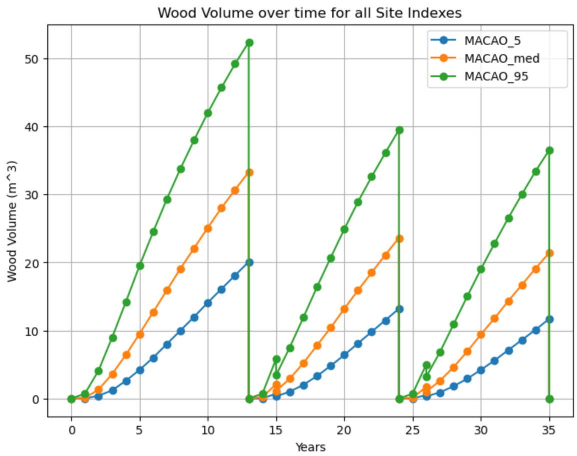

Fig 6.5 – Wood Volume Over Time for all Site Indexes

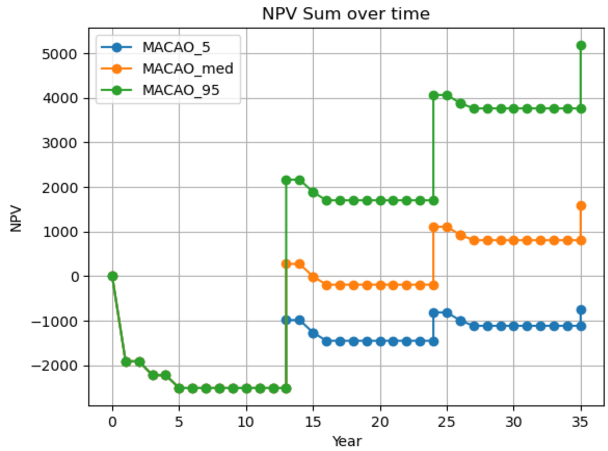

Figure 6.6 – Sum of NPV over time for all site indexes

6.8 Sensitivity Analysis

When analyzing economic models such as StandsSIM, it is crucial to perform a sensitive analysis to understand the impact of each input parameters. As per this, the following analysis aims to assess each input individually and identify the optimal combination of factors. To achieve this, both univariate and multivariate analysis were conducted, with Tableau graphs.

6.8.1 Univariate Analysis

The univariate analysis isolates each input and varies its value within a realistic range to observe its impact. For a correct analysis, the NPV will be studied in projects with the same duration and the EAA when this does not apply. The main objective is to compare the results obtained to Mação's current strategy that is as follows: three rotations with 13, 11, and 11 years, a wood price of €34, a plantation density of 1,250 trees per hectare, and a beat-up rate of 15%.

6.8.1.1 Final Cut Age

The duration of each rotation was adjusted between 8 and 14 years, corresponding to a final cut age of 24 to 42 years. In addition, as Mação performs shoot selection two years after harvest, this was kept unchanged. Given the varying project lifetimes, the EAA was calculated for each combination of rotation years and each site index. To visualize these findings, the sum of each rotation was plotted with the EAA. However, for a correct comparison, as Mação performs silvicultural operations until year 32, final cut ages lower than 32 years were not considered.

Figure 6.7 shows that, for low site indexes (*Mação 5*), extending the final cut age yields better results. This is justified by lower site indexes producing less wood and so, there is a need to extend the eucalyptus lifespan to gather more wood and increase revenues. The same trend happens in *Mação med*, representing average site indexes, however with a less step trend line.

Lastly, high productive lands benefit from shorter rotation durations as sufficient wood is produced early to cover costs. While expanding the project one additional year results in more wood produced (Figure 6.7), the increment gains are diminishing. As such, the negative sloped trend line shows that prolonging the eucalyptus lifetime reduces the EAA.

The red points in all graphs represent Mação's strategy. For *Mação 5* the EAA is always negative, meaning that eucalyptus should not be planted. For average site indexes, Mação yields an EAA of €84.4 and could increase it to €88, if the final cut age is performed between age 37 and 40, rather than 35. In high soil productivities, Mação is yielding an EAA of €277.8 and could increase to €303, if final cut was performed at ages 32 or 33. However, because final cut age is the sum of rotation durations, an analysis on those was undertaken.

An individual visualization of each scenario in Figure 6.9 is presented in the Appendix VI.3.

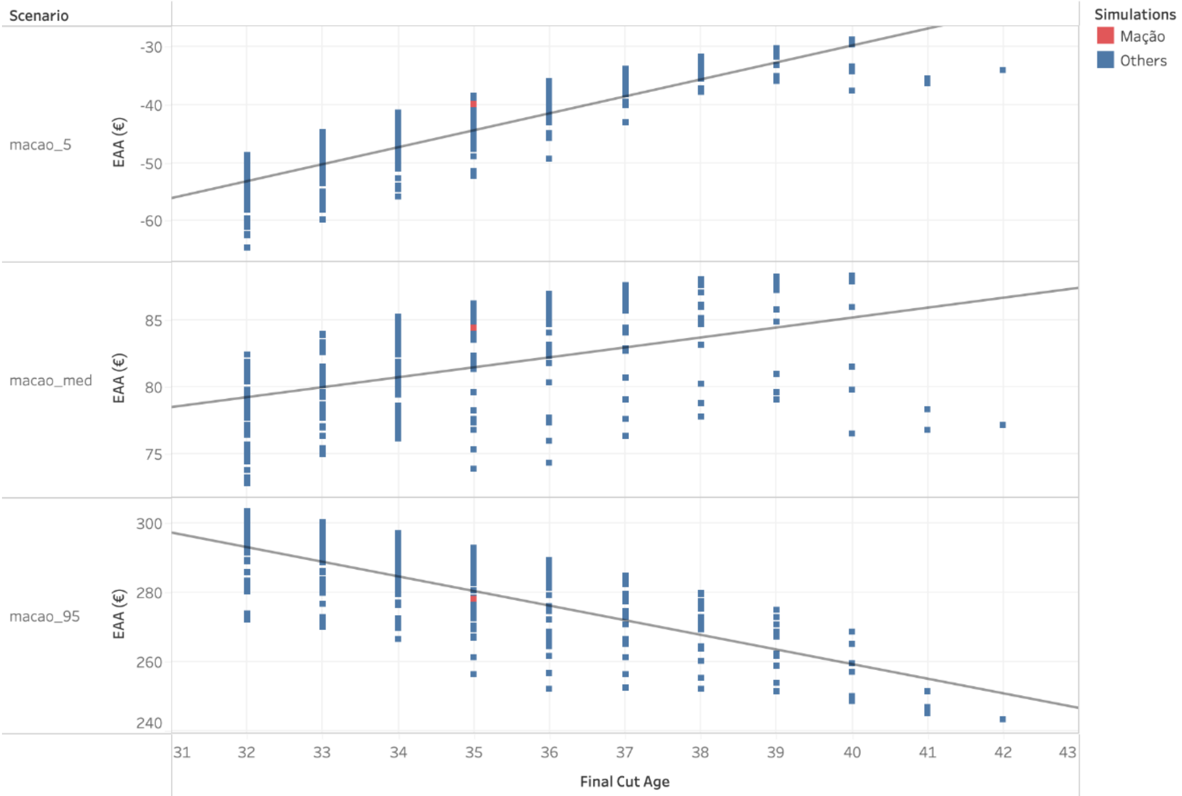

Figure 6.7 – Final Cut Age VS EAA for all site indexes

6.8.1.2 Rotation Duration

The rotations' duration was adjusted using the same ranges as Section 6.8.1.1, enabling analysis of the most profitable duration with shoot selection performed two years after harvest.

Figures 6.8, 6.9 and 6.10 compares the EAA yield for each site index, showing the relationship between the duration of the first and second rotations. Agreeing with conclusions taken in the previous section, lower site indexes yield higher annual profit when rotations are longer. Contrarily, high site indexes maximize their EAA in shorter rotations, as wood produced is more than enough to cover costs. These graphs have a darker color in combinations with higher EAA, and label of the maximum EAA yield when combining the third rotation.

This rational is the same for studying changes on only the first rotation, or even when adding the second (Figures 6.8, 6.9, 6.10) or third. For a more in-depth analysis with graphs similar to these, comparing only the duration of the first rotation, adding the second and finally the third is in the Appendix VI.3.

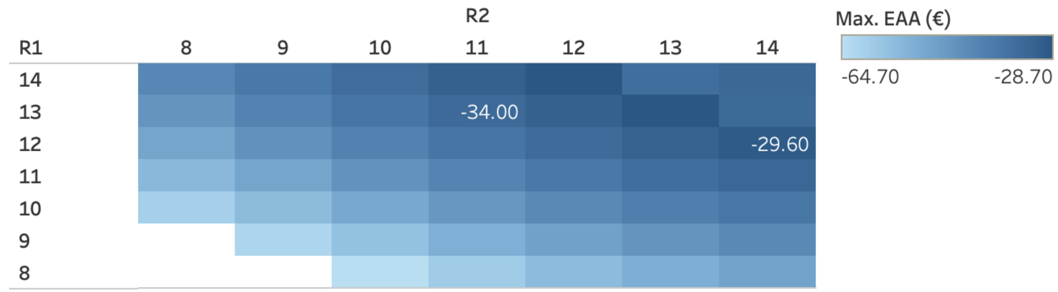

Figure 6.8 – Rotation 1 and 2 VS EAA for Mação 5

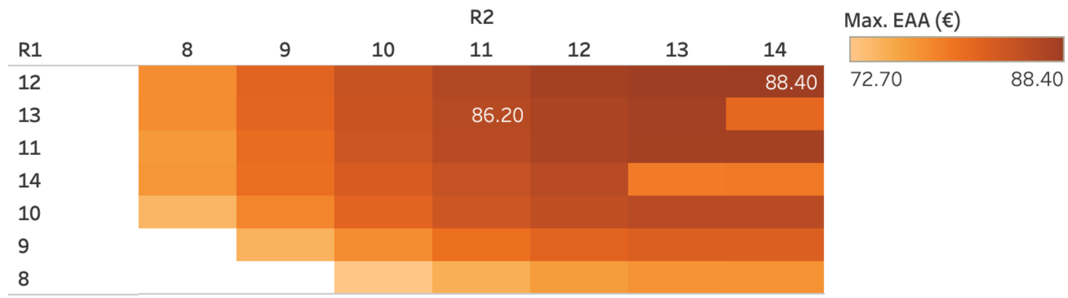

Figure 6.9 – Rotation 1 and 2 VS EAA for Mação med

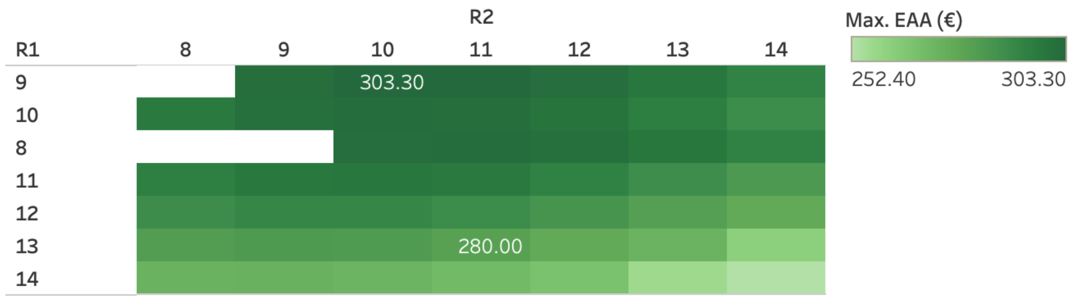

Figure 6.10 – Rotation 1 and 2 VS EAA for Mação 95

6.8.1.3 Number of Trees

Eucalyptus plantations have a maximum density of 1,400 trees per hectare. Considering this, the analysis used values from 1,000 and 1,400 trees per hectare, with increments of 10.

As shown in Figure 6.11, increasing the number of trees planted leads to a higher NPV in all site indexes. Therefore, planting 1,400 trees instead of the base 1,250 may lead to an increase €52 per hectare on lower site index lands. For mean and top site indexes the increase is €116 and €190, respectively. Both these numbers and the Figure 6.11 demonstrate that increasing tree density has a minor impact on the project's overall profitability.

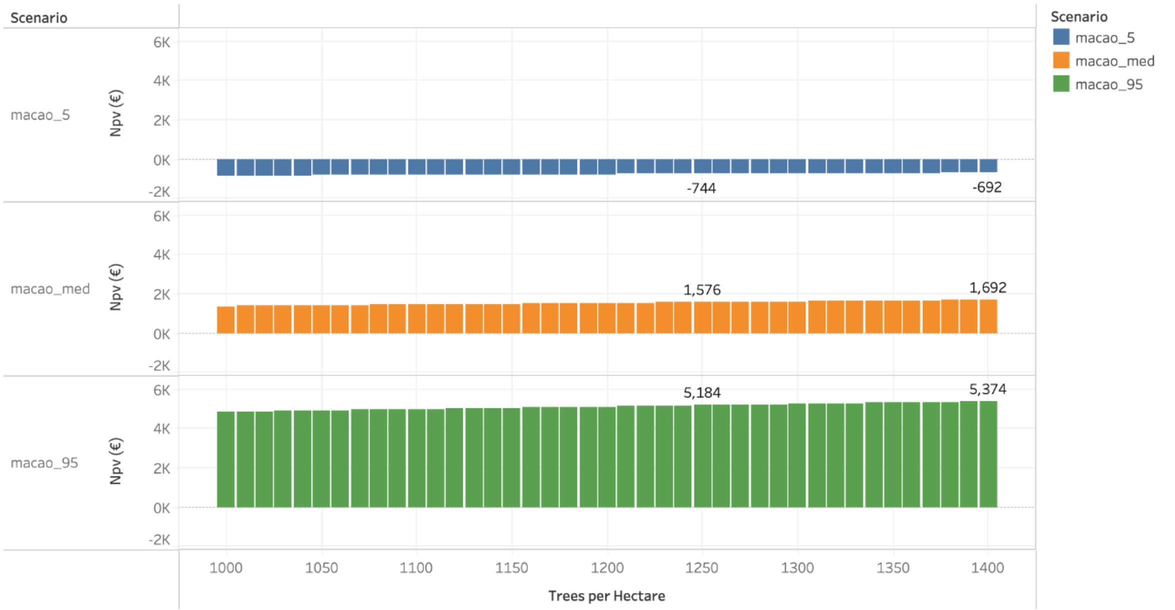

Figure 6.11 – NPV for different number of trees planted per hectare

6.8.1.4 Beat-Up Rate

Beat-up is the process of replacing dead trees after planting, and its value represents the percentage of planted trees that are expected to die during this process. The standard beat-up rate is 15%, though factors such as weather, diseases and soil conditions can influence it. The analysis was conducted by varying the beat-up rate between 5%, 10%, 15%, and 20%. With the current management schedule applied by Mação, Figure 6.12 shows that , the beat-up rate has a minimal impact on NPV. A table for a more numerical view is in the Appendix VI.3.

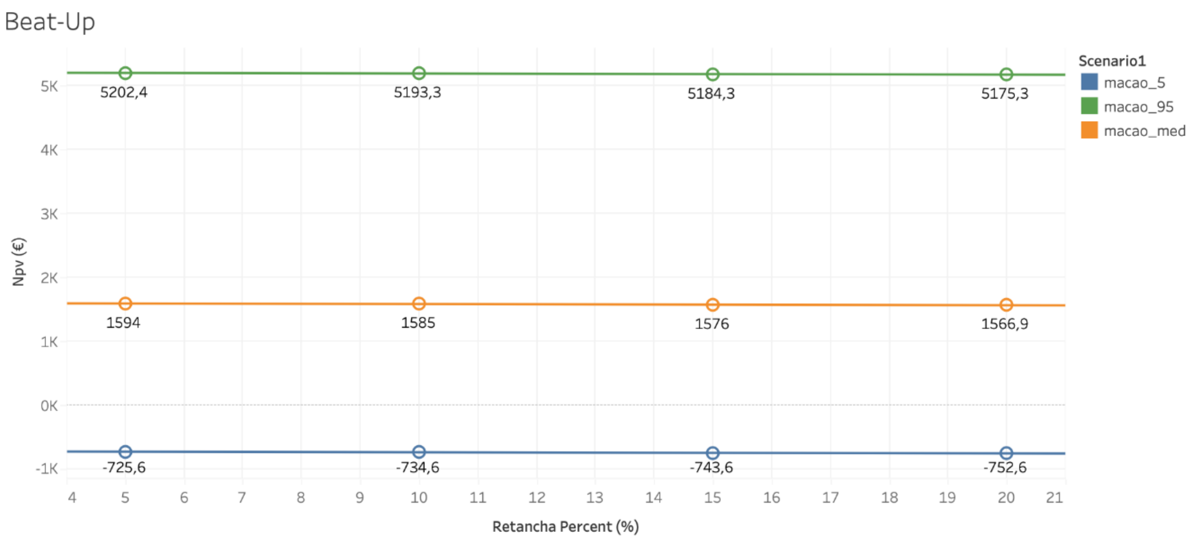

Figure 6.12 – Beat-up Rate VS NPV for all site indexes

6.8.1.5 Management Schedule – Shoot Selection

Upon meetings with Mação, it was easy to understand that they use the same management schedule for all lands. However, studying small changes in this schedule could be important to analyze the influence of some practices and their regularity in the NPV. As such, an analysis was done with shoot selection being performed between the first and fourth year of the second and third rotation. Figure 6.13 show that performing shoot selection 1 year after harvest is the most profitable strategy for all site indexes, contrasting with Mação's strategy of second year.

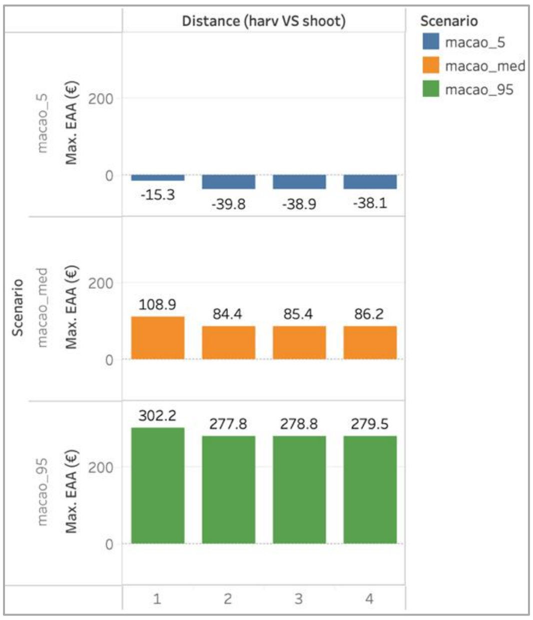

Figure 6.13 – Management Schedule VS EAA for all site indexes

6.8.2 Multivariate Analysis

To identify the optimal combination of inputs, a multivariate analysis was performed by simultaneously varying all parameters within the same range chosen in the univariate analysis. This analysis confirmed that, for all site indexes, the optimal strategy was to plant 1,400 trees per hectare, decrease beat-up rate to 5%, and perform shoot selection 1 year after harvest. Table 6.4 shows the rotation years that maximize profit in each site index, corresponding NPV values and percentage increases compared to the base scenario. Adopting the schedule that maximized NPV, Mação would increase its EAA in 94.22%, 13.2% and 14.8% for the low, average and top site indexes, respectively. However, this might not be the best strategy.

Scenario	Type	Trees per Hectare	Beat-up Percent (%)	Rotations	Shoot Selection	Final Cut Age	NPV (€)	EAA (€)	Difference EAA (%)
Maçao 5	Practiced	1250	15	13-11-11	2	35	-743.6	-39.8	-
Maçao 5	Max NPV	1400	5	13-13-14	1	40	-45.9	-2.3	94.22
Maçao Médio	Practiced	1250	15	13-11-11	2	35	1576.0	84.4	-
Maçao Médio	Max NPV	1400	5	11-12-13	1	36	1805.3	95.5	13.2
Maçao 95	Practiced	1250	15	13-11-11	2	35	5184.3	277.8	-
Maçao 95	Max NPV	1400	5	9-10-13	1	32	5702.2	319.0	14.8

Table 6.4 – NPV for base and recommended management schedule

6.9 Conclusion - Recommendations

Based on the sensitivity analysis conducted in Section 6.8, recommendations for optimizing the management schedule of Mação's eucalyptus plantations are presented below. As low site indexes yield negative NPV, only recommendations for mean and high will be conducted.

6.9.1 Beat-Up Rate

While reducing beat-up rates can improve profitability, associated costs such as improving seeding quality, soil preparation, planting techniques and weed control, will outweigh the minimal increase in NPV. Environmental factors such as weather, animal damage, and natural disasters further complicate efforts to reduce beat-up rates. Therefore, maintaining current practices, which result in a 15% beat-up is recommended as the most cost-efficient approach.

6.9.2 Tree Density

While planting 1,400 trees per hectare generates the highest NPV, the wildfire risk in Mação makes a lower density of 1,250 trees per hectare more attractive. This approach reduces biomass and flammable material, lowering the likelihood and impact of fires. Moreover, reduced density decreases competition for resources, enhancing individual tree growth.

6.9.3 Final Cut Age, Rotation Duration and Management Schedule – Shoot Selection

Due to Mação vulnerability to wildfires, cutting trees earlier is preferred to decrease this risk. Taking this into consideration, for *Mação med* and *Mação 95* the combinations with earlier final cut are presented in Figure 6.14 and 6.15. All scenarios have a tree density of 1,250, beat-up of 15% and perform shoot selection during the first year after each harvest, as it is the best.

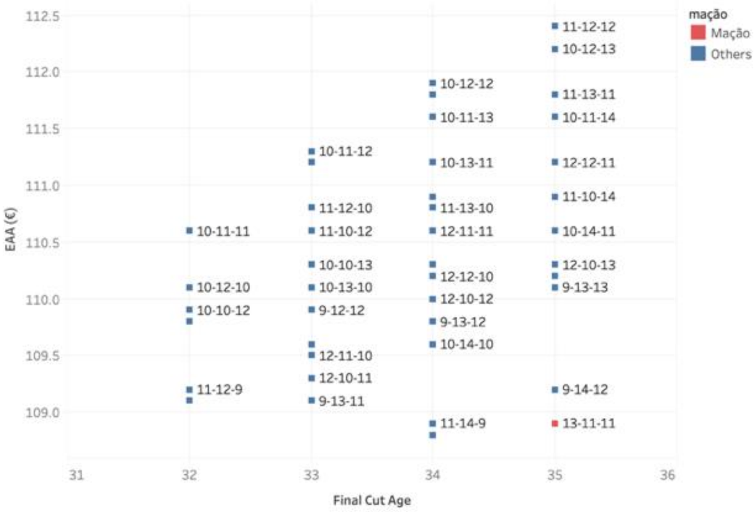

Figure 6.14 – Recommendations for Mação med

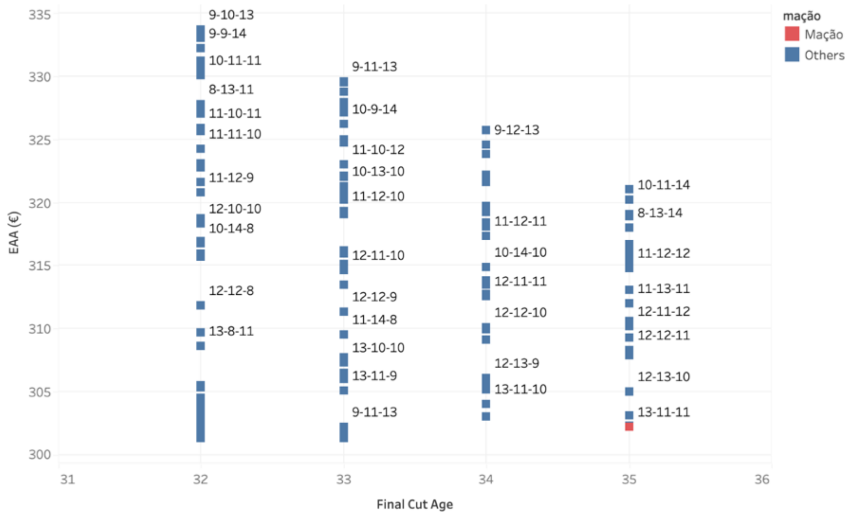

Figure 6.15 – Recommendations for Mação 95

6.9.4 Proposed Management Strategy

The recommended strategy for Mação's eucalyptus plantations based on the findings of this study, aims to maximize profitability while ensuring sustainable plantation management, is:

- Decreasing final cut age with one of the combinations presented in Figure 6.14 and 6.15.
- Plant 1,250 trees per hectare is the best trade-off between profitability and fire risk.
- Keep the same management schedule that translates into a beat-up rate of 15%.
- Perform shoot selection in the first year after each harvest.

6.10 Limitations

The API model presented little limitations, mostly related the unavailability of data.

The absence of site indexes for each AIGP prevented a more tailored forecast for each land parcel. Having access to such site-specific information would have enhanced the precision of the model's predictions and tailor the final output for each AIGP. However, the use of percentiles to estimate site conditions has provided a viable solution, enabling an approximated result. This mimics the outcomes that would have been obtained with the site-specific data.

Another constraint of the model arises from the treatment of some costs as fixed inputs. This assumption overlooks the reality that prices fluctuate over time and can vary across different locations, due to differing service providers, and different terrain characteristics. These factors could affect the accuracy of financial predictions and reduce the overall reliability of the model.

Moreover, the StandsSIM simulator assumes that scaling the simulation by hectares results in directly proportional financial and productivity outcomes. However, economies of scale may lead to unproportional relationships, which reduces the accuracy of the model's predictions.

Lastly, the StandsSIM simulator requires the eucalyptus management schedule to be consistent in the second and third rotations, meaning that the operations and years at which those were performed need to be the same. This proves to be a limitation as simulations with operations taking place in different ordinary years, within the second and third rotations, are not supported.

6.11 Future Work

The StandsSIM simulator is capable of handling complex scenarios, including irregular-aged stands. However, the API does not yet support these specific features. Enhancing the API to accommodate this scenario would fully leverage the simulator’s advanced capacities, providing more comprehensive results. Additionally, data regarding existing eucalyptus stands in Mação was not available in time to be integrated into the API. Addressing this is critical for LAND IT users to simulate both new and existing stands effectively. These updates would ensure that all available features in StandsSIM are integrated into the API to being used by LAND IT users.

7. The Case of Cork Oak

7.1 Cork Oak in Portugal

The cork oak is part of the native Portuguese forest (Biodiversity 2024). In the past, in many regions, the cork oak was overlooked in favor of other species to take the most advantage out of fertile lands (Quercus 2024). As a result, the area covered by the original forest was reduced (Quercus 2024). In the Natura 2000 Network Sectoral Plan the cork oak got recognized as a protected species (Biodiversity 2024) and is currently protected under the Portuguese legislation (Decreto-Lei n.º169/2001, de 25 de maio de 2001). According to the most recent “Inventário Florestal Nacional”, in 2015, approximately 23% of Portugal's forest area is made up of cork oaks (ICNF 2015). It covers 720,000 hectares, which represents about one third of the total world cork oak forest (Amorim Cork Composites 2024). The cork oak agroforestry systems, known as “montados”, are most present in Alentejo as represented in Appendix VII.1. Over 600,000 hectares of cork oak are located in this region (Biodiversity 2024).

An analysis of the latest “Inventário Florestal Nacional”, present in Table 7.1, indicates that both the area and the number of trees in pure stands has not changed significantly from 1995 to 2015. Although, in 2005, the number of trees decreased to 36 million trees. The area of dense pure stands decreased, while there was an increase in the area of stands with lower cover (ICNF 2015).

Total Area and Pure Stands by Tree Cover % Class

	Total Area (thousands of ha)	Pure Stands (trees in millions)	Pure Stands (trees per ha)	Sparse Forests (Pure Stands with 10% - 30% of cover) (thousands of ha)	Open Forests (Pure Stands with 30% - 50% of cover) (thousands of ha)	Dense Forests (Pure Stands with more than 50% of cover) (thousands of ha)
IFN4 - 1995	712.8	50.0	85	85.3	192.6	314.4
IFN5 - 2005	715.9	36.0	66	112.1	180.3	255.4
IFN6 - 2015	719.9	51.1	78	331.7	243.7	68.0

Table 7.1 - Development of the Cork Oak Stands according to the latests “Inventário Florestal” (ICNF)

In case the market for cork recedes, there is an increasing risk for everything it represents, since those forests are mainly viable because of their economy (Amorim Cork Composites 2024). The sustainability of the cork oak forests has been threatened worldwide, specifically with the occurrence of several wildfires in the last decades (AFINET 2019), with the same happening in Mação territory as discussed in Section 2.

Regarding the current presence of the cork oak in Mação, it is sparse, with only a few small areas identified in the POSA of the analyzed AIGPs. The analyzed areas show limited presence of cork oak forests and agroforestry systems where cork oaks coexist with other agricultural cultures. However, in Mação the cork oak is now lizastarting to be more valued and, according to POSP, for the future an increase in the number of cork oak forests and agroforestry systems is planned. This is visible in Table 7.2.

Location	Category	POSA (ha)	POSA (%)	POSP (ha)	POSP (%)
Amêndoa	Cork Oak AFS	0.03	0.001	108.77	5.14
Amêndoa	Cork Oak Forests	2.72	0.13	147.3	6.95
Carvoeiro	Cork Oak AFS	70.82	2.04	165.08	4.76
Carvoeiro	Cork Oak Forests	13.22	0.38	38.59	1.11
Castelo	Cork Oak AFS	-	-	104.47	4.9
Castelo	Cork Oak Forests	-	-	20.11	0.94
Ortiga	Cork Oak AFS	41.29	2.19	162.53	8.61
Ortiga	Cork Oak Forests	2.05	0.11	27.87	1.48

Table 7.2 - Actual and Planned Cork Oak Forests and Agroforestry Systems with Cork Oak in 4 AIGPs in Mação

7.2 Cork Oak Characteristics

The cork oak has a big lifespan that can vary from 300 to 500 years (ICNF 2012). However, its longevity decreases with the cork harvesting (Silva and David 2020), living on average around 200 years, when its production cycle finishes (APCOR 2024).

Cork oaks can reach 20 meters high; their canopy is broad and irregular, has solid and twisted branches and its thick trunk tends to branch at a low high (ICNF 2012). All year has green foliage and can adapt to different soil types (ICNF 2012). It also shows good resistance to summer drought but is more sensitive to frost (ICNF 2012).

The cork oak is a natural fire retardant, due to the slow combustion of the cork that has thermal and weak combustion properties (Amorim Cork Composites 2024). Cork is a natural raw material extracted from the tree in a manual process of harvesting. Cork also has the particularity of being reusable and once transformed, cork can re-enter the production process (APCOR 2024). It consists of suberin (45%), responsible for the elasticity of the cork, lignin (27%), that is an insulating compound, polysaccharides (12%), that help define the texture of the cork, tannins (6%), responsible for the color, and seroids (5%), that guarantee the impermeability of the cork (Amorim Cork Composites 2024).

7.3 Growing Cycle

The trees reach maturity for exploitation between 110 and 130 years, with the primary objective of cork production (ICNF 2012). Normally cork is harvested at the end of spring and during summer, since in windy or rainy conditions the cork does not come off the trees and can potentially cause harm to the tree (APCOR 2024). In the process of harvesting, it is not required to cut down the tree and so there is no harm to the tree's normal development, allowing new cork to regrow (APCOR 2024).

In the first harvest, "Desbóia", the cork is commonly known as virgin cork, which has a very irregular structure, making it difficult to work with (Silva and David 2020). Due to the legislation, there are strict rules regulating the harvesting and maintenance of the trees (APCOR 2024). A young tree can only be stripped when the trunk has reached a perimeter of 70 centimeters, measured at 1.3 meters from the ground (Decreto-Lei n.º169/2001). It is also not allowed to harvest the tree above a height equal to twice the perimeter of the trunk in the first harvesting, or no more than three times for a mature cork oak (Decreto-Lei n.º169/2001). The legislation does not allow cork to be removed from branches of the trees with less than 70 centimeters in perimeter as well (Decreto-Lei n.º169/2001).

After the first harvest, the following are carried out at intervals of at least 9 years (Amorim Cork Composites 2024), since it is forbidden to harvest the cork at intervals lower than 9 years (Decreto-Lei n.º169/2001). In the second extraction, called "Secundeira", it is produced a cork with a more regular softer structure, but still not with the highest quality (Silva and David 2020). Starting on the third harvesting, the cork starts having higher levels of quality and is known as "Amadia" or "Reproduction" Cork (Silva and David 2020). However, it is difficult to predict the quality, since it depends on several factors, such as the climate, soil and genetics (Paulo 2024). This results in a considerable difference in cork prices between cork oak trees (Paulo 2024). The cycle described, from the planting until each of the harvests, is described in Figure 7.1.

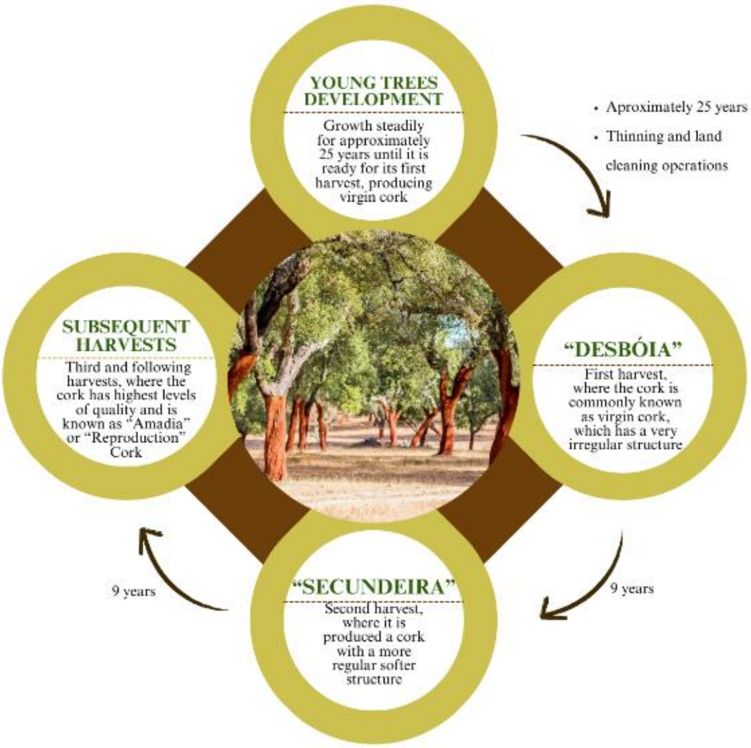

Figure 7.1 - Growing Cycle of the Cork Oak

7.4 Related Work and State of the Art

The existing literature on cork oak in Portugal highlights the importance of ensuring the productivity and sustainability of cork oak stands. The articles in review provide detailed analysis of specific factors influencing its growth and the optimal conditions for its development. The functioning of SUBER 5.0 model and the simulator were also analyzed in detail.

According to Paulo, Palma, et al. (2014), certain climatic variables are more associated with site index values, while some soil variables significantly influence soil water availability throughout the year. The developed models highlight water availability and the soil's capacity to retain it as critical factors for productivity. Among climatic variables, evaporation and frost showed the strongest correlation with site index values and, additionally, soil variables such as lithology, texture, depth, thickness of the A horizon (mineral layer at or below the surface, rich in organic matter (Owens and Rutledge 2005)), and soil classification were found to have a substantial impact on soil water availability. This study demonstrates that the existing cork oak stands are in optimal regions.

Sánchez-González, Tomé and Montero (2005) developed height and diameter growth models for dominant cork oak trees in Spain, defining a site index for these areas. These models increased the knowledge of the growth of this species and enabled improvements in the planning and management of cork oak stands. Diameter growth allowed the estimation of the minimum time required for a tree to reach 20 cm in diameter at breast height, approximately corresponding to 70 centimeters in perimeter, the point at which cork can be extracted for the first time. It made it possible to predict the time required for regeneration and cork production. It was also concluded that height is more reliable than diameter for measuring the site index, as it is less influenced by stand density or some forest management practices.

Some years later, Paulo, Tomé and Tomé (2011) developed a generalized height–diameter model that can be applied to cork oak trees both harvested and not harvested, with a diameter at breast height over cork larger than 2.5 cm in Portugal. The study focused on comparing two models: a nonlinear fixed effects model (NLFEM) and a nonlinear mixed effects model (NLMEM). The results showed that the NLMEM had higher precision and flexibility than the NLFEM, particularly for young trees. This makes the NLMEM more suitable for varying conditions and allows it to be used simultaneously for both young and mature trees, eliminating the need for separate models.

The inclusion of variables such as density and height significantly improved the precision of the predictions. The relationship between height and diameter demonstrated high variability among individual trees, reflecting the species' high genetic diversity and the influence of practices like pruning. The study concluded that both stand density and dominant height are important factors for accurately predicting tree height.

Estimations of the volume and biomass of cork oak trees were developed by Paulo and Tomé (2006). These equations are based on simple measurements of diameter at breast height and tree height, making them particularly valuable for use in forest inventories. This revealed to be important for cork oak, since it was a species with limited historical data available for such estimations.

Another methodology developed by Paulo and Tomé (2010), predicts mature cork biomass for cork oak trees at any age *t*, also based on measurements taken at a specific point in time. Its applications include sustainable management, economic analyzes, and carbon stock monitoring. The method also facilitates predictions outside the most common 9 year cork extraction interval.

Additionally, Almeida, Tomé and Tomé (2010) developed a model to predict individual tree cork caliber based on measurements taken at a specific point in time. This model can be used for forecasting cork caliber evolution and its impact on production, by allowing the maximization of high-quality cork production while reducing waste. Later, Paulo and Tomé

(2014) developed an equation system specifically with the purpose of estimating virgin cork production in young stands, with a particular focus on thinning and the first cork harvesting. This system helps forest managers and landowners in predicting virgin cork yields, enhancing planning and management practices.

To calculate the probability of a cork oak tree being thinned in a regular stand, Paulo and Tomé (2005) developed a distance independent logistic model. It was found that larger diameter trees are less likely to be thinned, while those closer to the stand's average diameter have a higher probability of remaining. Naturally, it was concluded that higher thinning intensities increase the likelihood of a tree being removed.

A model developed by Fonseca, et al. (2017) evaluates the maximum potential stocking level in cork oak stands. The developed self-thinning model suggests that traditional density guidelines are conservative and underestimate the potential of the species. Higher densities than currently recommended are viable, addressing potential growing cork demand and supporting sustainability.

The environmental impacts associated with cork production and extraction in Portuguese cork oak stands were assessed by González-García, Dias and Arroja (2013) using Life Cycle Assessment (LCA). Lower cork yields were found to worsen the environmental profile, as forest operations maintain the same intensity. Cleaning and pruning significantly increase impacts, while cork harvest itself has a low impact but is linked to mechanized activities like transportation and storage. It is recommended the adoption of management practices that reduce the frequency of maintenance operations in less productive areas and simultaneously improve the environmental sustainability of cork oak stands.

As seen previously, one of the integrated models in the sIMfLOR platform was the SUBER model, version 5.0 which was developed by Paulo (2011). This model aligned with the sIMfLOR platform can support decision-making processes by simulating forest management in the long term. This is explained in further detail in Section 4.2.

7.5 Methodology and Approach

The main objective was to create an economic model for cork oak to be incorporated into the LAND IT platform. The process started by reviewing the existing literature to identify the existing and most updated growth functions needed for reliable predictions.

When creating an economic model, it is important to follow the existing rules and regulations for cork oak harvesting, with those affecting the timing of the first and subsequent harvests. The cork oak's longevity is also an important factor to be considered in an economic analysis, as it allows for multiple cycles of cork production over its lifetime.

The initial idea was to build a model that could calculate cork production and financial outcomes for each tree individually and then to aggregate the results to represent the entire stand. However, the complexity of the existing growth and cork yield functions requires the use of specific data, such as measurements of tree diameter, height, or cork caliber. However, this data is not always accessible for every stand. The missing data represents a limitation for accurate modelling and consequently compromises the accuracy of the predictions. Additionally, the genetic variability of the cork oak creates significant differences in the different individual tree's growth and cork characteristics within a stand.

Given these limitations and the existence of SUBER 5.0 model integrated in the sIMfLOR platform, with proven equations, make them more effective for managing cork oak stands. As a result, the focus shifted to integrate these tools into the LAND IT platform through an API. For the specific context of the cork oak in Mação, as the cork oak stands are almost inexistent in the region and have no data available, the objective is to estimate the productivity of new stands. To achieve this, the approach for newly established stands available on the SUBER is used.

7.6 Integration and Application of the SUBER

With the literature presented in this previous section, a growth and economic model in Python and the details regarding this modulation can be found in the Appendix VII.2 Section. Due to the previously mentioned reasons, the approach changed so, in the present section, only the development of the API that will integrate SUBER into LAND IT will be explained.

7.6.1 Inputs

The inputs are defined from the already existing inputs in SUBER simulator and managed by the API. Through the API, users can input data in an organized way and support scenario evaluation and optimization of cork oak management practices. The selected inputs, explained in Table 7.3, were the ones identified as the most relevant and important factors to consider when planning a new cork oak stand.

Input	Explanation	Default Value
Production Cycle	Entire duration in years from the planting of the cork oak stand until the final cork harvest, covering all harvests throughout the stand's lifecycle	200 years
Area (ha)	Area. Important for determining production scale	1 hectare
Wood Price (€ / m³)	Price per cubic meter of wood, based on market tables	€59
Virgin Cork Price (€ / @)	Price per arroba (15 kg) of virgin cork, analyzed based on market trends	€12
Amadia Cork Price (€ / @)	Price per arroba (15 kg) of 'amadia' cork, analyzed based on market trends	€37
Trees Planted	Number of trees planted in the first year. Defines stand density	1 hectare
Tree Age at First Harvest	Starting point for the cork harvesting cycle	25 years
Harvest Interval	Years between each cork harvest	9 years
Operations in the First Year	Operations that occur during the the first year	Years and Costs in Appendix VII.3
Operations Across the Years	Operations that occur over the years	Years and Costs in Appendix VII.3
List of Years for Operations	Defines when operations occur. Exceptions include harvesting	Years and Costs in Appendix VII.3

Table 7.3 - Defined Inputs for the SUBER Integration in the API and their Default Values used on the Analysis

For the cork price an analysis was made, considering the price trends observed between 2008 and 2022 in the “Cork Market Bulletins” from UNAC and recorded in their annual “Cork Market Surveys”. Due to limited information on cork price ranges for different calibers and quality levels, the cork from the second harvest is grouped into the same price category as "amadia" cork.

In line with information provided by the municipality of Mação, the operations considered, its schedule, and the operation’s cost are currently implemented in Mação. Due to the low number of cork oaks trees compared to other forestry cultures presence in Mação, in some cases the costs were indeterminate, and the used costs were defined by “Comissão de Acompanhamento para as Operações Florestais” (CAOF). This is seen further in detail in Appendix VII.3.

7.6.2 Simulation Process

The simulation process starts with the integration of validated inputs through the API, with the API automating the configuration of these inputs. Then, the simulation follows a structured sequence.

During the simulation process cork production is a central aspect. At the start of each year, if cork harvesting occurs, it is considered the harvesting height to ensure maximum cork productivity. Then, considering for each year if the cork is harvested or not, cork production is evaluated, with the model calculating the total yield and revenues for each of those years.

At the end of each year, the model calculates the stand variables, both at the start and end of the projection year with the cycle being repeated for all projection years. The whole simulation process is explained in Section 4.3.2 in more detail.

7.6.3 Outputs

Once the simulation has been executed over the defined years, producing estimates of tree growth, cork yield, and economic returns, the model generates outputs, accessible through the API. The selected outputs are represented in Table 7.4.

Output	Explanation
Total Cash Inflows (€)	Represent the revenues. Directly influenced by inputs such as cork, cork harvest schedules, and production volumes
Total Cash Outflows (€)	Represent the expenses related to essential management practices
Net Present Value (NPV) (€)	Assesses the profitability of the cork oak stand over its lifecycle
Equivalent Annual Annuity (EAA) (€)	Calculated by taking the NPV of all future cash inflows and outflows and converting that total into an annual amount
Wood Volume (m³)	Natural growth considered in the model, representing the total wood volume produced
Virgin Cork (@)	Natural growth considered in the model, representing the virgin cork extracted
"Amadia" Cork (@)	Natural growth considered in the model. Represents the 'amadia' cork extracted. The cork in the second harvest is grouped into this category. Due to the high genetic varibiality is difficult to assess a specific cork quality per harvest

Table 7.4 - Defined Outputs for the SUBER Integration in the API

7.7 Results

This section analyzes how different combinations of inputs impact the results, with the goal of understanding how various factors can influence and improve profitability. The analysis of the results includes both univariate and multivariate approaches, to understand the individual and combined impact of the inputs in analysis.

7.7.1 Univariate Sensitivity Analysis

For the univariate sensitivity analysis, the following three inputs were analyzed individually: trees planted, harvest interval and tree age at first harvest. These represent key controllable inputs in cork oak management that significantly influence the results. Other inputs, such as cork price, are externally driven and not subject to direct management. The default values considered for the analysis were explained previously and are in Table 7.3. The analysis is conducted for a production cycle of 200 years to account for the natural variations that may occur over time in cork oak stands.

Regarding the operation related inputs, their impact on long-term dynamics is more limited compared to the chosen inputs for the analysis. Except for the cork harvesting, with a direct impact on revenues, the rest of the operations did not have a significant impact on the revenues. The operations are directly related to its costs, having a major impact on the expenses, although mostly restricted to the first years of the simulation. For this reason, in the analysis, it is not considered a variation for each operation.

Regarding the baseline values of each individual variable in the analysis, were used 100 trees planted, an approximated value of the national average; a tree age at first harvest of 25 years, an approximated age for the maturity required for its first cork extraction (age that can vary due to genetic variability among trees); and a harvest interval of 9 years, the minimum allowed by law and the most common. During the univariate analysis, these values were varied individually to assess their impact.

7.7.1.1 Trees Planted

As seen in Section 7.1, the average number of cork oaks per hectare is 78, with this being one of the values considered in this analysis. However, a range from 50 to 1,000 (with intervals of 50) was also defined to assess the potential of increasing the tree's density. In this analysis another goal was to assess the impact of the planting density on the evolution of tree numbers over the years and then on the revenue.

For the national average of 78 trees per hectare, the Net Present Value is negative throughout the years analyzed: -€511 for 200 years, -€1,017 at 100 years, and –€1,976 at 51 years. This indicates that the national average number of trees for a hectare never becomes profitable.

Analyzing Figure 7.2, for 700 trees per hectare, the Net Present Value is positive, reaching €10,148 at 100 years and €14,705 at 200 years. Between 100 and 200 years, the Net Present Value increases by approximately 45%, reflecting a significant improvement over this period. The similar happens for 750 trees per hectare, with the Net Present Value being also positive, and reaching €10,390 at 100 years and €14,777 at 200 years. For this density, between the 100 and the 200 years of the analysis, the Net Present Value has an increase by around 42%. These two values correspond to the planting densities that have the biggest Net Present Value.

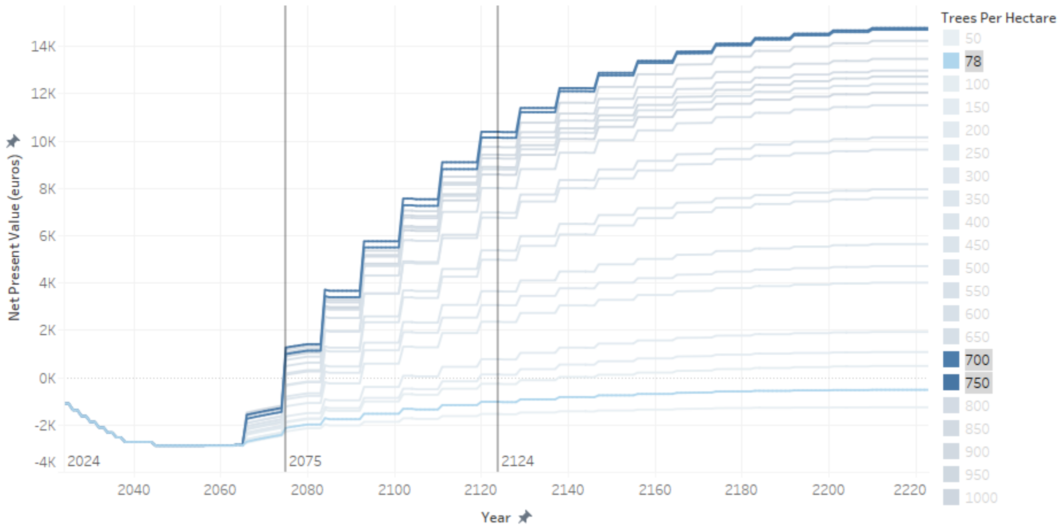

Figure 7.2 - Net Present Value Evolution Across 200 years for Different Planted Trees Densities

At 51 years (a year where a harvest operation occurs), the Net Present Value ranges between €915 (for 1,000 trees per hectare) and €1,277 (for 750 trees per hectare), with 700 trees per hectare registering €1,002. Between 51 and 100 years, the Net Present Value for 700 and 750 trees per hectare increases considerably. Comparing this to the values above, it is evident that the Net Present Value has a higher increase between the year 51 and year 100, than in later years. This corresponds to the period cork oak start reaching their maturity for exploitation, and also to a period where the density of operations is lower.

This is explained by the evolution of tree numbers within the stand, present in Figure 7.3. The decrease observed in year 2054 corresponds to a thinning year, during which the stand density is intentionally reduced. Thinning improves the growing conditions for the remaining trees by reducing competition, enhancing their productivity and longevity. The planting densities with more trees lived along the years are the ones that provide best growing condition for the trees, consequently the ones that have better conditions for the cork production and generate more revenues. That is precisely the case of the highlighted densities of 700 and 750.

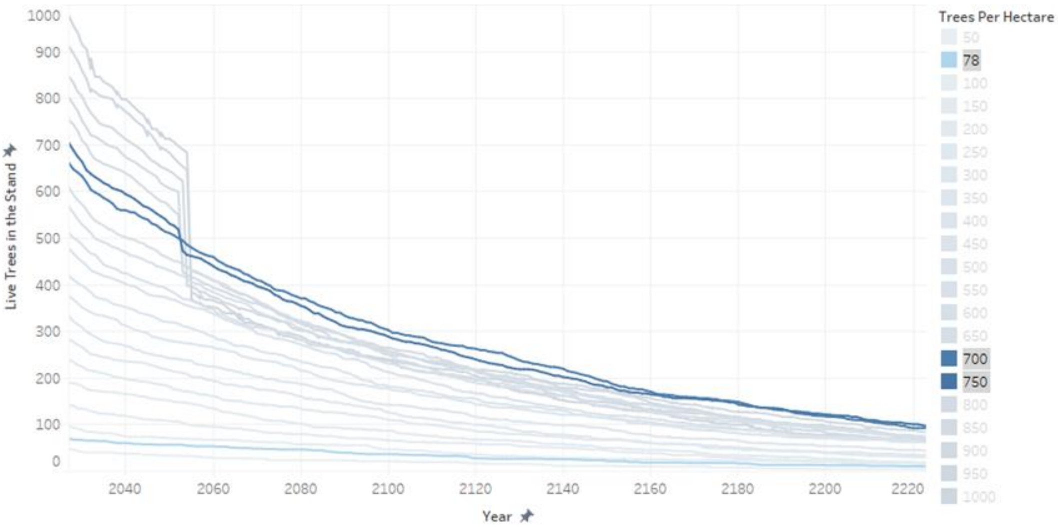

Figure 7.3 - Live Trees in the Stand Evolution Across 200 years for Different Planted Trees Densities

The Figure 7.4 also supports this idea. After 200 years, 93 trees (13.3% of the initial tree density of 700 per hectare) and 97 trees (12.93% of the initial tree density of 750 per hectare), remain alive from the initial planting. In contrast, for densities above 800 trees per hectare, the percentage of trees still alive falls below 10%. The higher initial densities, despite planting more trees, may not provide the necessary conditions for cork oak development. The results confirm that densities of 700 and 750 trees per hectare have the best balance, ensuring both survival and productivity of the stand over time.

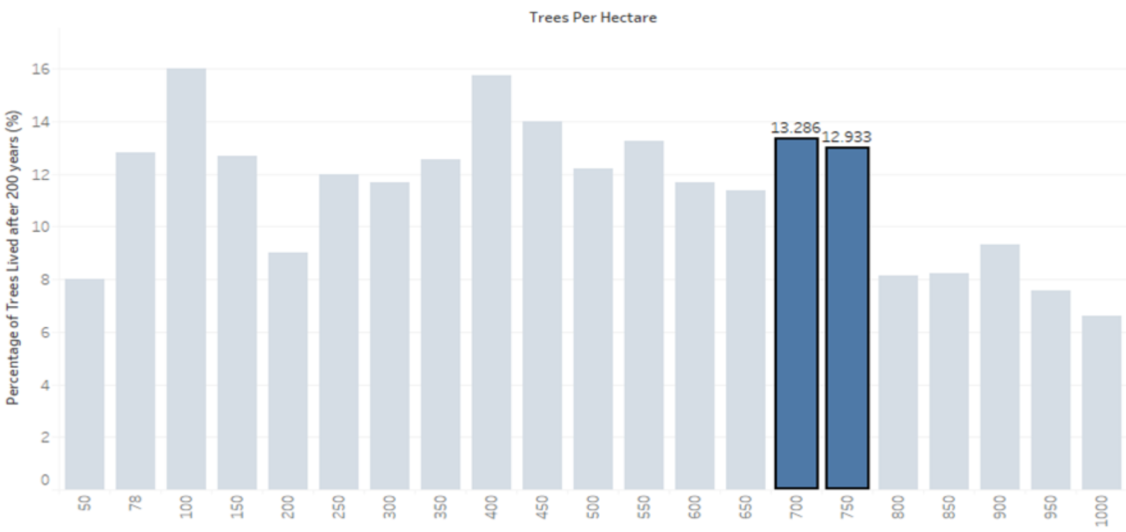

Figure 7.4 -Percentage of Tress Alive After 200 Years by Planted Trees Densities

7.7.1.2 Harvest interval

For the harvest interval a range of 9 to 20 years was defined. From the analysis to Figure 7.5 it is clear that shorter cork harvesting intervals result in a higher Net Present Value. Specifically, the 9-year interval is the highest with a Net Present Value of €497, calculated for the default scenario of 100 trees planted per hectare. This result demonstrates the economic advantage of shorter harvesting cycles, as more frequent cork extraction leads to higher cumulative revenue over time.

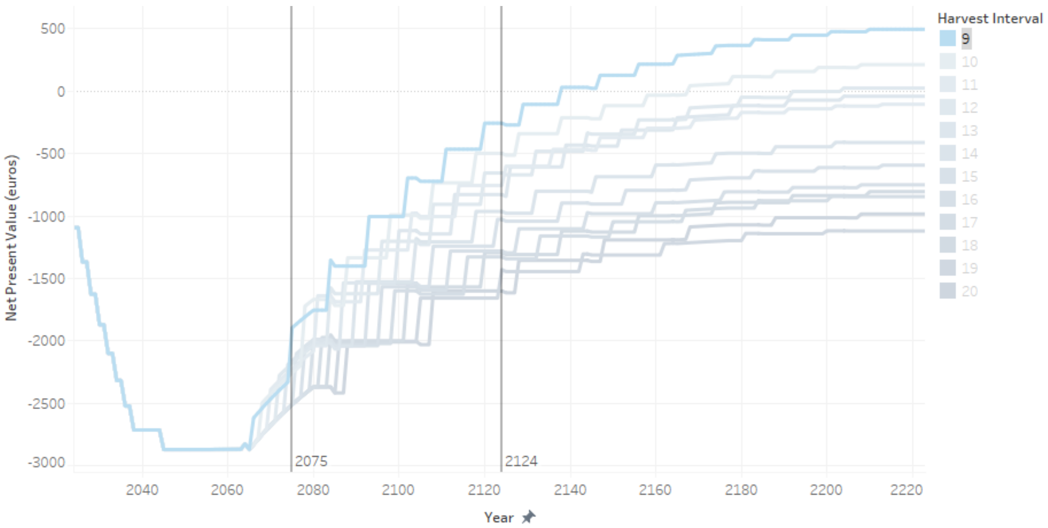

Figure 7.5 - Net Present Value Evolution Across 200 years for Different Harvest Intervals

This result is mainly justified by the amount of "amadia" cork extracted over the years, responsible for the greater part of the revenues. In shorter harvesting intervals, although the cork yield per extraction is smaller, the cumulative amount of cork extracted from the stand over 200 years is greater. For a 9-year interval, the total "amadia" cork extracted reaches 1,785 arrobas at 200 years. In comparison, the cumulative cork yield is significantly lower in earlier periods: 501 arrobas at 100 years and only 71 arrobas at 51 years. This information is represented on the tables on Appendix VII.3.

The difference becomes even more pronounced when comparing shorter and longer harvesting intervals. Over the same period, particularly when the Net Present Value is negative, fewer harvests occur in scenarios with longer intervals. For these scenarios, this results in reduced returns from cork extraction during initial periods of the stand's life cycle.

The 9-year harvesting interval proves to have more advantages both in the short term, by providing quicker returns, and in the long term, through higher cumulative cork yields. This trend is further confirmed in the figures for revenues, expenses, and profit presented on Appendix VII.3

7.7.1.3 Tree Age at First Harvest

The tree age at first harvest was also subject of analysis, with a range of 10 to 40 years to be considered. However as observed in the results, in Figure 7.6, there is no clear pattern relating this variable to the Net Present Value. However, it is important to highlight that when analyzing the amount of cork extracted over 200 years by tree age at first harvest class, a consistent pattern emerges. The results, visible in the Appendix VII.3, show that higher amounts of cork extracted per tree age at first harvest class aligns with intervals of 9 years, which corresponds to the default harvest interval used in the simulations. This suggests that the harvest interval and its timing have a greater impact on cork extraction dynamics than the tree age at first harvest itself as it was observed in the previous section.

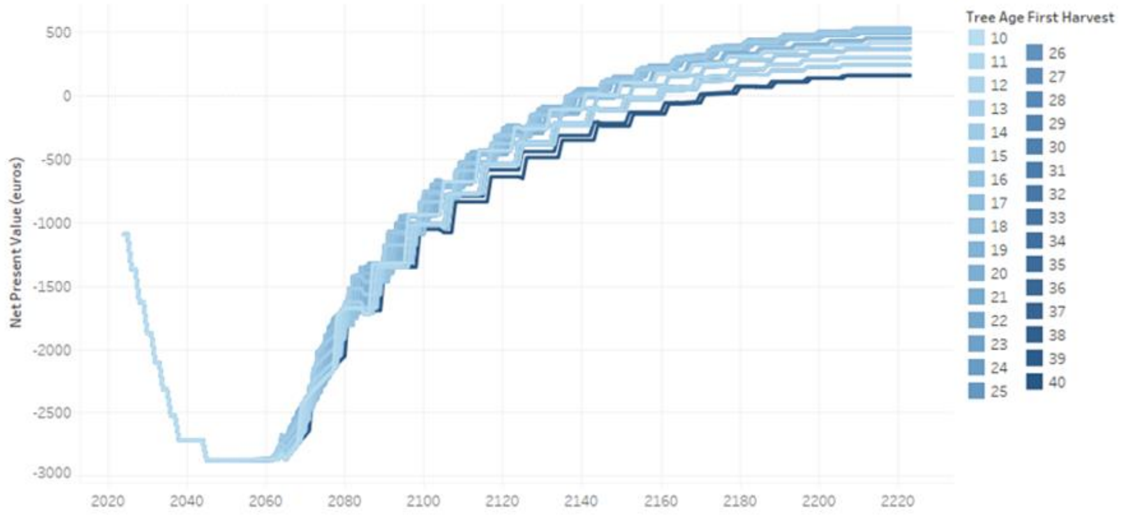

Figure 7.6 - Net Present Value Evolution Across 200 years for Different Planted Tree Age at First Harvest

7.7.2 Multivariate Sensitivity Analysis

This multivariate sensitivity analysis evaluates the combined impact variables in analysis, providing a better understanding of how the simultaneous changes of the variables influence the results. In the analysis of the best combinations of the variables for the total number of trees lived, the densities of 700 and 750 trees per hectare, independently of the tree age at first harvest, have more trees lived. A lower harvest interval is predominant. The best scenario has 117 live trees after 200 years. This scenario has 750 trees planted, the first harvest occurs at 22 or 33 years and has a harvest interval of 11 years.

The results show similar trends for the best combinations of the variables for the maximization of the cumulative “amadia” cork extracted. The highest cumulative “amadia” cork yields reach 10,313.044 arrobas. These scenarios also maintain a relatively high number of live trees (103). It is possible to conclude that a higher number of living trees does not necessarily mean more revenue. The number of living trees impact but it is also important to consider the extracted cork and that depends on the growing conditions of the stand. The tables presenting the best ten combinations for "amadia" cork extracted and the lived trees after 200 years can be found in Appendix VII.3.

Regarding the different variable combinations for maximizing Net Present Value and the analysis was made across time horizons of 50 (Table 7.5), 100 (Table 7.6) and 200 years (Table 7.7). The ten best combinations are in the Appendix VII.3.

NPV (50 Years)

Order	Trees Per Hectare	Tree Age at First Harvest	Harvest Interval	Net Present Value
1	900	32	9	791.55
2	900	23	9	791.55
5	750	23	9	705.36

NPV (100 Years)

Order	Trees Per Hectare	Tree Age at First Harvest	Harvest Interval	Net Present Value
1	700	35	9	10737.39
2	700	26	9	10737.39
3	700	17	9	10737.39

NPV (200 Years)

Order	Trees Per Hectare	Tree Age at First Harvest	Harvest Interval	Net Present Value
1	700	17	9	15112.09
2	700	35	9	15112.09
3	700	26	9	15112.09

Table 7.5 - Best 3 Combinations of Variables to Maximize NPV For 50 Years, Table 7.6 - Best 3 Combinations of Variables to Maximize NPV For 100 Years and Table 7.7 - Best 3 Combinations of Variables to Maximize NPV For 200 Years

For the 50-year horizon the best scenarios involve planting 900 trees per hectare, with a tree age at first harvest of 32 or 23 years, and a harvest interval of 9 years. These combinations have a Net Present Value of €791.55, reflecting the shorter time frame for returns.

For the 100-year horizon planting 700 trees per hectare becomes the best option, with a tree age at first harvest of 35, 26 or 17 years and a harvest interval of 9. These combinations have a Net Present Value significantly increasing to €10,737.39, demonstrating the advantage of considering an extended production cycle.

For the 200-year horizon, the results indicate that planting 700 trees per hectare, with a tree age at first harvest of 17, 35 or 26 years and a harvest interval of 9 years, maximizes profits. Once again, the best scenario has an increasing Net Present Value that reaches €15,112.09.

7.8 Conclusion - Recommendation

The results provide important insights into optimizing both the productivity and economic viability of cork oak stands. Firstly, it is evident that the current number of trees per hectare in Portugal does not reach its potential, presenting a clear opportunity to increase stand densities. The findings suggest that planting a density of 700 or 750 trees per hectare is an ideal target for maximizing cumulative "amadia" cork yield and, consequently, stand profitability. If the focus is on short-term profit, then this density can be increased even further. However, this would compromise the optimal growing conditions of the stand and would not maximize the profits in the long-term.

As analyzed, thinning is especially important in densely planted stands, as it helps ensure better long-term sustainability. While older trees at first harvest produce more cork, the tree age at first harvest has limited influence on stand structure and cork yields over the production cycle. It is recommended to find a balanced approach for this input. According to the literature, harvesting trees at a significantly younger age may compromise optimal growth, whereas delaying the first harvest too long can postpone revenue generation.

Regarding harvest intervals, shorter intervals allow for more frequent cork extraction, maximizing cumulative revenue. However, they also lead to higher operational costs. Despite this, shorter intervals consistently have higher Net Present Value making them more economically advantageous. Based on these findings, a harvest interval of 9 years, the minimum allowed under Portuguese legislation, is recommended to balance economic benefits and sustainability.

Considering everything, in cork oak stand management the results emphasize the importance of careful planning and balanced management to achieve both short term profitability and long-term viability in cork oak stand management.

7.9 Limitations

There are some limitations that should be considered when interpreting the results. One significant limitation is the limited data sources available for cork oak stands. As a result, the analysis may not represent possible tree age diversity and characteristics present in a single stand, due to the cork oak's genetic variability.

The analysis relies on growth models to project tree and stand development over time. While these models are valuable tools, they are inherently simulations and may not fully represent the complexity of the cork oak populations. Additionally, flaws in the economic outputs from SUBER were identified and had to be addressed manually.

The analysis is also based on historical price trends for cork and wood, assuming constant prices throughout the simulation period of 200 years. It does not account for potential future variations in market conditions, and for such a large period of simulation it is important to consider shifts in demand and production costs.

7.10 Future Work

The limitations highlight the importance of improving the data availability and consequently incorporate into the analysis to better reflect the complexities of cork oak management. Future integrations of existing cork oak stands should have accurate measurements of stand characteristics.

Future work should also focus on improving the API's flexibility, enabling it to handle more scenarios and stand characteristics for the specific case of the cork oak. This should include the introduction of variables that consider the genetic variability of cork oaks, allowing its comparison, since it represents a difference from this species compared to others. It would also be necessary to align this with the SUBER, since contrary to other forest management models, SUBER allows just the simulation of a single scenario simultaneously.

8. The Case of the Olive Tree

8.1 Olive Tree in Portugal and Mação

Portugal has become one of the most important regions for growing olive trees, due to its favorable climatic conditions. Thus, the olive tree has not only become a crucial element of Portuguese countryside, but also an economic pillar, mainly due to the olive oil's production, which is recognized for its high quality (Jordão 2014). As a result, Portugal is the fourth-largest olive oil producer in the EU, accounting for around 5% of total production (European Commission 2024), which reflects strong investment in modern olive growing systems and the strategic importance of olive tree in the national economy.

The olive tree is widely cultivated in Portugal, with the main producing regions in the Alentejo and Trás-os-Montes. Alentejo is a region that stands out for its high productivity, which is the result of the introduction of more modern olive groves, potted and hedge, explained later. This region, which covers around 50% of the country's olive area, is responsible for approximately 80% of national olive oil production, benefiting from the Alqueva irrigation perimeter, which has led to exponential growth in olive oil production since the early 2000s (BPI Research 2023).

Other regions such as Trás-os-Montes, Beira Interior, where the district of Mação is located, and Ribatejo maintain more traditional practices, with a focus on preserving quality and local varieties. Figure 8.1, clearly shows that different olive grove management techniques, but also different soil and climatic conditions result in significant variations in productivity, as an example, while Alentejo has an average production of 4833kg/ha, regions such as Between Douro and Minho have considerably lower values, such as 1379kg/ha, which represents almost four times less production than Alentejo (INE 2023).

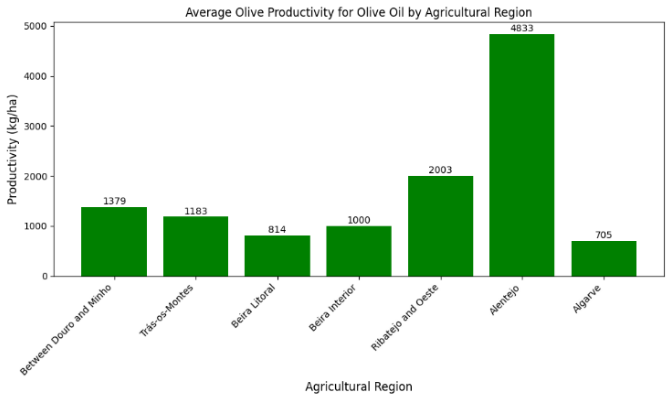

Figure 8.1 - Average production by agricultural region. (INE 2023)

High national production reinforces the critical role of the olive oil sector in the Portuguese economy. Since 2011, Portugal has been a net exporter of olive oil, and in 2023 exports reached around €1.06 billion, while imports totalized €505.74 million (Comtrade Plus 2024). This positive trade balance, which exceeded €552 million, highlights the competitiveness of Portuguese olive oil on the global market. Analyzing Figure 8.2, we can observe that olive oil exports significantly outstrip imports, with a considerable difference between the lines. This performance is sustained not only by the increase in production, but also by investment in modern technology in the plant, ensuring that Portuguese olive oil has high quality and is highly competitive (BPI Research 2023).

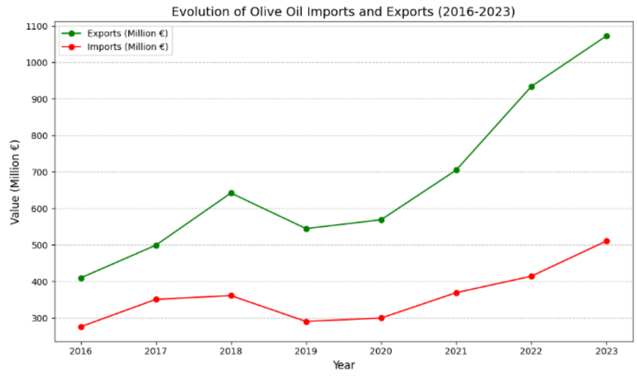

Figure 8.2 - Olive oil imports and exports in Portugal (Comtrade Plus 2024)

To obtain a more detailed understanding of the distribution and impact of olive cultivation in Portugal, it is essential to look at specific areas where the activity is extremely important. In this sense, the Mação region stands out not only for its vast expanse of land dedicated to olive cultivation, but also for being a clear example of the importance of the crop, with approximately 50% of the cultivated agricultural area.

The olive tree is predominantly present compared to other crops such as vineyards, strawberry trees and lemon trees (Matias 2023). By analyzing Figure 8.3, we can observe that in the four AIGP's under study, Carvoeiro, Castelo, Ortiga, and Amêndoa, the olive tree stands out in relation to the other crops. This improves the understanding of the olive tree's economic contribution to local agriculture, but also its central role in the region's rural identity.

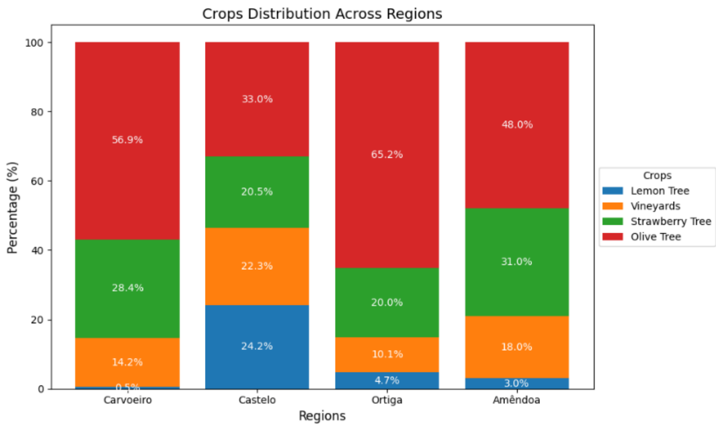

Figure 8.3 - Distribution of agricultural crops in four AIGPs in Mação (Municipality of Mação)

After emphasizing the economic importance of the culture in the region, it is also important to consider its ecological value, since the culture also makes a significant contribution to environmental sustainability. The valorization of biomass, using waste such as branches and leaves from pruning, enables the production of renewable energy and other valuable products, reducing environmental contamination and minimizing CO2 emissions. Separately, Traditional rainfed olive groves, which dominate in Mação, represent the most resource-efficient cultivation system, requiring minimal external inputs, which makes them inherently more sustainable, supporting local biodiversity and improving the resilience of rural ecosystems. Together, these practices underscore the olive tree's pivotal role in promoting sustainability in regional agriculture (Sales et al. 2022).

8.2 Olive Growing Systems

The olive tree's life cycle is influenced by environmental factors, such as temperature and the availability of water, which determine yields and the overall sustainability of olive growing. The impact of these factors varies according to the cultivation system used, which rises to three completely different olive groves: traditional, potted and hedge, which are going to be analyzed ahead.

8.2.1 Traditional Olive Grove

The traditional olive grove is characterized by low density, between 80 and 100 trees per hectare. In this growing system, the trees are planted with wide space, which allows the development of extensive canopies and deep roots. The trees start producing between 5 and 7 years, reaching 100% productivity around 10 and 12 years, and can live and produce for quite a long time, up to 100 years, with consistent production cycles of up to 25 years (AGRO.GES 2021).

According to Mação's Municipality, this system is the most widely used in the region, where tradition and environmental sustainability are priority factors. This growing system has the advantage of preserving the soil structure, maintaining biodiversity and using fewer external resources, which make it ideal for areas that value sustainable practices. However, productivity is lower compared to other modern types of olive groves, and climatic variations usually have a significant impact, since the system depends solely on seasonal rainfall (Oliveira 2022).

8.2.2 Potted Olive Grove

Potted Olive Grove has a higher density than traditional groves, between 200 and 500 trees per hectare. In terms of the planting method, the trees are spaced less widely apart and are irrigated in order to optimize growth and production. In this way, the olive tree starts producing earlier, between 3 and 4 years old, reaching its peak productivity at 8 years, with lifespan of 25 years

(AGRO.GES 2021). The fact that this growing system is irrigated allows more efficient growth management and significantly higher productivity.

This system is mostly used in regions such as Alentejo, where Alqueva irrigation project has helped to maximize the potential of plantings (Ferreira 2020). In Mação's case, the transition from traditional to potted olive grove is considered to increase productivity and consequently economic income, although investment in irrigation system is one of the challenges that need to be considered (Pereira 2014).

8.2.3 Hedge Olive Grove

The Hedge olive grove is the most up-to-date and has a density between 1600 and 2000 trees per hectare. In this olive grove, trees start producing around 3 years old and reach maximum production at 5 years, earlier than in the two previous olive groves, although their lifespan is the shortest, between 12 and 15 years (AGRO.GES 2021).

The main advantage of this system is its high productivity and efficient harvesting, which is completely mechanized, reducing labor costs. Although it is the type of olive grove with the highest production values, it requires investments in technology and demanding resource management, as well as having a significant environmental impact, especially in terms of water consumption and soil composition (Silva 2022).

In order to make easier to compare the three types of olive groves, Figure 8.4 shows the main differences between the characteristics of each olive grove, the planting density, the age at which production starts, the age at which maximum production is reached and the longevity of the tree, as well as the irrigation method and the main olive tree varieties that are most suitable.

Characteristic	Traditional Olive Grove	Potted Olive Grove	Hedge Olive Grove
Plantation Density	80-100 trees/ha	200-500 trees/ha	1600-2000 trees/ha
Age of Start of Production	5-7 years	2-3 years	3 years
Age of Maximum Production	10-12 years	8 years	5 years
Tree Longevity	>100 years	Around 25 years	12-15 years
Irrigation Method	Rainfed	Irrigation	Irrigation
Main Varieties	Galega, Cobrançosa, Cordovil, Verdeal	Arbequina, Cobrançosa, Picual	Arbequina, Arbosana

Figure 8.4 - Characteristics of the three types of olive groves (AGRO.GES 2021).

For each olive grove, the best main varieties chosen are most adapted to the conditions and characteristics of each growing system. In traditional olive grove, "Galega", "Cobrançosa", "Cordovil" and "Verdeal" are the most used due to their resilience to drought conditions and low water requirements. For potted and hedge olive groves, varieties such as "Arbequina", "Picual" and "Arbosana" are the most suitable, as they have a positive response to the irrigation method, which results in mechanized harvesting and more efficient production, but also a significant reduction in labor costs.

8.3 Related Work and State of the Art

During the research, several models were analyzed to estimate olive grove production, to use them later in the simulation; however, each model has limitations that could make its practical application unfeasible.

8.3.1 Linear Regression Model based on Root System

The Root-based Linear Regression Model is based on the characteristics of olive tree's root system to predict yield, using three variables: Root Weight Density, that represents the tree's ability to absorb water and nutrients; Root Length, that correlates with the surface area for nutrient absorption; and Root Biomass, that indicates the overall health and vigor of the tree. This model is useful for management practices that seek to improve root growth; however, it assumes a constant linear relationship between root growth and yield, which may not be verified in different soil types and climatic conditions. In addition, measuring root characteristics on a large scale can be laborious and costly (López-Bernal et al. 2018).

8.3.2 Yield Estimation using Weight and Number of Fruits

The Yield Estimation Model using weight and the number of fruits consists in a simple formula that multiplies the number of fruits per tree by the average weight of each fruit. In this way, the model provides a direct and practical estimate of production, especially useful in smaller groves or in experimental studies. Despite this, the model assumes uniformity in the fruit of all trees and disregards variations caused by age, management practices and environmental factors, which once again limits its application (Fernández et al. 2021).

8.3.3 Trunk Cross-Sectional Area (TCSA) Model

In this model, production is estimated based on the cross-sectional area of the trunk, considering that a larger trunk generally indicates a more resilient and productive tree. This method is useful in orchards where tree size reflects potential production, but it does not consider factors such as pruning and irrigation that can influence productivity, nor differences in age or even specific characteristics of each variety (Martin-Verdedor et al. 2020).

8.3.4 Tree crown area method (TCA)

This method, as the name suggests, uses the area of the tree's crown as an indicator of production, assuming that a larger crown increases the tree's photosynthetic capacity. TCA is particularly advantageous in potted or hedge olive groves, where the size of the canopy is more uniform and controlled. However, it assumes that whenever the canopy is larger, production is also higher, disregarding effects such as excessive pruning and shading. Furthermore, measuring the crown is very challenging in irregular trees (Oliva et al. 2022).

Each model examined had limitations that restricted its applicability for accurate and practical olive grove production forecasts. As a result, detailed and specific information on the olive crop was gathered, and a customized simulation was developed to meet the specific needs and conditions of the olive grove, intended for later integration into the LAND IT platform.

8.4 Methodology

The extraction of the data needed to build the model and the simulation of olive grove production was carried out using a structured methodology that was articulated in different stages. The main objective was to ensure that the information collected was specific, taking into account the variation in maintenance costs and productivity.

The first step involved identifying credible sources of information. To this end, contact was made with the company Fitolivos, recognized for its expertise in foliar nutrients and bio protection of agricultural crops, including olive trees.

With the help of Fitolivos, it was possible to establish contact with a professional with consolidated experience in olive cultivation. This expert contributed to a detailed analysis of the model's needs, emphasizing the importance of adjusting cost and production data based on variables such as the age of the trees and the cultivation system used (traditional, potted or hedge). The exchange of knowledge at this stage was crucial for identifying errors in the data and directing the next stages of the research.

Based on the guidance provided, it was decided to carry out further research with agricultural consultancies, Consulai and AGRO.GES, both recognized for their consultancy experience in the agricultural, food and rural sectors. Both consultancies were contacted to collaborate in providing data and after a detailed presentation of the study's needs, a response was obtained from AGRO.GES.

After analyzing the requests, the consultant provided detailed information on annual maintenance costs, productivity and other essential parameters. Finally, the data was analyzed, taking into account the specific challenges of growing olive trees in different systems and stages of development. The methodology adopted ensured the integration of practical and theoretical information from experts and a renowned agricultural consultant, resulting in a model adjusted to the real conditions of the olive sector.

8.5 Developed Model

The goal of the developed model was to create a practical tool for assessing the economic viability of different cultivation systems. The model is based on carefully collected inputs, combines information with olive tree's lifecycle and presents clear and intuitive outputs that allow an objective assessment of the results.

8.5.1 Inputs

The model's inputs have been organized into three main categories, as can be observed in Annex VIII.1: (1) those provided by AGRO.GES, (2) those defined by the user, and (3) those obtained via the European Commission's API, making it possible to personalize the simulation calculations according to real information and user-adjustable criteria.

The inputs provided by Category (1) focuses on olive groves in Portugal, highlighting modernization and sustainability in Alentejo's region, especially the Alqueva irrigation area. These inputs from AGRO.GES include three essential elements for the simulation purposes: annual maintenance costs, installation costs, and the annual yield production.

Annual maintenance costs (€/ha) cover detailed operational expenses such as pruning, fertilization, irrigation, herbicide use and vegetation management, and harvest and transport of olives, varying according to the type of cultivation system. Figure 8.5 shows how these expenses are distributed. In the traditional system, the highest costs are related to harvest and transport of olives, while in the potted and hedge systems, the most significant costs are concentrated in fertilization, irrigation and phytosanitary treatments.

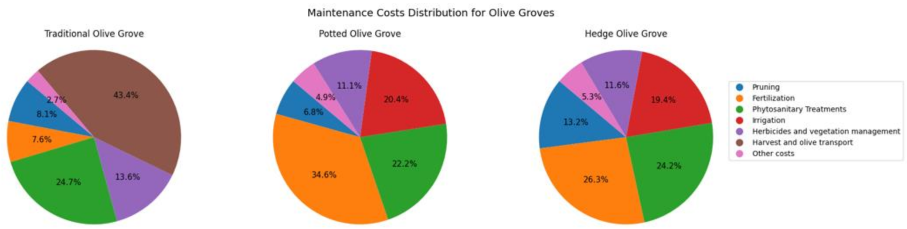

Figure 8.5 - Distribution of Maintenance costs for the three cultivation system's types (AGRO.GES 2021).

On the other hand, olive grove's installation costs (€/ha) include land preparation, planting, trellising and the irrigation system, reflecting the initial investments needed to implement two cultivation systems, potted and hedge. Unlike these modern systems, traditional growing systems generally don't have significant installation costs as they rely on existing trees and traditional farming practices, that's why it's not shown in the representation below. In this way, Figure 8.6 highlights the differences between potted and hedge groves, showing that the costs of the hedge olive grove are higher, due to its higher density and complex structure, compared to the potted olive grove.

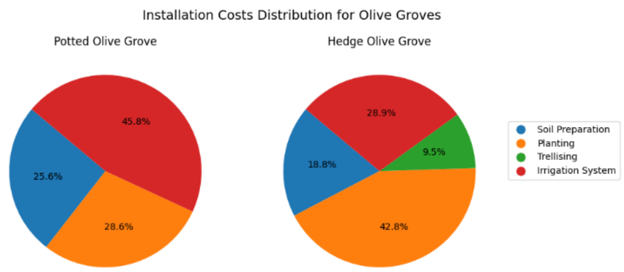

Figure 8.6 - Installation costs' distribution for potted and hedge olive groves (AGRO.GES 2021).

Lastly, the Annual yield (kg/ha) mainly varies with the type and age of olive grove. Figure 8.7 highlights the yield differences between the three systems: traditional system exhibit a slower productivity, only starting production in year 5 with steady yield of 2,000kg/ha thereafter; potted system begin production earlier in year 4 with 2,500 kg/ha, quickly increasing to 9,000 kg/ha by year 8 and maintaining this peak; and hedge system show the fastest growth, achieving significant yields as early as year 3 with 5,400 kg/ha, reaching 12,000kg/ha by year 5, and sustaining this high productivity through year 10.

Annual Yield (Kg/ha/year)

Type of Olive Grove	Year 1	Year 2	Year 3	Year 4	Year 5	Year 6	Year 7	Year 8	Year 9	Year 10
Traditional	0	0	0	0	2000	2000	2000	2000	2000	2000
Potted	0	0	0	2500	4250	6900	8000	9000	9000	9000
Hedge	0	0	5400	9000	12000	12000	12000	12000	12000	12000

Figure 8.7 - Annual Yield Production by Year (Kg/ha) (AGRO.GES 2021).

Additionally, the simulation can be tailored to specific needs through Category (2), which include five key variables: the cultivation system (traditional, potted, or hedge), the age of the olive grove, the simulation duration in years, the cultivated area, and the selling price of table olives. Adjusting the cultivation system and the cultivated area ensures the data reflects the unique characteristics of each olive grove. Additionally, factoring in the age of the olive grove aligns costs and yields with the various stages of the crop's lifecycle, improving the simulation's accuracy and relevance.

According to the European Commission table olive's price shows a general increase, between 2020 and 2023, in the main European and productive countries, which can be observed in Figure 8.8. Italy consistently leads with the highest prices, Greece shows some fluctuations, with a peak in 2021, followed by a decline in 2022 and a sharp recovery in 2023, Portugal, on the other hand, has maintained moderate growth, with relatively low prices.

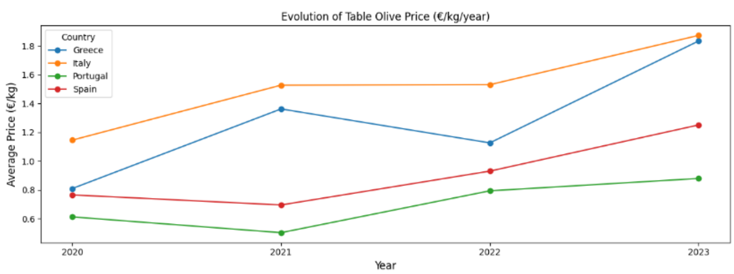

Figure 8.8 - Evolution of table olives' price (European Commission)

Lastly, data obtained through Category (3) that provides up-to-date information on the average price of olive oil (€/kg), a variable automatically adjusted in the simulation based on periodic reports from the European Commission, allowing a precise analysis of the olive oil price, ensuring the simulation keeps pace with market fluctuations. Figure 8.9 shows the olive oil's evolution between 2010 and 2024, with Croatia standing out with a sharp increase, especially from 2022 onwards. The other countries, such as Greece, Italy, Spain and Portugal had more gradual increases. In Portugal, the price raised the most in 2021, reaching around €6/kg in 2024.

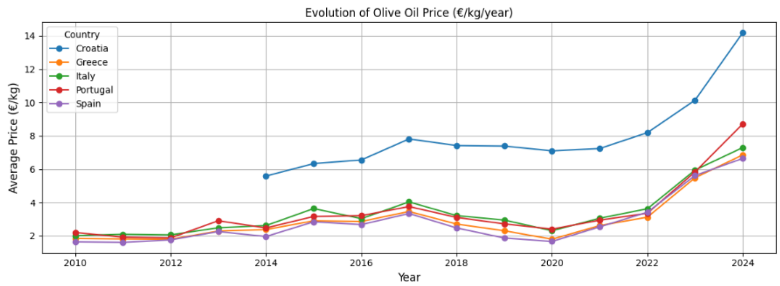

Figure 8.9 - Evolution of olive oil price by year (European Commission)

Despite the successive increase in prices, recent sources, such as El País, expect a significant increase in olive and olive oil production in Spain, which is expected to grow by around 50% (El País 2024). This increase in supply could put downward pressure on olive and olive oil prices, resulting in a stabilization or reduction of prices in Europe, which is extremely important for future forecasts.

8.5.2 Simulation

The simulation model evaluates the economic performance of olive groves by accounting for installation costs, annual maintenance costs, and productivity, tailored to the specific type of cultivation system, and olive grove's age, as seen in Annex VIII.2. Installation costs are applied exclusively in the first year, reflecting the initial investment required for establishment, such as planting and system setup. These are combined with maintenance costs for the first year to capture the total initial financial effort.

On the other hand, maintenance costs are incurred annually and vary according to the cultivation system, the area cultivated, and the grove's lifecycle stage. The simulation recognizes three main stages: (1) Establishment Period, during which trees are maturing, there is no productivity, and maintenance costs are relatively high to support growth; (2) Peak Productivity, when the grove reaches maximum production potential with regular maintenance costs; and (3) Decline or End-of-Life, when productivity drops and maintenance costs are minimized.

The model dynamically adjusts costs and yield based on the grove's age and type, using specific functions for each cultivation system to reflect their unique characteristics. For example, traditional groves have a longer establishment phase and steady productivity, while hedge systems reach peak production faster but have a shorter productive lifespan.

8.5.3 Outputs

The simulation model focuses on key financial outputs that provide valuable insights for producers and investors, which ensures a comprehensive understanding of olive grove economic viability. These outputs include: (1) Annual Operating costs that encompasses maintenance costs incurred each year, as well as installation costs during the first year; (2) Annual Revenue calculated based on the income from table olives (80% of production) and olive oil (20% of production), using average market prices given by the user and the European commission respectively; and (3) Financial Metrics, like cumulative profit, that enable a holistic assessment of grove's financial performance throughout its lifecycle, in order to capture the relation between investment, operational costs, and revenue generation. The production percentages (80% table olives and 20% olive oil) were determined by the Municipality of Mação and reviewed by a professional from Fitolivos. To facilitate practical observation, Annex VIII.3 clearly represents the selected outputs.

8.6 Sensitivity Analysis

A sensitivity analysis is a critical step to evaluate the robustness of the developed model for olive cultivation, because it allows for a comprehensive understanding of how variations in key input variables influence the overall outcomes, such as operational costs, revenue and profitability. The analysis spans a 25-year timeframe, which corresponds to the productive lifespan of traditional and potted olive groves, ensuring a consistent comparison even as the hedge olive grove concludes its shorter productive cycle at 15 years. By focusing on parameters directly influenced by user decisions, such as the type of olive grove, the cultivated area, and the average olive price; the sensitivity analysis assesses their individual impact on the model's performance, which ensures that the simulation remains both realistic and adaptable to varying conditions, providing insights for strategic decision-making.

8.6.1 Univariate Analysis

The univariate analysis focuses on three main variables, type of olive grove, cultivated area, and table olive's price because they are primary drivers of model's outcomes' variation. Each of these variables plays a different role: the olive grove type determines directly the correspondents' operational costs and productivity values; the cultivated area scale these costs and influences economies of scale, and the average olive price defines the potential revenue. Together, these parameters capture the most critical interactions between user-defined choices and the economic viability.

8.6.1.1 Type of Olive Grove

The traditional olive grove stands out for its low operational costs driven by minimal reliance on external inputs, like irrigation or fertilization. Figure 8.10 shows the costs remain stable and relatively low throughout the 25-year period, which makes this system a highly sustainable for long-term investments, however the start of production year is delayed compared to the other systems, requiring patience before seeing significant returns.

The potted olive grove represents a middle ground between the traditional and hedge systems, because its moderate installation and maintenance costs reflect the higher input requirements compared to the traditional, such as irrigation and pruning. While these costs stabilize after the first years, they remain consistently higher than those of the traditional grove. The potted olive grove benefits from earlier production compared to traditional grove, which makes it attractive for medium-term economic goals.

The hedge olive grove has the highest installation costs, due to its high-density planting and reliance on mechanized systems, however the operational costs stabilize at a level higher than both the traditional and potted systems, as can be observed in Figure 8.11. The hedge grove's key advantage lies in its accelerated production cycles and efficiency, despite its productive lifespan ends after 15 years, which limits its long-term economic viability.

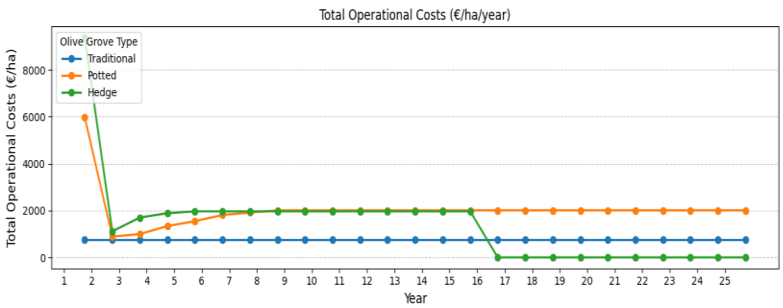

Figure 8.11 - Evolution of Annual operational costs through 25-year period for 50 hectares

The analysis of the operational costs reveals clear trade-offs among the three olive grove systems; the traditional grove is the most cost-efficient, with low operational costs and long-term sustainability, however its delayed production might discourage those that aim for faster returns. On the other hand, hedge grove is the most expensive due to high initial investments and mechanization, delivers high production quicker but is limited by its 15 -year productive lifespan. Lastly, the potted grove balances the two systems before, offering earlier returns than traditional system with moderate costs, which makes it a versatile option.

8.6.1.2 Hectares

The operational costs of the three olive grove systems were analyzed across three different cultivated areas (15ha, 50ha and 100ha). This analysis provides insights into how costs scale with the size of the operation, which can be analyzed in Figure 8.12.

For traditional olive groves, operational costs are stable across all areas of cultivation, with slight decrease in costs per hectare as the cultivated area increases, which reflects the minimal dependency on installation cost and technological advanced techniques, despite its high dependence on labor costs.

In the potted grove system, operational costs are higher than in traditional groves but follow a similar stability over time. Figure 8.12 shows that the costs per hectare slightly decrease with increasing area showcasing the benefits of economies of scale.

The hedge system demonstrates the most substantial scaling effects; despite the initial investment is the highest across all cultivated areas, the per-hectare operational costs decrease with larger areas, also represented in Figure 8.12. This reflects the high level of mechanization, which becomes more cost-effective, despite the shorter productive.

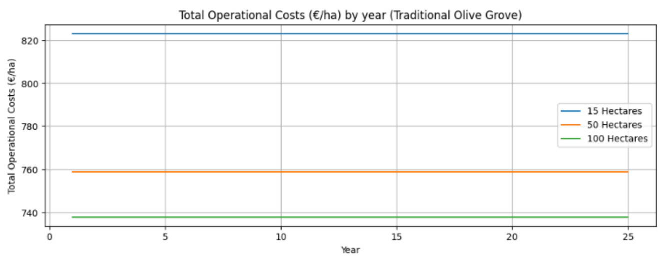

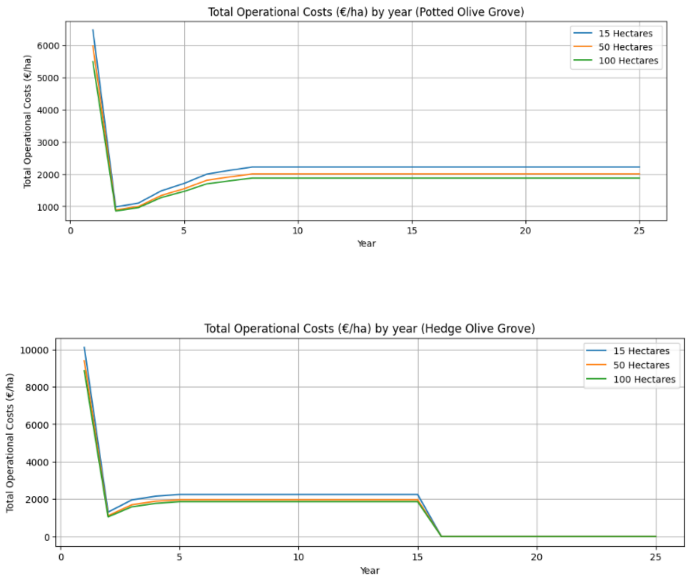

Figure 8.12 - Evolution of annual operational costs through 25-year period for 3 different areas

8.6.1.3 Average Olive Price

The cumulative profit was chosen as the key metric because the average olive price influences directly the revenue, which is a major component of profitability. To conduct this analysis, the cumulative profit was evaluated across three olive grove systems, while considering the same cultivated area of 50 hectares.

Starting with traditional olive grove, in this system the cumulative profit increases steadily with higher average olive prices. Figure 8.13 shows the linear impact of price, with higher price points, like €2/kg, resulting in significantly higher profits compared to lower prices.

Potted groves show a more pronounced sensitivity to average olive price due to their higher production levels, compared to traditional groves. In this system, the cumulative profit increases more sharply as the price rises.

Hedge groves demonstrate the highest sensitivity to average olive prices due to their high productivity during shorter lifecycle. As we observe, Figure 8.13 shows that the cumulative profit rises rapidly at higher price points, despite after a 15-year lifespan the profits stabilize, due to the limited long-term viability of this system.

Across the three olive grove's types, the cumulative profit increases linearly with higher average olive prices, highlighting its significant impact on profitability. Figure 8.13 shows that traditional groves are the least sensitive to price changes due to their lower production, which makes them suitable for stable or low-price markets; potted groves achieve higher profits at moderate price levels while benefiting from scalability, and hedge groves generate the highest profits at elevated price points, especially in larger areas, though their shorter productive life constrains long-term returns.

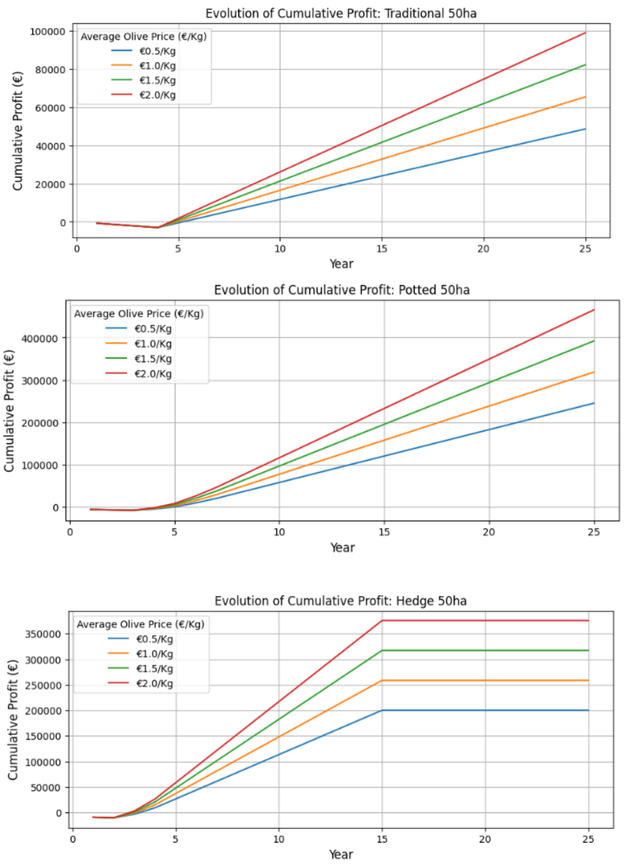

Figure 8.13 - Evolution of cumulative profit through 25-year period for 50 hectares

8.6.2 Multivariate Analysis

In the multivariate analysis, only the type of olive grove and cultivated area were variable, however the average olive price was fixed, as the univariate analysis demonstrated a consistent linear relationship between olive price and profit. This choice simplified the analysis to focus on understanding the impact of grove type and scale on cumulative profits.

The potted olive grove consistently emerges as the most profitable option, because it achieves the highest cumulative profit across all cultivated areas. For 15ha the profit is approximately €313,000 increasing sightly to €318,000 for 50ha and €321,000 for 100ha, these values demonstrate that potted system not only provides the greatest overall profitability but also scales effectively with increasing cultivated area.

The hedge olive grove ranks second in profitability, with cumulative profits of approximately €254,000 for 15ha, €258,000 for 50ha, and €260,000 for 100ha. This system doesn't match the performance of the potted system but offers a moderate profit and remains scalable as the cultivation area expands, so it provides a viable alternative for scenarios where high-density mechanized systems are preferred.

On the other hand, traditional olive grove consistently yields the lowest profits across all cultivated areas; with cumulative profits €64,000 for 15ha, €65,000 for 50ha, and €66,000 for 100ha, despite being the system with lower operational costs. However, the traditional grove limited production capacity and delayed returns make it the least economically competitive, even when cultivated area is bigger. Despite that, this system is suitable in situations where the input dependency is lower and long-term sustainability is prioritized over profitability.

This analysis, observed in Figure 8.14, demonstrates the differences of profitability between the three types of olive grove, standing out the potted system in terms of cumulative profit for 25 years. In the case of Municipality of Mação, the preference expressed is for the installation of a potted olive grove in all AIGPs, with the aim of balancing profitability and sustainability throughout the production cycle.

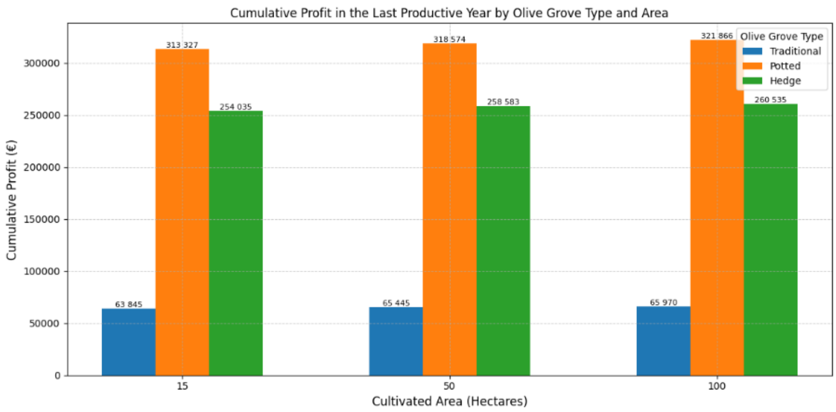

Figure 8.14 - Cumulative Profit in the last productive year (25-year period for Traditional and Potted, and 15 for Hedge)

8.7 Conclusion - Recommendations

8.7.1 Potted Olive Grove

The potted olive grove is the ideal option for Mação if the municipality's primary objectives are to balance longevity and sustainability, because this system delivers the highest cumulative profit over its 25-year productive lifespan. Furthermore, the potted grove scales effectively across different cultivated areas, which shows stable profitability even when the area increases.

Additionally, the moderate inputs requirements and long-term economic viability is ideal for producers who value sustainability alongside profitability, aligned with Mação's goals to foster productive and resource-efficient agricultural practices while maintaining economic returns.

8.7.2 Hedge Olive grove with replacement

Mação could adopt a hedge olive grove system with replacement after its lifespan of 15-year, if the main purpose be based on profit's maximization. In this scenario, a new grove is replanted, resulting in a cumulative profit of approximately €514,000 over the same 25-year timeframe, exceeding profits of both potted (€318,000) and traditional (€65,000) systems. The hedge system's mechanized and high-density planting yields rapid production and high profitability during each cycle, however, requires a larger initial investment and careful management for replanting after 15 years. Thus, this approach is best suited for producers who can accommodate higher operational demands and aim to achieve maximum financial returns.

8.8 Limitations

Despite the model's practical utility, it has some limitations that arise from the assumptions made during the model's development and the scope of data used, so addressing these issues in future versions could improve the model's accuracy and usefulness.

One notable limitation is that the model is based on general data for all Portugal regions, overlooking specifics like Mação's microclimate, soil conditions, and farming practices, which results in a reduced accuracy when assessing localized scenarios.

The model excludes key factors such as agriculture subsidies, government incentives, and policy impacts, that could significantly vary the costs, and in turn profitability, which limits the model's ability to assess economic viability in regions influenced by policy-driven factors.

Lastly, the model assumes a uniform price for olive oil, disregarding the differences arising from the characteristics and costs associated with the different cultivation systems.

8.9 Future Work

A future direction is the development of a regionalized data model tailored to Mação, this model would integrate the region's characteristics, such as its microclimate, soil composition, and traditional growing system, improving accuracy of economic assessments for olive cultivation.

The process would involve collecting localized data through contact with farmers, cooperatives, and institutions in Mação. Some examples of tools that provide detailed inputs are surveys, climatic data, soil analysis, and remote sensing technologies. These efforts would refine cost structures, capture variations in productivity, and account for specific challenges, such as irrigation and logistic costs.

9. The Case of Solar Panels

9.1 Introduction

The initial plan for the photovoltaic research involved creating a model to simulate the economic feasibility of installing a specified number of solar panels in Mação over time. However, this approach was hindered by a severe lack of localized data on solar panel productivity, terrain usability, and other crucial factors specific to Mação. Without robust, region-specific data, it proved challenging to develop reliable simulations for energy output and to generate meaningful economic projections.

This realization led to a shift in focus toward evaluating pre-designated sites within Mação's OIGP, identified in part through consultations with the OIGP team. Although these areas were selected based mainly on important criteria such as slope and south-facing orientation, a more comprehensive site assessment was necessary to determine their suitability and long-term economic potential for utility-scale solar installations.

9.2 Fundamental Concepts

9.2.1 What are Solar Panels?

A solar panel is a device designed to convert solar energy into electricity through photovoltaic (PV) cells, which capture sunlight and create an electric current by establishing a charge differential between two layers. This process enables the conversion of solar energy into electricity by exploiting the photovoltaic effect. Solar panels play a crucial role in sustainable energy systems, with their PV cells enabling the direct transformation of solar radiation into usable electrical energy. To maximize energy output, it is essential to position solar panels in locations with high solar exposure, for direct, unobstructed sunlight (National Grid. 2023).

9.2.2 How a Solar Panel Works

A photovoltaic solar panel is made from cells composed of semiconductor materials like silicon (National Grid. 2023). When photons (particles of sunlight) come into contact with the panel, they cause electrons in the silicon atoms to become dislodged and move from the negative to the positive side, creating an electron flow, which generates a direct current (DC).

From Alharbi, F. H., & Kais, S. 2020 it important to note that not all solar energy is converted into electricity. Consequently, only a portion of the energy can be harnessed by the panels to generate electricity, as there are losses due to electrical and physical factors within the panel.

9.2.3 Types of Solar Panels

Monocrystalline Solar Panels

Monocrystalline solar panels are made from a single, continuous silicon crystal, giving them a sleek, black appearance. They are highly efficient, often exceeding 20%, and perform well in low-light conditions (Aurora Solar. (2024)).

Polycrystalline Solar Panels

These panels are made by melting silicon crystals together, creating a blue look. They are less efficient than monocrystalline panels, achieving 15-17% efficiency (Aurora Solar. (2024)).

Thin-Film Solar Panels

Thin-film panels are created by depositing thin layers of photovoltaic material, such as cadmium telluride or amorphous silicon, onto substrates like glass or plastic. They are lightweight, flexible, and suitable for non-traditional applications, including curved surfaces or portable solar products. These panels have lower efficiency, typically 10-12%, but their low production cost and adaptability are significant advantages (Aurora Solar. (2024)).

9.2.4 Efficiency and Technological Advancements

The efficiency of solar panels has steadily improved over the years due to advancements in photovoltaic technology. Early solar panels had relatively low efficiency rates, often below 10%, but modern panels can achieve efficiencies of 25% or more. Innovations in materials, such as the use of monocrystalline silicon and the development of multi-junction cells, have contributed to these improvements (Lafayette College. 2014.).

9.2.5 Utility-Scale Solar Panel System Energy Production Formulas

Utility-scale solar panel systems rely on several key formulas to estimate their energy production. The Efficiency of a solar panel can be calculated using the panel power, irradiance (G) and panel's surface area (A), shown in Equation 9.1:

$$(1)\ Efficiency = \frac{\text{Module Power (kW)}}{G \times \text{A}}$$

Equation 9.1 – Solar Panel Efficiency Formula

The Energy Production per Panel formula calculates the energy output from a single solar panel using its efficiency, the local solar irradiance (G), and the panel's surface area (A), shown in Equation 9.2:

$$(2)\ E_{\text{panel}} = \text{Efficiency} \times G \times A$$

Equation 9.2 – Solar Panel Power Output Formula

This formula is used to estimate how much energy a single panel can generate. Finally, the Total Energy Output for the System formula helps scale this to the entire system, considering the total number of panels (N) and the average sunlight hours (H), show in Equation 9.3:

$$(3)\ E_{\text{system}} = N_{\text{panels}} \times E_{\text{panel}} \times H$$

Equation 9.3 – Total Energy Output Formula

These formulas are pivotal for assessing the performance and operational efficiency of utility-scale solar power installations (Photonic Universe. 2024) (Anker Solix. 2024).

9.2.6 How Produced Energy is Delivered to Consumers

The energy delivery process involves a pipeline from production to the consumer, with grid operators playing a central role. Initially, energy is produced, often by sources such as solar, wind, hydroelectric, or fossil fuel plants and transmitted over long distances at high voltages to reduce losses (GridX. 2024). Grid Operators distribute power through high or low voltage networks directly to homes being part of the pipeline of energy production to consumption, explained in Figure 9.1, and serve as the middleman who maintains the operation of the grid, monitoring its performance, ensuring it operates within capacity. In Europe they are split into Transmission System Operators (TSO) and Distribution System Operators (DSO).

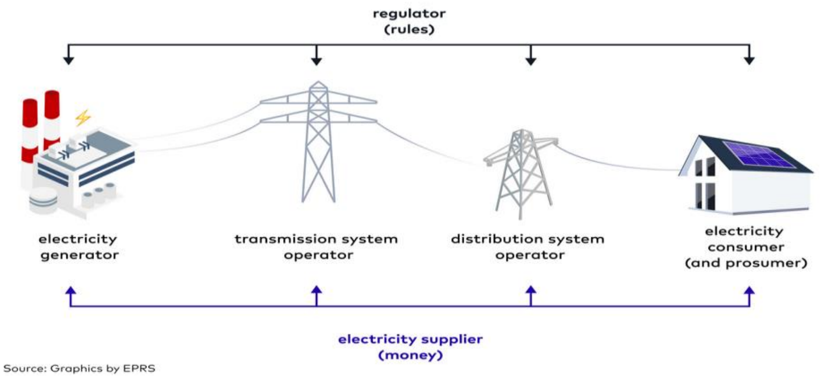

Figure 9.1 – Pipeline from energy production to consumption | Source: (GridX. 2024)

Transmission System Operators are responsible for the transmission of electricity from generational plants via the power grid to regional distributors, dealing with very high voltages. On the other hand, Distribution System Operators grids usually consist of low and medium voltage networks (6-50 kV) like renewables, transporting electricity to the end user (GridX. .2024).

In Portugal REN serves as a Transmission System Operator (TSO), while E-Redes takes the role of Distribution System Operator (DSO), differentiating in the levels of voltage in their substations - E-Redes allows up to 150 kilo Volts (kV), while REN has substations at 150, 220 and 400 kV (Portugal/Energia/Subestações).

9.2.7 Photovoltaic Market in Portugal

The Photovoltaic (PV) market has seen increasingly high growth in Portugal. Referencing Santos, B. 2022, Portugal's cumulative PV capacity reached 2.19 GW by the end of June 2022, with Solar being the technology with the greatest growth in installed capacity, going from 299 MW in 2013 to 2192 MW in 2022. According to (REN. 2024.), Between January and August 2024, 75% of the electricity consumed in Portugal came from renewable sources, with hydropower accounting for 33% of the energy, wind power for 26%, solar for 10%, and biomass for 6%. Natural gas supplied 8% of consumption, while the remaining 17% corresponded to imported energy. Nearly half of Portugal's solar energy production is concentrated in the Alentejo region, which represents 12% of all electricity consumed in that area.

9.2.8 How Photovoltaic Farms Sell Energy

Historically, in order to incentivize investments in the renewable energy sector, governments have provided financial incentives, like subsidies or guaranteed prices per MWh, to increase supply (ABN AMRO Bank. 2022.). However, in recent years, the number of subsidies given by governments has been decreasing. To hedge against decreasing incentives from governments and avoid the price competition and volatility of global markets, renewable energy providers are increasingly using Power Purchase Agreements (PPAs) – A typically long-term contract between buyers and sellers of energy, under a pre-defined price.

PPA structures can take a Pay-As-Produced approach, where a fixed price is paid for produced volumes, up to a predetermined amount (ABN AMRO Bank. 2022.). In this case, the risk is on the buyer as the producer is not under any obligation to deliver a specific volume.

9.3 Related Work and State of the Art

The development of solar photovoltaic (PV) farms requires a comprehensive understanding of both technical and economic factors that determine site suitability and long-term profitability. Researchers in the field have employed advanced methodologies, such as Multi-Criteria Decision-Making (MCDM) frameworks - structured methods used to evaluate and prioritize multiple conflicting criteria when making decisions, analyzing the trade-off and ranking the alternatives -, Geographic Information Systems (GIS) models - systems used to capture, store, analyze, and visualize spatial or geographic data -, and economic feasibility tools, to optimize PV site selection and economic evaluation. These approaches help identify areas with optimal solar resources, evaluate topographic and infrastructure conditions, and estimate financial returns under different scenarios.

In Hasti et al. 2023., the authors study the potential of the Kurdistan Province, in Iran, for Solar Photovoltaic farms by using geographic information systems-based modelling techniques and the comparison of using confidence levels in the analysis. In their work, they use a Multi Criteria Decision-Making (MCDM) framework placing factors influencing site selection in two main categories - meteorological and topographic conditions; and non-meteorological constraints such as human infrastructure, energy-grid accessibility, legal protections, and urbanization. The paper reviews different MCDM approaches that have been employed in the context of renewable energy site selection. Techniques such as the Analytical Hierarchy Process (AHP), Technique for Order Preference by Similarity to Ideal Solution (TOPSIS) and the Dempster-Shafer Theory, utilized to incorporate uncertainty, by combining evidence from various sources, providing a more robust assessment of site suitability compared to traditional methods that do not account for uncertainty. In their methodology a two-stage framework was used. In the first stage, a fuzzy system, a technique that helps to homogenize and process input parameters. Then, the fuzzy outputs are processed using the AHP model and Dempster-Shafer theory to evaluate the suitability of different sites. The results include a comparison between the suitability maps generated using the fuzzy_AHP method (which does not consider the probability that an interval contains the true parameter value, otherwise called confidence level) and those produced using the fuzzy_DS method (which incorporates different confidence levels of 95%, 99%, and 99.5%). One of the significant findings is that as the confidence level in the fuzzy_DS method increases, the area identified as suitable for solar PV farms decreases. This indicates that higher confidence levels lead to more conservative estimates of suitable locations, reflecting the uncertainty in the input data. In the end of the analysis, it's emphasized that the southeastern region of Faro has favorable conditions, such as adequate solar radiation and appropriate land use, making it an ideal candidate for solar energy projects.

Furthermore, recent studies have underscored the importance of adopting robust, data-driven methodologies that minimize subjective bias and enhance predictive accuracy. One such approach is presented in the work of Li, X et al. 2023. which developed an Interaction Linear Model combined with GeoDetector – a statistical tool to analyze and measure how factors influence a target variable - to improve PV siting in China. This approach skips traditional subjective weighting and focuses on how different factors, like slope or direct radiation, and their combined effects, influence site suitability. For example, instead of just ranking slope and radiation separately, it considers how good they, together, make a site more PV suitable. In the analyzing accuracy increased by 8% over a basic linear model and identified the region of Xinjiang, compared to the other two candidates, as an optimal region for solar PV farms due to its high determinant power in the interaction-based evaluation system.

Aside from selecting the location, it is of pivotal importance to assess the economic feasibility of a photovoltaic farm, to understand its effectiveness in the long run. The work of Kim, Y et al. 2022. studies the economic feasibility of potential PV farms in three locations in Kentucky, USA, in terms of Cumulative Cash flow (Sum of amount of cash generated or spent over time) and Payback Time (Time to recover cost of investment, in years) by using the Cost of Renewable Energy Spreadsheet Tool (CREST), as well as estimating the output power (kWh) annually, for the three sites. The CREST is a tool used to assess and calculate the costs associated with renewable energy projects, made by the National Renewable Energy Laboratory, a U.S. government research organization. Similarly to the previously reviewed studies, the authors use MCDM framework with the main site-choosing criteria being terrain and solar irradiance, but also incorporate Cost and Size (Average property cost, state and county taxes, and upfront costs) as well as Infrastructure (Existence of coal powered plants, dams, transmission lines, substations, etc.). For the modelling, the authors used three main tools, PVWatts and System Advisor Model (SAM) for the mathematical modelling, and CREST for the financial modelling. The analysis can be summarized in three steps: (1) Used PVWatts, Google Earth, topographical maps, and other relevant maps to study which of the three sites gathered the best weather, topographic and orography criteria. (2) Enter parameters into SAM's detailed PV Model to estimate annual power output (TWh) and graph generation. (3) Enter variables requested by the financial model, which include degradation rate, income tax rates and incentives. CREST's output includes cash flows, market value, revenue, operating expenses, debt service, reserves, pre-tax cash flow, federal taxable income, state taxable income, federal tax benefits/liability, state tax benefits/liability, after tax cash flow, payback time, after tax IRR, debt service coverage, etc. Out of all these, cumulative cash flow and payback time were the primary decision factors. Out of the three possible locations described in the paper, Smithland, Hickman and Falls of Rough, the Hickman Farm appears to generate the most TWh and has the largest profit. However, Falls of Rough generates the most money per MWh at over $11,300 per MWh produced. Therefore, while all the farms were determined to be profitable based on the rough estimates using CREST, Hickman is the largest producer and has the largest net profit. Falls of Rough would be the most profitable percentage wise.

These models prove that solar is not only feasible but could potentially be profitable. They show a return on investment within 6 years, positive profit margins, and annual generation of over 2.2 Terawatt Hours (TWh).

The studies reviewed highlight various advanced methodologies for solar photovoltaic (PV) site selection and economic evaluation. Methods like Multi-Criteria Decision-Making (MCDM), Geographic Information Systems (GIS), and economic feasibility tools, such as CREST, offer solid frameworks for assessing both technical and financial factors. MCDM techniques, such as Analytical Hierarchy Process (AHP) and Dempster-Shafer Theory, provide structured decision-making by integrating multiple conflicting criteria. GIS models enable spatial analysis and visualization of optimal areas, while economic tools like CREST assess financial viability through metrics like cumulative cash flow and payback time. The use of these tools minimizes subjective bias, enhances predictive accuracy, and accounts for uncertainty.

However, these methods also have some limitations like data quality and the complexity of integrating multiple criteria can make results sensitive to data inaccuracies. For example, higher confidence levels in the Dempster-Shafer method led to more conservative estimates of suitable sites, which may overlook potentially viable areas. Additionally, while MCDM frameworks and economic tools like CREST provide valuable insights, they often require significant computational resources and expertise.

The following methodology uses a similar approach to prior work on PV feasibility assessments, including a thorough analysis based on pre-defined criteria, modelling using Geographic Information Systems and an economic modelling spreadsheet similar to CREST. However, it is uniquely focused on the Mação region, where there is limited data on solar panel feasibility and potential economic impact. Unlike established regions with extensive studies on PV system viability, Mação remains largely hindered in terms of available information on suitability for utility-scale solar installations. By applying an established methodology to an under-researched area, this paper seeks to fill the gap on solar energy output potential and economic assessment specific to Mação.

9.4 Methodology and Approach

This section outlines the structured approach employed to assess the feasibility of a utility scale solar park. Starting with site selection criteria explanation, followed by a comprehensive analysis of all available polygons in the OIGP based on site selection criteria, the approach applies techniques to evaluate potential locations. Following site availability and initial exclusion factors, this thesis then narrows down potential options before moving into assessments of the final three sites. After the potential sites are laid down, a comprehensive financial analysis is shown with revenues and expenditure, being the focus that supports the final selection, integrating both quantitative metrics and qualitative considerations.

9.4.8 Site Selection Criteria for Maximizing Solar Panel Performance

In this site selection analysis, defining criteria is split into 5 different sections, inspired by the work of Rediske, G. et al. 2018. : Socio-environmental, Location, Climate, and Orography.

9.4.1.1 Socio-environmental Criteria

Socio-environmental criteria elaborate on how the land is used currently and, in the future (Rediske, G. et al. 2018.), which can be evaluated by the POSA and POSP of the respective OIGP. There must be some precautions taken when considering land use as reserves, forests, water bodies, humid areas and urban/populated areas are all restrictions to the creation of a utility-scale solar park.

Further, the agrological capacity should also be considered, as land with great agricultural potential should be utilized for the aforementioned purposes. Moreover, areas with high vegetation index, should be avoided, because the shaded areas resulting from tall vegetation can hinder the allocation/efficiency of solar panels, resulting in lower energy production (Rediske, G. et al. 2018.).

9.4.1.2 Location Criteria

Location criteria address potential problems like the proximity to a substation, which can impact the costs by having to build longer infrastructure to connect them (Rediske, G. et al. 2018.). Furthermore, the nearby substation also needs to have the capacity to receive the energy produced by the solar farm.

Another important factor to consider is the proximity to roads, as on one side, the absence of nearby roads can hinder the transportation of necessary materials and infrastructure (Rediske, G. et al. 2018.). However, if roads are located within the selected site, fencing will need to be constructed around them, which increases costs.

Additionally, a pre-defined distance must be maintained between the fence and the solar panels, reducing the area available for photovoltaic installation (MacDonald, M. 2017). Furthermore, the site must not have water courses running through it, as they increase the risk of flooding in an event of bad weather and soil erosion, which can lead to displacement of foundations (Liu, H et al. 2023.).

Finally, literature says it's very important to distance any prospective solar park from residential or environmentally protected areas as these can destroy habitats and/or affect urban growth (Rediske, G. et al. 2018.).

9.4.1.3 Climate Criteria

The first important climate-related criteria is solar radiation, typically measured in Global Horizontal Irradiance (GHI). As per the efficiency equation presented above, the output of a solar panel is a function of its wattage rating and the solar irradiance. As such, the amount of energy a solar panel can produce is directly proportional to the amount of solar energy that its surface receives on any given period. Literature utilizing GIS and MCDA confirm solar radiation as the primary factor influencing the long-term viability of a solar farm (Alhammad, A. et al. 2022).

Another important factor is the average temperature, given that the operating temperature of the cells in a PV panel is one of the key determinants of efficiency. According to Khan, M. et al. 2017. whenever the temperature of the solar panel increases above the operating temperature (25 degrees Celsius), the band gap of the semiconductor material in solar cell decreases, resulting in the drop of efficiency and maximum power output.

Duration of sunlight, or the time of insulation, represents how long energy is received from the sun, on any given time period (Rediske, G. et al. 2018.). Conversely, when there is no insulation, none or very reduced energy production happens. Moreover, and tied to duration of sunlight, accounting for cloudiness is also important, as an overcast sky severely affects PV Efficiency.

9.4.1.4 Orography Criteria

Recent studies (Freeing Energy. 2021.) suggest that around one hectare of land is needed for every 1 MW of solar power capacity, particularly for crystalline silicon panels. Furthermore, Slope of the terrain is a dealbreaker for many terrains, especially those with zones above 20%, as they present several challenges like structural stability, shading issues and potential soil erosion problems (Heo, J. et al. 2021.).

Finally, orientation, or the cardinal direction to which the piece of land faces. The orientation of the site will limit the solar radiance solar panels receive (Rediske, G. et al. 2018.). The general understanding is that the solar panels facing south (in locations north of the equator) will receive the most sunlight (De Rooij, D. 2023.). However, recent studies have proven differently: according to a new study from Pecan Street Research Institute (Katherine Tweed.

2013.), West-facing solar panels produced 49 percent more electricity during peak demand compared to south-facing panels, concluding that the optimal direction is Southwest.

With the selection criteria established, this study now moves to analyzing the initial 16 polygons available in Mação's OIGP.

9.4.2 OIGP Initial Site Analysis

The site selection analysis was conducted in three phases. In the initial phase, a basic orographic analysis was performed, including slope and perimeter evaluations. In the second phase, the remaining sites were assessed based on additional relevant criteria, resulting in the identification of four final sites. In the third phase, the final sites were reviewed, with the help of a specialist team, to gather measurements of the terrain and assess potential PV output.

9.4.2.1 First Phase of Analysis

For this analysis, QGIS, a versatile geographic information system (GIS) software, was employed to view, edit, print, and analyze geospatial data across various formats. This tool facilitated the evaluation of sites according to Mação's OIGP, which initially identified 16 polygons across nine OIGP - Aboboreira, Amêndoa, Cardigos, Carvoeiro, Castelo, Envendos, Mação, Ortiga, and Penhascoso - as potential locations for photovoltaic (PV) development.

From the 16 identified polygons, two sites in Cardigos were excluded: one already designated for a wind farm and the other due to a predominant steep slope, making it unsuitable for PV development across most of its area. The three sites in the municipality of Aboboreira were excluded from the final selection due to their limited dimensions, measuring only 3, 5, and 6 hectares, which do not align with the land area requirements to satisfy the energy output demand in Mação, according to Eng. António Louro. In Envendos, two out of the three potential sites were similarly excluded: One due to its reduced dimension of 3 hectares, and the other due to being under the ownership of the Portuguese electric power distribution company, EDP

Renováveis. Lastly, within the municipality of Mação, the northernmost site was removed due to its pronounced slope, which complicates construction and energy efficiency.

9.4.2.2 Second Phase of Analysis

In phase 2, a deeper analysis, considering the majority of the criteria presented above, was conducted on 9 remaining polygons, to be presented to Eng. António Louro, specialist in the forestry sector and current forest manager for the Mação's OIGP. Using the aforementioned criteria and Geographical Information Systems (GIS) for the research, and a further discussion with Eng. António Louro, the following sites were excluded:

Polygon 2, the largest polygon in Penhascoso, despite having 13 Ha of usable terrain, much of this potential is hindered by high slopes (See appendix IX.1). In addition, polygon 3, the southernmost site in Penhascoso, was excluded for the increased number of external roads passing through it, thus reducing the usable area for PV. Furthermore, Polygon 4, the only one in Carvoeiro, is situated on a hill, hence having a high slope (with some parts reaching 40%), making it hard for a Solar Farm (See Appendix IX.2). Polygon 7, in Envendos, has many water courses running through it, making the terrain unstable, as mentioned in the location criteria. In Mação, Polygon 8 consists of an area of just 6 Ha, small compared to some of the other potential sites. It is also situated close to an urban area, which can have further complications, as mentioned in the socio-environmental criteria. Finally, Polygon 9 has a large amount of water bodies close to it, as well as being situated very close to an urban area.

	Polygon 1	Polygon 2	Polygon 3	Polygon 4	Polygon 5	Polygon 6	Polygon 7	Polygon 8	Polygon 9
AIGP	Ortiga	Penhascoso	Penhascoso	Carvoeiro	Castelo	Castelo	Envendos	Mação	Mação
Area	24.2 Ha	13 Ha	11.2 Ha	9.1 Ha	14,6 Ha	22.6 Ha	8.54 Ha	6.2 Ha	10Ha
Perimeter	6.5 Km	1.8 Km	3.5 Km	1.6 Km	2.7 Km	5.1 Km	2.4 Km	1.4Km	3.3Km
POSA	Olive Trees	Maritime Pine	Stone Pine	Invasive Species Forest	Eucalyptus	Eucalyptus and Pine	Pine Tree	Eucalyptus	Mixed Forest
Southwest POSP	Olive Trees	Maritime Pine	Stone Pine	Eucalyptus and Pine	Orchard	Pine and Cork Oak	Eucalyptus	Pine Tree	Mixed Forest
Vegetation Index (South)	Low	Low	Low	Low	Low	Medium	Medium	High	Low
Slope	0-15%	10-30%	5-20%	15-40%	5-20%	5-20%	5-20%	5-20%	0-15%
Hypsometry	50-100m	200-300m	100- 200m	350-450m	500-600m	300-450m	150-200m	300-350m	200-250m
Guidance	South	East-South	South	South	South – East	South – West	South – West	West	South-west
Roads	Yes	No	Yes	No	Yes	Yes	Yes	Yes	Yes

Table 9.1 1 - Quantitative Criteria for remaining 9 polygons

9.4.3 Final Site Selection Simulations

In the final phase, with the assistance of Professor Álvaro Rodrigues, Business Development and Operational Adviser, and Eng. Tiago Barata, at GENERG, a comprehensive evaluation of the three remaining sites was conducted using PVSyst and PVCase, software tools used in the design, simulation, and optimization of solar photovoltaic (PV) systems. With the aforementioned sites defined, Meteonorm, a source for solar and meteorological data, was used to retrieve solar radiation and wind speed in the area of Mação. Next, using the extracted data and in-house cartographic resource as inputs in PVCase, a detailed simulation of the yearly potential power output of the sites was generated, allowing for a robust estimate of production. Finally, the power output was used to calculate the financial potential of the PV farm in each site, based on the cost estimate provided by GENERG, combined in an Excel spreadsheet.

For this simulation and power output simulation, the following premises were considered:

(1) 2x7 string PV modules (2 vertical, 7 horizontal) of 665Wp each with 20% angle;

(2) Site is unusable if slope of terrain is above 10% in north-facing zones, and 20% elsewhere;

(3) Exclusion zones were considered where waterbodies were found (with a setback of 3.0 m), existing access roads (with a setback of 2.0 m), and municipal roads (with a setback of 4.0 m);

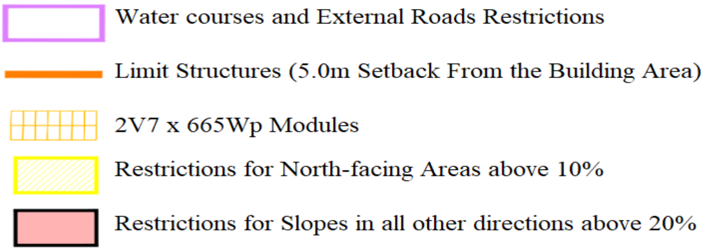

Figure 9.5 - Labels for Polygon Use Figures

9.4.3.1 Polygon 5 (Castelo)

Polygon 5 has a usable solar panel area of 42,381.5m^2 (4.238 Ha) out of 142,205.54m^2 (14.22 Ha), representing 29.8% area coverage and a perimeter of around 5100m. This 71.2% difference from the total area stems from the fact that 21.18% of its area has a slope of above 20%, and another 0.67% of its area faces North and has a slope of above 10% (Appendix IX.3). The rest of the unusable area is made up of restrictions from water courses and road access, as well as the 5m mandatory distance from fencing all around, as seen below in figure 9.6.

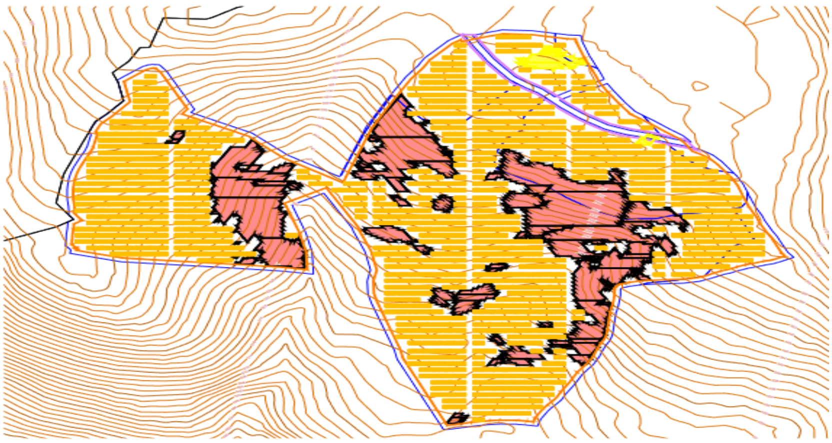

Figure 9.6 – Polygon 5's Total Terrain Use

Overall, following the PVCase output, this site supports the use of 1017 2x7 PORTRAIT 665W, totaling 14 238 PV modules. Thus, total output power (MWp), the product of the number of modules by their capacity would be 9468 kWp (9.47 MWp).

9.4.3.2 Polygon 6 (Castelo)

The other polygon in Castelo has a total usable PV area of 24,670.46m^2 (2.47 Ha) out of 224,501.41m^2 (22.4 Ha), representing a coverage area of 10.989%. According to the analysis, 59.5% of the terrain has a slope above 20% and according to PVCase data, 11% of the total area faces north and has a slope above 10%, making it unusable (Appendix IX.4). The rest of the unusable area is composed by access water courses and external roads, as well as their setback distances, as seen in figure 9.7.

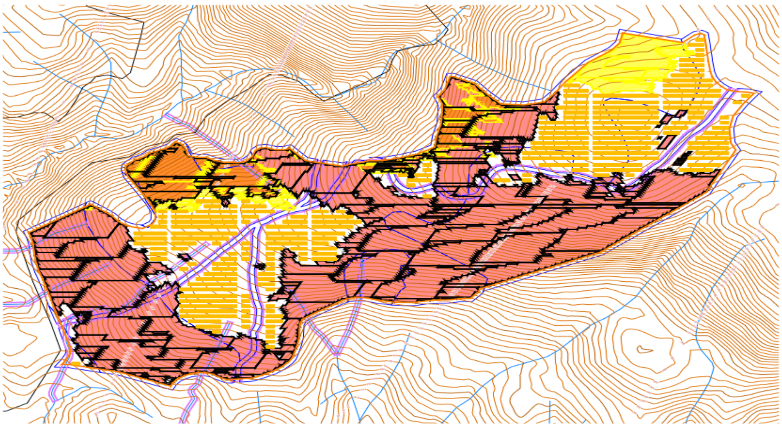

Figure 9.7 – Polygon 6's Total Terrain Use

Overall, this site supports the use of 592 2x7 PORTRAIT 665W, totaling 8288 PV modules. Thus, Total output power (MWp), would be 5511 kWp (5.51 MWp).

9.4.3.3 Combining Polygon 5 and Polygon 6

Given the close distance between the two sites (Figure 9.8), in conversation with Eng. Tiago Barata and Professor Álvaro Rodrigues, the possibility of building a PV park in the two locations and connecting them came up. After running the simulations for this idea, using the same tools, the simulated PV Farm totaled 22533 665W modules (777 strings x 29 in series), with a total PV power of 14984 kWp (14.98 MWp) (For a more detailed analysis on the simulations check appendix Figure IX.6, IX.7, IX.8, IX.9, IX.10, IX.11, IX.12, and IX.13).

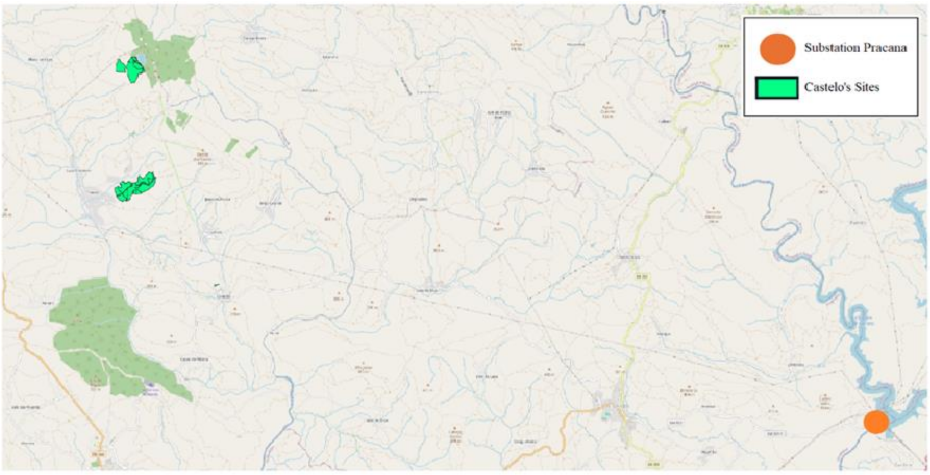

Figure 9.8 - Map of Castelo's Sites and Substation

9.4.3.4 Polygon 1 (Ortiga)

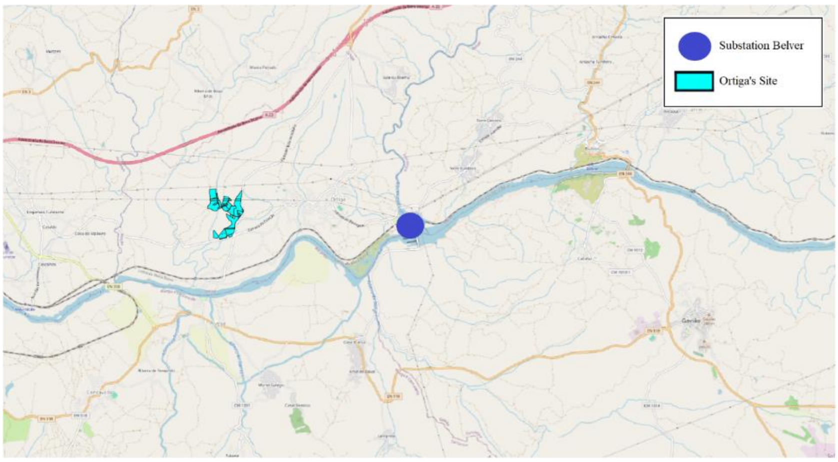

Figure 9.9 - Map of Ortiga's sites and Substation

This polygon (Figure 9.9) has a total usable PV area of 67,743m^2 (6.77 Ha) out of 242,117.15m^2 (24,21 Ha), representing a coverage area of 27.96%. Overall, 13.89% of the terrain has a slope above 20% and according to PVCase data, 9.19% of the total area faces north and has slope above 10%, making it unusable (Appendix IX.5). Furthermore, as is visible in figure 9.10, this polygon has an increased amount of water courses and road accesses, causing a significant area to be hindered by the 5m mandatory distance from fencing. Overall, this site supports the use of 752 string x 29 bifacial 665W modules in series, totalling 21808 PV modules. Thus, total output power (MWp), would be 14502 kWp (14.5 MWp). (For a more detailed analysis on the simulations check appendix Figure IX.14, IX.15, IX.16, IX.17, IX.18, IX.19, IX.20 and IX.21).

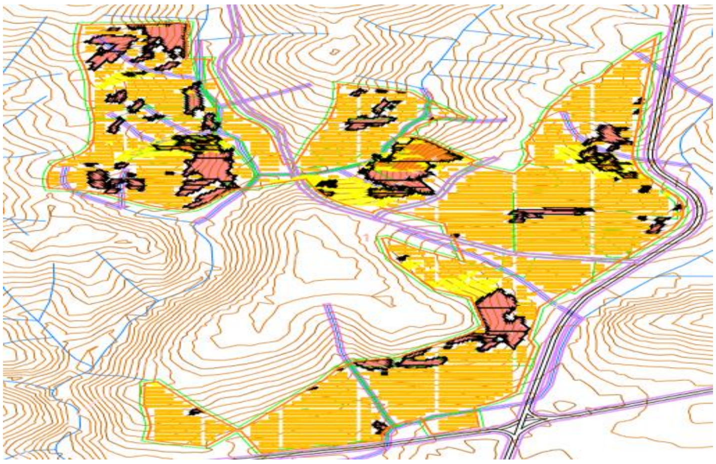

Figure 9.10 - *Polygon 1's Total Terrain Use*

While the combination of the two sites in Castelo yielded a marginally higher total PV power (14.98 MWp compared to 14.5MWp), there is still an important detail to consider before looking at the financials. As mentioned in the first sections, the PV park grid connection is made through a cable connection to a substation. The site in Ortiga has E-REDES' substation Belver at a distance of 3km, while the two in Castelo have substation Pracana at a distance of 16km, which will result in higher costs.

9.4.4 Cost Assessment

To assess the Engineering, Procurement and Construction (EPC) cost - total capital needed to build the solar farm – and other costs, estimates for parameters were provided by GENERG using internal market analysis and industry averages.

9.4.4.1 Economic Feasibility of the Castelo Solar Park

The total main cost of the solar PV project is €12.42 million, averaging €0.83 per Wp. The largest expense is the delivery and installation of balance of plant (BoP) - costs to support the infrastructure and systems of a power plant needed to deliver the energy-, materials and equipment, totaling €5.08 million. PV module supply, including handling, amounts to €1.65 million. Civil works cost €869,000, while studies, design, and engineering account for €554,000. Interconnection-related expenses, due to the distance of 16km to the substation, totals

€3.25M. Other miscellaneous costs amount to €1.66 million (For a more detailed breakdown on the costs for Castelo's joint solar park, check appendix IX.22 and IX.23)

The overall investment value is equal to the total cost (€12.42m + €1.66m = €14.08m), divided by the Direct Current (DC) Capacity, the aggregated rated power output of the solar panels, 14,984 kWp. Thus, the investment for the project is €945,824.0/MWp. For the capital structure to accomplish the investment value, in conversation with Eng. Tiago Barata, a Debt-to-Equity ratio of 65% (Total debt equal to €614,785.60) was established, as per industry averages, with a debt maturity of 15 years, paying 4.5% interest. The values for taxes and inflation were pre-defined at 23.5% and 2.0%, respectively.

Finally, to compare the two projects the €/MWh was calculated for the project to break even, in this case, to get a 0% Total Internal Return (TIR) on Equity. This value at maturity (25 years), holds when the MW/h price was fixed to €38.00 (Meaning that a PPA of €38.00/MWh is the minimum price to break even on the project at maturity). This value is otherwise called the Levelized Cost of Energy (LCOE) and is pivotal when assessing PV projects. (Check appendix IX.24 for information on the debt, investment, LCOE and IX.25 for the income statement).

9.4.4.2 Economic Feasibility of the Ortiga Solar Park

The main project cost is €9.28 million (€0.64 per Wp). Key expenses include €1.6 million for PV module supply, €4.92 million for BoP materials and installation, and €841,000 for civil works. Studies, design, and engineering cost €537,000, while interconnection expenses amount to €660,000, much less than Castelo's due to a 3km distance to the substation, rather than 16km. Other costs, like land acquisition, and contingencies, total €1.66 million (For a detailed breakdown on the costs for Ortiga's solar park, check appendix IX.26 and IX.27).

The overall investment value is then equal to the total cost (€9.28m + €1.66m = €10.94m), divided by the DC Capacity, the aggregated rated power output of the solar panels, 14,502 kWp.

Thus, the investment for the project is €735,834.38/MWp. For the capital structure, the same Debt-to-Equity ratio of 65% (Total debt equal to €478,292.35) with a debt maturity of 15 years, paying 4.5% interest. The same values for taxes and inflation were also used (23% and 2.0%, respectively). In this case, to get a 0% Total Internal Return (TIR) on Equity, the LCOE is lower than in the Castelo PV Park, at €31.3 Megawatt/Hour (Meaning that a PPA of €31.3/MWh is the minimum price to break even on the project at maturity). (Check appendix IX.28 for information on the debt, investment, LCOE and IX.29 for the income statement).

9.4.4.3 Conclusions and Price Sensitivity Analysis on ROE

The final sites reflect the culmination of an in-depth analysis of the initial pool of 16 candidates. Both projects exhibit robust financial structures and competitive investment metrics. Even so, Ortiga shows a slight advantage with a lower Levelized Cost of Energy (LCOE) of €31.3/MWh, compared to Castelo's €38.0/MWh, suggesting a more favorable break-even price over its 25-year operational lifespan. Figure 9.11 illustrates the sensitivity of Return on Equity (ROE) to variations in the €/MWh price defined in the Power Purchase Agreement (PPA), with the Q1 2024 average of €44/MWh (Future Energy GO. 2024) highlighted (Appendix IX.30 shows a simple overview of both projects' outcome).

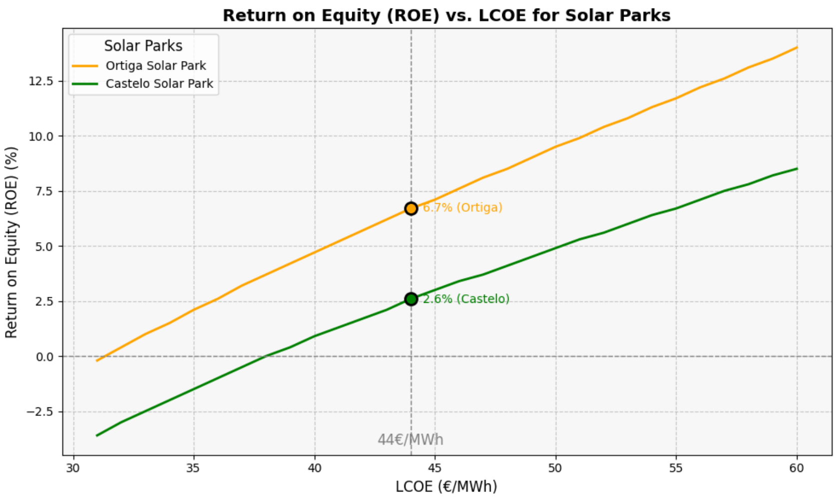

Figure 9.11 - Sensitivity Analysis of PPA price to ROE in Ortiga and Castelo

At this PPA value, Ortiga’s 25-year project yields a projected ROE of 6.7%, compared to Castelo’s 2.6%. While both sites present strong potential, this analysis underscores the advantages Ortiga holds, due to the close distance to the substation, yielding much lower interconnection costs and thus higher ROE.

9.5 Limitations

While there is a solid foundation for this analysis, outputting detailed results, the simulations are made by software that is not publicly available, meaning that, to replicate this study for other sites, it would require the use of the software and simulators that were provided by GENERG, which are not publicly available, thus limiting any additional analysis in the region.

9.6 Conclusion - Recommendations and Future Work

The sites analyzed in this section were initially selected from the predefined solar panel locations in Mação’s OIGP. Future research could explore other areas of Mação using similar methodologies to identify additional potential sites that could feasibly undergo POSP modifications, potentially meeting similar or even superior orographic criteria. Regarding the two final proposed sites, which demonstrate strong financial viability, it is recommended that a comprehensive study be conducted by relevant entities, such as E-REDES, GENERG, and the AZR, to further validate the project's potential as a sustainable source of revenue for Mação.

References

European Commission. *Recovery plan for Europe*. European Commission. https://commission.europa.eu/strategy-and-policy/recovery-plan-europe_en

População de Mação. 2001. "O Concelho." Accessed September 22, 2024. https://populacaodemacao.jimdofree.com/o-concelho/.

Gabinete de Estratégia e Estudos (GEE). 2023. "Mação: Estatísticas Regionais." Accessed September 30, 2024. https://www.gee.gov.pt/pt/lista-publicacoes/estatisticas-regionais/distritos-concelhos/santarem/macao/3190-macao/file.

Médio Tejo. 2019. "Mação: Exemplo florestal elogiado em todo o mundo, mas em Portugal falta coragem política." Médio Tejo, November 15. Accessed September 30, 2024. https://mediotejo.net/macao-exemplo-florestal-elogiado-em-todo-o-mundo-mas-em-portugal-falta-coragem-politica/.

Fernandes, Patrícia, Fernando Miguel Granja-Martins, Celestina Pedras, and Helena Maria Fernandez. 2020. "Análise dos Incêndios no Município de Mação num Período de 30 Anos (1991–2019)." Universidade do Algarve, Faro.

ICNF (Instituto da Conservação da Natureza e das Florestas). 2019. *8.º Relatório Provisório de Incêndios Rurais de 2019*. Lisboa: ICNF.

ICNF (Instituto da Conservação da Natureza e das Florestas). 2017. *10.º Relatório Provisório de Incêndios Florestais -2017*. Lisboa: ICNF.

Câmara Municipal de Mação. 2021. *Propostas para o Concelho de Mação: Áreas Integradas de Gestão da Paisagem (AIGP)*. Mação: Câmara Municipal de Mação. Acessed September 24, 2024. http://www.cm-macao.pt/index.php/pt/83-info-municipal/noticias/1146-propostas-concelho-macao-aigp.

Direção-Geral do Território. 2023. *Ordenamento Integrado e Gestão da Paisagem (OIGP)*. Acessed 17 October, 2024. https://www.dgterritorio.gov.pt/paisagem/ptp/oigp

Direção-Geral do Território. 2023. *Quadro de referência para o Ordenamento Integrado e Gestão da Paisagem - Versão 4 (2023-11-28)*. Acessed 17 October, 2024. https://www.dgterritorio.gov.pt/sites/default/files/ficheiros-paisagem/Quadro_referencia_OIGP_versao4_20231128.pdf

Racius. 2024. "AZR Gestão Territorial, S.A." Acessed 24 September, 2024. https://www.racius.com/azr-gestao-territorial-s-a/.

FCT (Faculdade de Ciências e Tecnologia). 2024. "Faculdade de Ciências e Tecnologia da Universidade Nova de Lisboa." Acessed 24 September, 2024. https://www.fct.unl.pt/.

Instituto Superior de Agronomia. 2024. "Margarida Tomé – Investigadora." Acessed 24 September, 2024. https://www.isa.ulisboa.pt/id/magatome.

Instituto Superior de Agronomia. 2024. "Instituto Superior de Agronomia – Universidade de Lisboa." Acessed 24 September, 2024. https://www.isa.ulisboa.pt/.

Mediotejo.net. 2023. "António Louro Renuncia ao Mandato na Câmara de Mação para se Dedicar à Reforma da Floresta." Acessed 24 September, 2024. https://mediotejo.net/antonio-louro-renuncia-ao-mandato-na-camara-de-macao-para-se-dedicar-a-reforma-da-floresta/.

Aflomação – Associação Florestal do Concelho de Mação." Acessed 24 September, 2024. https://www.aflomacao.pt/.

ICNF (Instituto da Conservação da Natureza e das Florestas). 2019. *IFN6 – Principais Resultados – Relatório Sumário*. Lisboa: Instituto da Conservação da Natureza e das Florestas.

Autoridade Florestal Nacional. 2012. *Regiões de Proveniência: Portugal*. Lisboa: Autoridade Florestal Nacional.

Florestas.pt. 2023. "Pinheiro-bravo: A Conífera Mais Abundante em Portugal." Acessed September 24, 2024. https://florestas.pt/conhecer/pinheiro-bravo-a-conifera-mais-abundante-em-portugal/

Figueiral, Isabel. 1995. "Charcoal Analysis and the History of *Pinus pinaster* (Cluster Pine) in Portugal." *Review of Palaeobotany and Palynology* 89(1-2): 441–454.

Matias, Márcia Batalha. 2023. *Sistema de Apoio à Decisão para as Áreas Integradas de Gestão da Paisagem*. Mestrado em Engenharia Informática, Universidade NOVA de Lisboa.

Oliveira, A. 1999. *Boas Práticas Florestais para o Pinheiro Bravo – Manual*. Porto: Centro *Pinus* – Associação para a Valorização da Floresta de Pinho.

Centro *Pinus*. 2016. *Silvicultura: O Futuro é Crescer – Boas Práticas na Floresta de Pinheiro-Bravo*. Porto: Centro *Pinus* – Associação para a Valorização da Floresta de Pinho.

Gonçalves, João, Pedro Teixeira, and Susana Carneiro. 2020. *Valorizar o Pinheiro-Bravo: A Perspetiva de Mercado*. Lisboa: Centro *PINUS*.

Mendes, Amélia, Teresa Fonseca and Jorge Branco. 2017. *Pinhais Bravos: Um Sistema Baseado em Ecogestão de Povoamentos*. Lisboa: Instituto Superior de Agronomia. Accessed September 26, 2024.

https://www.repository.utl.pt/bitstream/10400.5/14258/1/Pinhais%20bravos-sbPbEcoges.pdf.

Centro *PINUS*. 2015. *Manual de Boas Práticas: Melhoria da Gestão do Pinhal Bravo*. Porto: Centro *PINUS*. Accessed September 26, 2024.

https://www.centropinus.org/files/upload/edicoes_tecnicas/manual02.pdf.

Centro *PINUS*. *Centro PINUS – Associação para a Valorização da Floresta de Pinho.* Accessed September 26, 2024. https://www.centropinus.org/.

Centro *PINUS*. 2018. *Silvicultura do Pinhal Bravo: Recomendações Técnicas*. Porto: Centro *PINUS*. Accessed September 26, 2024.

https://www.centropinus.org/files/upload/edicoes_tecnicas/silvicultura-centro-pinus-digital.pdf.

Oliveira, Ângelo Carvalho, João Santos Pereira, and Alexandre Vaz Correia. 2000. *A Silvicultura do Pinheiro Bravo*. Porto: Centro Pinus.

Tomé, Margarida, Susana Barreiro, Joana Amaral Paulo, e Sónia Pacheco Faias. 2007. *Seleção de Equações para Estimação de Variáveis da Árvore em Inventários Florestais a Realizar em Portugal*. Lisboa: Universidade Técnica de Lisboa, Instituto Superior de Agronomia, Centro de Estudos Florestais.

Rodríguez-García, Aida, Rosana López, Juan Antonio Martín, Felix Pinillos, and Luis Gil. 2014. "Resin Yield in *Pinus pinaster* Is Related to Tree Dendrometry, Stand Density, and Tapping-Induced Systemic Changes in Xylem Anatomy." *Forest Ecology and Management* 313: 47–54.

ScienceDirect. 2024. "Pinus Pinaster." Acessed September 24, 2024.

https://www.sciencedirect.com/topics/agricultural-and-biological-sciences/pinus-pinaster.

Fernandes, Paulo, Hermínio Botelho, e Francisco Rego. 2005. "A Piroecologia do Pinheiro Bravo." *Silva Lusitana* 13(2): 233–248.

Gómez-García, Esteban, Teresa F. Fonseca, Felipe Crecente-Campo, Luís R. Almeida, Ulises Diéguez-Aranda, Shongming Huang, and Carlos P. Marques. 2015. "Height-Diameter Models for Maritime Pine in Portugal: A Comparison of Basic, Generalized, and Mixed-Effects Models." *iForest* 9: 72-78.

Alegria, Cristina Maria Martins. 2004. "PBIRROL: Modelo de Crescimento e Produção para os Povoamentos de Pinheiro Bravo de Estrutura Irregular do Concelho de Oleiros." Castelo Branco: Instituto Politécnico de Castelo Branco, Escola Superior Agrária.

Alegria, Cristina Maria Martins. 2007. "Modelos para a Predição de Volumes do Pinheiro Bravo na Região de Castelo Branco." *Agroglobal* 19: 17-18.

Ogana, Friday Nwabueze, Sacramento Corral-Rivas, and José Javier Gorgoso-Varela. 2020. "Nonlinear Mixed-Effect Height-Diameter Model for *Pinus pinaster* Ait. and *Pinus radiata* D. Don." *Cerne* 26(1): 150–161.

Msaouak, Khaoula. 2016. "Modeling Height-Diameter Relationship in *Pinus pinaster* Ait. in the Forest Intervention Zone of Lomba, NE-Portugal." Master's thesis, Escola Superior Agrária, Instituto Politécnico de Bragança.

Barreiro, Susana, João Rua, and Margarida Tomé. 2016. "StandsSIM-MD: A Management Driven Forest Simulator." *Forest Systems* 25(2): eRC07. https://doi.org/10.5424/fs/2016252-08916.

ICNF (Instituto da Conservação da Natureza e das Florestas). 2021. *Plano Nacional de Gestão Integrada de Fogos Rurais (PNGIFR) – Relatório de Progresso 2021*. Lisboa: ICNF. Acessed October 23, 2024. https://www.icnf.pt/api/file/doc/73ec1b0d36d0261f.

ICNF (Instituto da Conservação da Natureza e das Florestas). 2022. *Projeto de (Re)Arborização – Envendos (B50)*. Lisboa: ICNF.

Produtores Florestais. 2024. "As Melhores Opções na Plantação." Acessed November 2, 2024. https://www.produtoresflorestais.pt/as-melhores-opcoes-na-plantacao/.

Centro de Estudos Florestais (CEF). 2022. *FMM5 – Forest Management Model Version 5*. Lisboa: Instituto Superior de Agronomia. Acessed November 3, 2024. https://www.isa.ulisboa.pt/cef/wp-content/uploads/2022/08/FMM5_v2.pdf.

La Billardière, J. J. H. 1800. *Relation du voyage à la recherche de La Pérouse*. Vols. 1, 2, and Atlas. Paris: H. J. Jansen.

La Billardière, J. J. H. 1804–1806. *Novae Hollandiae plantarum specimen*. Vols. 1 and 2. Parisiis: Huzard.

Cabral, J. P. 2019. "A entrada na Europa e a expansão inicial do eucalipto em Portugal Continental." História da Ciência e Ensino: Construindo Interfaces 20: 8–27.

Navigator Company. 2020. “The Newsletter: Junho 2020”

Alves, António Monteiro, João Santos Pereira, e João M. Neves Silva. 2007. *A introdução e a expansão do eucalipto em Portugal*. Lisboa: Instituto Superior de Agronomia.

Instituto da Conservação da Natureza e das Florestas (ICNF). 2021. *6.º Inventário Florestal Nacional: Relatório Final.*

Stape, J. L. 1997. “Planejamento Global e Normatização de Procedimentos Operacionais da Talhadia Simples em Eucalyptus.” *Em Série Técnica IPEF* 11.30: 51-52. (ver p.7).

Marques, H., et al. 2012. *Regiões de Proveniência. Portugal.*

"Rearboreação." *Melhor Eucalipto.* Accessed October 1, 2024. https://www.biond.pt/melhoreucalipto/rearborizacao/.

Peng, C. 2000. "Growth and Yield Models for Uneven-Aged Stands: Past, Present and Future." *Forest Ecology and Management* 132: 259–79.

Vanclay, J. 1994. *Modelling Forest Growth and Yield: Applications to Mixed Tropical Forests.* Wallingford, UK: CAB International.

Tomé, Margarida, Susana Barreiro, Joana Amaral Paulo, and Sónia Pacheco Faias. *Selecção de Equações para Estimação de Variáveis da Árvore em Inventários Florestais a Realizar em Portugal*. Lisbon: Universidade Técnica de Lisboa - Instituto Superior de Agronomia, Centro de Estudos Florestais.

Richards, F. J. 1959. "A Flexible Growth Function for Empirical Use." *Journal of Experimental Botany* 10 (29): 290–300.

Goes, Francisco de Almeida. *Modelação do Crescimento da Árvore Individual de Eucalyptus globulus Labill.* Master's thesis, Instituto Superior de Estatística e Gestão de Informação da Universidade Nova de Lisboa, 2012.

Biond. n.d. "Homepage." Accessed September 24, 2024. https://www.biond.pt/.

Direção-Geral do Território. n.d. "SNIG - Sistema Nacional de Informação Geográfica." Accessed October 2, 2024. https://snig.dgterritorio.gov.pt.

Produtores Florestais. 2023 "Calculadora CO_2." Accessed October 2, 2024. https://produtoresflorestais.pt/calculadora-co2/.

Produtores Florestais. 2023 "Eucalipto Sequestra Mais Carbono." Accessed October 2, 2024. https://produtoresflorestais.pt/eucalipto-sequestra-mais-carbono/.

Navigator Paper. "Get to Know Eucalyptus Better." *Navigator Paper*, 2020. https://navigator-paper.com/en/blog/article/get-to-know-eucalyptus-better.

Caldas, Carlos, e Marlene Marques. *Modelos de Gestão Florestal - Vale do Sousa*. Centro de Estudos Florestais, Instituto Superior de Agronomia, Universidade de Lisboa, 2022.

The Navigator Company. *Exploring Eucalyptus: Environmental, Social, and Economic Impacts in Portugal*. Lisbon: The Navigator Company, June 2020, 5.

Behera, L.K., Lala I.P. Ray, M.R. Nayak, A.A. Mehta, and S.M. Patel. "Carbon Sequestration Potential of *Eucalyptus* spp.: A Review." *e-Planet* 18, no. 1 (2020): 79-84.

Carvalho, Samuel de Pádua Chaves e, Mariana Peres de Lima Chaves e Carvalho, Natalino Calegario, Adriano Ribeiro de Mendonça, Valdir Carlos Lima de Andrade, Marcos Felipe Nicoletti, and Carlos Alberto Silva. 2021. "Modeling Growth of Total Height Using Early Data from Forest Inventories in Fast Growing *Eucalyptus* spp. Plantations." *Advanced Forest Science* 8, no. 3: 1567-1573

Mhamdi, Sameh, Mohamed Tahar Elaieb, Naoufel Souayah, Mariem Khouja, Mohamed Larbi Khouja, Ali Aloui, and Kévin Candelier. 2022. "Growth and Productivity Modeling of Seven Eucalyptus Species in Souiniet's Arboretum in the Northwestern of Tunisia." *Forestist* 72, no. 1: 48–61

Goes, Francisco de Almeida. 2012. Modelação do Crescimento da Árvore Individual de Eucalyptus globulus Labill.

Burkhart, H., and M. Tomé. 2012. Modelling Forest Trees and Stands. Dordrecht: Springer Science+Business Media.

Brealey, Richard A., Stewart C. Myers, and Franklin Allen. 2020. Principles of Corporate Finance. 13th ed. New York: McGraw-Hill Education.

Richards, F. J. 1959. "A Flexible Growth Function for Empirical Use." *Journal of Experimental Botany* 10 (29): 290–300.

Cunha, M. Ricardo F., and Dalila B. M. M. Fontes. "A Real Options Approach to the Valuation of an Investment in Eucalyptus." Lancaster University and Universidade Católica Portuguesa, Faculdade de Economia da Universidade do Porto and LIACC, 2004.

Tomé, Margarida, Susana Barreiro, Joana Amaral Paulo, and Sónia Pacheco Faias. 2007. *Selecção de equações para estimação de variáveis da árvore em inventários florestais a realizar em Portugal*. Centro de Estudos Florestais, Instituto Superior de Agronomia, Universidade Técnica de Lisboa.

Malik, M. S., C. Surendran, and K. Kailasham. 2003. *A Mathematical Model for Predicting the Growth of Eucalyptus Globulus under Agroforestry Plantation*.

Martins, Fabrina Bolzan, Carlos Pedro Boechat Soares, and Gilson Fernandes da Silva. 2014. *Individual Tree Growth Models for Eucalyptus in Northern Brazil*.

Kiernan, D., E. Bevilacqua, and R. Nyland. 2008. “Individual-Tree Diameter Growth Model for Sugar Maple Trees in Uneven-Aged Northern Hardwood Stands under Selection System.” *Forest Ecology and Management* 256: 1579–1586.

Tomé, M., J. Tomé, S. Barreiro, and J. A. Paulo. 2006. “Age-Independent Difference Equations for Modelling Tree and Stand Growth.” *Canadian Journal of Forest Research* 36: 1621–1630.

Peng, Changhui. 1999. *Growth and Yield Models for Uneven-Aged Stands: Past, Present and Future*. Ontario Forest Research Institute, Ministry of Natural Resources.

Matias, Márcia Batalha. 2023. *Sistema de Apoio à Decisão para as Áreas Integradas de Gestão da Paisagem*.

Zhao-gang, L., and L. Feng-ri. 2003. "The Generalized Chapman-Richards Function and Applications to Tree and Stand Growth." *Journal of Forestry Research* 14: 19–26. https://doi.org/10.1007/BF02856757.

Simflor Platform. "StandsSIM." Forest Simulators. https://www.isa.ulisboa.pt/cef/forchange/fctools/en/SimflorPlatform/ForestSimulators/StandsSIM.

National Grid. (n.d.). *How does solar power work?* https://www.nationalgrid.com/stories/energy-explained/how-does-solar-power-work

Aurora Solar. (2024). *Solar panel types: A complete guide*. https://aurorasolar.com/blog/solar-panel-types-guide/

Rediske, G., Siluk, J. C. M., Gastaldo, N. G., Rigo, P. D., & Rosa, C. B. (2023). Determinant factors in site selection for photovoltaic projects: A systematic review. *Renewable Energy*. https://onlinelibrary.wiley.com/doi/full/10.1002/er.4321

Wang, Y., et al. (2020). *Quantum dot solar cells: Challenges and opportunities.* https://www.researchgate.net/publication/278397872_Quantum-Dot-Based_Solar_Cells_Recent_Advances_Strategies_and_Challenges

Lee, J. W., et al. (2021). *Advances in perovskite solar cells: Progress, challenges, and opportunities*. https://onlinelibrary.wiley.com/doi/full/10.1002/inf2.12141

Heo, J., Moon, H., Chang, S., Han, S., & Lee, D.-E. (2021). *Case Study of Solar Photovoltaic Power-Plant Site Selection for Infrastructure Planning Using a BIM-GIS-Based Approach*. https://www.mdpi.com/2076-3417/11/18/8785

Freeing Energy. (2021). *How much land does solar need to generate a megawatt hour?*https://www.freeingenergy.com/math/solar-pv-land-acres-hectares-miles-m118/

SolarGIS. (n.d.). *Free maps and GIS data for Portugal*. SolarGIS. https://solargis.com/resources/free-maps-and-gis-data?locality=portugal

REN. (n.d.). *Eletricidade*. REN - Redes Energéticas Nacionais. https://www.ren.pt/pt-pt/atividade/eletricidade

REN21. (2024). *Renewables 2024 Global Status Report.* https://www.ren21.net/renewables-2024-global-status-report-economic-social-value-creation/

REN. (2024). *Renewables supply 75% of electricity consumption in the first eight months of the year*. https://www.ren.pt/en-gb/media/news/renewables-supply-75-of-electricity-consumption-in-the-first-eight-months-of-the-year

Alharbi, F. H., & Kais, S. (2020). *Theoretical limits of photovoltaics efficiency and possible improvements by intuitive approaches learned from photosynthesis and quantum coherence* https://www.sciencedirect.com/science/article/pii/S136403211401048X

Liu, H., Wu, C., Yu, Y., & Zhao, W. (2023). Effect of solar farms on soil erosion in hilly environments: A modeling study from the perspective of hydrological connectivity. *ResearchGate*. https://www.researchgate.net/publication/376450038_Effect_of_Solar_Farms_on_Soil_Erosion_in_Hilly_Environments_A_Modeling_Study_From_the_Perspective_of_Hydrological_ConnectivityOpenStreetMap. (n.d.). *Portugal/Energia/Subestações*.

OpenStreetMap Wiki.https://wiki.openstreetmap.org/wiki/Portugal/Energia/Subesta%C3%A7%C3%B5es

Smith, J., & Johnson, R. (2024). Evaluating the potential of solar energy in urban areas. *Energy Reports*, 10(3), 123-135. https://onlinelibrary.wiley.com/doi/full/10.1002/er.4321

International Renewable Energy Agency (IRENA). (2021). *Renewable Power Generation Costs 2021*. Retrieved from IRENA

National Renewable Energy Laboratory (NREL). (2022). *Solar Photovoltaic System Performance*. Retrieved from NREL

AGRO.GES - Sociedade de Estudos e Projetos, Lda. 2022. *Sustainability of olive groves in Portugal - Challenges and Responses.* Cascais: Princípia Editora.

Jordão, P. 2014. *Manual Boas Práticas no Olival e no Lagar.* National Institute for Agricultural and Veterinary Research.

European Commission. 2024. *Olive Oil: Agriculture and Rural Development.* Brussels: European Commission.

BPI Research (2023). *A small portrait of the olive oil sector in Portugal.*

National Statistics Institute (INE). 2024. *Agricultural Statistics 2023.* Lisbon: National Statistics Institute.

Oliviculture Economic Analysis. OLIVUM - Associação de Olivicultores e Lagares de Portugal (2024).

Characterization of the olive and olive oil sectors in mainland Portugal (2008).

Comtrade Plus. 2024. *Trade Flow: Olive Oil (Commodity Code 1509) - Import and Export Data for Portugal (2016-2023).*

Pereira, João. 2014. *Manual Boas Práticas no Olival e no Lagar.* Lisbon: Editora Agrícola.

Ferreira, Luís. 2020. *Phenological Growth Stages of Olive Trees.* Madrid: Olive Research Institute.

Oliveira, Ana. 2022. *The Rhythms of the Reproductive Cycle in Olive Varieties.* Coimbra: University of Coimbra.

Silva, Maria, and Costa, Pedro. 2021. *Lifecycle Assessment for Olive Production: A Case Study for the Region of Trás-os-Montes.* Porto: University of Porto.

López-Bernal, Álvaro, and Teresa Villalobos. 2018. *A Linear Model for Predicting Olive Yield Using Root Characteristics.* Madrid: Olive Research Institute.

Fernández, José, and Manuel Hernández. 2021. *A Process-Based Model of Development, Growth, and Yield of Olive Trees.* Sevilla: University of Sevilla Press.

Martin-Verdedor, David, and Sara Parras. 2020. *Trunk Cross-Sectional Area and Yield Estimation in Olive Cultivation.* Lisbon: Olive Cultivation Research Council.

Oliva, Marta, and Luís Silva. 2022. *Tree Canopy Geometry and Olive Yield Estimation Using UAS Imagery.* Coimbra: University of Coimbra.

Sales, Hélia, Filipa Figueiredo, Maria Carlota Vaz Patto, and João Nunes. 2022. "Assessing the Environmental Sustainability of Portuguese Olive Growing Practices from a Life Cycle Assessment Perspective." Journal of Cleaner Production 355: 131692.

El País. 2024. "Olive oil production will grow by almost 50% this season and pave the way for a drop in prices." El País, October 4, 2024. Accessed November 21, 2024. https://elpais.com/economia/2024-10-04/la-produccion-de-aceite-de-oliva-crecera-casi-un-50-esta-campana-y-abre-el-camino-a-una-bajada-de-precios.html.

2024. *Suber Stand Level Simulator.* Accessed 0 15, 2024. https://www.isa.ulisboa.pt/cef/forchange/fctools/en/SimflorPlatform/StandSimulators/Suber.

Biodiversity. 2024. *Cork Oak.* https://biodiversity.com.pt/biogallery/cork-oak/

Quercus. 2024. *A Importância dos montados de sobro em portugal.* Accessed 09 10, 2024. https://quercus.pt/2021/03/a-importancia-dos-montados-de-sobro-em-portugal/

2001. “Decreto-Lei n.º 169/2001, de 25 de maio.” *Diário da República.* 25 05. Accessed 09 11, 2024. https://diariodarepublica.pt/dr/detalhe/decreto-lei/169-2001-332749

ICFN. 2015. “6.º Inventário Florestal Nacional (IFN6).”

Amorim Cork Composites. 2024. Accessed 09 10, 2024. https://amorimcorkcomposites.com/pt/

Matias, Magda. 2008. “A IMPORTÂNCIA DOS MONTADOS PARA O DESENVOLVIMENTO RURAL NO DISTRITO DE BEJA: IDENTIFICAÇÃO DOS FACTORES DE DEGRADAÇÃO. CASO-ESTUDO-HERDADE DO REGUENGO GRANDE E HERDADE DO BEBEDOURO.”

AFINET. 2019. “Post-Fire Management of Cork Oak Forest (Quercus suber).” *EURAF.* 08. Accessed 10 03, 2024. https://euraf.isa.utl.pt/files/pub/20191119_factsheet_37_en_web.pdf

ICNF. 2012. "Regiões de Proveniência." 30 01. Accessed 09 13, 2024. https://www.icnf.pt/api/file/doc/7eba73fd7d9976f1

Silva, Conceição Santos, and Teresa Soares David. 2020. "Sobreiro: a árvore mãe da cortiça." *florestas.pt.* 22 09. Accessed 09 12, 2024. https://florestas.pt/conhecer/sobreiro-a-mae-da-cortica/

Paulo, Joana Amaral. 2024. *Calibre e qualidade condicionam preço da cortiça.* Accessed 09 17, 2024. https://florestas.pt/valorizar/calibre-e-qualidade-condicionam-preco-da-cortica/.

APCOR. 2024. Accessed 09 10, 2024. https://apcor.pt/

Paulo, Joana Amaral, João H. N. Palma, Alberto Azevedo Gomes, Sónia Pacheco Faias, José Tomé, and Margarida Tomé. 2014. "Predicting site index from climate and soil variables for cork oak (Quercus suber L.) stands in Portugal." *New Forests* 293–307.

Owens, P. R., and E. M. Rutledge. 2005. "Horizons." In *Encyclopedia of Soils in the Environment*.

Sánchez-González, Mariola, Margarida Tomé, and Gregorio Montero. 2005. "Modelling height and diameter growth of dominant cork oak trees in Spain." *Annals of Forest Science* 355–364.

Paulo, Joana Amaral, José Tomé, and Margarida Tomé. 2011. "Nonlinear fixed and random generalized height–diameter models for Portuguese cork oak stands." *Annals of Forest Science* 295–309.

Paulo, Joana Amaral, and Margarida Tomé. 2006. "Equações para Estimação do Volume e Biomassa de Duas Espécies de Carvalhos: Quercus suber e Quercus ilex."

Paulo, Joana Amaral, and Margarida Tomé. 2010. "Predicting mature cork biomass with t years of growth from one measurement." *Forest Ecology and Management* 1993–2005.

Almeida, Alice M., José Tomé, and Margarida Tomé. 2010. "Development of a system to predict the evolution of individual tree mature cork." *Forest Ecology and Management* 1303–1314.

Paulo, Joana Amaral, and Margarida Tomé. 2014. "Estimativa das Produções de Cortiça Virgem Resultantes das Operações de Desbastes e Desboia em Montados de Sobro em Fase Juvenil." *Silva Lusitana* 29-42.

Paulo, J. A., and M. Tomé. 2005. *Modelo Probabilístico Independente da Distância para Implementação de Desbastes em.* SPCF.

Fonseca, Teresa, Luísa Monteiro, Teresa Enes, and Adelaide Cerveira. 2017. "Self-thinning dynamics in cork oak woodlands: providing a baseline." *Forest Systems* 26(1), e006, 10 pages.

González-García, Sara, Ana Cláudia Dias, and Luís Arroja. 2013. "Life-cycle assessment of typical Portuguese cork oak woodlands." *Science of the Total Environment* 355–364.

Paulo, Joana Amaral. 2011. *Desenvolvimento de um sistema para apoio à gestão sustentável de montados de sobro.* Lisboa: Universidade Técnica de Lisboa, Instituto Superior de Agronomia.

Tomé, Margarida. 2004. "Modelo de crescimento e produção para a gestão do montado de sobro em Portugal."

2024. UNAC. Acedido em 12 de 10 de 2024. https://www.unac.pt/.

2024. *CAOF - Comissão de Acompanhamento para as Operações Florestais.* Accessed 10 12, 2024. https://www.dgadr.gov.pt/mecanizacao/caof.

National Grid. 2023. *How does solar power work?* https://www.nationalgrid.com/stories/energy-explained/how-does-solar-power-work

Alharbi, F. H., & Kais, S. 2020. *Theoretical limits of photovoltaics efficiency and possible improvements by intuitive approaches learned from photosynthesis and quantum coherence* https://www.sciencedirect.com/science/article/pii/S136403211401048X

Aurora Solar. 2024. *Solar panel types: A complete guide*. https://aurorasolar.com/blog/solar-panel-types-guide/

Lafayette College. 2014. *History of PV Technology*. Lafayette College: Technology and the Environment. Retrieved from https://sites.lafayette.edu/egrs352-sp14-pv/technology/history-of-pv-technology/

Istafaul et al. 2018. *Frontiers, opportunities, and challenges in perovskite solar cells: A critical review* https://onlinelibrary.wiley.com/doi/full/10.1002/inf2.12141

Wang, Y., et al. 2020. *Quantum dot solar cells: Challenges and opportunities.* *https://www.researchgate.net/publication/278397872_Quantum-Dot-Based_Solar_Cells_Recent_Advances_Strategies_and_Challenges*

Photonic Universe. 2024. https://www.photonicuniverse.com/en/resources/articles/full/7.html

Anker Solix. 2024. https://www.anker.com/blogs/solar/solar-panel-calculation

GridX. *What is a grid operator?* GridX. https://www.gridx.ai/knowledge/what-is-a-grid-operator

Portugal/Energia/Subestações. OpenStreetMap Wiki. https://wiki.openstreetmap.org/wiki/Portugal/Energia/Subesta%C3%A7%C3%B5es

REN. 2024. *Renewables supply 75% of electricity consumption in the first eight months of the year*. https://www.ren.pt/en-gb/media/news/renewables-supply-75-of-electricity-consumption-in-the-first-eight-months-of-the-year

Santos, B. 2022 *Portugal added 546 MW of solar in H1*. Pv Magazine International. https://www.pv-magazine.com/2022/09/02/portugal-registered-546-mw-of-solar-in-h1/

Myllyvirta, L. 2024. *Analysis: Clean energy was top driver of China's economic growth in 2023*. Carbon Brief. https://www.carbonbrief.org/analysis-clean-energy-was-top-driver-of-chinas-economic-growth-in-2023/

Platform, C. A. 2024. *China's solar panel boom is making solar energy more affordable - Climate Adaptation platform*. Climate Adaptation Platform. https://climateadaptationplatform.com/chinas-solar-panel-boom-is-making-solar-energy-more-affordable/

BloombergNEF. 2023. *3Q 2023 Global PV Market Outlook | BloombergNEF*. https://about.bnef.com/blog/3q-2023-global-pv-market-outlook/

ABN AMRO Bank. 2022. *The rise of Power Purchase Agreements*. https://www.abnamro.com/research/en/our-research/the-rise-of-power-purchase-agreements-ppas

Market.us. 2024. *Power Purchase Agreement Market Size | CAGR of 31.7%*. https://market.us/report/power-purchase-agreement-market/

Hasti et al. 2023. *Optimal solar photovoltaic site selection using geographic information system–based modeling techniques and assessing environmental and economic impacts: The case of Kurdistan.* https://www.sciencedirect.com/science/article/pii/S0038092X23004322

MacDonald, M. 2017. https://cms.eirgrid.ie/sites/default/files/publications/Solar-Farm-Clearances-Report-Rev-A.PDF

Li, X et al. 2023. *An interaction model applied to optimize photovoltaic farm location: A case study of China.* https://www.sciencedirect.com/science/article/pii/S0306261923017853?ref=cra_js_challenge&fr=RR-1

Kim, Y et al. 2022. *United States solar investment: A feasibility study of solar farms in Kentucky.* https://www.mdpi.com/2673-9941/2/4/28

Rediske, G. et al. 2018. *Determinant factors in site selection for photovoltaic projects: A systematic review.* https://onlinelibrary.wiley.com/doi/abs/10.1002/er.4321

Liu, H et al. 2023. *Effect of solar farms on soil erosion in hilly environments: A modeling study from the perspective of hydrological connectivity.* https://www.researchgate.net/publication/376450038_Effect_of_Solar_Farms_on_Soil_Erosion_in_Hilly_Environments_A_Modeling_Study_From_the_Perspective_of_Hydrological_Connectivity

Alhammad, A. et al. 2022. *Optimal solar plant site identification using GIS and remote sensing: Framework and case study.* https://www.mdpi.com/1996-1073/15/1/312

Khan, M. et al. 2017. *Effect of temperature on performance of solar panels: Analysis.* https://ieeexplore.ieee.org/document/8455109

SolarGIS. *Free maps and GIS data for Portugal*. SolarGIS. https://solargis.com/resources/free-maps-and-gis-data?locality=portugal

Admin_Gbsolar. 2024. *How much Photovoltaics in 1 Hectare?* GBSOLAR. https://gbsolar.it/en/how-much-photovoltaic-in-1-acre/

Freeing Energy. 2021. *How much land does solar need to generate a megawatt hour?*https://www.freeingenergy.com/math/solar-pv-land-acres-hectares-miles-m118/

Heo, J. et al. 2021. *Case Study of Solar Photovoltaic Power-Plant Site Selection for Infrastructure Planning Using a BIM-GIS-Based Approach*. https://www.mdpi.com/2076-3417/11/18/8785

De Rooij, D. 2023. *Solar Panel Direction: what direction should solar panels face?* Sinovoltaics (Hong Kong Office). https://sinovoltaics.com/learning-center/system-design/solar-panel-direction-what-direction-should-solar-panels-face/

Katherine Tweed. 2013. from Green Tech Media http://www.greentechmedia.com/articles/read/are-solar-panels-facing-the-wrong-direction.

Future Energy GO. 2024. PPA Price Trends Q1 2024: Power Purchase Agreement Price Trends Revealed. https://futureenergygo.com/ppa-price-trends-q1-2024/

Appendix

Appendix II - Mação

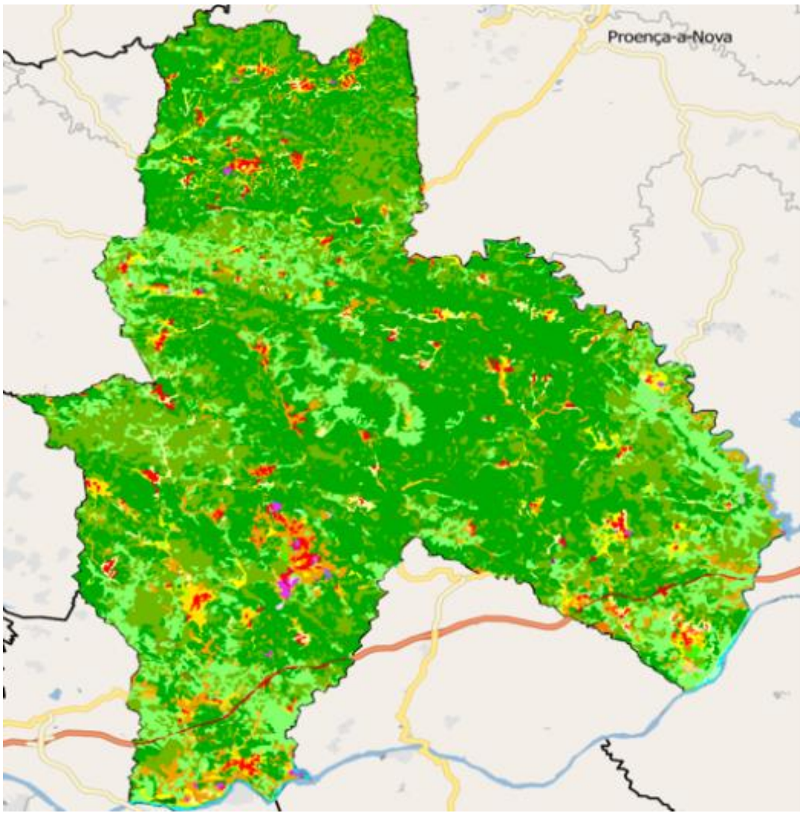

Figure II.1: COS Map | Source: Matias 2023

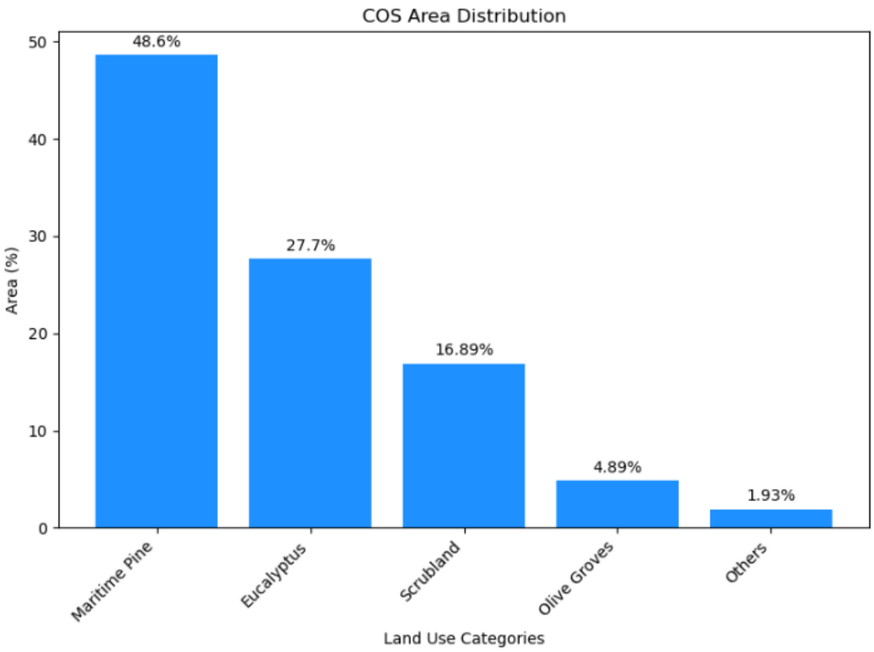

Figure II.2: COS Area distribution

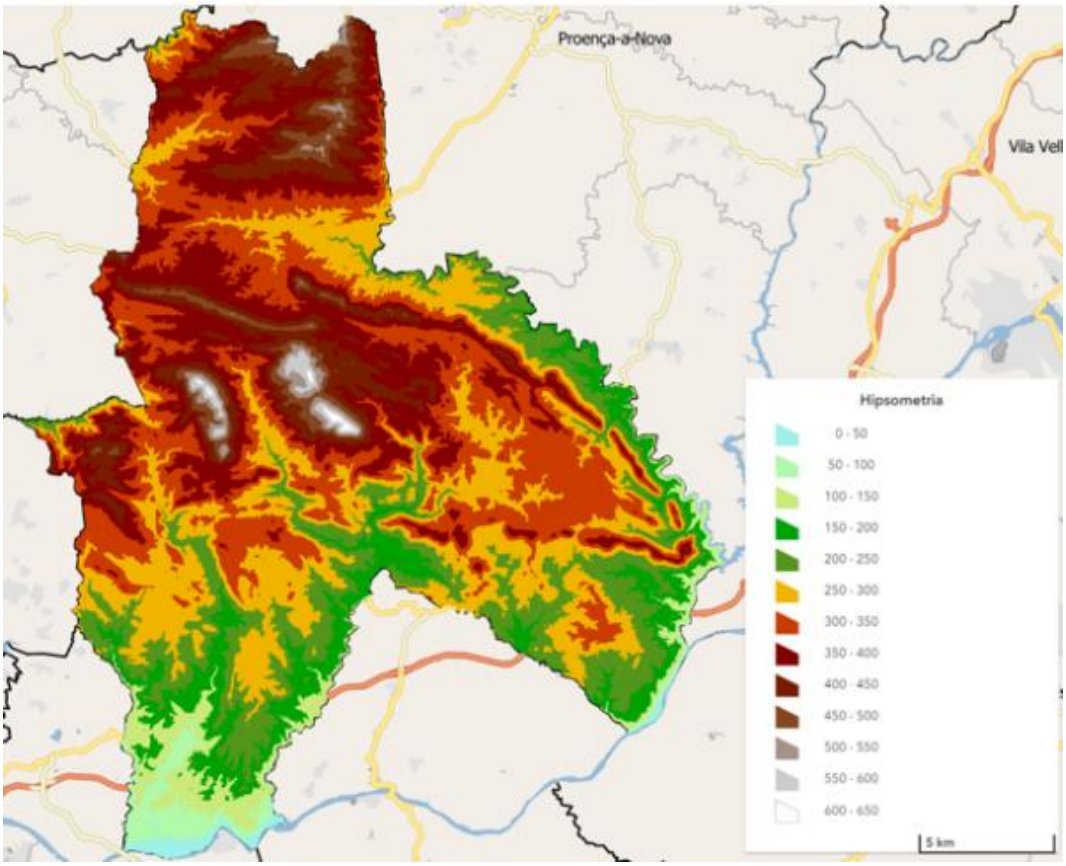

Figure II.3: Hypsometry in Mação

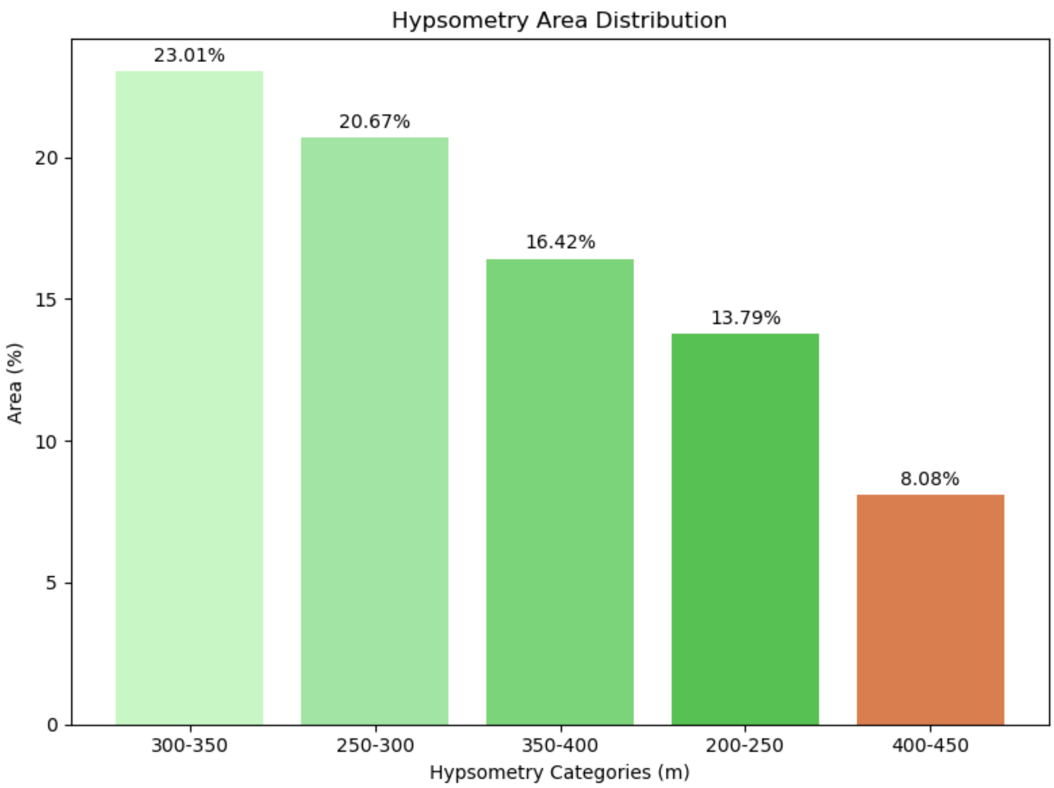

Figure II.4: Map Hypsometry in Mação | Source: Matias 2023

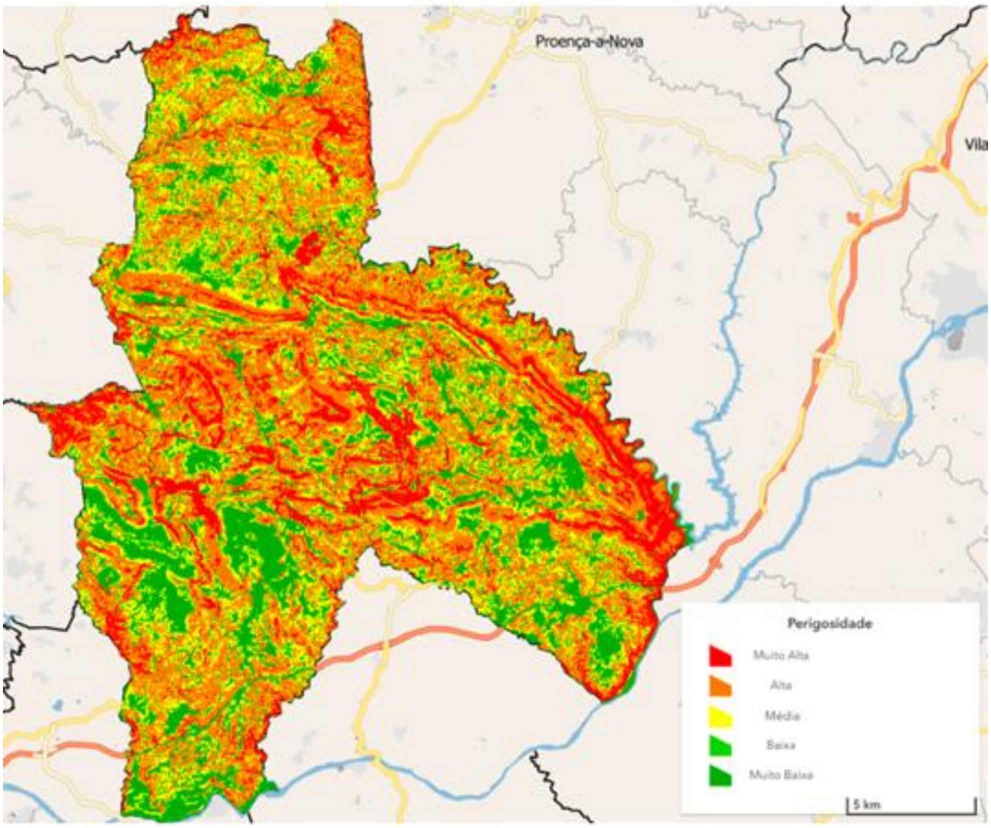

Figure II.5: COS Hypsometry in Mação

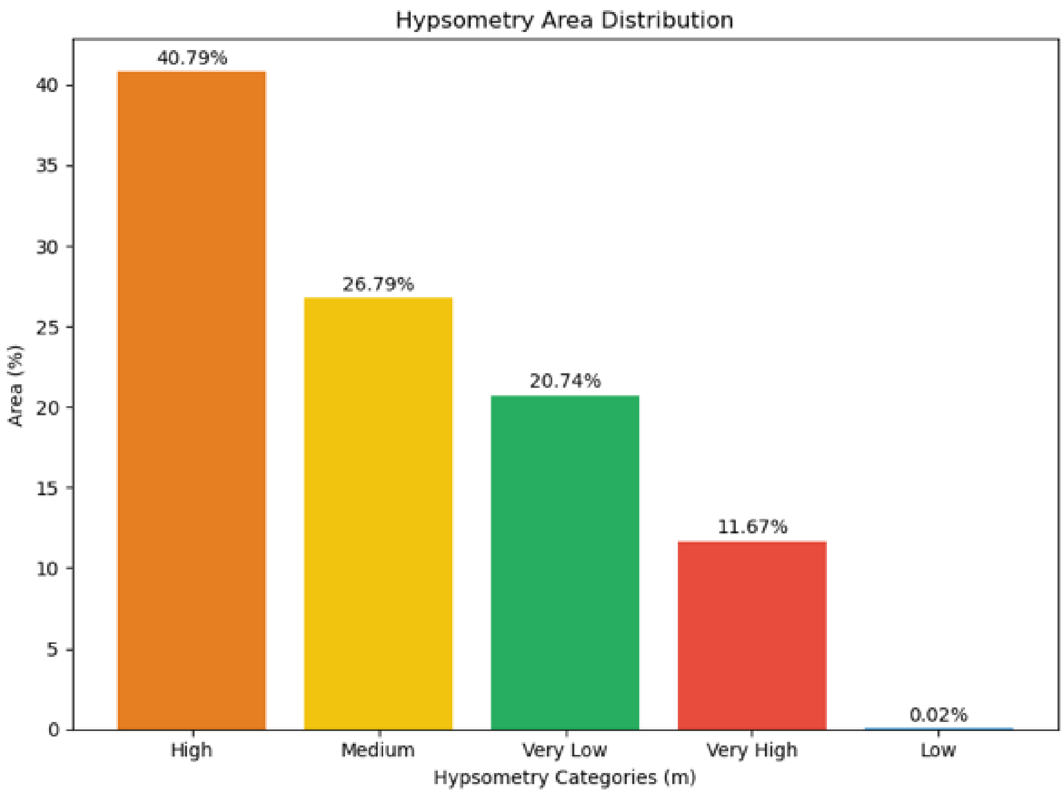

Figure II.6: COS Map Mação | Source: Matias 2023

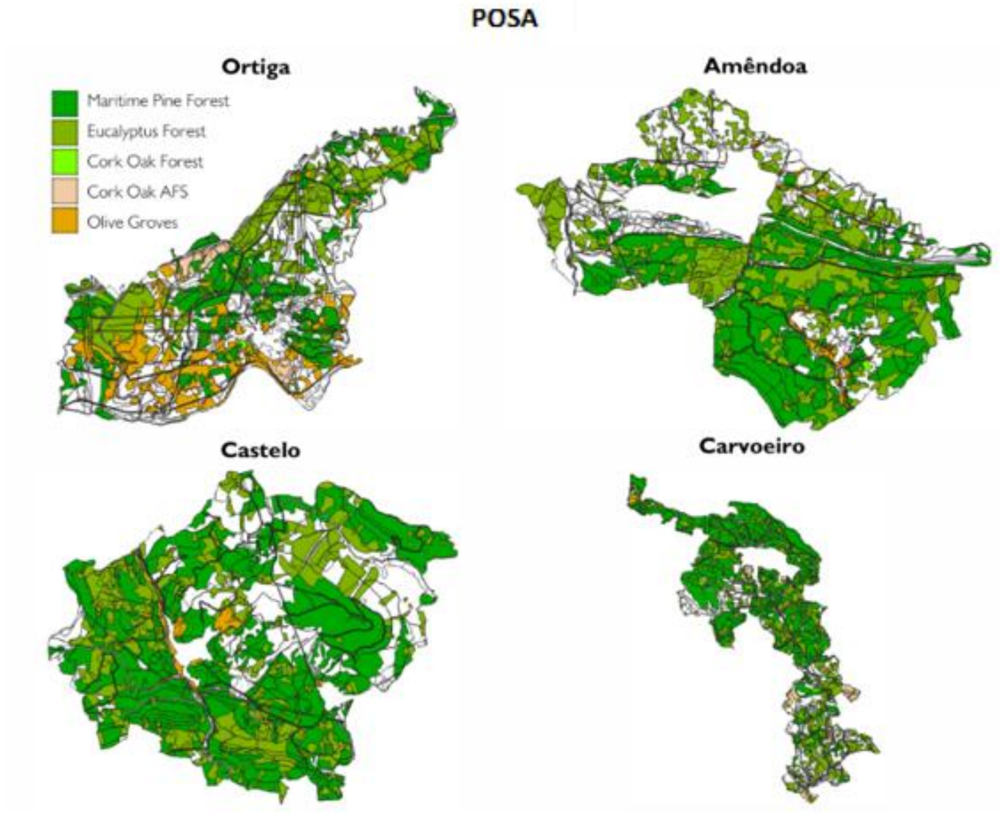

Figure II.7: Current Land Use Map in four specific AIGPS

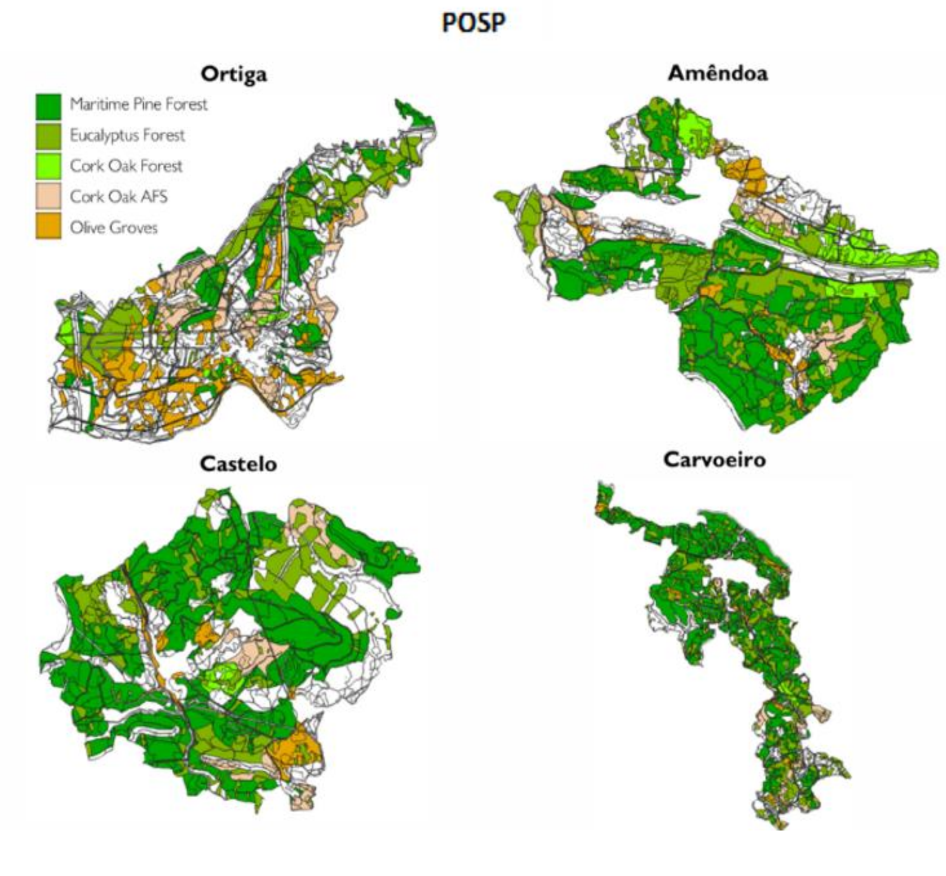

Figure II.8: Proposed Land Use Map in four specific AIGPs

Appendix IV – StandsSIM

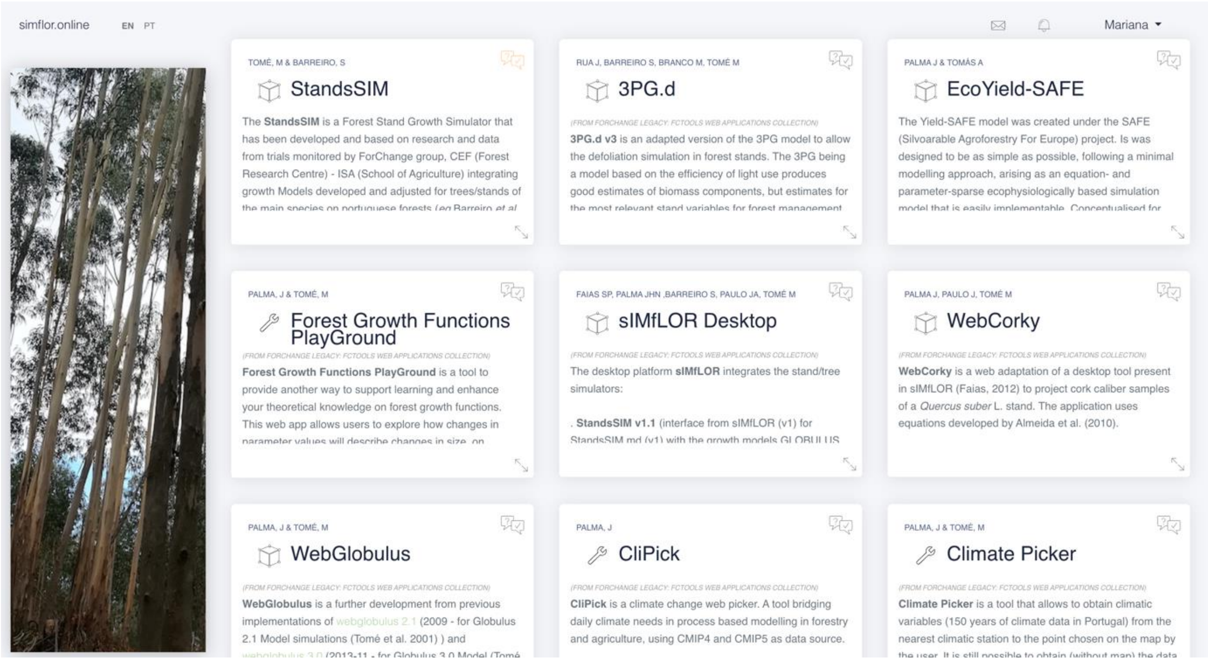

Figure IV.1 – Online Simflor Interface

id_stand	id_presc	year	Thinning	Debark	t	0	5	10	15	20	25	30	35	40	45	50	55	60	65	70	75	80
MACAO_5	ID1	2024	0	0	0.0	0.	0.	0.	0.	0.	0.	0.	0.	0.	0.	0.	0.	0.	0.	0.	0.	0.
MACAO_5	ID1	2025	0	0	1.0	0.	0.	0.	0.	0.	0.	0.	0.	0.	0.	0.	0.	0.	0.	0.	0.	0.
MACAO_5	ID1	2026	0	0	2.0	0.	0.	0.	0.	0.	0.	0.	0.	0.	0.	0.	0.	0.	0.	0.	0.	0.
MACAO_5	ID1	2027	0	0	3.0	0.	0.	0.	0.	0.	0.	0.	0.	0.	0.	0.	0.	0.	0.	0.	0.	0.
MACAO_5	ID1	2028	0	0	4.0	0.	0.	0.	0.	0.	0.	0.	0.	0.	0.	0.	0.	0.	0.	0.	0.	0.
MACAO_5	ID1	2029	0	0	5.0	0.	0.	0.	0.	0.	0.	0.	0.	0.	0.	0.	0.	0.	0.	0.	0.	0.
MACAO_5	ID1	2030	0	0	6.0	0.	0.	0.	0.	0.	0.	0.	0.	0.	0.	0.	0.	0.	0.	0.	0.	0.
MACAO_5	ID1	2031	0	0	7.0	0.	0.	0.	0.	0.	0.	0.	0.	0.	0.	0.	0.	0.	0.	0.	0.	0.
MACAO_5	ID1	2032	0	0	8.0	0.	0.	0.	0.	0.	0.	0.	0.	0.	0.	0.	0.	0.	0.	0.	0.	0.
MACAO_5	ID1	2033	0	0	9.0	0.	0.	0.	0.	0.	0.	0.	0.	0.	0.	0.	0.	0.	0.	0.	0.	0.
MACAO_5	ID1	2034	0	0	10.0	0.	0.	0.	0.	0.	0.	0.	0.	0.	0.	0.	0.	0.	0.	0.	0.	0.
MACAO_5	ID1	2035	0	0	11.0	0.	0.	0.	0.	0.	0.	0.	0.	0.	0.	0.	0.	0.	0.	0.	0.	0.
MACAO_5	ID1	2036	0	0	12.0	0.	0.	0.	0.	0.	0.	0.	0.	0.	0.	0.	0.	0.	0.	0.	0.	0.
MACAO_5	ID1	2037	0	0	13.0	0.	0.	0.	0.	0.	0.	0.	0.	0.	0.	0.	0.	0.	0.	0.	0.	0.
MACAO_5	ID1	2038	0	0	14.0	0.	0.	0.	0.	0.	0.	0.	0.	0.	0.	0.	0.	0.	0.	0.	0.	0.
MACAO_5	ID1	2039	0	0	15.0	0.	0.	0.	0.	0.	0.	0.	0.	0.	0.	0.	0.	0.	0.	0.	0.	0.
MACAO_5	ID1	2040	0	0	16.0	0.	0.	0.	0.	0.	0.	0.	0.	0.	0.	0.	0.	0.	0.	0.	0.	0.
MACAO_5	ID1	2041	0	0	17.0	0.	1470.	0.	0.	0.	0.	0.	0.	0.	0.	0.	0.	0.	0.	0.	0.	0.
MACAO_5	ID1	2042	0	0	18.0	0.	1390.	80.	0.	0.	0.	0.	0.	0.	0.	0.	0.	0.	0.	0.	0.	0.
MACAO_5	ID1	2043	0	0	19.0	0.	1390.	80.	0.	0.	0.	0.	0.	0.	0.	0.	0.	0.	0.	0.	0.	0.
MACAO_5	ID1	2044	0	0	20.0	0.	1040.	430.	0.	0.	0.	0.	0.	0.	0.	0.	0.	0.	0.	0.	0.	0.
MACAO_5	ID1	2045	0	0	21.0	0.	710.	760.	0.	0.	0.	0.	0.	0.	0.	0.	0.	0.	0.	0.	0.	0.
MACAO_5	ID1	2046	0	0	22.0	0.	180.	1290.	0.	0.	0.	0.	0.	0.	0.	0.	0.	0.	0.	0.	0.	0.
MACAO_5	ID1	2047	0	0	23.0	0.	0.	1470.	0.	0.	0.	0.	0.	0.	0.	0.	0.	0.	0.	0.	0.	0.
MACAO_5	ID1	2048	0	0	24.0	0.	0.	1470.	0.	0.	0.	0.	0.	0.	0.	0.	0.	0.	0.	0.	0.	0.
MACAO_5	ID1	2049	0	0	25.0	0.	0.	1470.	0.	0.	0.	0.	0.	0.	0.	0.	0.	0.	0.	0.	0.	0.
MACAO_5	ID1	2050	0	0	26.0	0.	0.	1470.	0.	0.	0.	0.	0.	0.	0.	0.	0.	0.	0.	0.	0.	0.
MACAO_5	ID1	2051	0	0	27.0	0.	0.	1390.	80.	0.	0.	0.	0.	0.	0.	0.	0.	0.	0.	0.	0.	0.
MACAO_5	ID1	2052	0	0	28.0	0.	0.	1390.	80.	0.	0.	0.	0.	0.	0.	0.	0.	0.	0.	0.	0.	0.
MACAO_5	ID1	2053	0	0	29.0	0.	0.	1290.	180.	0.	0.	0.	0.	0.	0.	0.	0.	0.	0.	0.	0.	0.
MACAO_5	ID1	2054	0	0	30.0	0.	0.	1110.	360.	0.	0.	0.	0.	0.	0.	0.	0.	0.	0.	0.	0.	0.
MACAO_5	ID1	2055	0	0	31.0	0.	0.	980.	490.	0.	0.	0.	0.	0.	0.	0.	0.	0.	0.	0.	0.	0.
MACAO_5	ID1	2056	0	0	32.0	0.	0.	840.	630.	0.	0.	0.	0.	0.	0.	0.	0.	0.	0.	0.	0.	0.
MACAO_5	ID1	2057	0	0	33.0	0.	0.	710.	760.	0.	0.	0.	0.	0.	0.	0.	0.	0.	0.	0.	0.	0.
MACAO_5	ID1	2058	0	0	34.0	0.	0.	560.	910.	0.	0.	0.	0.	0.	0.	0.	0.	0.	0.	0.	0.	0.
MACAO_5	ID1	2059	0	0	35.0	0.	0.	180.	1290.	0.	0.	0.	0.	0.	0.	0.	0.	0.	0.	0.	0.	0.
MACAO_5	ID1	2060	0	0	36.0	0.	0.	180.	1210.	80.	0.	0.	0.	0.	0.	0.	0.	0.	0.	0.	0.	0.
MACAO_5	ID1	2061	0	0	37.0	0.	0.	0.	1390.	80.	0.	0.	0.	0.	0.	0.	0.	0.	0.	0.	0.	0.
MACAO_5	ID1	2061	1	0	37.0	0.	0.	0.	1010.	80.	0.	0.	0.	0.	0.	0.	0.	0.	0.	0.	0.	0.
MACAO_5	ID1	2062	0	0	38.0	0.	0.	0.	1010.	80.	0.	0.	0.	0.	0.	0.	0.	0.	0.	0.	0.	0.
MACAO_5	ID1	2063	0	0	39.0	0.	0.	0.	960.	130.	0.	0.	0.	0.	0.	0.	0.	0.	0.	0.	0.	0.
MACAO_5	ID1	2064	0	0	40.0	0.	0.	0.	910.	180.	0.	0.	0.	0.	0.	0.	0.	0.	0.	0.	0.	0.
MACAO_5	ID1	2065	0	0	41.0	0.	0.	0.	840.	250.	0.	0.	0.	0.	0.	0.	0.	0.	0.	0.	0.	0.
MACAO_5	ID1	2066	0	0	42.0	0.	0.	0.	730.	360.	0.	0.	0.	0.	0.	0.	0.	0.	0.	0.	0.	0.
MACAO_5	ID1	2067	0	0	43.0	0.	0.	0.	660.	430.	0.	0.	0.	0.	0.	0.	0.	0.	0.	0.	0.	0.
MACAO_5	ID1	2068	0	0	44.0	0.	0.	0.	600.	490.	0.	0.	0.	0.	0.	0.	0.	0.	0.	0.	0.	0.
MACAO_5	ID1	2069	0	0	45.0	0.	0.	0.	600.	410.	80.	0.	0.	0.	0.	0.	0.	0.	0.	0.	0.	0.

Figure IV.2 – StandsSIM output file: output_dd

id_stand	id_presc	ttotal	S	NPV	EAA	0.030	0.040	0.050	0.000	0.000	maiV	Vharv	Vuharv
MACAO_5	ID1	36	15.4	-716.6	-38.4	-20.0	-38.4	-57.4	0.0	0.0	11.2	160.2	129.5
MACAO_med	ID1	36	20.7	1603.0	85.9	110.1	85.9	61.1	0.0	0.0	20.9	311.9	256.6
MACAO_95	ID1	36	25.9	5211.4	279.2	312.9	279.2	245.1	0.0	0.0	36.2	550.9	458.2

Figure IV.3 – StandsSIM output file: output_npv

id_stand	S	AreaUG	id_presc	FMA	opt	year	ttotal	t	rot	FinalCut	Thinning	Debark	hdom	Nst	N	Ndead	N_ing	Fw	G	dg	Vu_st	Vb_st	Vst	V	V_as1	V_as2	V_as3	V_as4	V_as5	Vu_as1	Vu_as2	Vu_as3	Vu_as4	Vu_as5	Vharv	Vuharv	Vtot	maiV	iV	Ww	Wb
MACAO_5	15.44	1.00	ID1	4	1	2024	0	0.0	1	0	0	0	0.0	1250.	1250.	0.	0.	0.00	0.0	0.0	0.0	0.0	0.0	0.0	0.0	0.0	0.0	0.0	0.0	0.0	0.0	0.0	0.0	0.0	0.0	0.0	0.0	0.0		0.0	0.0
MACAO_5	15.44	1.00	ID1	4	1	2025	1	1.0	1	0	0	0	4.1	1250.	1250.	0.	0.	0.68	0.1	1.1	0.2	0.0	0.0	0.2	0.0	0.0	0.0	0.0	0.0	0.0	0.0	0.0	0.0	0.0	0.0	0.0	0.2	0.2	0.2	0.1	0.0
MACAO_5	15.44	1.00	ID1	4	1	2026	2	2.0	1	0	0	0	7.2	1250.	1250.	0.	0.	0.39	0.7	2.7	1.8	0.5	0.1	2.4	0.0	0.0	0.0	0.0	0.0	0.0	0.0	0.0	0.0	0.0	0.0	0.0	2.4	1.2	2.2	0.7	0.1
MACAO_5	15.44	1.00	ID1	4	1	2027	3	3.0	1	0	0	0	9.3	1250.	1250.	0.	0.	0.30	1.7	4.1	5.3	1.4	0.2	7.0	0.0	0.0	0.0	0.0	0.0	0.0	0.0	0.0	0.0	0.0	0.0	0.0	7.0	2.3	4.6	2.4	0.3
MACAO_5	15.44	1.00	ID1	4	1	2028	4	4.0	1	0	0	0	10.8	1233.	1233.	17.	0.	0.26	2.8	5.3	10.1	2.6	0.3	13.0	0.0	0.0	0.0	0.0	0.0	0.0	0.0	0.0	0.0	0.0	0.0	0.0	13.0	3.3	6.1	4.7	0.6
MACAO_5	15.44	1.00	ID1	4	1	2029	5	5.0	1	0	0	0	12.0	1217.	1217.	16.	0.	0.24	3.9	6.4	15.6	3.9	0.5	20.0	0.0	0.0	0.0	0.0	0.0	0.0	0.0	0.0	0.0	0.0	0.0	0.0	20.0	4.0	7.0	7.4	0.9
MACAO_5	15.44	1.00	ID1	4	1	2030	6	6.0	1	0	0	0	12.9	1201.	1201.	16.	0.	0.22	4.9	7.2	21.5	5.3	0.6	27.4	0.0	0.0	0.0	0.0	0.0	0.0	0.0	0.0	0.0	0.0	0.0	0.0	27.4	4.6	7.4	10.5	1.3
MACAO_5	15.44	1.00	ID1	4	1	2031	7	7.0	1	0	0	0	13.7	1185.	1185.	16.	0.	0.21	6.0	8.0	27.5	6.7	0.7	35.0	0.0	0.0	0.0	0.0	0.0	0.0	0.0	0.0	0.0	0.0	0.0	0.0	35.0	5.0	7.6	13.7	1.7
MACAO_5	15.44	1.00	ID1	4	1	2032	8	8.0	1	0	0	0	14.4	1169.	1169.	16.	0.	0.20	7.0	8.7	33.6	8.1	0.8	42.5	0.0	0.0	0.0	0.0	0.0	0.0	0.0	0.0	0.0	0.0	0.0	0.0	42.5	5.3	7.6	17.0	2.2
MACAO_5	15.44	1.00	ID1	4	1	2033	9	9.0	1	0	0	0	14.9	1153.	1153.	16.	0.	0.20	7.9	9.4	39.5	9.5	1.0	50.0	0.0	0.0	0.0	0.0	0.0	0.0	0.0	0.0	0.0	0.0	0.0	0.0	50.0	5.6	7.4	20.2	2.6
MACAO_5	15.44	1.00	ID1	4	1	2034	10	10.0	1	0	0	0	15.4	1138.	1138.	15.	0.	0.19	8.8	9.9	45.4	10.8	1.1	57.3	0.0	0.0	0.0	0.0	0.0	0.0	0.0	0.0	0.0	0.0	0.0	0.0	57.3	5.7	7.3	23.5	3.0
MACAO_5	15.44	1.00	ID1	4	1	2035	11	11.0	1	0	0	0	15.9	1123.	1123.	15.	0.	0.19	9.7	10.5	51.1	12.1	1.2	64.3	0.0	0.0	0.0	0.0	0.0	0.0	0.0	0.0	0.0	0.0	0.0	0.0	64.3	5.8	7.1	26.6	3.5
MACAO_5	15.44	1.00	ID1	4	1	2036	12	12.0	1	0	0	0	16.3	1108.	1108.	15.	0.	0.18	10.5	11.0	56.5	13.3	1.3	71.2	0.0	0.0	0.0	0.0	0.0	0.0	0.0	0.0	0.0	0.0	0.0	0.0	71.2	5.9	6.8	29.7	3.9
MACAO_5	15.44	1.00	ID1	4	1	2037	13	13.0	1	1	0	0	16.7	1093.	1093.	15.	0.	0.18	11.3	11.4	61.9	14.5	1.4	77.8	0.0	0.0	0.0	0.0	0.0	0.0	0.0	0.0	0.0	0.0	71.9	58.2	77.8	6.0	6.6	32.7	4.3
MACAO_5	15.44	1.00	ID1	4	1	2037	13	0.0	1	0	0	0	0.0	0.	0.	0.	0.	0.00	0.0	0.0	0.0	0.0	0.0	0.0	0.0	0.0	0.0	0.0	0.0	0.0	0.0	0.0	0.0	0.0	0.0	0.0	0.0			0.0	0.0
MACAO_5	15.44	1.00	ID1	4	1	2038	14	1.0	2	0	0	0	4.1	875.	4019.	0.	0.	0.38	0.1	0.7	0.2	0.1	0.0	0.3	0.0	0.0	0.0	0.0	0.0	0.0	0.0	0.0	0.0	0.0	0.0	0.0	78.0	5.6	0.3	0.1	0.0
MACAO_5	15.44	1.00	ID1	4	1	2039	15	2.0	2	0	0	0	7.2	875.	4019.	0.	0.	0.22	1.3	2.1	3.3	0.9	0.1	4.3	0.0	0.0	0.0	0.0	0.0	0.0	0.0	0.0	0.0	0.0	0.0	0.0	82.1	5.5	4.1	1.4	0.2
MACAO_5	15.44	1.00	ID1	4	1	2039	15	2.0	2	0	1	0	7.2	875.	1050.	0.	0.	0.43	0.6	2.7	1.4	0.4	0.1	1.9	0.0	0.0	0.0	0.0	0.0	0.0	0.0	0.0	0.0	0.0	0.0	0.0	82.1	5.5	4.1	0.6	0.1
MACAO_5	15.44	1.00	ID1	4	1	2040	16	3.0	2	0	0	0	9.3	875.	1050.	0.	0.	0.33	1.3	4.0	4.2	1.1	0.2	5.5	0.0	0.0	0.0	0.0	0.0	0.0	0.0	0.0	0.0	0.0	0.0	0.0	85.6	5.4	3.6	1.8	0.2
MACAO_5	15.44	1.00	ID1	4	1	2041	17	4.0	2	0	0	0	10.8	864.	1039.	11.	0.	0.29	2.2	5.2	8.0	2.0	0.3	10.3	0.0	0.0	0.0	0.0	0.0	0.0	0.0	0.0	0.0	0.0	0.0	0.0	90.5	5.3	4.8	3.6	0.4
MACAO_5	15.44	1.00	ID1	4	1	2042	18	5.0	2	0	0	0	12.0	854.	1028.	11.	0.	0.26	3.1	6.1	12.4	3.1	0.4	15.9	0.0	0.0	0.0	0.0	0.0	0.0	0.0	0.0	0.0	0.0	0.0	0.0	96.1	5.3	5.6	5.8	0.7
MACAO_5	15.44	1.00	ID1	4	1	2043	19	6.0	2	0	0	0	12.9	843.	1018.	11.	0.	0.24	3.9	7.0	17.2	4.2	0.5	21.9	0.0	0.0	0.0	0.0	0.0	0.0	0.0	0.0	0.0	0.0	0.0	0.0	102.1	5.4	6.0	8.3	1.0
MACAO_5	15.44	1.00	ID1	4	1	2044	20	7.0	2	0	0	0	13.7	833.	1007.	10.	0.	0.23	4.8	7.8	22.1	5.4	0.6	28.1	0.0	0.0	0.0	0.0	0.0	0.0	0.0	0.0	0.0	0.0	0.0	0.0	108.2	5.4	6.2	10.9	1.3
MACAO_5	15.44	1.00	ID1	4	1	2045	21	8.0	2	0	0	0	14.4	823.	997.	10.	0.	0.22	5.6	8.5	27.1	6.5	0.7	34.3	0.0	0.0	0.0	0.0	0.0	0.0	0.0	0.0	0.0	0.0	0.0	0.0	114.5	5.5	6.3	13.5	1.7
MACAO_5	15.44	1.00	ID1	4	1	2046	22	9.0	2	0	0	0	14.9	813.	986.	10.	0.	0.21	6.4	9.1	32.1	7.7	0.8	40.6	0.0	0.0	0.0	0.0	0.0	0.0	0.0	0.0	0.0	0.0	0.0	0.0	120.7	5.5	6.2	16.2	2.0
MACAO_5	15.44	1.00	ID1	4	1	2047	23	10.0	2	0	0	0	15.4	803.	976.	10.	0.	0.21	7.2	9.7	37.0	8.8	0.9	46.7	0.0	0.0	0.0	0.0	0.0	0.0	0.0	0.0	0.0	0.0	0.0	0.0	126.9	5.5	6.1	18.9	2.4
MACAO_5	15.44	1.00	ID1	4	1	2048	24	11.0	2	1	0	0	15.9	793.	966.	10.	0.	0.20	7.9	10.2	41.8	9.9	1.0	52.7	0.0	0.0	0.0	0.0	0.0	0.0	0.0	0.0	0.0	0.0	46.3	37.4	132.9	5.5	6.0	21.5	2.7
MACAO_5	15.44	1.00	ID1	4	1	2048	24	0.0	2	0	0	0	0.0	0.	0.	0.	0.	0.00	0.0	0.0	0.0	0.0	0.0	0.0	0.0	0.0	0.0	0.0	0.0	0.0	0.0	0.0	0.0	0.0	0.0	0.0	0.0			0.0	0.0
MACAO_5	15.44	1.00	ID1	4	1	2049	25	1.0	3	0	0	0	4.1	635.	2995.	0.	0.	0.44	0.1	0.7	0.2	0.1	0.0	0.2	0.0	0.0	0.0	0.0	0.0	0.0	0.0	0.0	0.0	0.0	0.0	0.0	133.1	5.3	0.2	0.1	0.0
MACAO_5	15.44	1.00	ID1	4	1	2050	26	2.0	3	0	0	0	7.2	635.	2995.	0.	0.	0.25	1.1	2.1	2.6	0.7	0.1	3.4	0.0	0.0	0.0	0.0	0.0	0.0	0.0	0.0	0.0	0.0	0.0	0.0	136.3	5.2	3.2	1.1	0.1
MACAO_5	15.44	1.00	ID1	4	1	2050	26	2.0	3	0	1	0	7.2	635.	762.	0.	0.	0.50	0.5	2.9	1.3	0.4	0.1	1.7	0.0	0.0	0.0	0.0	0.0	0.0	0.0	0.0	0.0	0.0	0.0	0.0	136.3	5.2	3.2	0.5	0.1
MACAO_5	15.44	1.00	ID1	4	1	2051	27	3.0	3	0	0	0	9.3	635.	762.	0.	0.	0.39	1.1	4.3	3.6	1.0	0.1	4.7	0.0	0.0	0.0	0.0	0.0	0.0	0.0	0.0	0.0	0.0	0.0	0.0	139.3	5.2	3.1	1.6	0.2
MACAO_5	15.44	1.00	ID1	4	1	2052	28	4.0	3	0	0	0	10.8	627.	754.	7.	0.	0.34	1.9	5.6	6.9	1.8	0.2	8.9	0.0	0.0	0.0	0.0	0.0	0.0	0.0	0.0	0.0	0.0	0.0	0.0	143.5	5.1	4.1	3.1	0.4
MACAO_5	15.44	1.00	ID1	4	1	2053	29	5.0	3	0	0	0	12.0	619.	747.	7.	0.	0.31	2.6	6.7	10.7	2.7	0.3	13.7	0.0	0.0	0.0	0.0	0.0	0.0	0.0	0.0	0.0	0.0	0.0	0.0	148.3	5.1	4.8	5.0	0.6
MACAO_5	15.44	1.00	ID1	4	1	2054	30	6.0	3	0	0	0	12.9	612.	740.	7.	0.	0.28	3.4	7.6	14.8	3.7	0.4	18.9	0.0	0.0	0.0	0.0	0.0	0.0	0.0	0.0	0.0	0.0	0.0	0.0	153.5	5.1	5.2	7.1	0.9
MACAO_5	15.44	1.00	ID1	4	1	2055	31	7.0	3	0	0	0	13.7	604.	733.	7.	0.	0.27	4.1	8.5	19.1	4.7	0.5	24.3	0.0	0.0	0.0	0.0	0.0	0.0	0.0	0.0	0.0	0.0	0.0	0.0	159.0	5.1	5.4	9.3	1.1
MACAO_5	15.44	1.00	ID1	4	1	2056	32	8.0	3	0	0	0	14.4	597.	726.	7.	0.	0.26	4.8	9.2	23.5	5.7	0.6	29.9	0.0	0.0	0.0	0.0	0.0	0.0	0.0	0.0	0.0	0.0	0.0	0.0	164.5	5.1	5.5	11.7	1.4
MACAO_5	15.44	1.00	ID1	4	1	2057	33	9.0	3	0	0	0	14.9	590.	719.	7.	0.	0.25	5.5	9.9	27.9	6.8	0.7	35.4	0.0	0.0	0.0	0.0	0.0	0.0	0.0	0.0	0.0	0.0	0.0	0.0	170.0	5.2	5.5	14.0	1.7
MACAO_5	15.44	1.00	ID1	4	1	2058	34	10.0	3	0	0	0	15.4	583.	712.	7.	0.	0.24	6.2	10.6	32.3	7.8	0.8	40.9	0.0	0.0	0.0	0.0	0.0	0.0	0.0	0.0	0.0	0.0	0.0	0.0	175.5	5.2	5.5	16.4	2.0
MACAO_5	15.44	1.00	ID1	4	1	2059	35	11.0	3	1	0	0	15.9	576.	705.	7.	0.	0.24	6.9	11.1	36.6	8.8	0.8	46.2	0.0	0.0	0.0	0.0	0.0	0.0	0.0	0.0	0.0	0.0	42.0	33.9	180.9	5.2	5.4	18.7	2.4
MACAO_5	15.44	1.00	ID1	4	1	2059	35	0.0	3	0	0	0	0.0	0.	0.	0.	0.	0.00	0.0	0.0	0.0	0.0	0.0	0.0	0.0	0.0	0.0	0.0	0.0	0.0	0.0	0.0	0.0	0.0	0.0	0.0	0.0			0.0	0.0
MACAO_med	20.69	1.00	ID1	4	1	2024	0	0.0	1	0	0	0	0.0	1250.	1250.	0.	0.	0.00	0.0	0.0	0.0	0.0	0.0	0.0	0.0	0.0	0.0	0.0	0.0	0.0	0.0	0.0	0.0	0.0	0.0	0.0	0.0	0.0		0.0	0.0
MACAO_med	20.69	1.00	ID1	4	1	2025	1	1.0	1	0	0	0	10.2	1250.	1250.	0.	0.	0.28	0.4	1.9	1.3	0.3	0.0	1.6	0.0	0.0	0.0	0.0	0.0	0.0	0.0	0.0	0.0	0.0	0.0	0.0	1.6	1.6	1.6	0.5	0.1
MACAO_med	20.69	1.00	ID1	4	1	2026	2	2.0	1	0	0	0	13.8	1250.	1250.	0.	0.	0.21	1.7	4.1	7.9	1.8	0.2	10.0	0.0	0.0	0.0	0.0	0.0	0.0	0.0	0.0	0.0	0.0	0.0	0.0	10.0	5.0	8.4	3.7	0.4
MACAO_med	20.69	1.00	ID1	4	1	2027	3	3.0	1	0	0	0	15.8	1250.	1250.	0.	0.	0.18	3.3	5.8	17.9	4.0	0.4	22.4	0.0	0.0	0.0	0.0	0.0	0.0	0.0	0.0	0.0	0.0	0.0	0.0	22.4	7.5	12.4	8.8	1.0
MACAO_med	20.69	1.00	ID1	4	1	2028	4	4.0	1	0	0	0	17.1	1233.	1233.	17.	0.	0.17	5.0	7.2	28.9	6.4	0.7	36.0	0.0	0.0	0.0	0.0	0.0	0.0	0.0	0.0	0.0	0.0	0.0	0.0	36.0	9.0	13.7	14.7	1.6

Figure IV.4 – StandsSIM output file: output_yieldtabl

Appendix V – The case of Maritime Pine

Appendix V.1: Growing Cycle

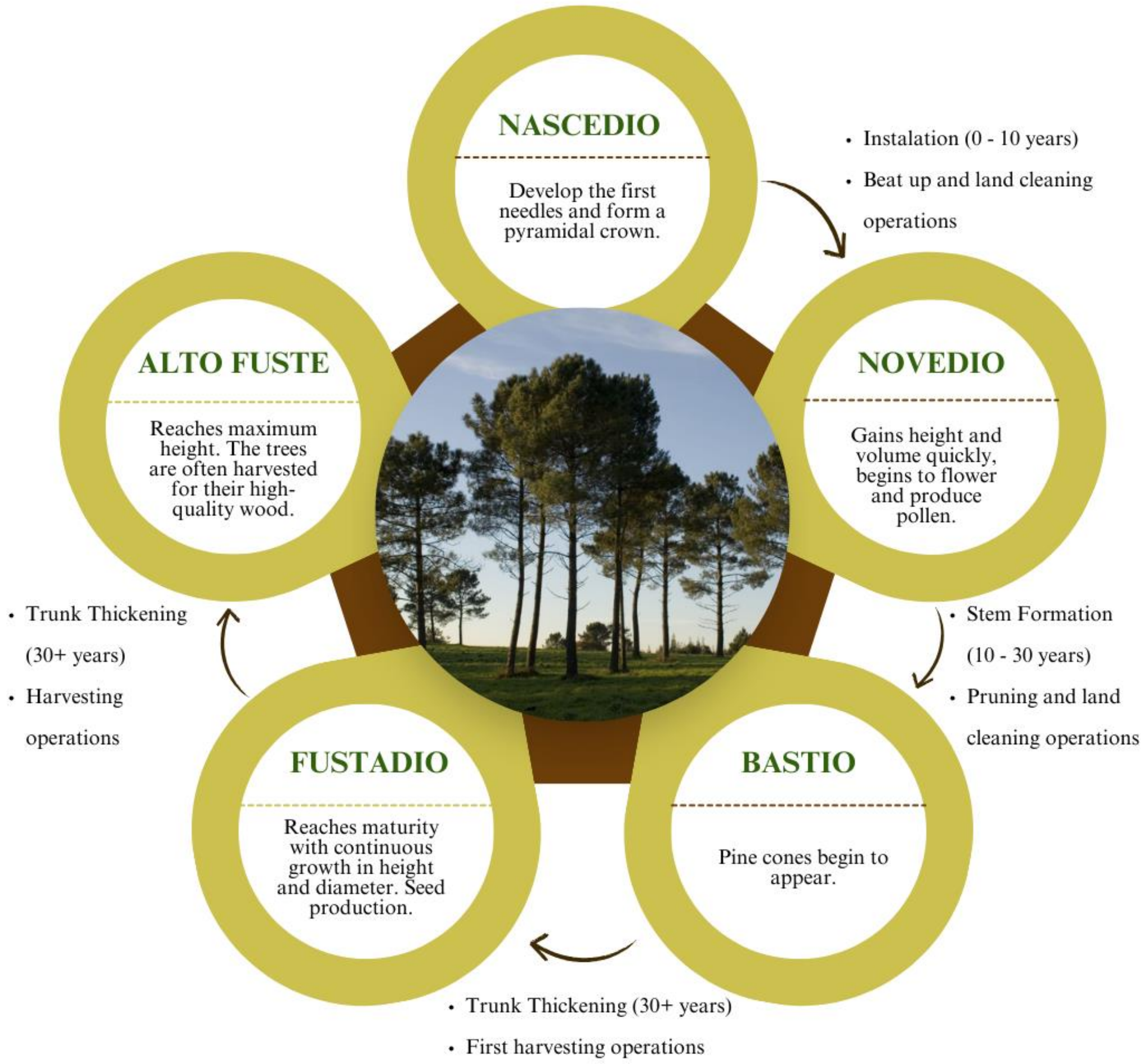

Figure V.1: Diameter and height variations in maritime pine (Matias, 2023)

Appendix V.2: Developed Models - Growth and Economic Model

The first goal was to develop a mathematical model to predict growth and economic return from maritime pine stands. This model aimed to simulate the lifecycle revenue generated from wood, resin and biomass, using user-provided data, such as the management that would be practiced in terms of thinning and final cut processes, as well as some characteristics of the stand itself, more properly, its age.

To begin, equations for calculating wood volume and biomass weight were adopted from existing research. For wood volume, Equation 1 was used,

$$(1)\ \ Pvudi = e^{-1{,}41300*\left(\frac{d_i^{4{,}3488}}{d^{4{,}3188}}\right)},\ \text{with}\ d_i = d\left(-2{,}1823*\left(\frac{h_i}{h}-1\right)+0{,}8591*\left(\frac{h_i^2}{h}-1\right)\right)^{0.5}$$

Equation 1: Equation selected for estimating the merchantable wood volume of Maritime Pine (excluding stump and bark) (Tomé et al. 2007)

In this equation, represents the diameter of an individual tree, in centimeters, measured at 1.30 m heigh h is the total height of the tree, d_i In this equation, d represents the diameter of an individual tree, in centimeters, measured at 1.30 m height, h is the total height of the tree, d_i is the diameter measured at height h_i and $Pvudi$ is the proportion of volume without bark and stump, up to the topping diameter d_i.

For biomass, separate Equations 2, 3 and 4 were applied to estimate the weight of the tree's bark, branches and needles,

$$(2)\ wb = 0{,}0114 * d^{1{,}8728} * h^{0{,}6694},$$

$$(3)\ \ wbr = 0{,}00308 * d^{2{,}75761} * \left(\frac{h}{d}\right)^{-0{,}39381}$$

$$(4)\ \ wl = 0{,}09980 * d^{1{,}39252} * \left(\frac{h}{d}\right)^{-0{,}71962}$$

Equations 2, 3, 4: Equations for estimating biomass weight (Tomé et al. 2007)

where (2), (3) and (4) represent the weight of the biomass, in kg, of the tree's bark, branches and needles respectively.

When it comes to resin's production, no equation was found, however, in average, trees with higher resin production were taller and thicker than trees with lower production (Rodríguez-García et al 2014), which means that both height and diameter are variables that have an influence in the amount of resin that can be extracted from a maritime pine.

While developing the model, several limitations were found, the primary one being the fact that there was no reliable age-dependent equation that accurately modeled the progression of height and diameter over the life cycle of *Pinus pinaster*. Accurate predictions for these attributes are essential because they directly influence calculations of wood volume, biomass weight, and resin production, which are the primary revenue sources for maritime pine stands.

Moreover, the initial modelling intention was to treat each tree individually, since that is how maritime pine stands are treated, however this approach required a more precise modelling that could capture the variations in individual growth patterns, which was not possible due to the lack of data.

Appendix V.3: Results Analysis

Dominant Height

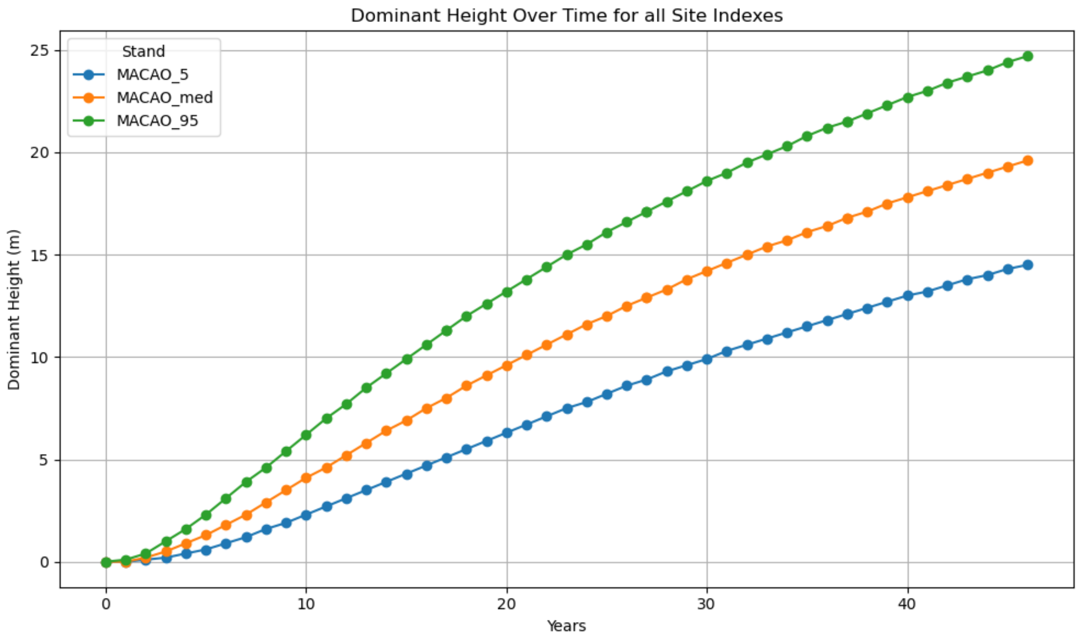

Figure V.2: Dominant Height over time for three site indexes

Number of trees

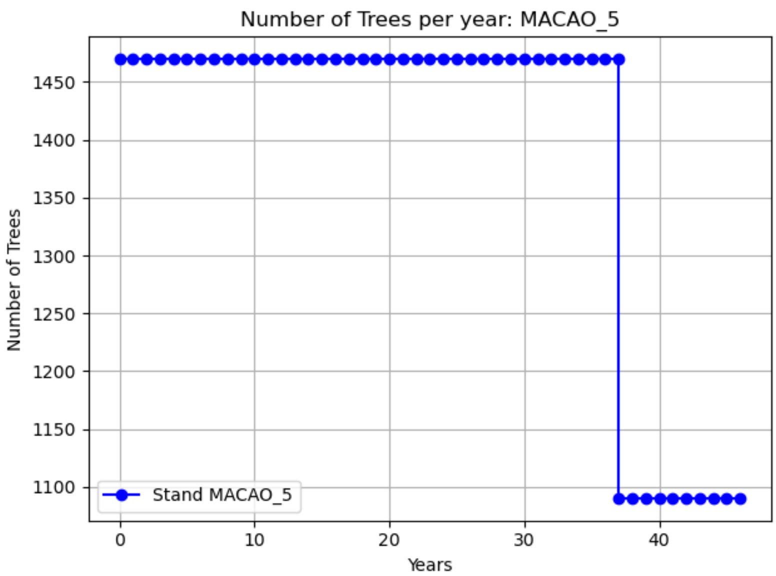

Figure V.3: Number of trees over time for Mação 5

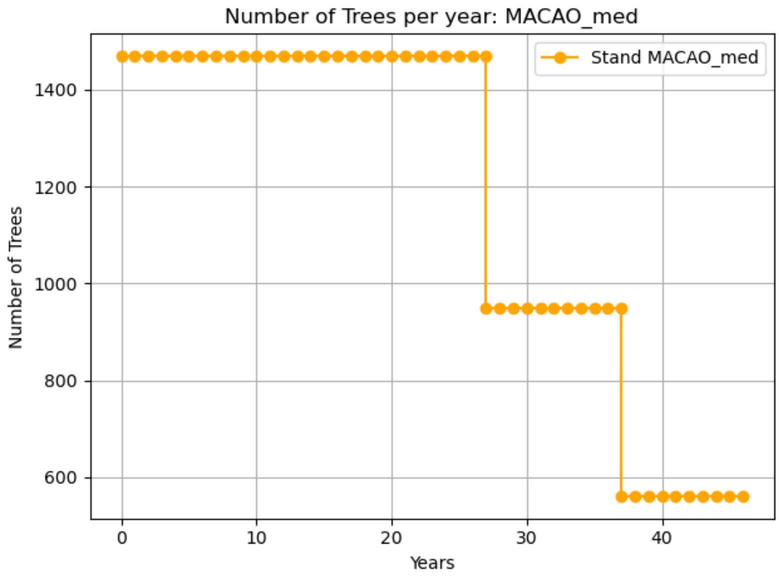

Figure V.4: Number of trees over time for Mação Med

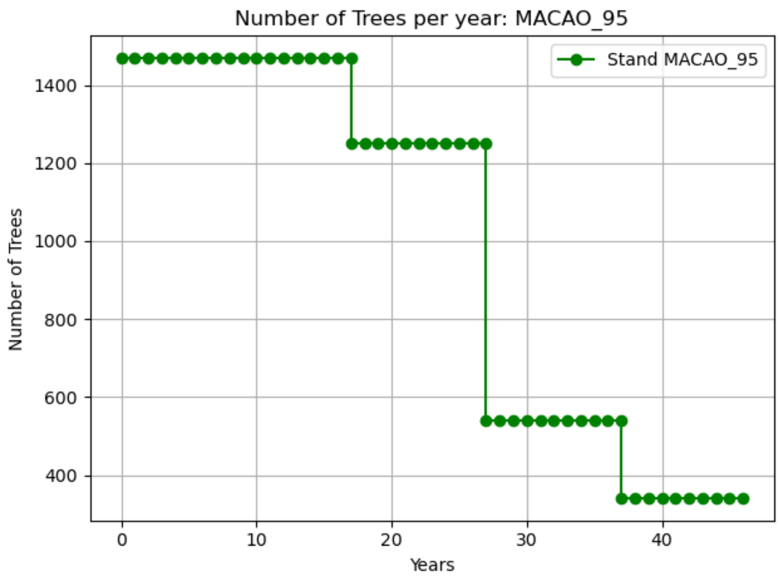

Figure V.5: Number of trees over time for Mação 95

Basal area and Wood Volume

Basal area consists in the total cross-sectional area of all tree trunks, at 1.3 meters above ground, per hectare and is a key measure for forest management and health assessment, since it indicates forest density, productivity and competition among trees.

As expected, in Figure V.6 is visible that *Mação 95* scenario has the highest wood volume, while *Mação 5* has the lowest. The growth in wood volume accelerates significantly after the initial phase and the lowest values, coordinated in all three scenarios, represent harvesting operations.

Moreover, higher productivity sites generally result in higher tree density and faster growth, consequently, leading to a higher basal area. In contrast, lower site indexes show the slowest growth in basal areas, with slower growth rates and fewer economic viable trees. These facts are clearly represented in Figure V.7, *Mação 95*, the higher productivity scenario, has high basal area, while *Mação 5* shows a clear slowest growth in basal area over the time.

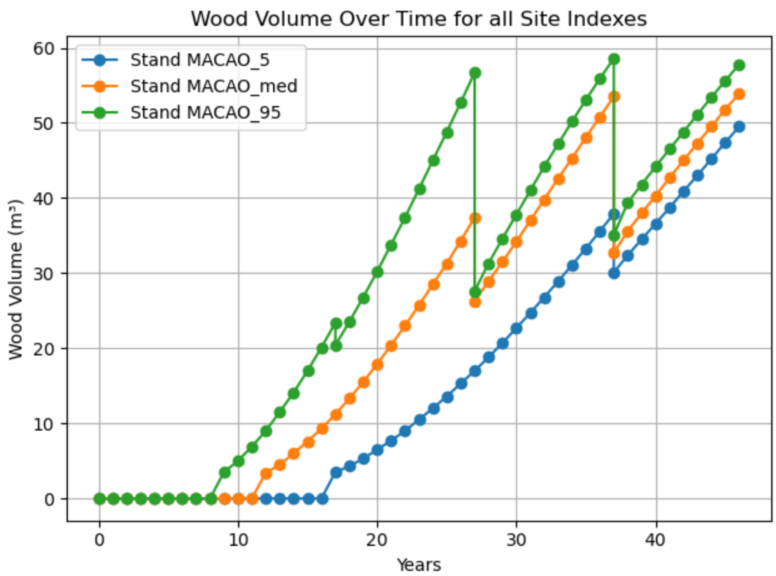

Figure V.6: Wood volume over time for all site indexes

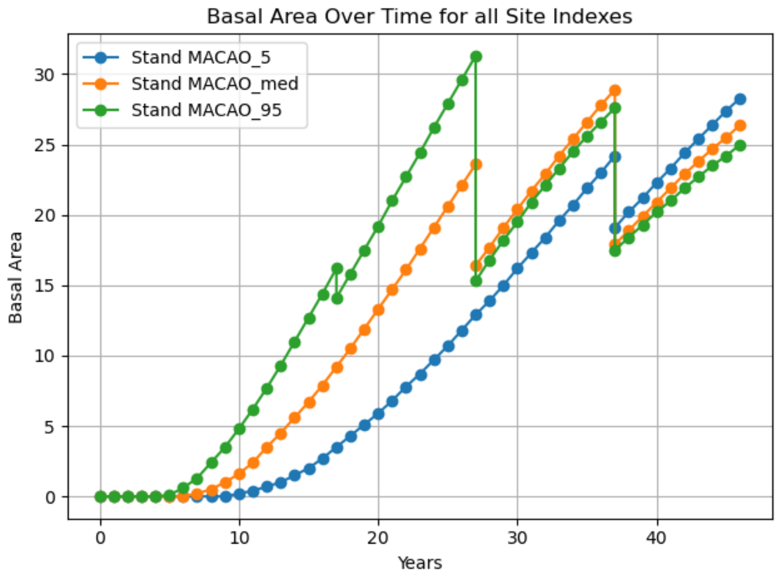

Figure V.7: Basal area over time for three site indexes

EAA, NPV and NPV Sum

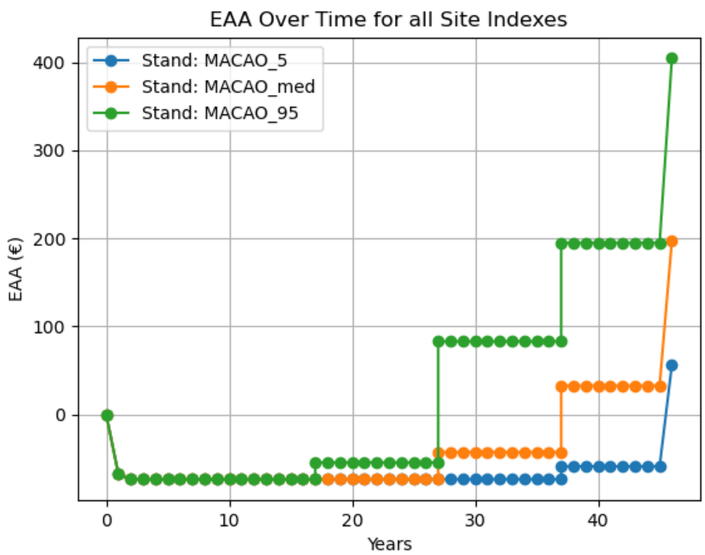

Figure V.8: EAA over time for three site indexes

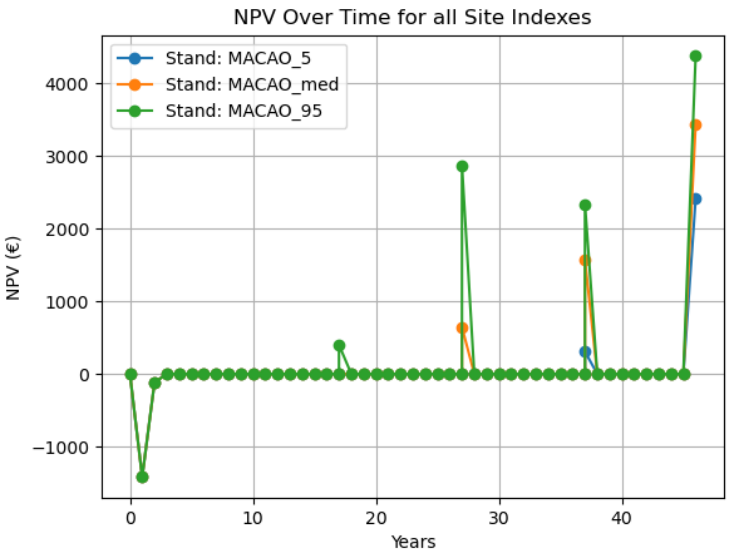

Figure V.9: NPV over time for three site indexes

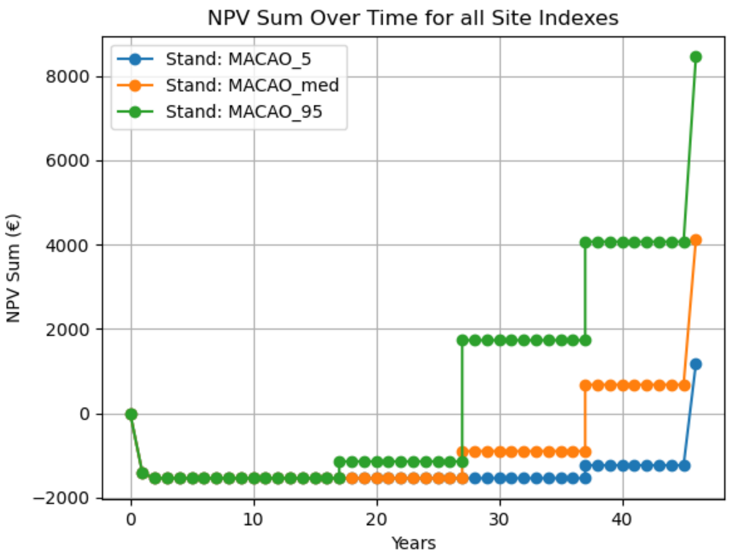

Figure V.10: Cumulative NPV over time for three site indexes

Appendix V.4: Sensitivity Analysis

Number of trees

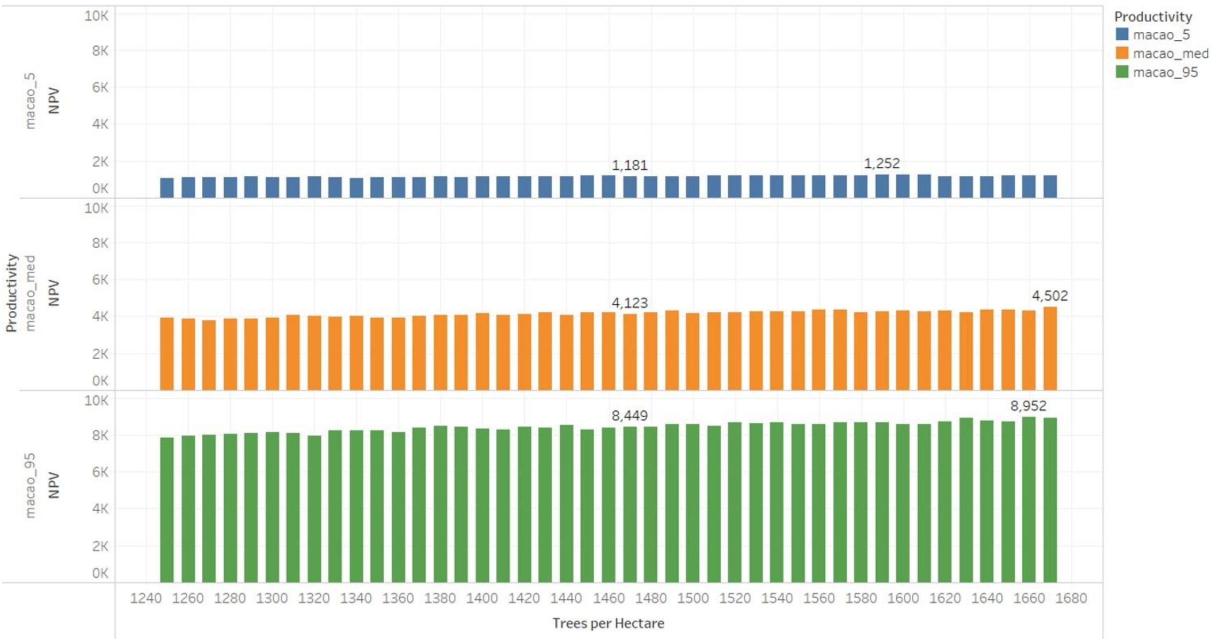

Figure V.11: Sensitivity Analysis of NPV with number of trees per hectare, for all three scenarios

Scenario	Type	Trees per hectare	NPV (€)	Difference (%)
Mação 5	Max NPV	1590	1252.2	6.03
Mação 5	Practiced	1470	1181.0	-
Mação med	Max NPV	1670	4501.6	9.18
Mação med	Practiced	1470	4123.2	-
Mação 95	Max NPV	1660	8951.8	5.95
Mação 95	Practiced	1470	8449.1	-

Table V.1: Summary of Sensitivity Analysis of NPV with Number of Trees per hectare

Beat-up Rate

Scenario	Site Index	Beat-up Percent (%)	NPV (€)	Difference (%)
Mação 5	15.44	5	1341.8	-
Mação 5	15.44	10	1261.4	-5.99
Mação 5	15.44	15	1181.0	-11.98
Mação 5	15.44	20	1100.6	-17.98
Mação 5	15.44	25	1020.2	-23.97
Mação med	20.69	5	4284.0	-
Mação med	20.69	10	4203.6	-1.88
Mação med	20.69	15	4123.2	-3.75
Mação med	20.69	20	4042.8	-5.63
Mação med	20.69	25	3962.4	-7.51
Mação 95	25.86	5	8609.9	-
Mação 95	25.86	10	8529.5	-0.93
Mação 95	25.86	15	8449.1	-1.87
Mação 95	25.86	20	8368.7	-2.8
Mação 95	25.86	25	8288.3	-3.74

Table V.2: Summary of Sensitivity Analysis of the NPV with different Beat-up percentages

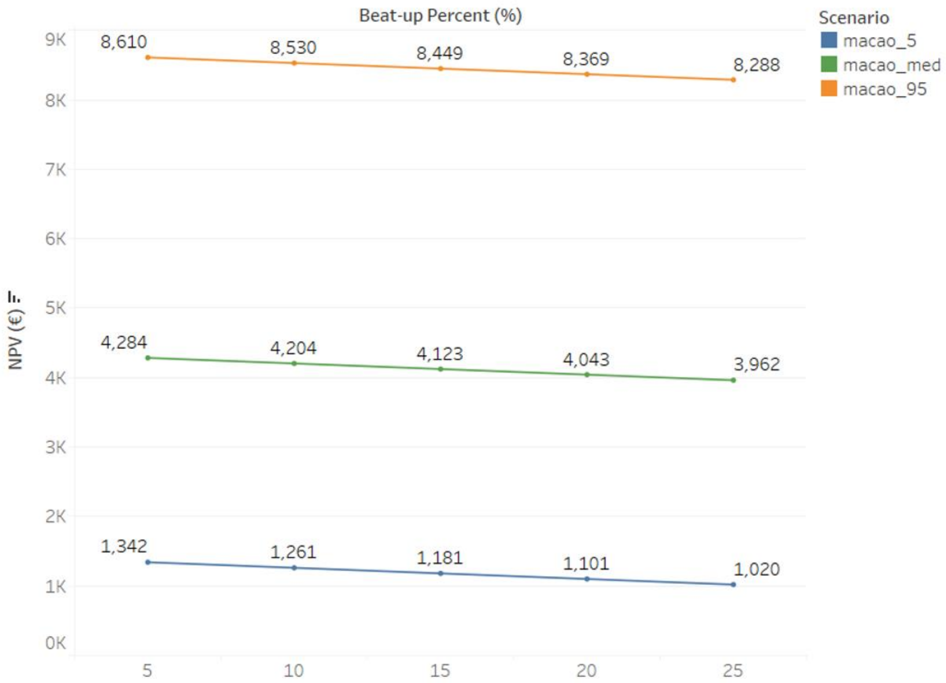

Figure V.12: Sensitivity Analysis of NPV with Beat-up percentages

Final Cut ages

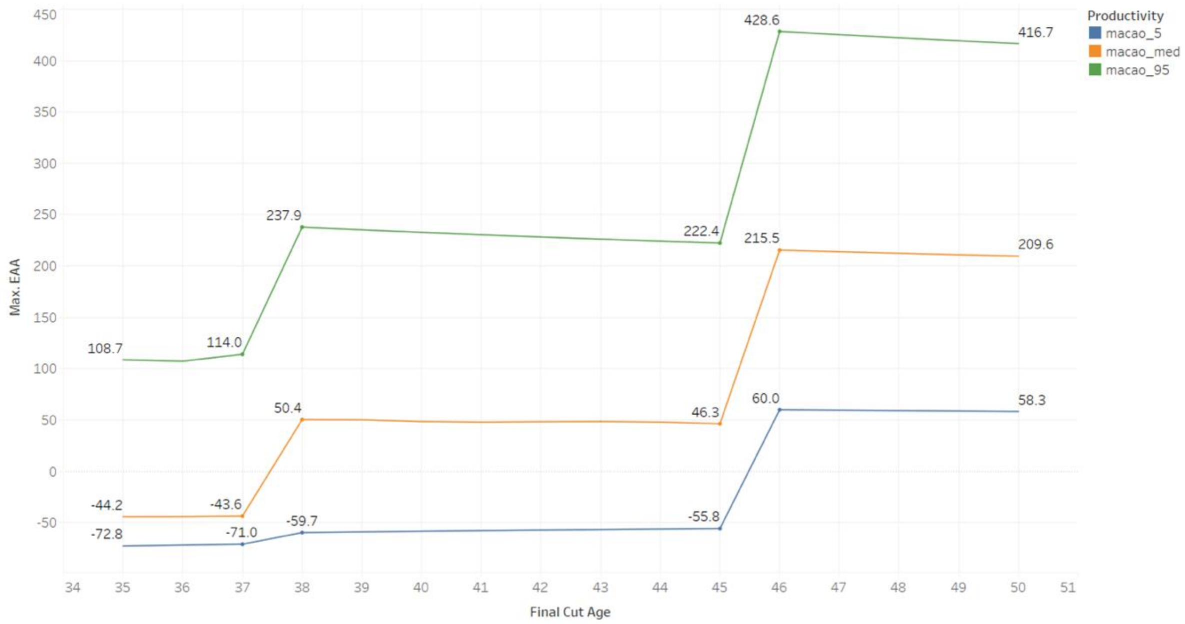

Figure V.13: Sensitivity Analysis of the NPV with different Final cut ages

Management Schedules

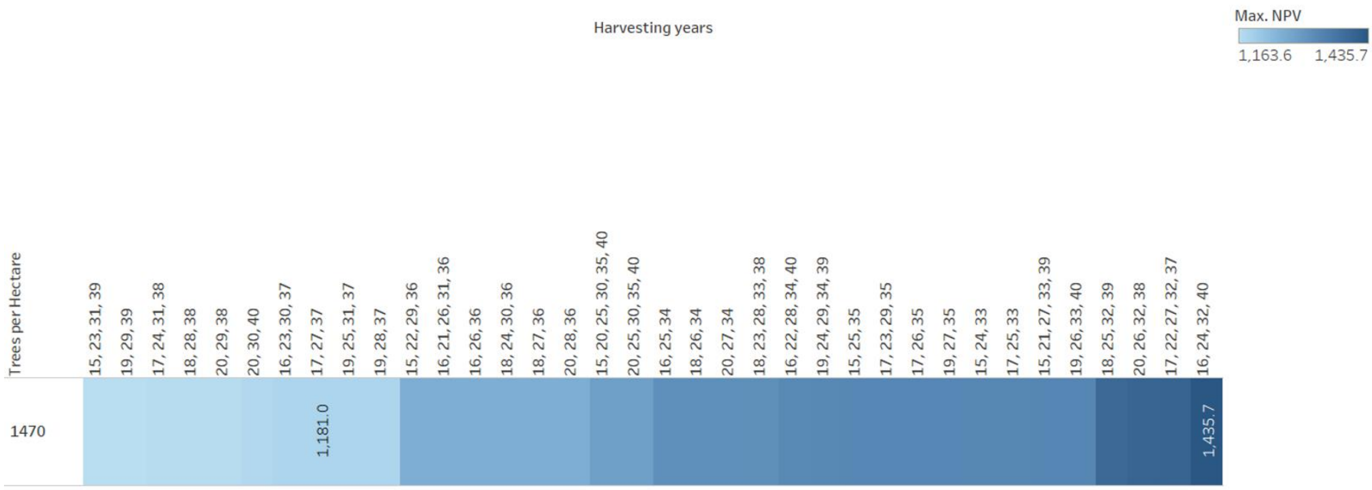

Figure V.14: Sensitivity Analysis of NPV with management schedules, Mação 5

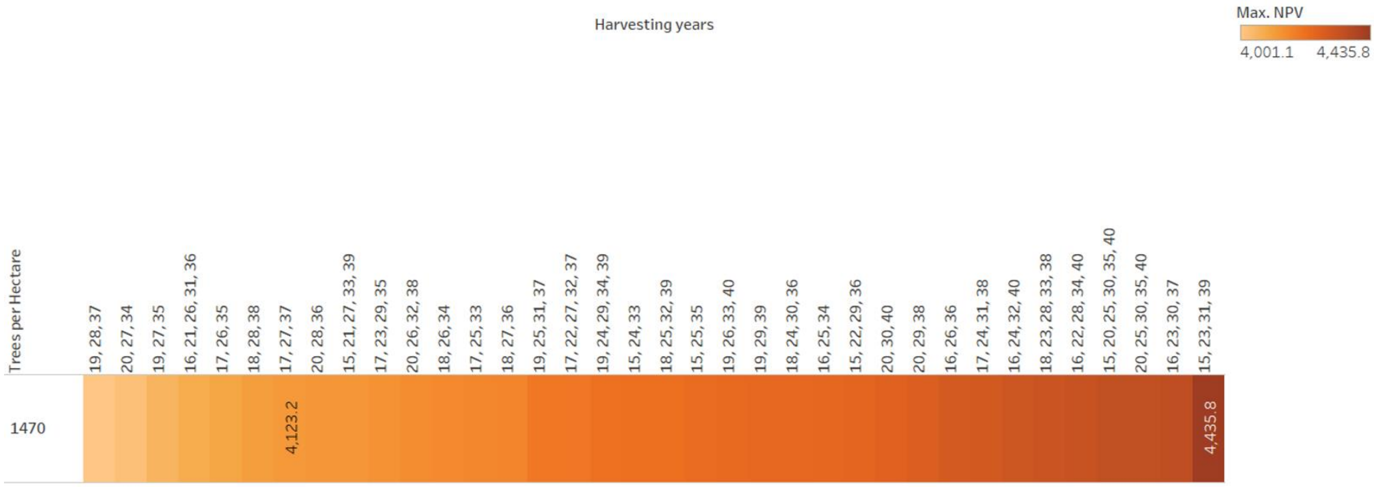

Figure V.15: Sensitivity Analysis of NPV with management schedules, Mação med

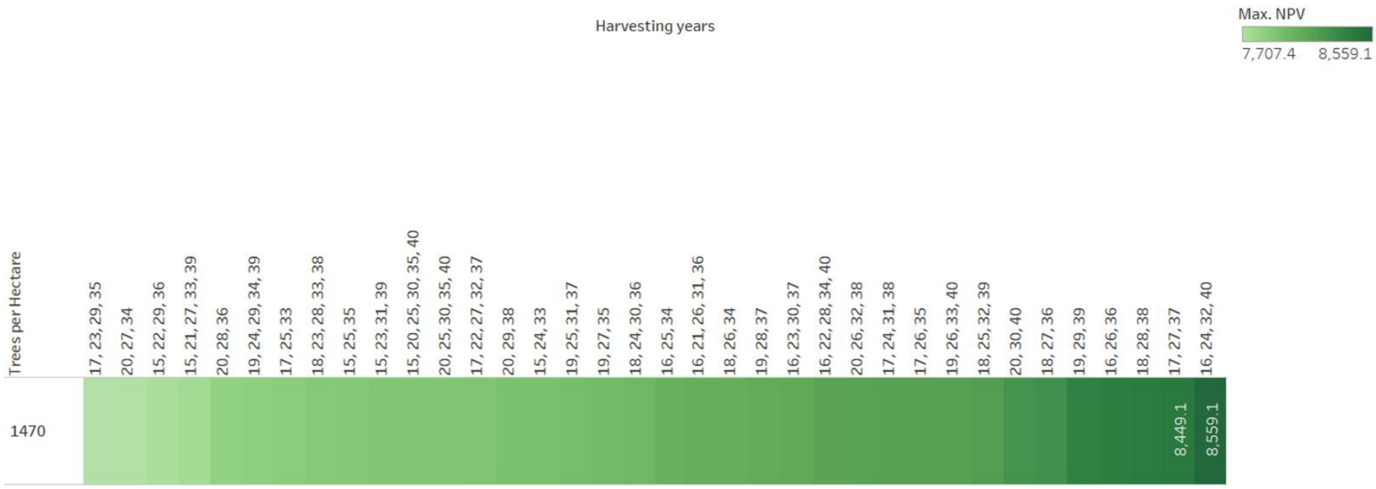

Figure V.16: Sensitivity Analysis of NPV with management schedules, Mação 95

Scenario	Type	Schedule	Actual Performing Thinning years	NPV (€)	Difference (%)
Mação 5	Max NPV	(16, 24, 32, 40)	(32, 40)	1435.7	21.57
Mação 5	Practiced	(17, 27, 37)	(37)	1181.0	-
Mação med	Max NPV	(15, 23, 31, 39)	(23, 31, 39)	4435.8	7.58
Mação med	Practiced	(17, 27, 37)	(27, 37)	4123.2	-
Mação 95	Max NPV	(16, 24, 32, 40)	(16, 24, 32, 40)	8559.1	1.3
Mação 95	Practiced	(17, 27, 37)	(17, 27, 37)	8449.1	-

Table V.3: Summary of the Sensitivity Analysis of the NPV with different management schedules

Multivariate sensitivity analysis

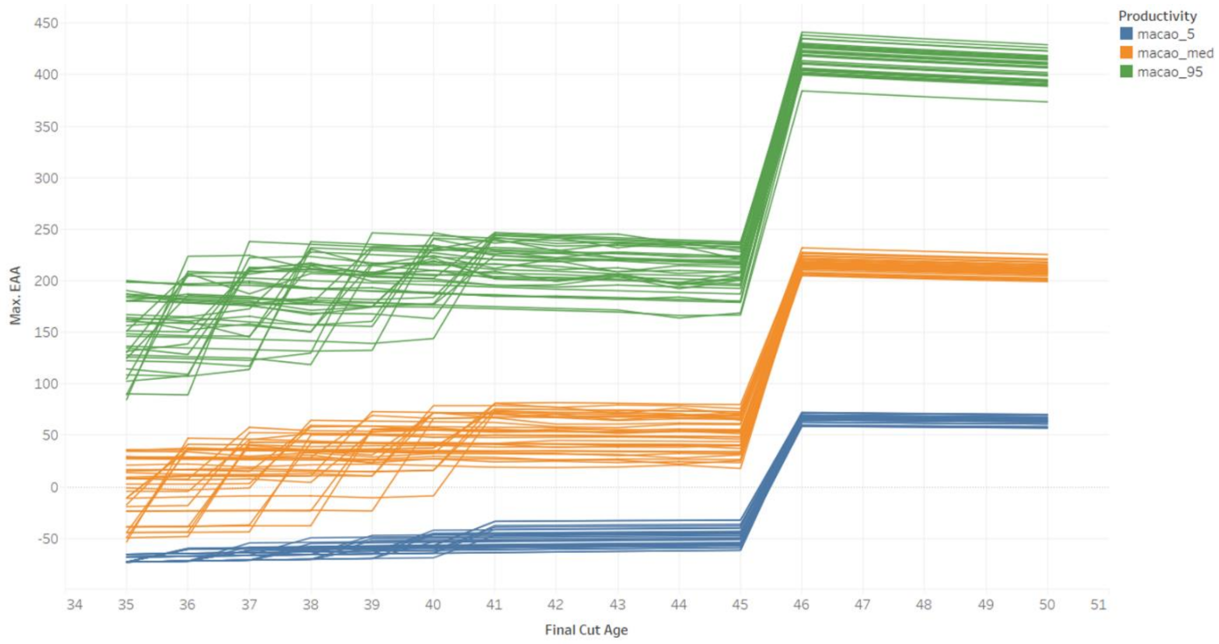

Figure V.17: Multivariate Analysis: Final Cut Age vs. Max EAA.

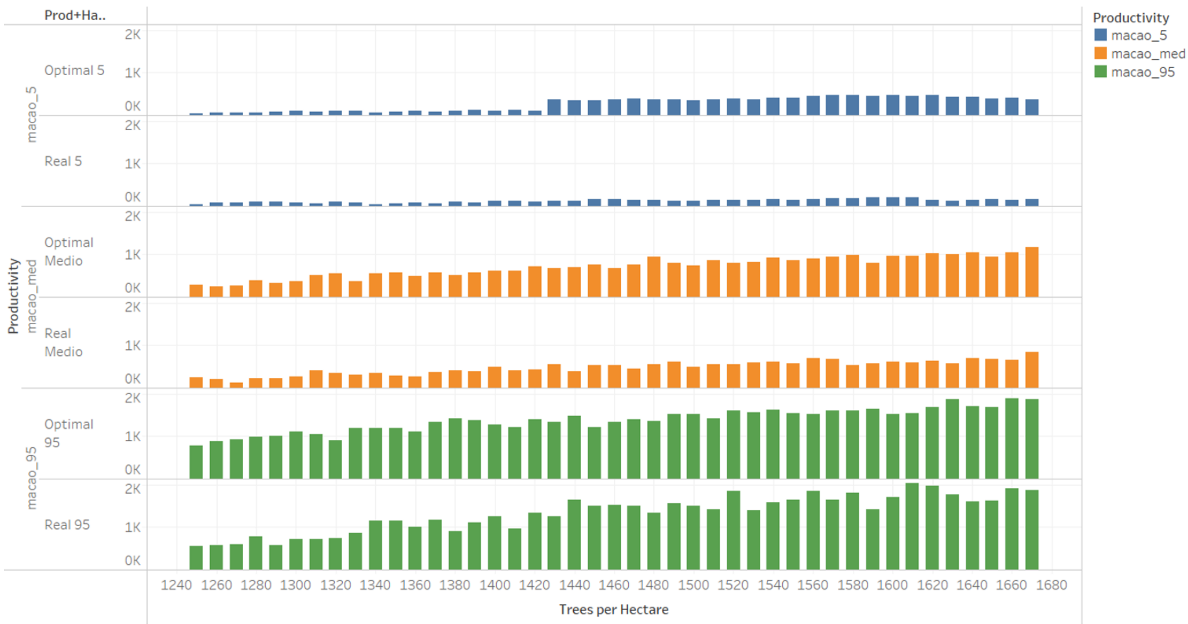

Figure V.18: Multivariate Analysis: Visualization of every combination of trees between the optimal and practiced schedules for all three productivity scenarios.

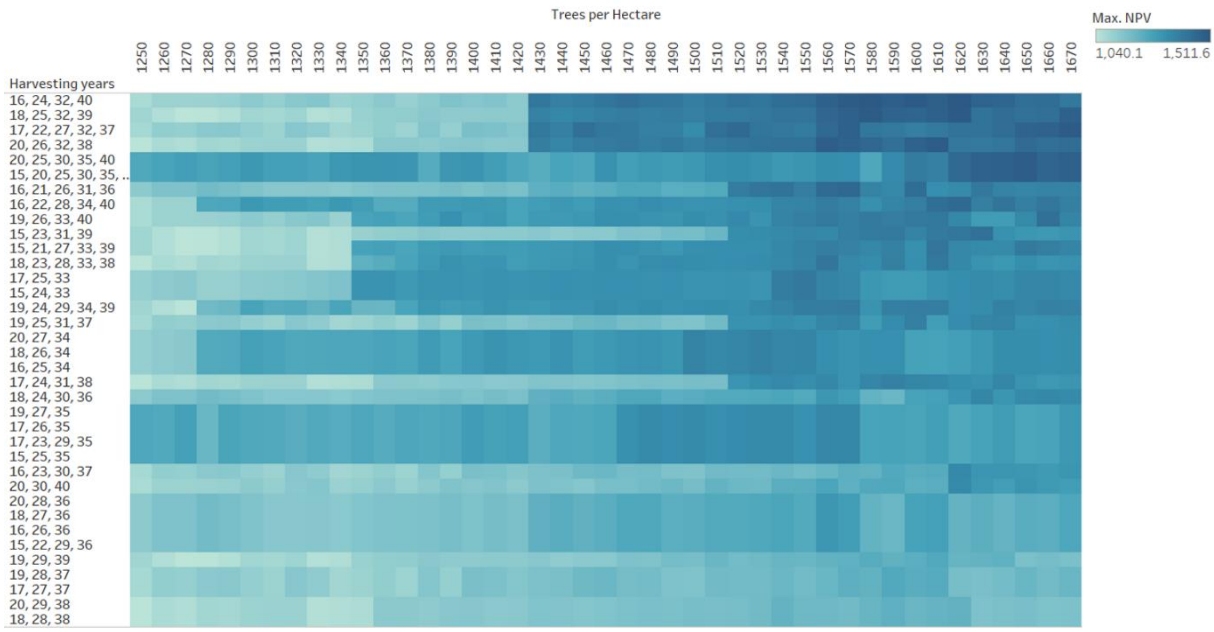

Figure V.19: Multivariate Analysis: Max NPV - Harvesting years vs. Trees per Hectare, Mação 5

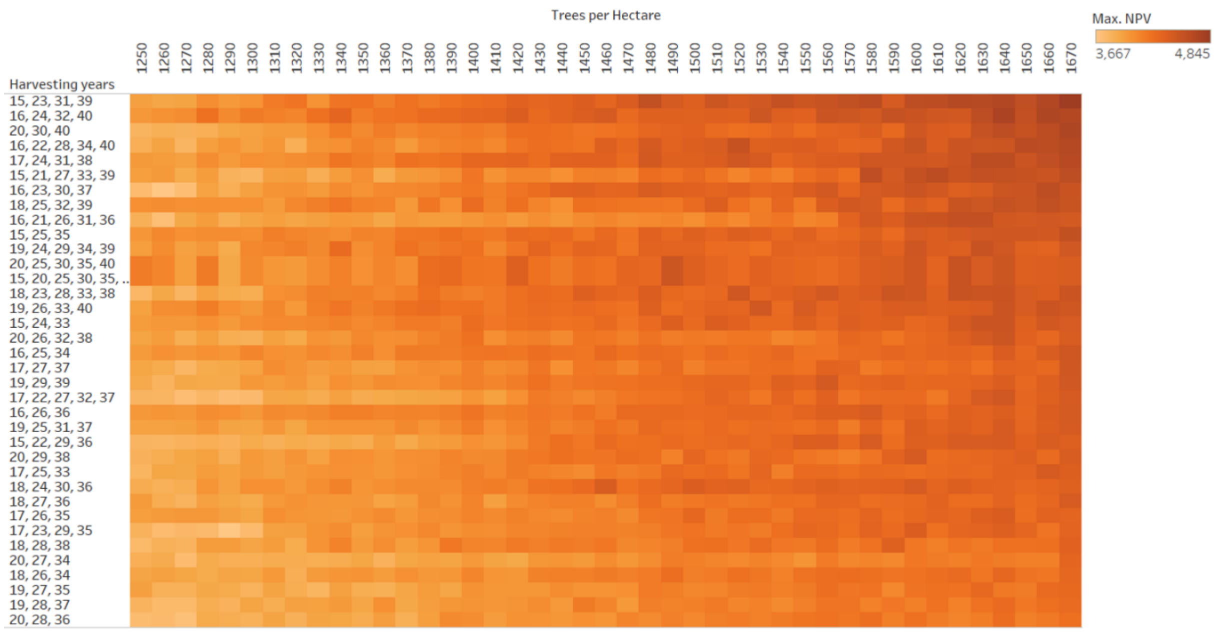

Figure V.20: Multivariate Analysis: Max NPV - Harvesting years vs. Trees per Hectare, Mação med

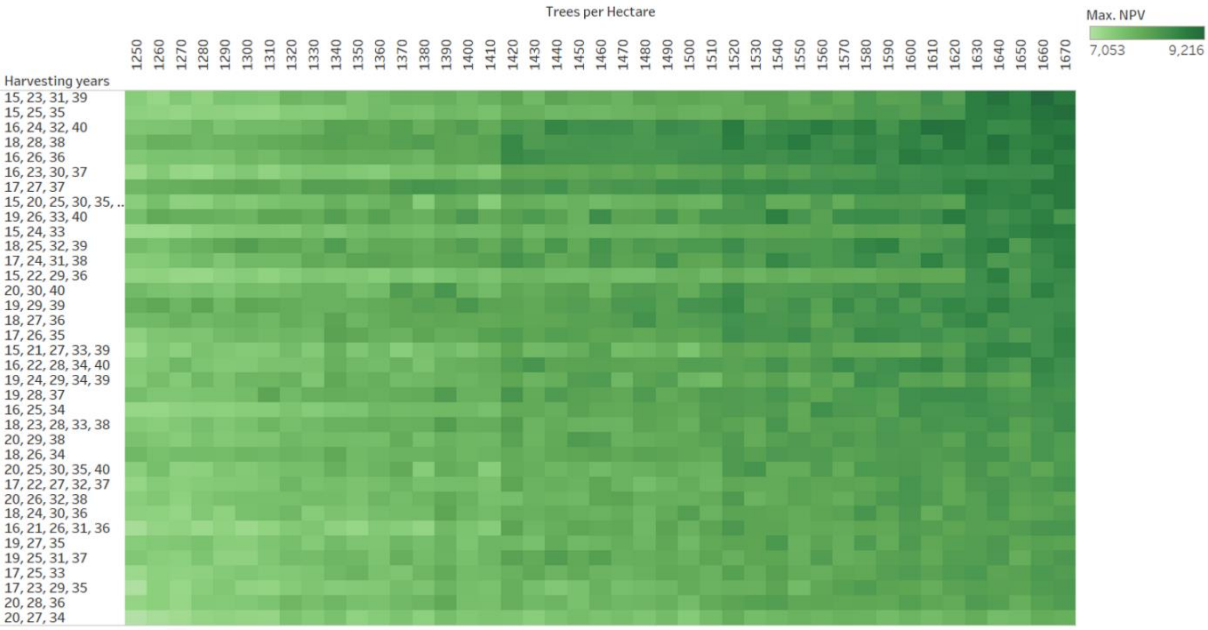

Figure V.21: Multivariate Analysis: Max NPV - Harvesting years vs. Trees per Hectare, Mação 95

Scenario	Type	Trees per Hectare	Beat-up Percent (%)	Schedule	Actual Performing Thinning years	Final Cut Age	NPV (€)	Difference (%)
Mação 5	Practiced	1470	15	(17, 27, 37)	(37)	46	1181.0	-
Mação 5	Max NPV	1580	15	(16, 24, 32, 40)	(32, 40)	46	1511.6	27.99
Mação med	Practiced	1470	15	(17, 27, 37)	(27, 37)	46	4123.2	-
Mação med	Max NPV	1670	15	(15, 23, 31, 39)	(23, 31, 39)	46	4845.0	17.5
Mação 95	Practiced	1470	15	(17, 27, 37)	(17, 27, 37)	46	8449.1	-
Mação 95	Max NPV	1660	15	(15, 23, 31, 39)	(15, 23, 31, 39)	46	9216.4	9.08

Table V.4: Summary of Multivariate Sensitivity Analysis

Appendix VI – The case of Eucalyptus

Appendix VI.1: Developed Models - Growth and Economic Model

The first approach was to develop a predictive growth and financial model. To start the model, *Tomé et al. (2007)* presented a selection of equations to estimate and predict all parameters needed for the model. eucalyptus's wood is commercialized without the stump and the bark. As such, the function to calculate the volume of wood produced is given by equation 5.

$$(5)\ Pvudi = e^{-0.6022*\left(\frac{d_i^{4.7767}}{d^{4.4125}}\right)} \text{ where } d_i = d\left(-\beta_0 * \left(\frac{h_i}{h} - 1\right) + \beta_1 * \left(\frac{h_i^2}{h} - 1\right)\right)^{0.5}$$

Equation 5 – Volume of wood produced | Source: Tomé et al. 2007

In this context, d represents the diameter in centimeters, h the height of the tree in meters and β needs to be estimated with data.

i. Age-Dependent Model

As for that with regard to age, developed by *Richards* (Richards 1959) is given by equation 6.

$$(6)\ Y_i = A(1 - e^{-kt_i})^{\frac{1}{1-m}}$$

Equation 6 – Estimations based on the tree's age

In this equation, Y_i represents the variable to be estimated at time t, A is the asymptote – maximum value that Y_i can reach –, k is the growth rate, m is the shape parameter and t is the tree's age. Therefore, by inputting the age at which the tree is harvested, this equation returns a prediction of the height and diameter of the tree, which can then be used to calculate the wood's volume production.

The unknown parameters were estimated by Francisco Goes (Goes 2012) and the final equations used to estimate the diameter in centimeters and height in meters are, respectively equations 7 and 8.

$$(7)\ D_i = 114.49(1 - e^{-0.02t_i})^{\frac{1}{1-0.183451}} \qquad (8)\ H_i = 71.74(1 - e^{-0.019280t_i})^{\frac{1}{1-(-1.432148)}}$$

Equation 7 – Diameter estimations based on the tree's age *Equation 8 – Height estimations based on the tree's age*

ii. Age-Independent Model

On the other hand, the function that does not consider age calculates both wanted parameters as an annual growth compound. So, if the user knows the current diameter and height of the tree, the equation calculates the values for the upcoming years annually until the harvest year. The general function was developed by *Richards* (Richards 1959) and is represented by equation 9.

$$(9)\ y_{i+1} = A\left(1 - e^{-k}\left(1 - {y_i}/{A}\right)^{1-m}\right)^{\frac{1}{1-m}}$$

Equation 9 – General age-independent equation to estimate height and diameter as a compound

For the diameter, this function is referred to as Richards-k, and the parameters were estimated by Francisco Goes (Goes 2012) as presented in equation 10.

$$(10)\ d_{i+1} = 114.495975(1 - e^{-k}(1 - {d_i}/{114.495975})^{1-0.183454})^{\frac{1}{1-0.183454}}$$

Equation 10 – Diameter estimations independent of the tree's age

where k is defined as shown in equation 11.

$$(11)\ k = 0.031391 + 0.001838\,puro - 0.000516G_L + 0.002904\frac{1}{G} - 0.000408\,Temp\,med\max mmq - 0.008075G_{perc}$$

Equation 11 –Estimation of the parameter k

For the height, the equation 12 is known as Richards-m with parameters also estimated by Francisco Goes (Goes 2012).

$$(12)\ h_{i+1} = 71.735833(1 - e^{-0.019280}(1 - {h_i}/{71.735833})^{1-m})^{\frac{1}{1-m}}$$

Equation 12 – Height estimation independent of the tree's age

where m is defined by equation 13:

$$(13)\ m = -1.432148 - 0.135726\, alto\ fuste + 0.039946 G_L - 0.223946 \frac{Nviv}{1000} + 0.073757\, Temp\ med + 0.188293\, G_{perc}$$

Equation 13 – Estimation of the parameter m

Finally, the biomass calculation was also included with the equations presented in Figure VI.1, present in the appendix, developed by *Tomé et al. (2007)*.

Modelos

(1) $w_i = \beta_0\ d^{\beta_1}\ h^{\beta_2}$

(2) $w_i = \beta_0\ d^{\beta_1}\ cl^{\beta_2}$

Componente	Modelo	β_0	β_1	β_2	Fonte
Lenho (ww)	1	0,0101	se $hdom \leq 10{,}71$: $\frac{hdom}{-0{,}6653 + 0{,}6243\ hdom}$ se $hdom > 10{,}71$: 1,7788 árvores dispersas noutros estratos: 1,7788	1,3638	António et al. 2006
Casca (wb)	1	0,0006	se $hdom \leq 18{,}27$: $\frac{hdom}{-0{,}6970 + 0{,}4586\ hdom}$ se $hdom > 18{,}27$: 2,3784 árvores dispersas noutros estratos: 2,384	1,0616	António et al. 2006
Ramos (wbr)	2	0,0224	se $hdom \leq 8{,}83$: $\frac{hdom}{-0{,}9130 + 0{,}7043\ hdom}$ se $hdom > 8{,}83$: 1,6640 árvores dispersas noutros estratos: 1,6640	0,6067	António et al. 2006
Folhas (wl)	2	0,0295	se $hdom \leq 7{,}39$: $\frac{hdom}{-1{,}0312 + 0{,}7069\ hdom}$ se $hdom > 7{,}39$: $1.7627 - 0.0106\ hdom$ árvores dispersas noutros estrato: 1.7627	0,6430	António et al. 2006
Total aérea (wa)	wa = ww+wb+wl+wbr				António et al. 2006
Raízes (wr)	wr = 0,2487 wa				Soares e Tomé, 2004
					Soares e Tomé, 2011

d – diâmetro da árvore medido a 1,30 m de altura (cm); *h* – altura total da árvore (m); *cl* – comprimento da copa; w_i – biomassa da componente i da árvore (kg); *wa* – biomassa total aérea da árvore (kg); *hdom* – altura dominante (m).

Figure VI.1 – Equations to estimate the eucalyptus' biomass (Tomé et al. 2007)

With the wood produced from the tree and its biomass, the only thing left is to multiply those values by the corresponding selling price, inputted by users. That will return the profit collected at the final harvesting of the stand per hectare. Multiplying this value by total hectares planted and the users get the total profit of their plantations.

Appendix VI.2: Results Analysis

Number of trees

Figures VI.2, VI.3 and VI.4 show that regardless of the site index, the number of trees remains the same for all scenarios. This result was expected, as the site index only influences the productivity (wood volume produced) rather than tree density. This graph fully illustrates the process of shoot regeneration in eucalyptus coppicing practices. As explained in Section 6.3, after harvest, the stumps left in the ground regenerate by producing multiple new shoots, leading to a sharp increase in tree numbers during years after harvest, 14-15 and 25-26. Then, during years 15 and 26, shoot selection is performed, reducing the number of shoots per stump back to the values seen during the first rotation.

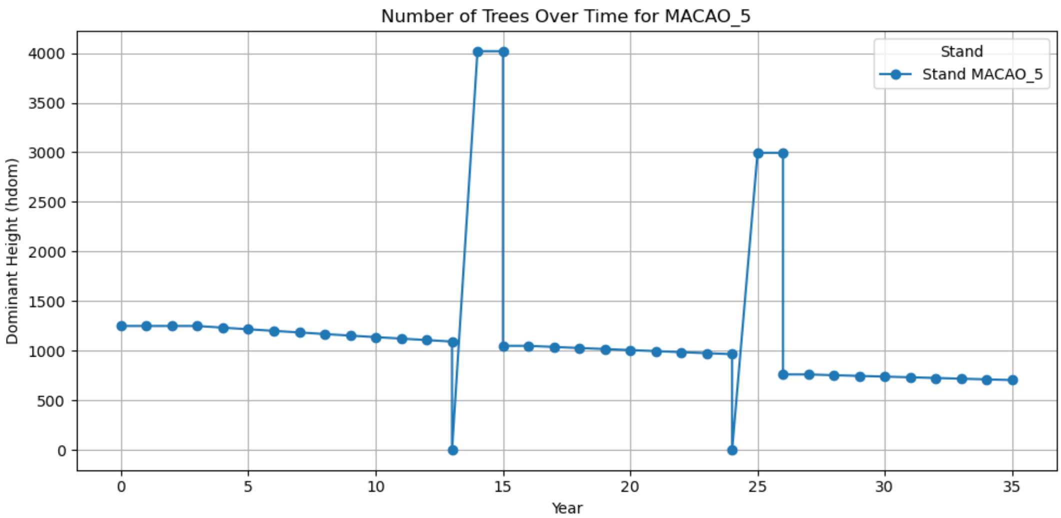

Figure VI.2 – Number of trees over time for Mação_5

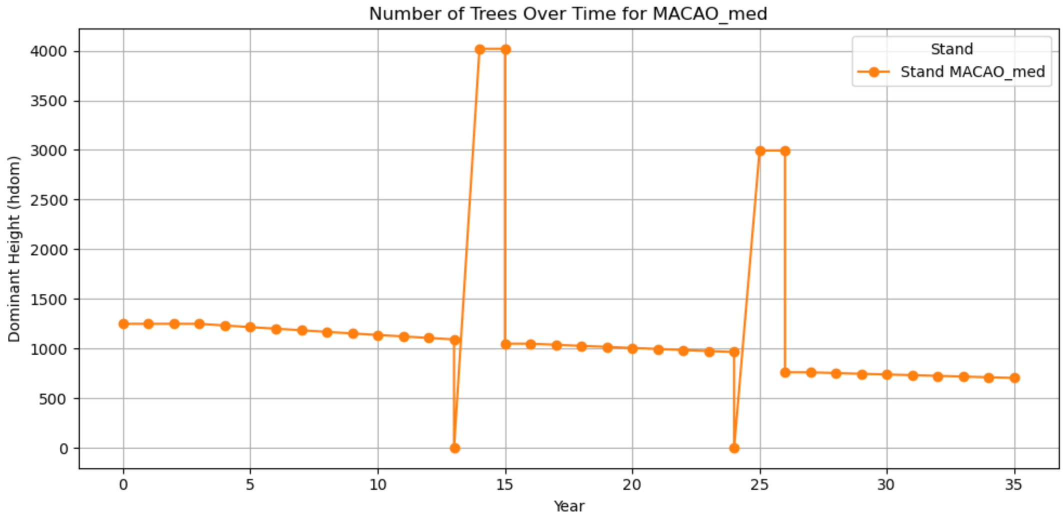

Figure VI.3 – Number of trees over time for Mação_med

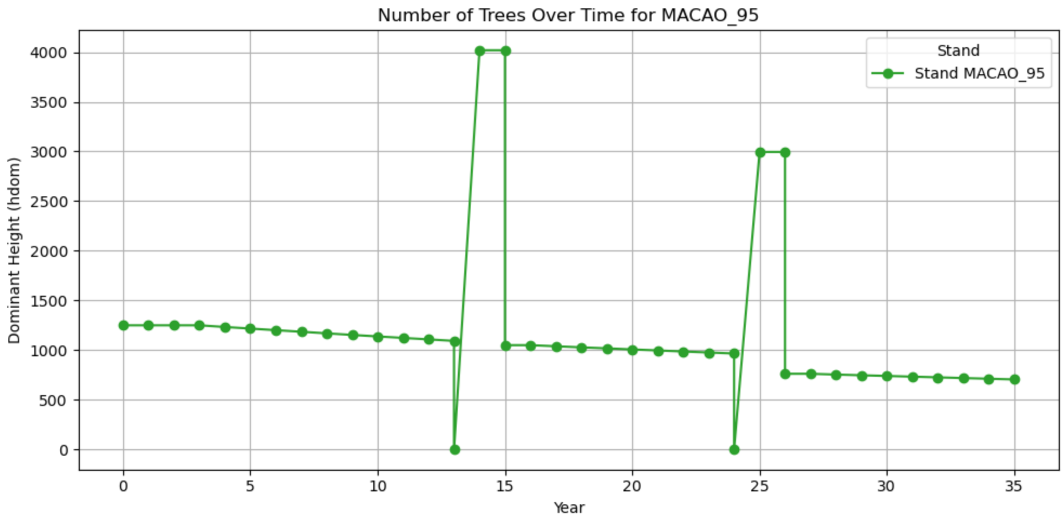

Figure VI.4 – Number of trees over time for Mação_95

Basal area

Another graph depicting basal area is shown in Figure VI.5. It represents the cross-sectional area of trees at 1.3 meters and is commonly used to describe a stand's density. In Mação, higher site indexes correspond to larger basal areas, justifying their superior productivity. After each harvest at 13, 24 and 35 years, the basal area is zero because there are no stumps. Shoot selection happened in year 15 and 26, represented by the fluctuation in those years. The observed decrease in the basal area during the second and third rotation can be justified by the decrease in number of trees, seen in Figures VI.2, VI.3 and VI.4.

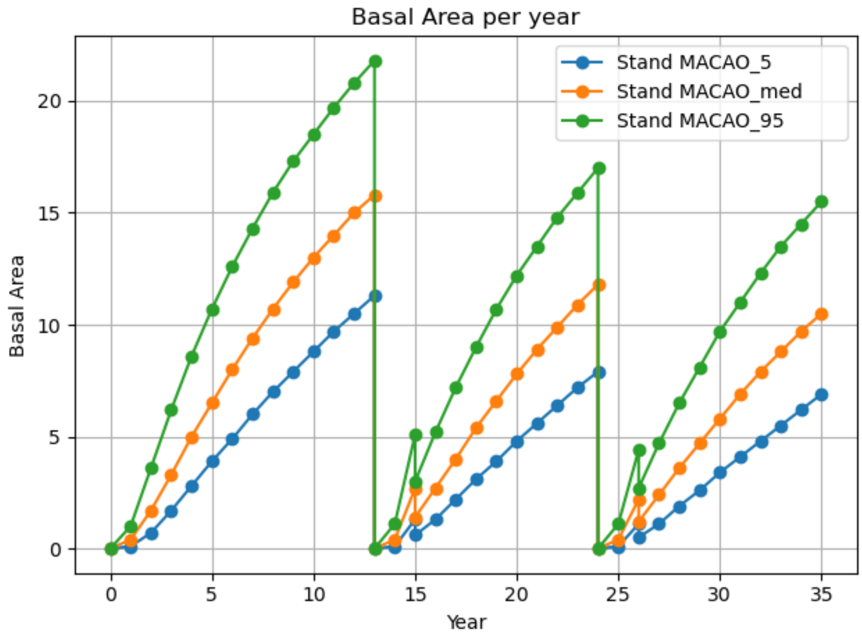

Figure VI.5 – Basal Area over time for all site indexes

EAA

Figure VI.6 shows that the EAA remains consistently negative for all site indexes until the first harvest at year 13, as the total costs are the same across all site indexes. As higher site indexes generate more wood volume and at a faster rate, the EAA is greater for *Mação 95*, whereas it remains negative for *Mação 5*. As the cycle progresses, the EAA rises further during the second and final cut. Contrarily, *Mação 5* remains unprofitable throughout the entire lifecycle, with a consistently negative EAA, highlighting that planting in low site indexes should not be considered.

The graph for yearly NPV is illustrated in Figure VI.7. As most costs occur in the first years due to land preparation, planting, and fertilization, the NPV is negative during these years in all site indexes. Moreover, yearly NPV becomes negative in years with silvicultural operations and remains null except for harvest years, when revenue is generated.

Although NPV turns positive during harvest years – years 13 and 24 – in *Mação 5*, these gains are insufficient to outweigh the negative NPV incurred during initial years. Additionally, the

NPV in the second rotation is lower than in the first due to fewer trees and reduced wood volume (Figure VI.2, VI.3, VI.4.)

Overall, the analysis confirms that higher site indexes yield significantly better financial outcomes, and plantations in low site indexes, like *Mação 5*, should be avoided.

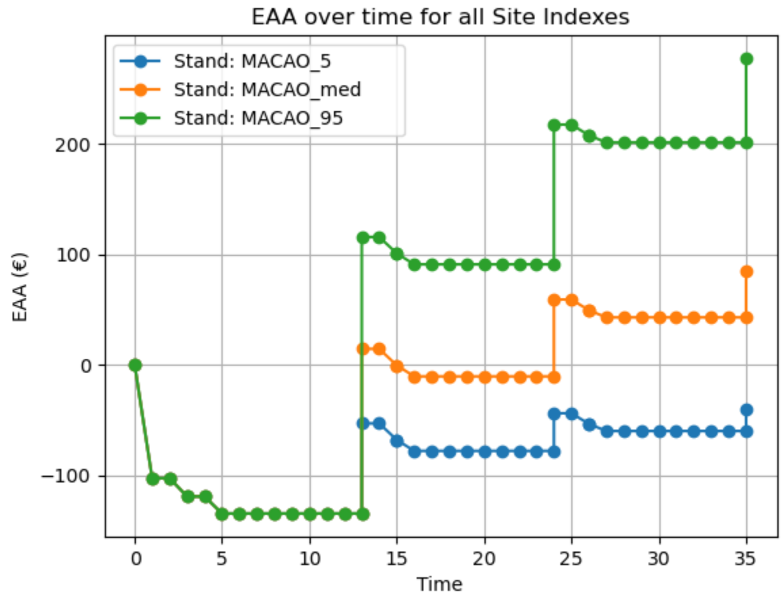

Figure VI.6 – EAA over time for all site indexes

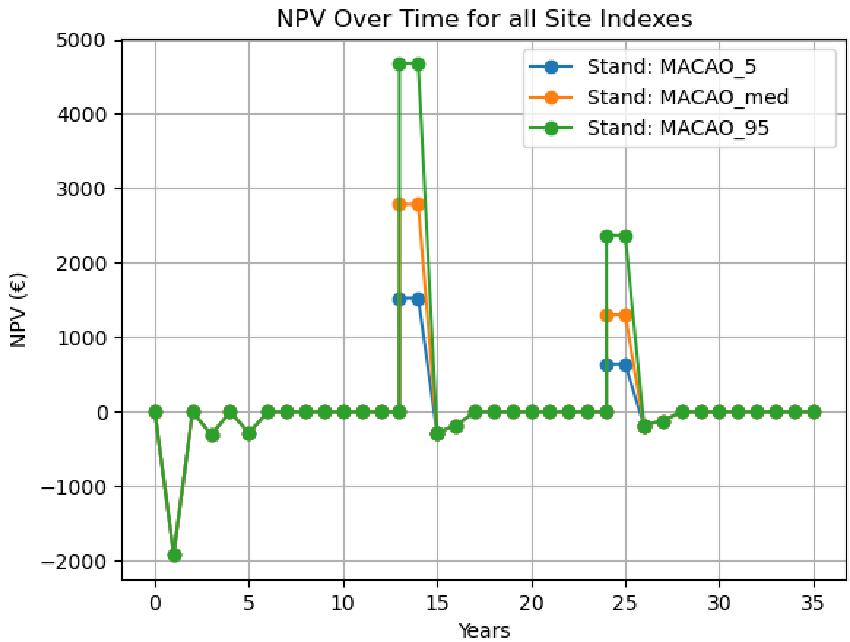

Figure VI.7 – Yearly NPV over time for all site indexes

Appendix VI.3: Sensitivity Analysis

Final Cut Age

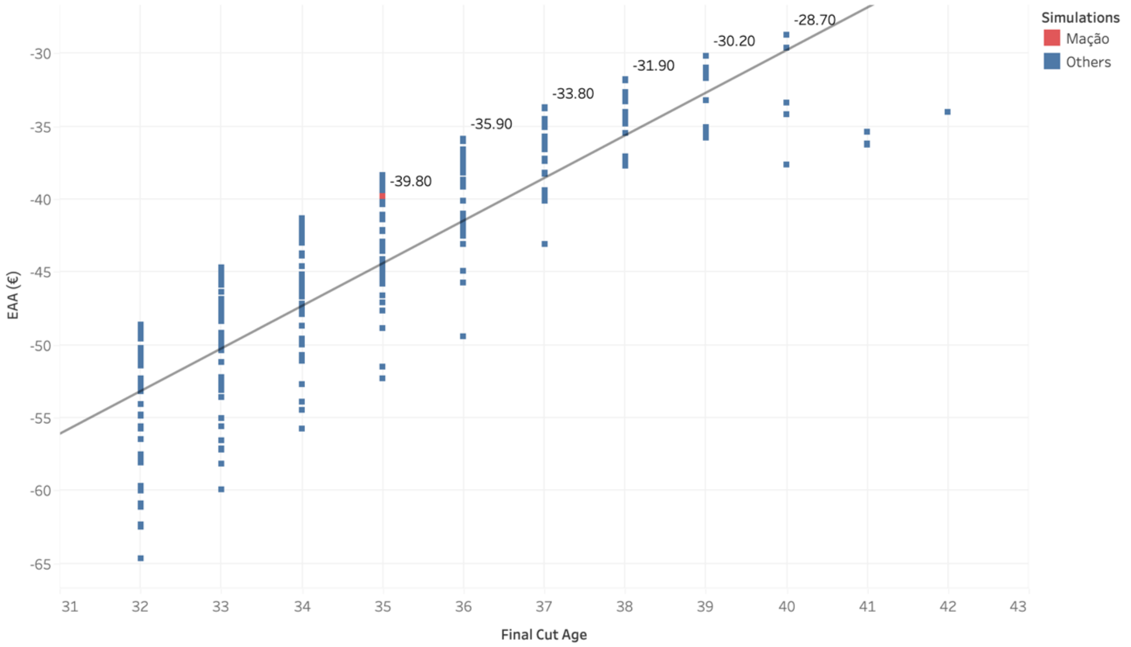

Figure VI.8 – Final Cut Age VS EAA for Mação 5

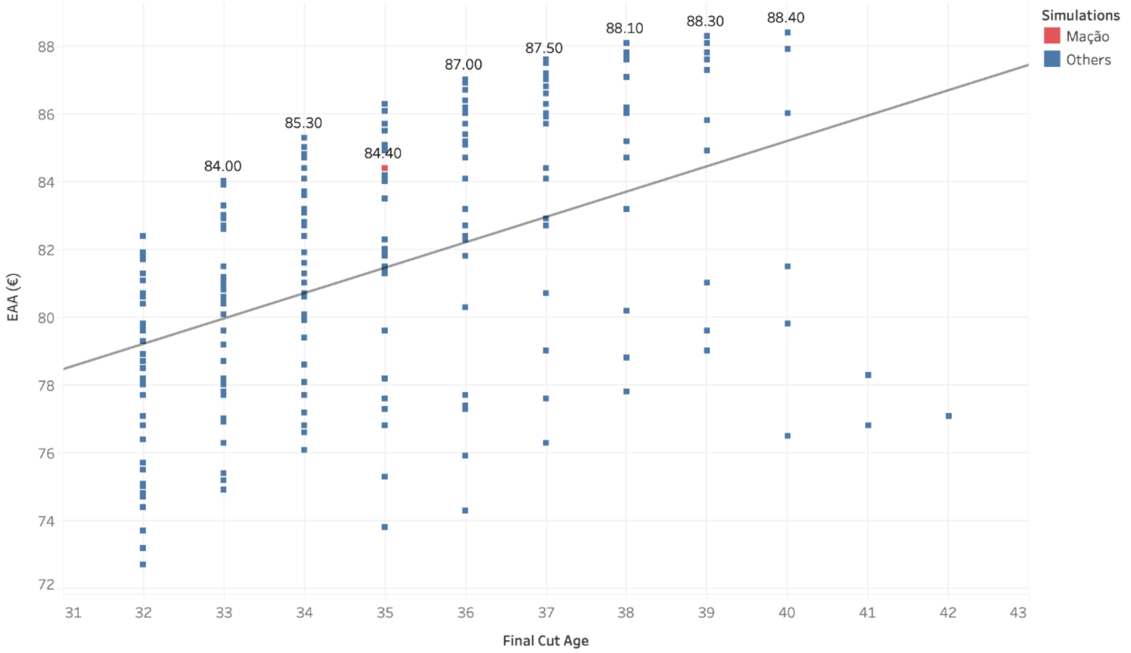

Figure VI.9 – Final Cut Age VS EAA for Mação med

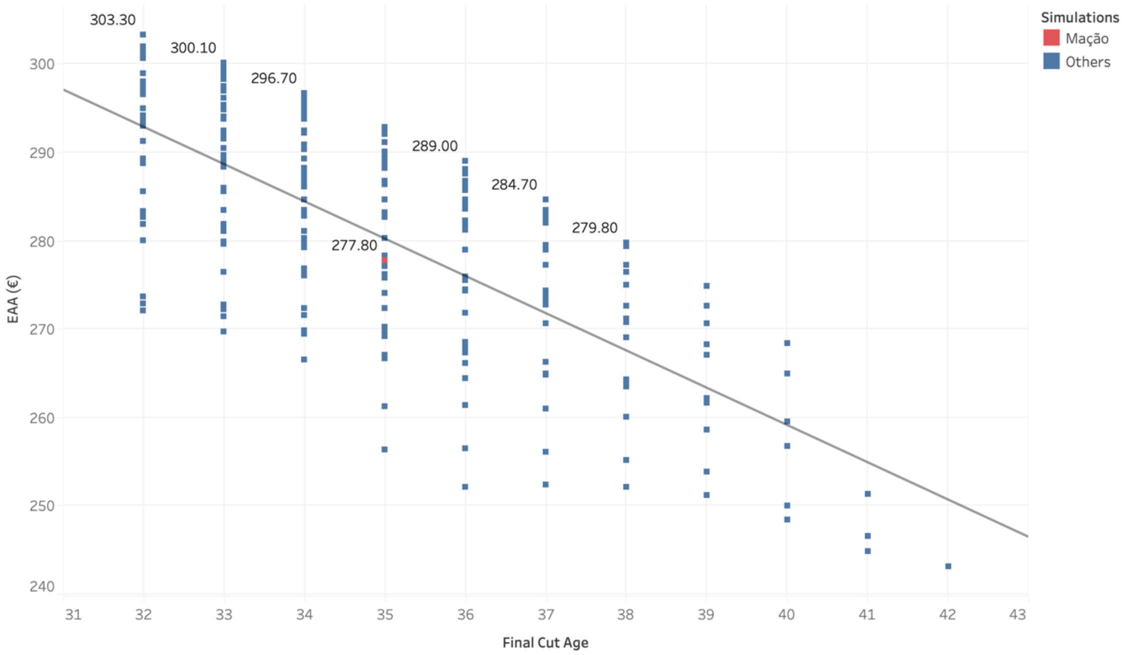

Figure VI.10 – Final Cut Age VS EAA for Mação 95

Rotation Duration

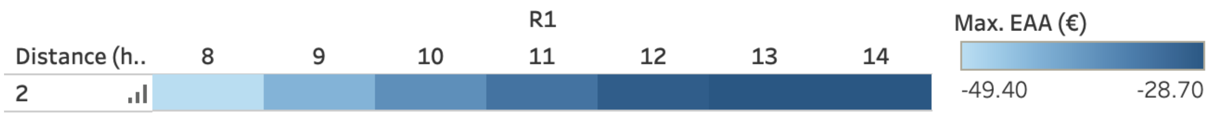

Figure VI.11 – Rotation 1 duration VS EAA for Mação 95

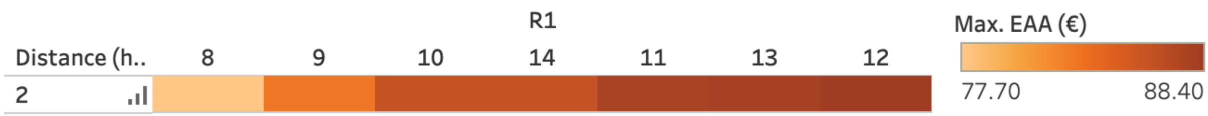

Figure VI.12 – Rotation 1 duration VS EAA for Mação med

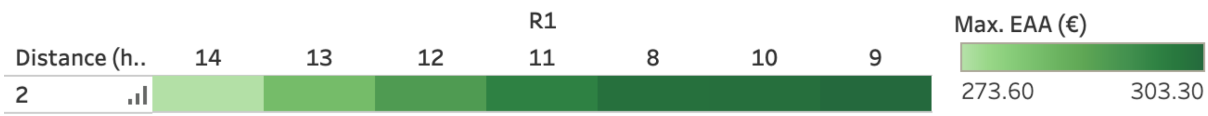

Figure VI.13 – Rotation 1 duration VS EAA for Mação 95

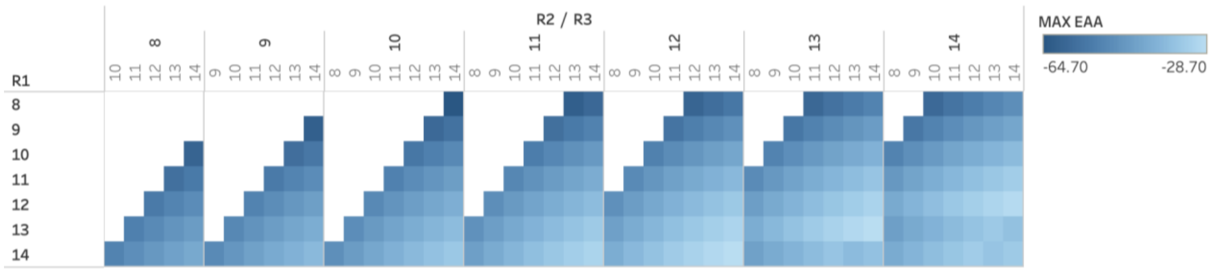

Figure VI.14 – Rotation 1, 2 and 3 durations VS EAA for Mação 5

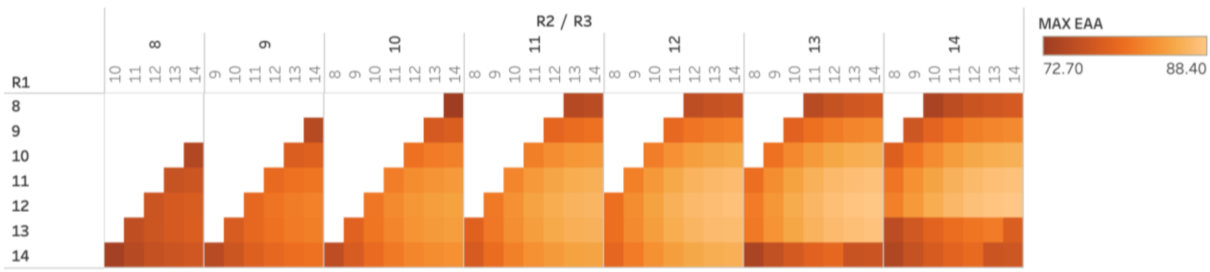

Figure VI.15 – Rotation 1, 2 and 3 durations VS EAA for Mação med

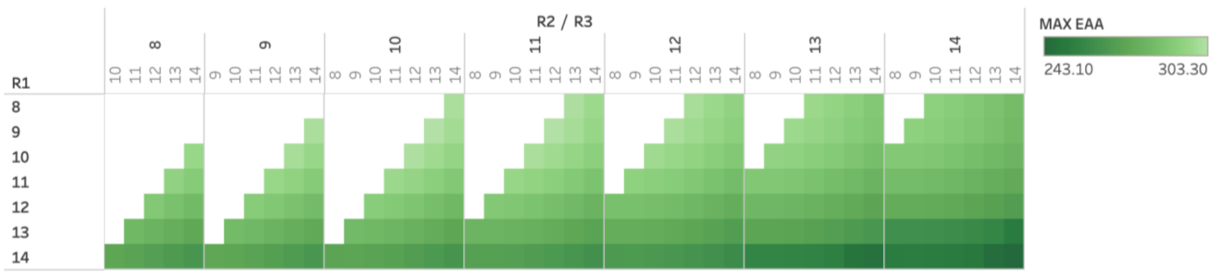

Figure VI.16 – Rotation 1, 2 and 3 durations VS EAA for Mação 95

Beat-up Rate

Scenario1	Retancha Percent (%)	Npv (€)
Mação 5	5	-725.6
Mação 5	10	-734.6
Mação 5	15	-743.6
Mação 5	20	-752.6
Mação 95	5	5202.4
Mação 95	10	5193.3
Mação 95	15	5184.3
Mação 95	20	5175.3
Mação med	5	1594.0
Mação med	10	1585.0
Mação med	15	1576.0
Mação med	20	1566.9

Figure VI17. – NPV for different beat-up rates

Appendix VII - The Case of Cork Oak

Appendix VII.1: Coark Oak Characteristics

Figure VII.1 - Distribution Area of "Montados" in Continental Portugal *(Matias 2008)*

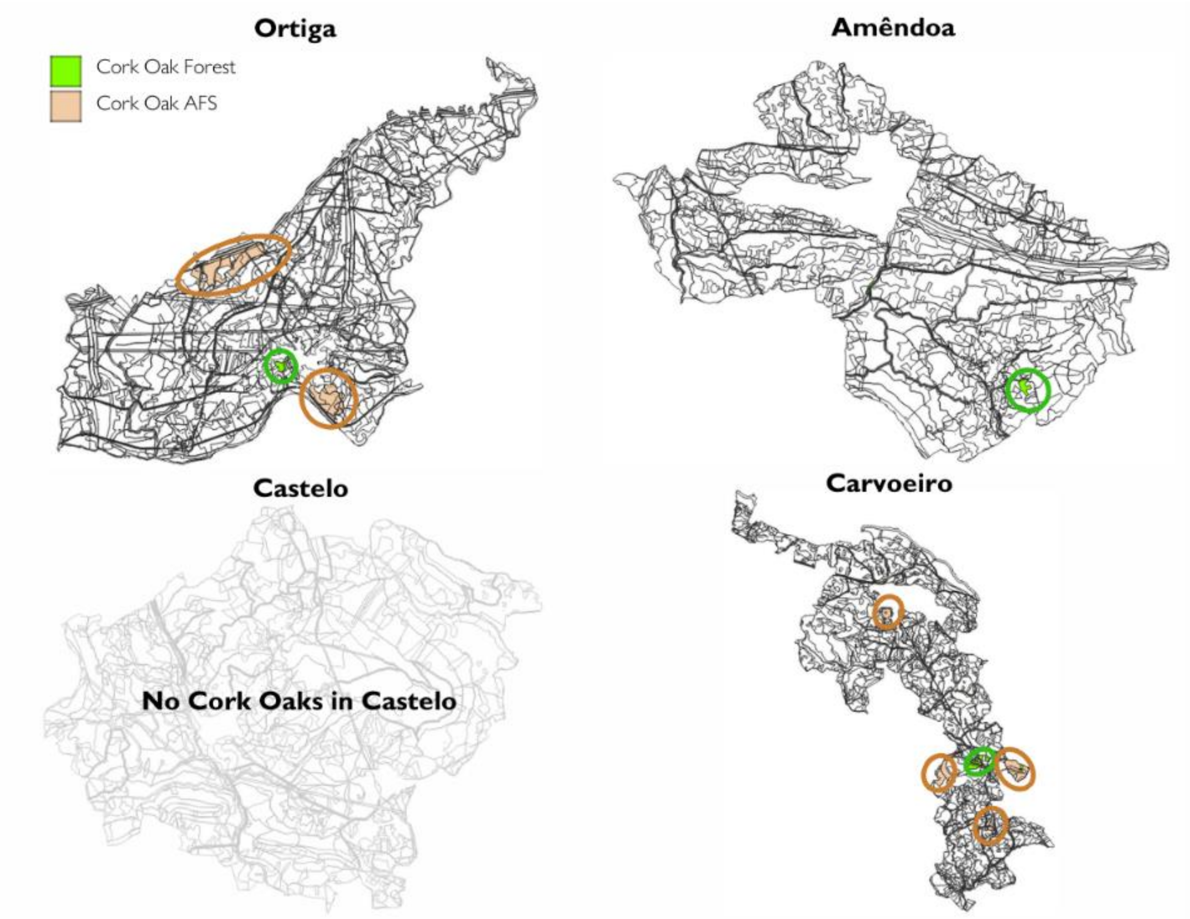

Figure VII.2 - Cork Oaks in Ortiga, Amêndoa, Castelo and Carvoeiro (according to POSA)

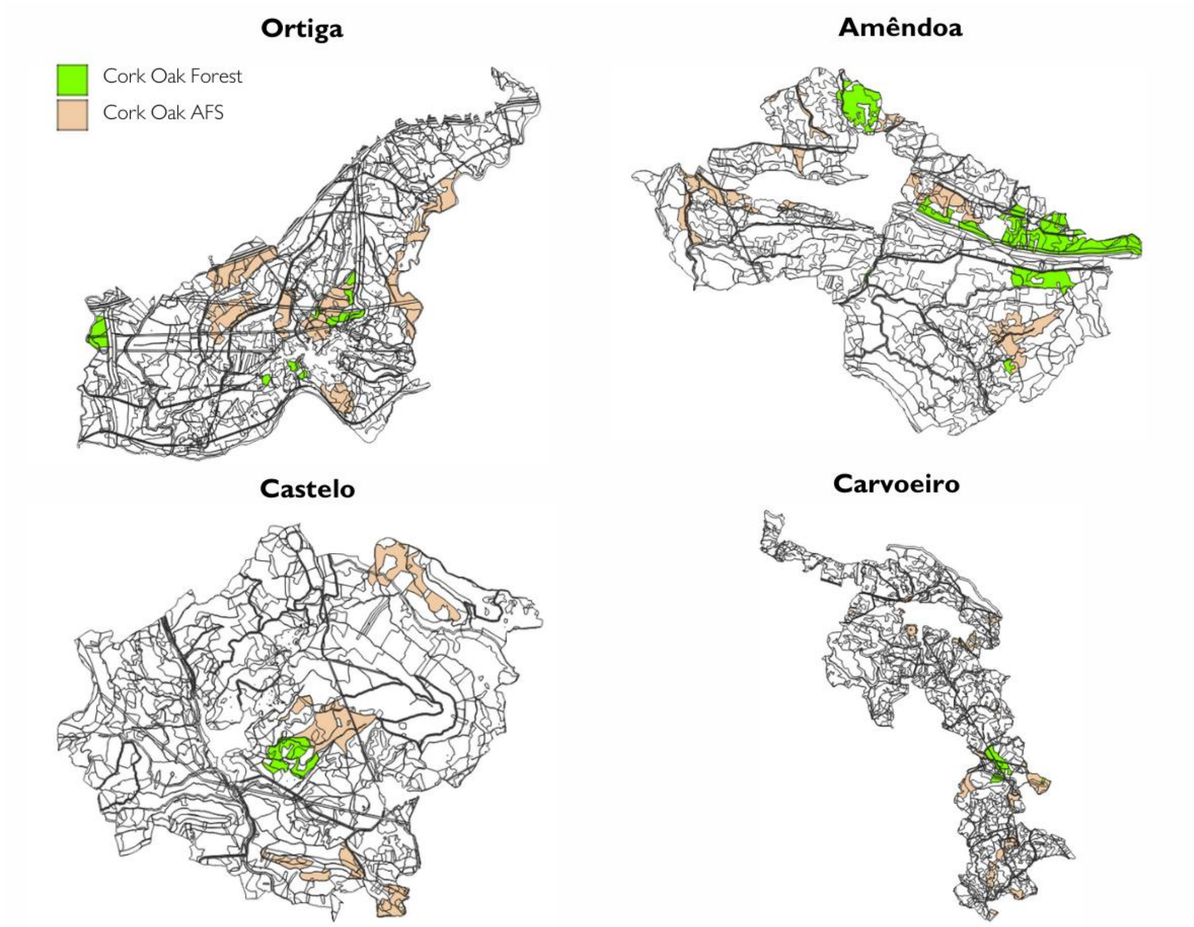

Figure VII.3 - Proposed Cork Oaks in Ortiga, Amêndoa, Castelo and Carvoeiro (according to POSP)

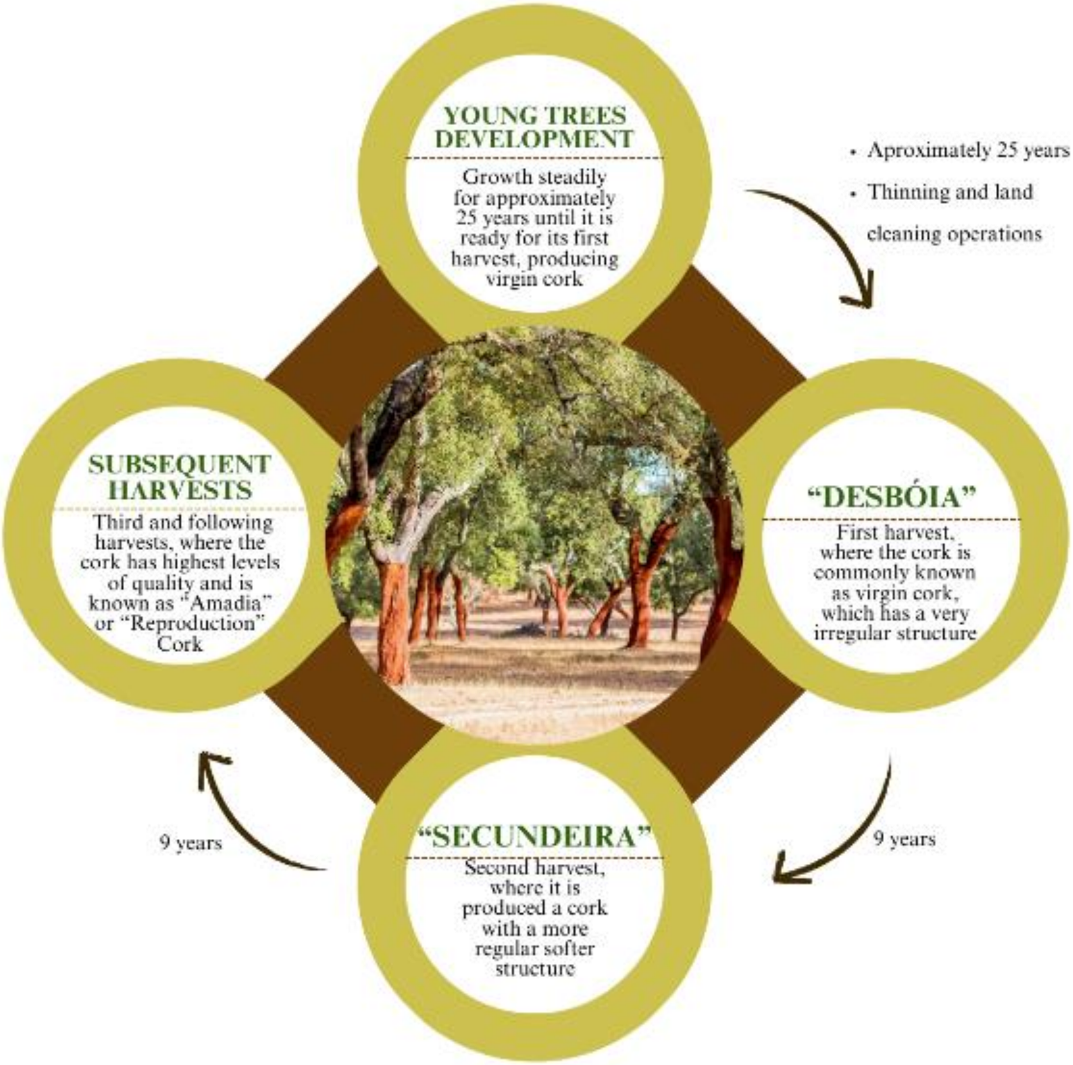

Figure VII.4 **-** *Growing Cycle of the Cork Oak*

Appendix VII.2: Developed Models - Growth and Economic Model

Baseline Economic Model for the Cork Oak

The baseline economic model serves as an initial model for the cork oak. It consists of a simplified approach designed to simulate the growth and yield of individual cork oak trees and its revenue, specifically the revenues generated from the cork extraction.

Key Parameters

The baseline economic model developed for a single cork oak uses specific parameters to simulate a cork oak growth and its economic results. For this model, other biomass beyond cork were not considered. The focus was on understanding the impact of cork extraction on revenues, since this is main purpose when planning a new cork oak stand.

For this model, growth rates are also important because they define the tree's yearly expansion. Furthermore, in this model the cork oak's age has a significant impact on both the quality and quantity of cork, especially when distinguishing between virgin cork and “amadia” cork. The cork extracted on the second harvest for the model is also classified as “amadia”, since determining its quality and price and how much it distinct is challenging with no concrete data available on that.

The management practices also play an important role in shaping this model. The operations include the harvest interval and the year of the last harvest, if it is not the first harvest and the tree have been harvested before, or the planting year, in case it is the first harvest. Other input is the maximum number of harvests, which determines how many times a cork oak can be stripped during its lifetime, in this context represents for how long the cork oak will generate revenues.

In this initial model, the virgin cork price indicates the value (€ per kg) of cork from the first harvest, and the “amadia” cork price, for the following harvests, were the only considered factors to calculate the revenue of an individual cork oak tree.

Logic and Functionality

To simulate the economic returns of cork oak management it is important to estimate the cork yield and the corresponding revenues over multiple harvests during the tree’s lifespan. The process is split into two main parts: calculating the cork weight and determining the revenues.

The sequence of harvests and their calculations follow the management practices mentioned above. If the cork oak is being harvested for the first time, the starting year is calculated by adding 25 years to the planting year, with this being the considered age for the tree to have a sustainable development. For subsequent harvests, the starting year is determined by adding the harvest interval to the year of the previous harvests.

After the starting year is determined, the model progresses through each harvest by incrementing the year by the harvest interval and updating the harvest count. This process repeats until the maximum number of harvests is reached, calculating, for each harvest, the cork weight and revenue using the appropriate equations.

For virgin cork the weight is calculated using equation:

$$(1) \quad Wv = -2.56859 + 0.02740 \times hd + 0.00074351 \times c^2$$

Equation 6.1 - Virgin Cork Oak Estimation for an Individual Tree(Tomé 2004)

In the equation, hd is the height of cork harvest (in meters), and c is the trunk circumference at 1.3 meters over cork (in meters). For the "amadia" cork the weight is calculated using the equation:

$$(2) \left(0.0618 \times du^{1.0418} \times hd^{0.6527} \times ct^{\{0.4588\}}\right\} \times \left(1 - \left(\frac{w \cos ta}{100}\right) \times \frac{ct}{ct9}\right) +$$

$$(0.0618 \times du^{1.0418} \times hd^{0.6527} \times ct^{0.4588}) \times \frac{w \cos ta}{100}$$

Equation 6.2 - Amadia Cork Weight Estimation for an Individual Tree (Tomé 2004)

In this equation du is the diameter at 1.30 meters (in centimeters), hd is the height of cork harvest (in meters), ct is the cooked cork caliber (in millimeters), and wcosta is the percentage weight of cork back. Revenues for each type of cork are then calculated by multiplying the respective weights by the market price:

$$(3) \quad Rv = Wv \times Pv$$

Equation 6.3 - Revenue for Virgin Cork Extracted from an Individual Tree

$$(4) \quad Ra = Wa \times Pa$$

Equation 6.4 - Revenue for Amadia Cork Extracted from an Individual Tree

In these two equations, P is the price per kilogram. Overall, this baseline model integrates growth dynamics, cork harvest schedules, and market factors to estimate cork yields and revenues, providing a comprehensive view of the economic potential throughout a cork oak's lifecycle.

Limitations

This model differs from the SUBER, particularly in how it handles growth dynamics. Cork oaks have considerable genetic and environmental variability, and while this model captures the specifics of one tree, it struggles to consider differences between trees. The use of simplified growth equations, which rely on fixed parameters and assumptions, may not fully capture the complexity of cork oak growth.

Moreover, this model only considers revenues and does not consider the costs related to forestry operations like planting, maintenance, and thinning. Because of this, the model does not provide a full economic assessment, ignoring the costs that have a significant impact on overall profitability.

SUBER addresses these limitations by considering genetic and environmental variability, using more detailed growth equations, and considering both revenues and costs. Its approach at the stand level and its ability to adjust growth and cork harvest schedules dynamically make it a completer and more realistic tool for managing cork oak forests.

Appendix VII.3: Sensitivity Analysis

Operations	Years of Operation	Cost Considered
Fertilization	1	0.11 eur/un
Stump Removal	1	0.4 eur/un
Harrowing	1	475 eur/ha
Planting	1	0.18 eur/un
Replanting	1 (6 Months After Planting)	0.18 eur/un
Ripping	1	650 eur/ha
Vegetation Control	3, 5, 7, 9, 11, 13, 15, 22 (And every 20 Years Thereafter)	300 eur/ha
Thinning	9, 15, 22, 30	0.745 eur/un
Prunning	9, 22, 25, 30	0.92 eur/un

Table VII.1 - Operations used in the Analysis, Years that Occur and their Costs

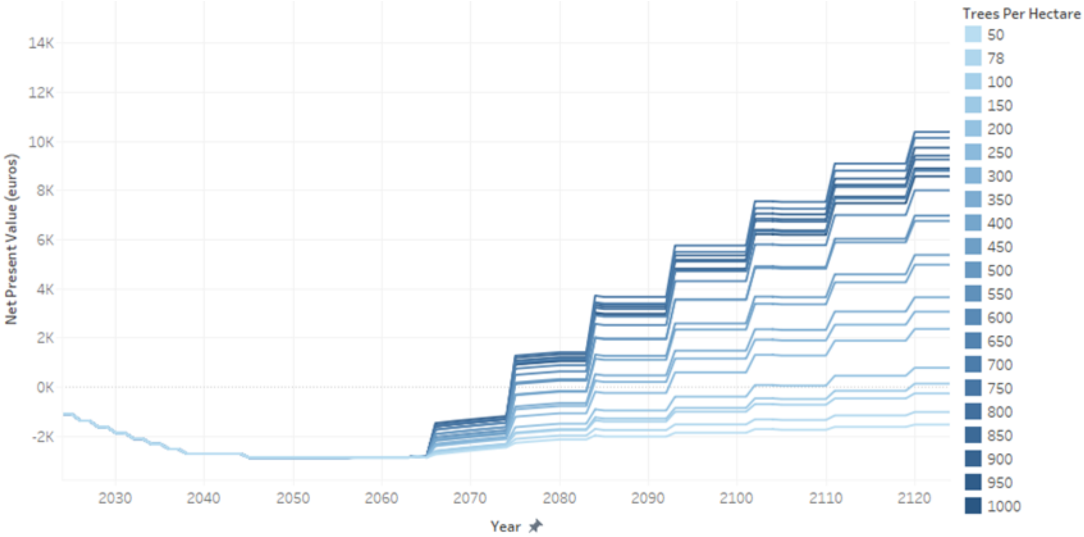

Figure VII.5 - Net Present Value Evolution Across 100 Years for Different Planted Trees Densities

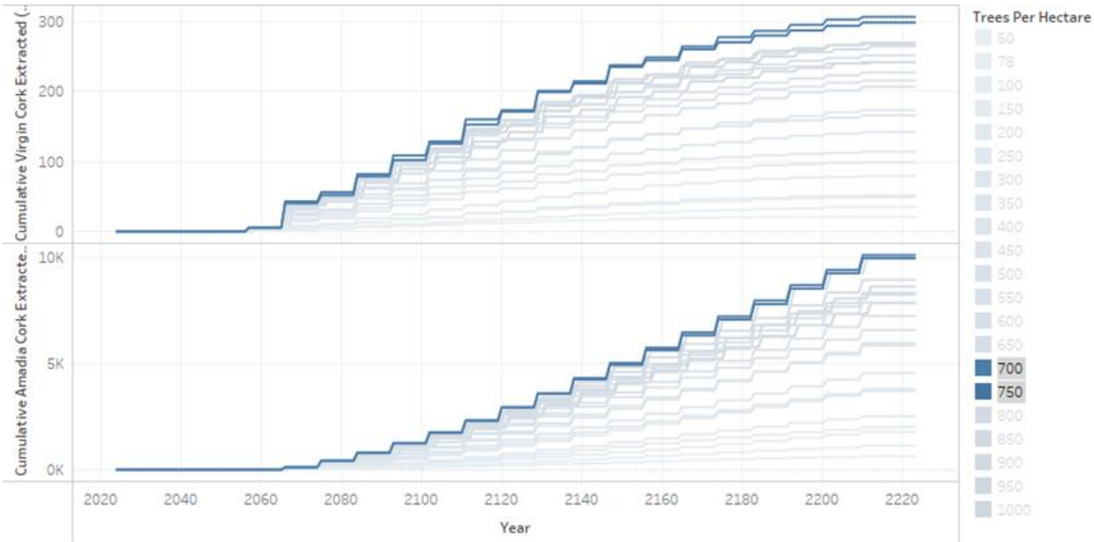

Figure VII.6 - Cumulative Virgin and "Amadia" Cork Extracted Evolution Across 200 Years for Different Planted Trees Densities

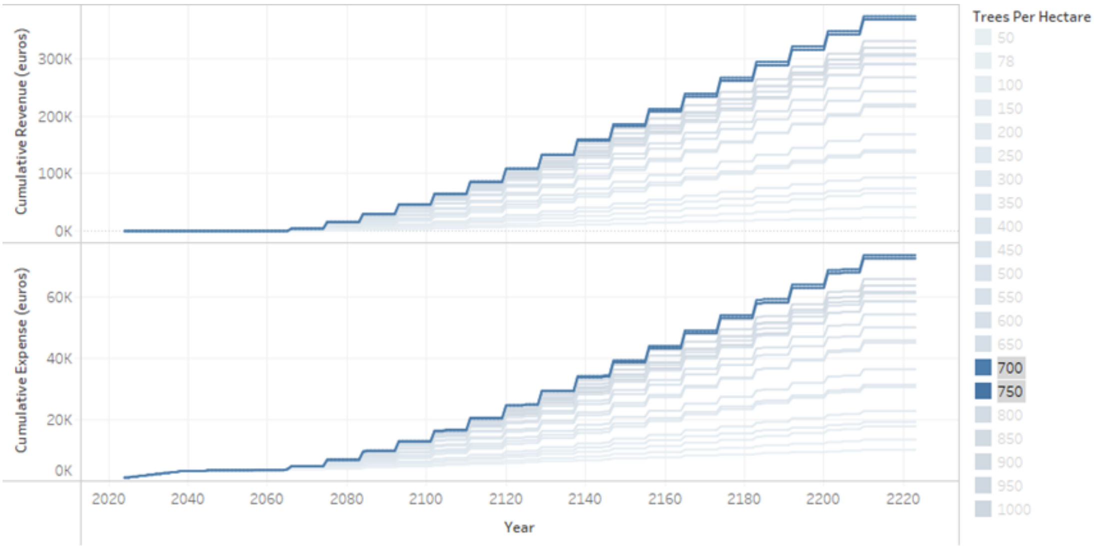

Figure VII.7 - Cumulative Revenues and Expenses Evolution Across 200 Years for Different Planted Trees Densities

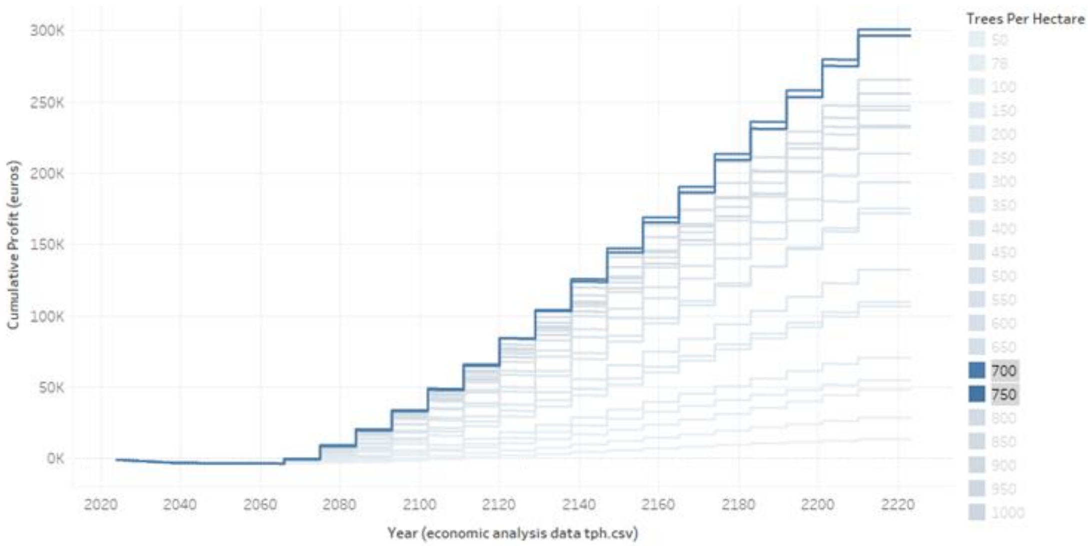

Figure VII.8 - Cumulative Profit Evolution Across 200 Years for Different Planted Trees Densities

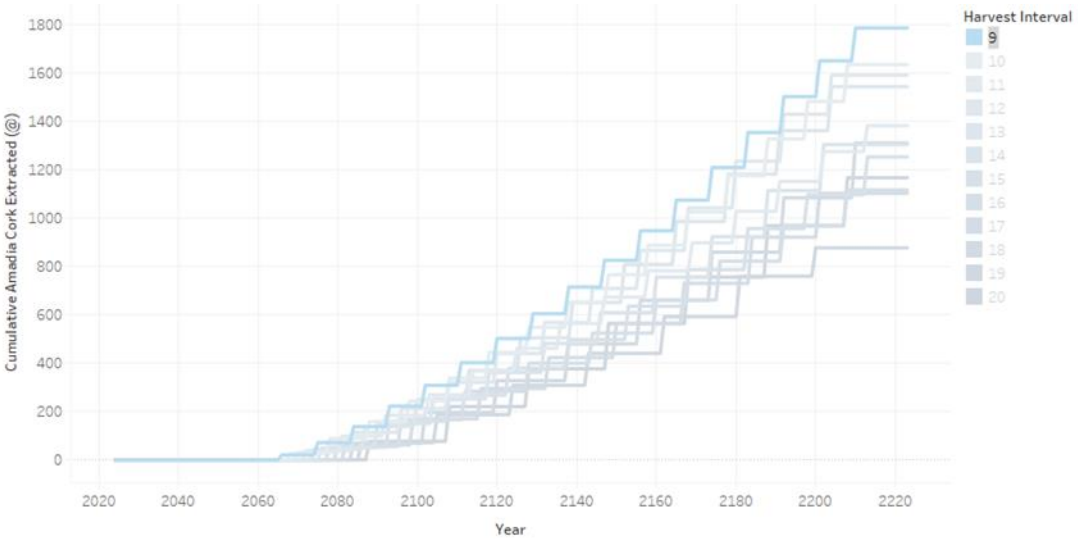

Figure VII.9 - Cumulative "Amadia" Cork Extracted Evolution Across 200 Years for Different Harvest Intervals

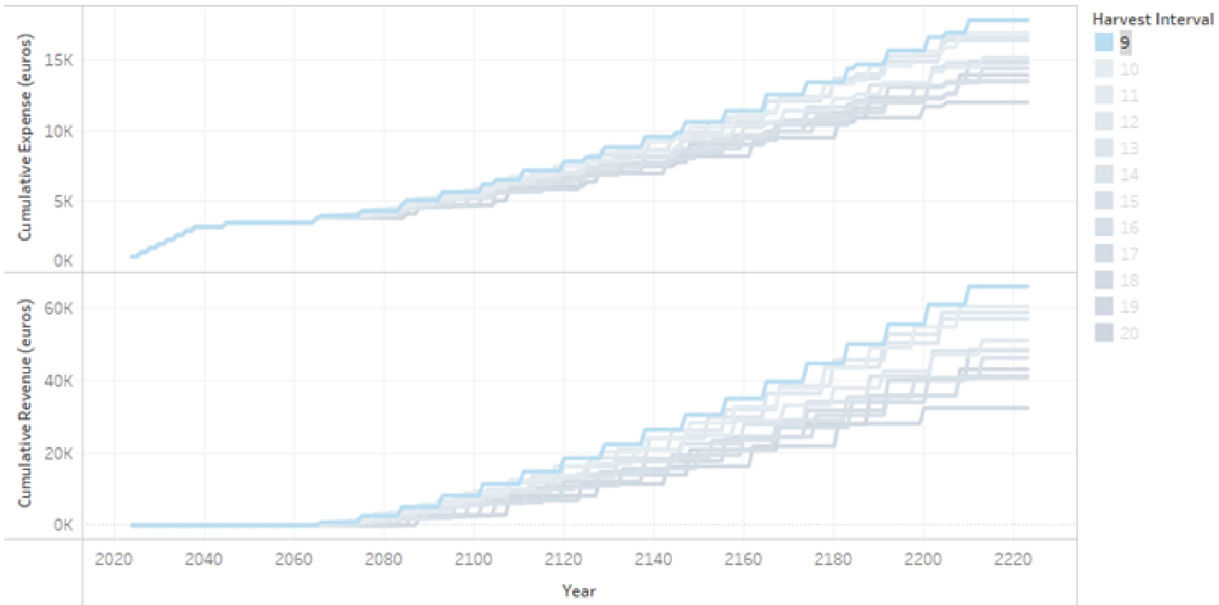

Figure VII.10 - Cumulative Expense and Revenue Evolution Across 200 Years for Different Harvest Intervals

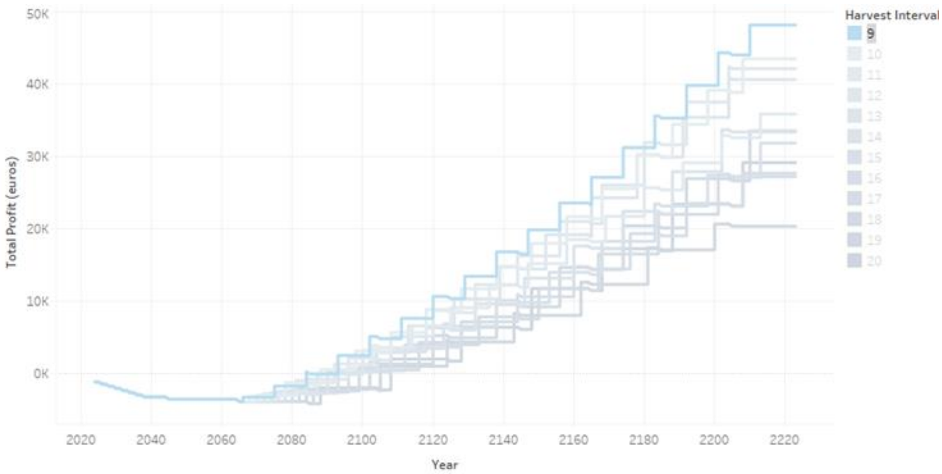

Figure VII.11 - Cumulative Total Profit Evolution Across 200 Years for Different Harvest Intervals

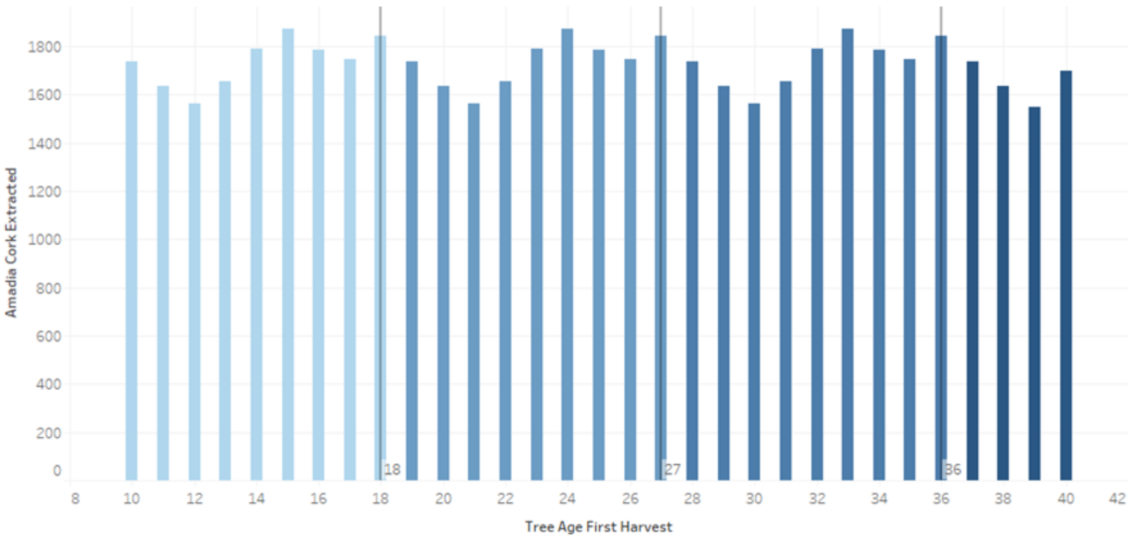

Figure VII.12 - Cumulative "Amadia" Cork Extracted by Tree Age at First Harvest

Top 10 Combinations for Live Trees (Year 2223)

Order	Trees Per Hectare	Tree Age at First Harvest	Harvest Interval	Total Live Trees	Total Amadia Cork (Cumulative)
1	750	22	11	117	10071.05
2	750	33	11	117	10071.05
3	700	22	13	106	8808.49
4	700	35	13	106	8808.49
5	700	26	12	105	8728.53
6	750	35	9	103	10154.66
7	750	20	12	103	10313.04
8	750	32	12	103	10313.04
9	700	26	13	103	8382.99
10	750	17	9	103	10154.66

Table VII.2 - Best 10 Variable Combinations for Maximizing Live Tress for 200 Years

Top 10 Combinations for Amadia Cork (Cumulative)

Order	Trees Per Hectare	Tree Age at First Harvest	Harvest Interval	Total Live Trees	Total Amadia Cork (Cumulative)
1	750	32	12	103	10313.04
2	750	20	12	103	10313.04
3	700	26	9	90	10219.1
4	700	35	9	90	10219.1
5	700	17	9	90	10219.1
6	750	17	9	103	10154.66
7	750	35	9	103	10154.66
8	750	26	9	103	10154.66
9	750	17	10	97	10133.79
10	750	27	10	97	10133.79

Table VII.3 - *Best 10 Variable Combinations for Maximizing Cumulative "Amadia" Cork Extraction for 200 Years*

Top 10 Combinations for NPV (50 Years)

Order	Trees Per Hectare	Tree Age at First Harvest	Harvest Interval	Net Present Value
1	900	32	9	791.55
2	900	23	9	791.55
3	900	32	9	791.55
4	900	23	9	791.55
5	750	23	9	705.36
6	750	32	9	705.36
7	750	32	9	705.36
8	750	23	9	705.36
9	850	23	9	688.6
10	850	23	9	688.6

Table VII.4 - *Best 10 Variable Combinations for Maximizing NPV for 50 Years*

Top 10 Combinations for NPV (100 Years)

Order	Trees Per Hectare	Tree Age at First Harvest	Harvest Interval	Net Present Value
1	700	35	9	10737.39
2	700	26	9	10737.39
3	700	17	9	10737.39
4	750	35	9	10474.9
5	750	17	9	10474.9
6	750	26	9	10474.9
7	750	25	9	10390.14
8	750	34	9	10390.14
9	750	16	9	10390.14
10	700	19	9	10337.65

Table VII.5 - *Best 10 Variable Combinations for Maximizing NPV for 100 Years*

Top 10 Combinations for NPV (200 Years)

Order	Trees Per Hectare	Tree Age at First Harvest	Harvest Interval	Net Present Value
1	700	17	9	15112.09
2	700	35	9	15112.09
3	700	26	9	15112.09
4	750	29	9	14859.65
5	750	20	9	14859.65
6	750	17	9	14776.99
7	750	26	9	14776.99
8	750	35	9	14776.99
9	750	16	9	14776.71
10	750	25	9	14776.71

Table VII.6 - Best 10 Variable Combinations for Maximizing NPV for 200 Years

Appendix VIII – The Case of Olive Tree

Appendix VIII.1 – Inputs of the Developed Model

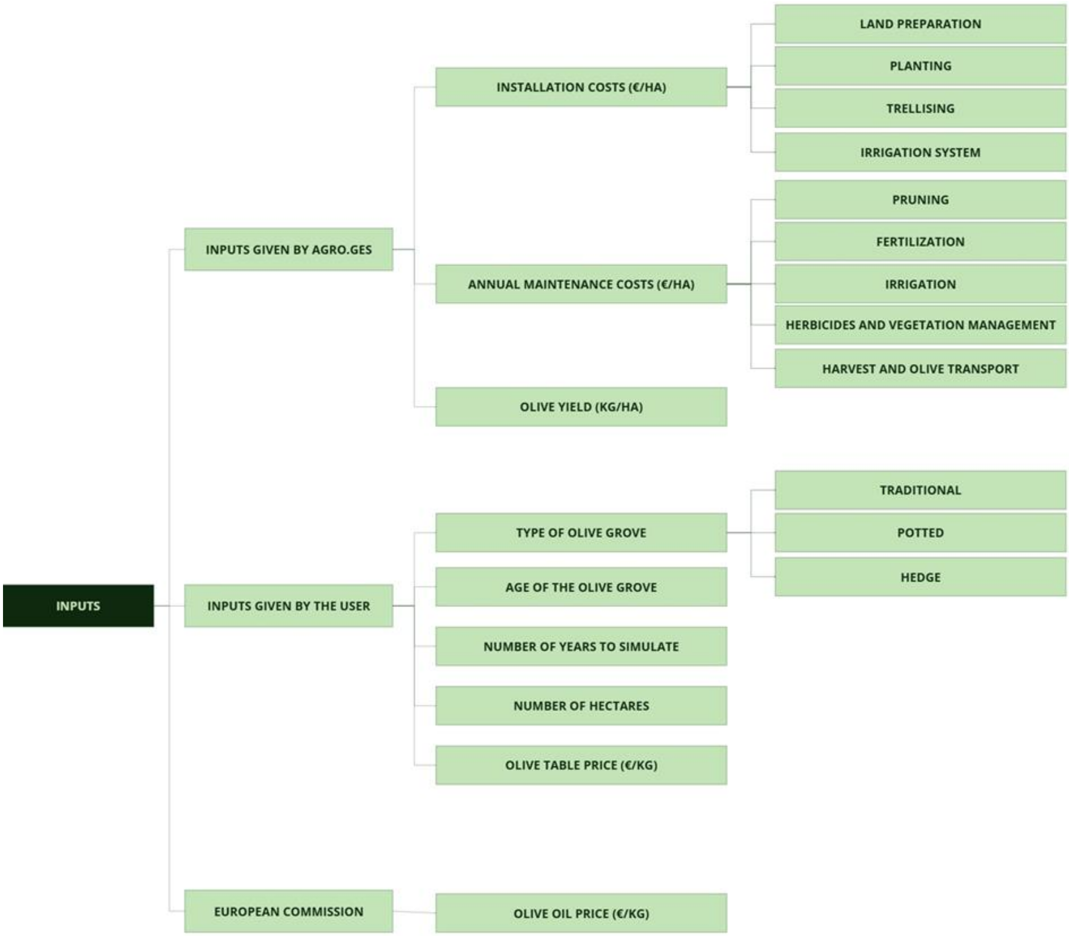

Figure VIII.1 – Inputs of the developed model's structure

Appendix VIII.2 – Simulation of the Developed Model

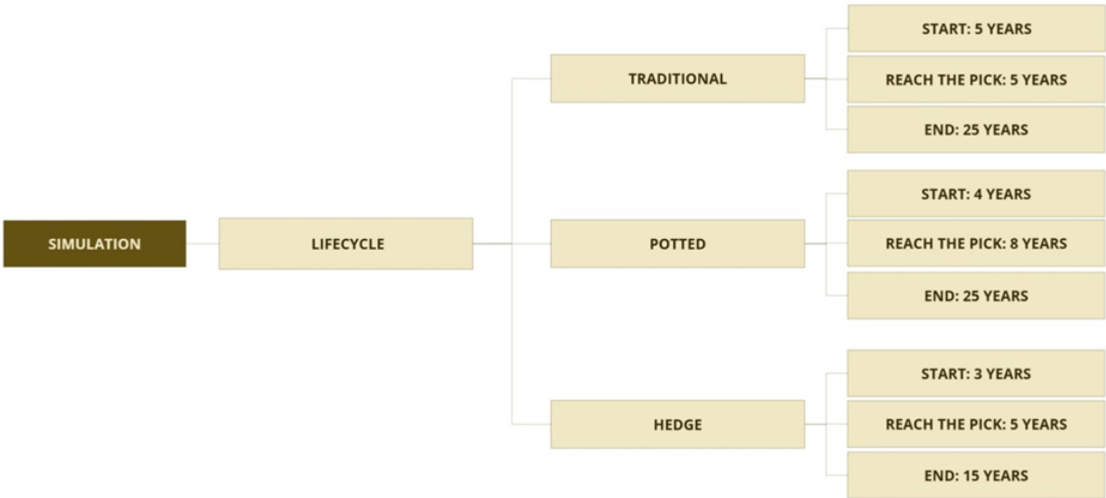

Figure VIII.2 – Simulation Structure

Appendix VIII.3 – Outputs of the Developed Model

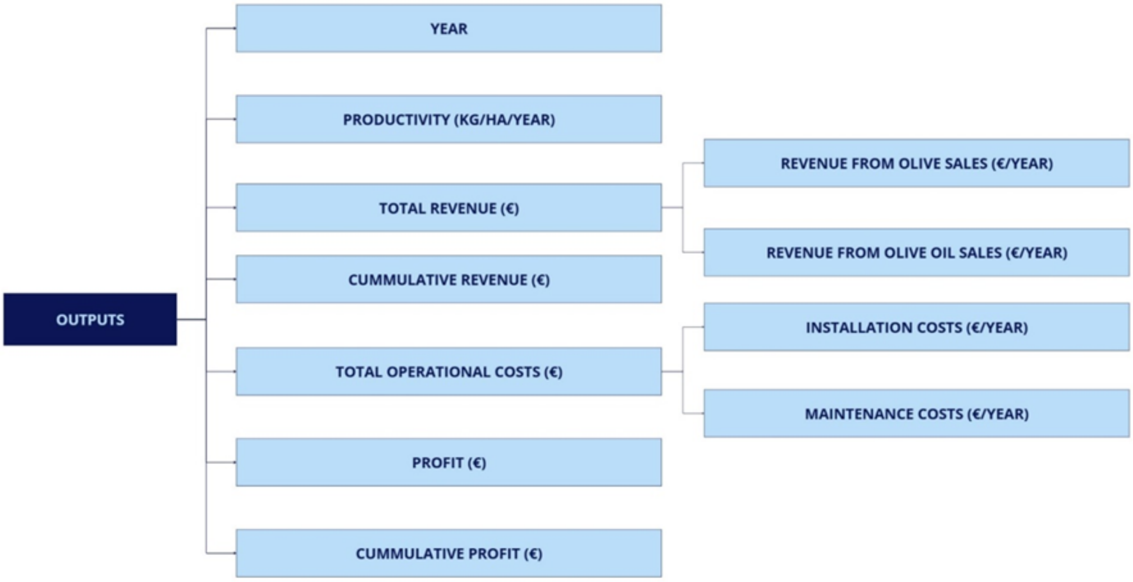

Figure VIII.3 – Outputs of the developed model's structure

Appendix IX – The Case of Solar Panels

Appendix IX.1: Initial Selection

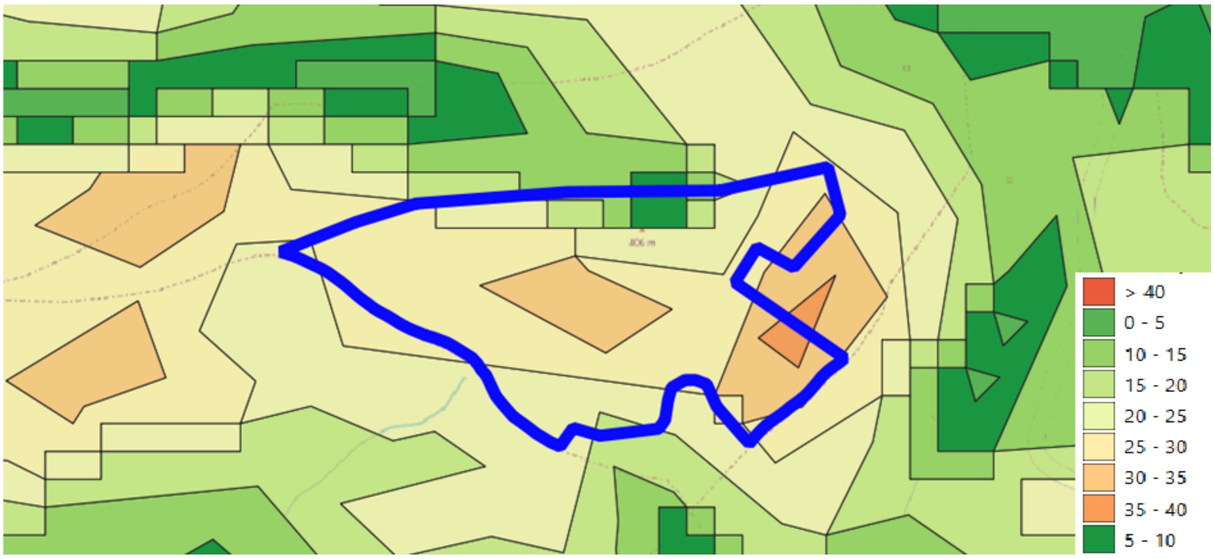

Figure IX.1 - Polygon 4's (Carvoeiro) Hipsometry (%) Visualized

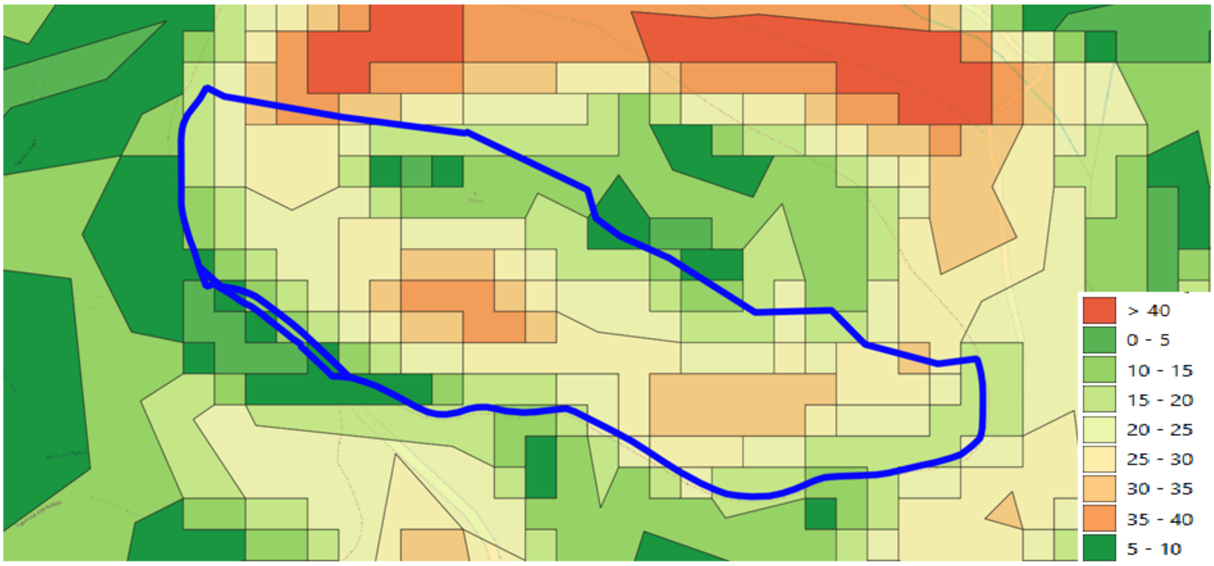

Figure IX.2 - Polygon 2's (Penhasocos) Hipsometry (%) Visualized

Appendix IX.2: Final Selection

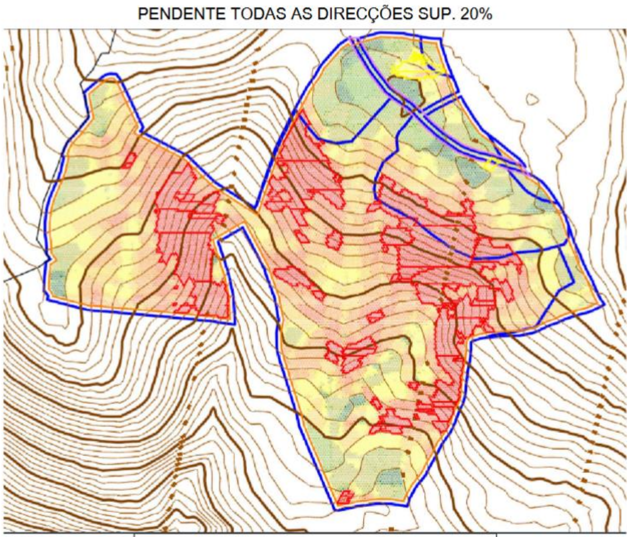

Angle min., %	Angle max., %	Color	Distribution, %
0.00	0.00		2.68
0.00	2.50		1.02
2.50	5.00		1.82
5.00	7.50		5.60
7.50	10.00		10.56
10.00	12.50		12.70
12.50	15.00		14.47
15.00	17.50		16.54
17.50	20.00		13.43
20.00	142.81		21.18

Figure IX.3 - Area of Polygon 5's terrain with slope above 20%

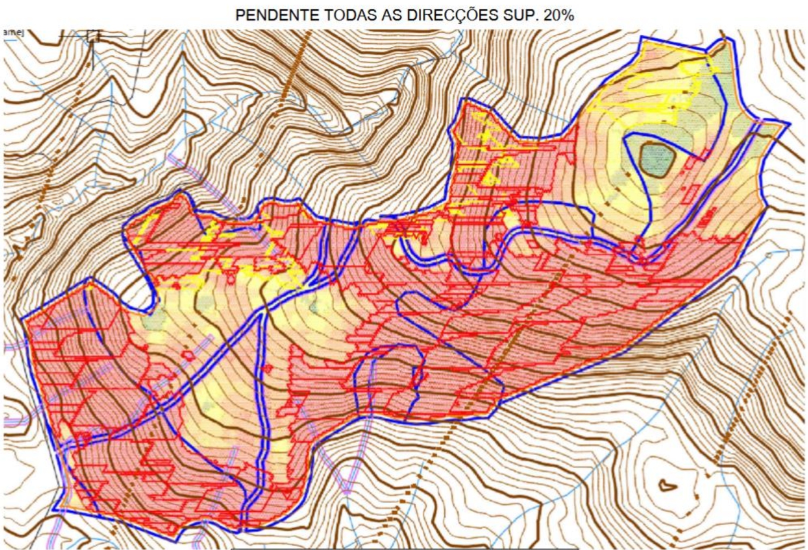

Angle min., %	Angle max., %	Color	Distribution, %
0.00	0.00		0.31
0.00	2.50		0.25
2.50	5.00		0.12
5.00	7.50		1.11
7.50	10.00		3.49
10.00	12.50		5.97
12.50	15.00		8.69
15.00	17.50		12.90
17.50	20.00		7.66
20.00	142.81		59.50

Figure IX.4 - Area of Polygon 6's terrain with slope above 20%

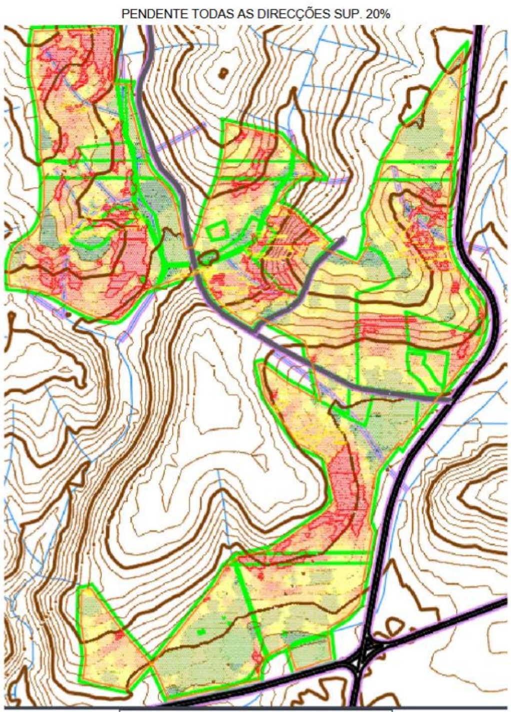

Angle min., %	Angle max., %	Color	Distribution, %
0.00	0.00		4.20
0.00	2.50		2.20
2.50	5.00		2.22
5.00	7.50		8.15
7.50	10.00		12.86
10.00	12.50		16.57
12.50	15.00		16.02
15.00	17.50		13.64
17.50	20.00		10.25
20.00	142.81		13.89

Figure IX.5 - Area of Polygon 1’s terrain with slope above 20%

Appendix IX.3: Final Sites Simulations

Project summary

Geographical Site	**Situation**		**Project settings**	
MAÇÃO	Latitude	39.63 °N	Albedo	0.20
Portugal	Longitude	-7.99 °W		
	Altitude	564 m		
	Time zone	UTC		

Weather data
MAÇÃO
MeteoNorm file - Synthetic

System summary

Grid-Connected System — **Ground system (tables) on a hill**

PV Field Orientation		**Near Shadings**	**User's needs**
Fixed plane		Linear shadings : Fast (table)	Unlimited load (grid)
Tilt/Azimuth	20.7 / 3.2 °		

System information

PV Array		**Inverters**	
Nb. of modules	22533 units	Nb. of units	39 units
Pnom total	14.98 MWp	Pnom total	11.70 MWac
		Pnom ratio	1.281

Results summary

Produced Energy	24776885 kWh/year	Specific production	1654 kWh/kWp/year	Perf. Ratio PR	82.83 %

Figure IX.6 - *Castelo’s Joint Sites Project Summary*

PV Array Characteristics

PV module		Inverter	
Manufacturer	Suntech	Manufacturer	Huawei Technologies
Model	STP665S-D66/Wmh_1500V_20V01_2384	Model	SUN2000-330KTL-H1-Preliminary V0.1
(Custom parameters definition)		(Custom parameters definition)	
Unit Nom. Power	665 Wp	Unit Nom. Power	300 kWac
Number of PV modules	22533 units	Number of inverters	39 units
Nominal (STC)	14.98 MWp	Total power	11700 kWac
Modules	777 string x 29 In series	Operating voltage	500-1500 V
At operating cond. (50°C)		Max. power (=>30°C)	330 kWac
Pmpp	13.64 MWp	Pnom ratio (DC:AC)	1.28
U mpp	998 V	Power sharing within this inverter	
I mpp	13659 A		
Total PV power		**Total inverter power**	
Nominal (STC)	14984 kWp	Total power	11700 kWac
Total	22533 modules	Max. power	12870 kWac
Module area	69995 m²	Number of inverters	39 units
Cell area	65585 m²	Pnom ratio	1.28

Figure IX.7 - Castelo's Photovoltaic Modules' Characteristics

Array losses

Array Soiling Losses
Loss Fraction 2.0 %

Thermal Loss factor
Module temperature according to irradiance
Uc (const) 29.0 W/m²K
Uv (wind) 0.0 W/m²K/m/s

DC wiring losses
Global array res. 1.2 mΩ
Loss Fraction 1.5 % at STC

LID - Light Induced Degradation
Loss Fraction 2.0 %

Module Quality Loss
Loss Fraction -0.8 %

Module mismatch losses
Loss Fraction 2.0 % at MPP

Strings Mismatch loss
Loss Fraction 0.1 %

IAM loss factor
Incidence effect (IAM): User defined profile

0°	30°	50°	60°	70°	75°	80°	85°	90°
1.000	1.000	1.000	0.981	0.946	0.920	0.857	0.707	0.000

Figure IX.8 - Castelo's Losses due to Direct current (DC), soiling and others

AC wiring losses

Inv. output line up to MV transfo

Inverter voltage	800 Vac tri
Loss Fraction	1.01 % at STC
Inverter: SUN2000-330KTL-H1-Preliminary V0.1	
Wire section (39 Inv.)	Copper 39 x 3 x 120 mm²
Average wires length	110 m

MV line up to Injection

MV Voltage	30 kV
Average each inverter	
Wires	Copper 3 x 95 mm²
Length	1500 m
Loss Fraction	0.16 % at STC

AC losses in transformers

MV transfo

Medium voltage	30 kV		
One transfo parameters		**Operating losses at STC (full system)**	
Nominal power at STC	4.90 MVA	Nb. identical MV transfos	3
Iron Loss (24/24 Connexion)	3.92 kVA	Nominal power at STC	14.71 MVA
Iron loss fraction	0.08 % at STC	Iron loss (24/24 Connexion)	11.77 kVA
Copper loss	61.70 kVA	Copper loss	185.10 kVA
Copper loss fraction	1.26 % at STC		
Coils equivalent resistance	3 x 1.64 mΩ		

Figure IX.9 – Castelo's Alternative Current (AC) Losses

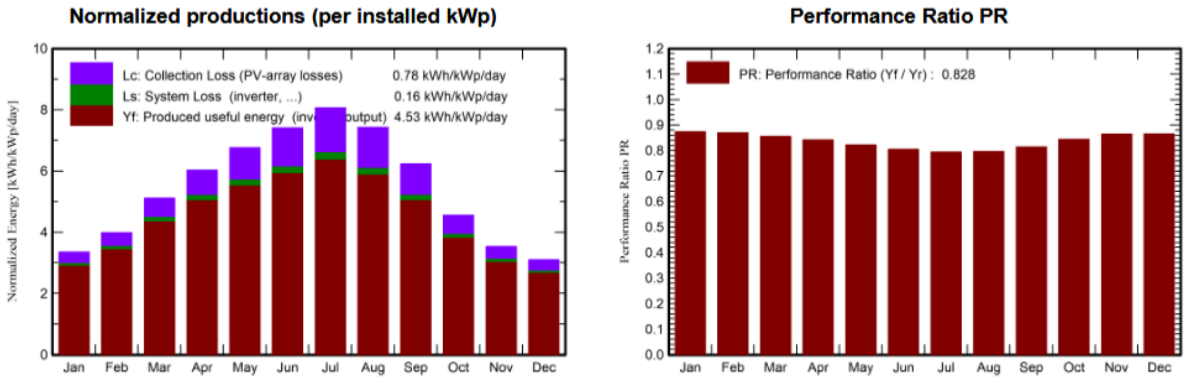

Figure IX.10 – Castelo's PV Energy Production Data

	GlobHor kWh/m²	DiffHor kWh/m²	T_Amb °C	GlobInc kWh/m²	GlobEff kWh/m²	EArray kWh	E_Grid kWh	PR ratio
January	69.9	28.98	7.87	103.9	96.7	1403469	1360186	0.874
February	83.4	32.14	9.25	111.6	104.7	1501313	1452924	0.869
March	132.7	55.05	11.69	158.3	148.3	2097494	2030033	0.856
April	166.6	66.49	12.51	180.8	168.6	2356807	2279671	0.841
May	207.9	70.54	16.68	209.4	194.6	2667803	2578072	0.821
June	225.7	64.08	21.84	222.1	206.4	2772231	2677275	0.804
July	250.1	52.30	23.63	249.9	232.5	3079839	2971060	0.794
August	217.1	49.13	24.32	230.2	214.8	2844872	2744770	0.796
September	161.2	50.28	20.94	186.8	174.9	2360582	2280479	0.815
October	109.0	41.04	16.16	141.1	132.4	1844155	1783960	0.844
November	74.0	29.34	10.65	106.0	99.2	1417055	1371816	0.864
December	61.1	21.23	8.25	96.2	89.1	1288173	1246639	0.865
Year	1759.0	560.62	15.35	1996.3	1862.2	25633794	24776885	0.828

Legends

GlobHor	Global horizontal irradiation	EArray	Effective energy at the output of the array
DiffHor	Horizontal diffuse irradiation	E_Grid	Energy injected into grid
T_Amb	Ambient Temperature	PR	Performance Ratio
GlobInc	Global incident in coll. plane		
GlobEff	Effective Global, corr. for IAM and shadings		

Figure IX.11 – Castelo's Summary of Monthly Irradiation, Temperature, Production and Performance

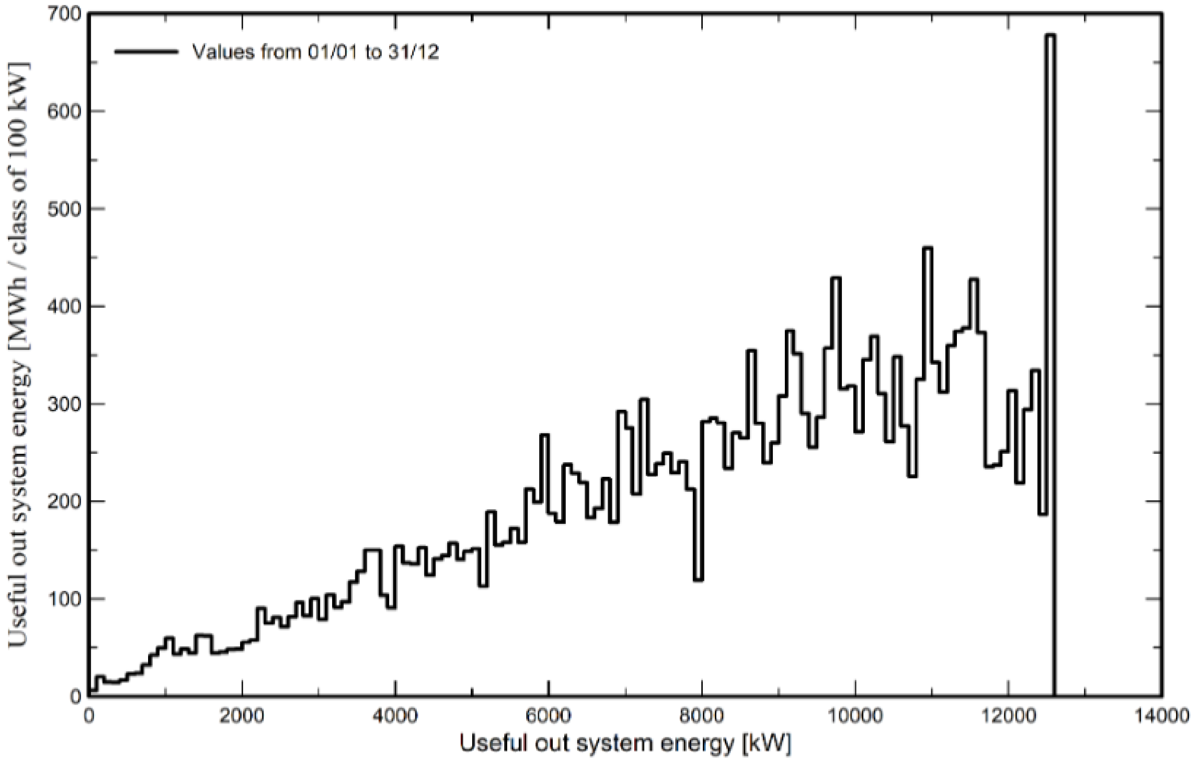

Figure IX.12 - Castelo's System Output Power Distribution

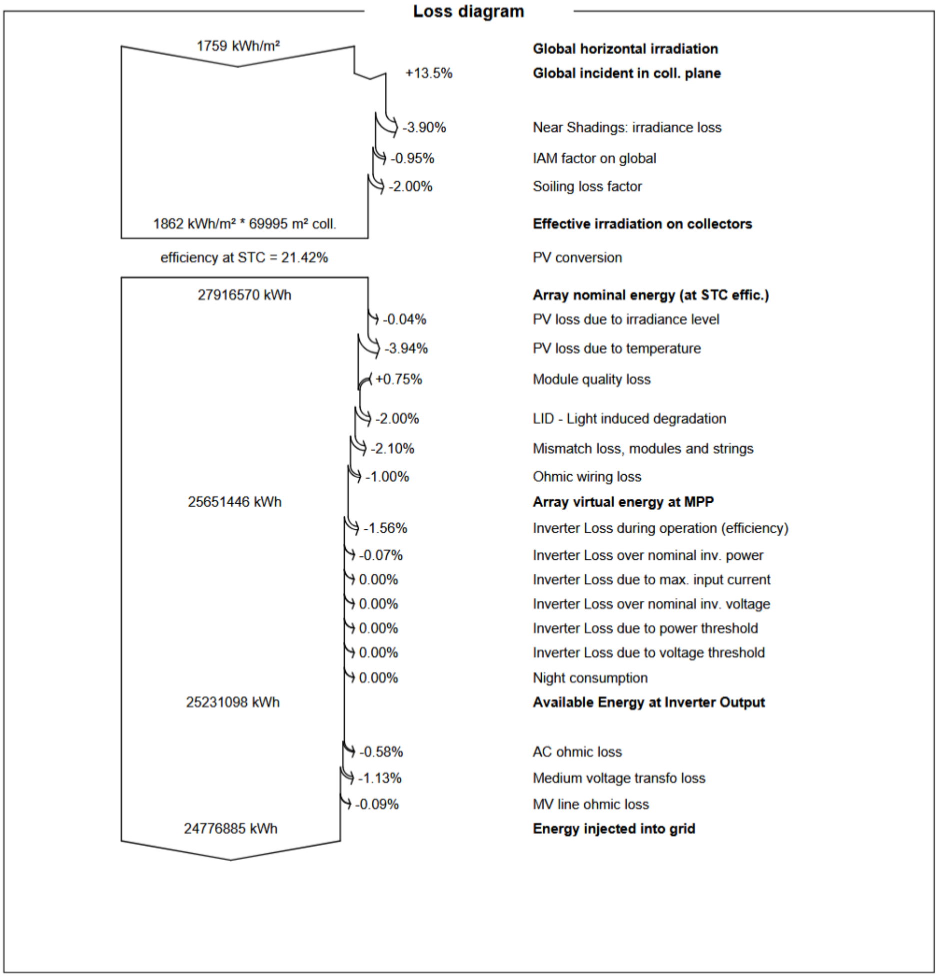

Figure IX.13 – Castelo's Loss Diagram

(Ortiga)

Project summary

Geographical Site
MAÇÃO
Portugal

Situation

Latitude	39.63 °N
Longitude	-7.99 °W
Altitude	564 m
Time zone	UTC

Project settings
Albedo 0.20

Weather data
MAÇÃO
MeteoNorm file - Synthetic

System summary

Grid-Connected System

Ground system (tables) on a hill

PV Field Orientation
Fixed plane
Tilt/Azimuth 20.4 / -5.4 °

Near Shadings
Linear shadings : Fast (table)

User's needs
Unlimited load (grid)

System information

PV Array		**Inverters**	
Nb. of modules	21808 units	Nb. of units	38 units
Pnom total	14.50 MWp	Pnom total	11.40 MWac
		Pnom ratio	1.272

Results summary

Produced Energy	24623863 kWh/year	Specific production	1698 kWh/kWp/year	Perf. Ratio PR	85.18 %

Figure IX.14 – Ortiga's Project Summary

PV Array Characteristics

PV module		Inverter	
Manufacturer	Suntech	Manufacturer	Huawei Technologies
Model	STP665S-D66/Wmh_1500V_20V01_2384	Model	SUN2000-330KTL-H1-Preliminary V0.1
(Custom parameters definition)		(Custom parameters definition)	
Unit Nom. Power	665 Wp	Unit Nom. Power	300 kWac
Number of PV modules	21808 units	Number of inverters	38 units
Nominal (STC)	14.50 MWp	Total power	11400 kWac
Modules	752 string x 29 In series	Operating voltage	500-1500 V
At operating cond. (50°C)		Max. power (=>30°C)	330 kWac
Pmpp	13.20 MWp	Pnom ratio (DC:AC)	1.27
U mpp	998 V	Power sharing within this inverter	
I mpp	13220 A		
Total PV power		**Total inverter power**	
Nominal (STC)	14502 kWp	Total power	11400 kWac
Total	21808 modules	Max. power	12540 kWac
Module area	67743 m²	Number of inverters	38 units
Cell area	63474 m²	Pnom ratio	1.27

Figure IX.15 – Ortiga's Photovoltaic Modules' Characteristics

Array losses

Array Soiling Losses
Loss Fraction 2.0 %

Thermal Loss factor
Module temperature according to irradiance
Uc (const) 29.0 W/m²K
Uv (wind) 0.0 W/m²K/m/s

DC wiring losses
Global array res. 1.3 mΩ
Loss Fraction 1.5 % at STC

LID - Light Induced Degradation
Loss Fraction 2.0 %

Module Quality Loss
Loss Fraction -0.8 %

Module mismatch losses
Loss Fraction 2.0 % at MPP

Strings Mismatch loss
Loss Fraction 0.1 %

IAM loss factor
Incidence effect (IAM): User defined profile

0°	30°	50°	60°	70°	75°	80°	85°	90°
1.000	1.000	1.000	0.981	0.946	0.920	0.857	0.707	0.000

Figure IX.16 – Ortiga's Losses due to Direct current (DC), soiling and others

AC wiring losses

Inv. output line up to MV transfo

Inverter voltage	800 Vac tri
Loss Fraction	1.01 % at STC
Inverter: SUN2000-330KTL-H1-Preliminary V0.1	
Wire section (38 Inv.)	Copper 38 x 3 x 120 mm²
Average wires length	110 m

MV line up to Injection

MV Voltage	30 kV
Average each inverter	
Wires	Copper 3 x 95 mm²
Length	1500 m
Loss Fraction	0.16 % at STC

AC losses in transformers

MV transfo

Medium voltage	30 kV		
One transfo parameters		**Operating losses at STC (full system)**	
Nominal power at STC	4.75 MVA	Nb. identical MV transfos	3
Iron Loss (24/24 Connexion)	3.85 kVA	Nominal power at STC	14.24 MVA
Iron loss fraction	0.08 % at STC	Iron loss (24/24 Connexion)	11.54 kVA
Copper loss	59.34 kVA	Copper loss	178.01 kVA
Copper loss fraction	1.25 % at STC		
Coils equivalent resistance	3 x 1.69 mΩ		

Figure IX.17 – Castelo's Alternative Current (AC) Losses

System Production

Produced Energy	24623863 kWh/year	Specific production	1698 kWh/kWp/year
		Perf. Ratio PR	85.18 %

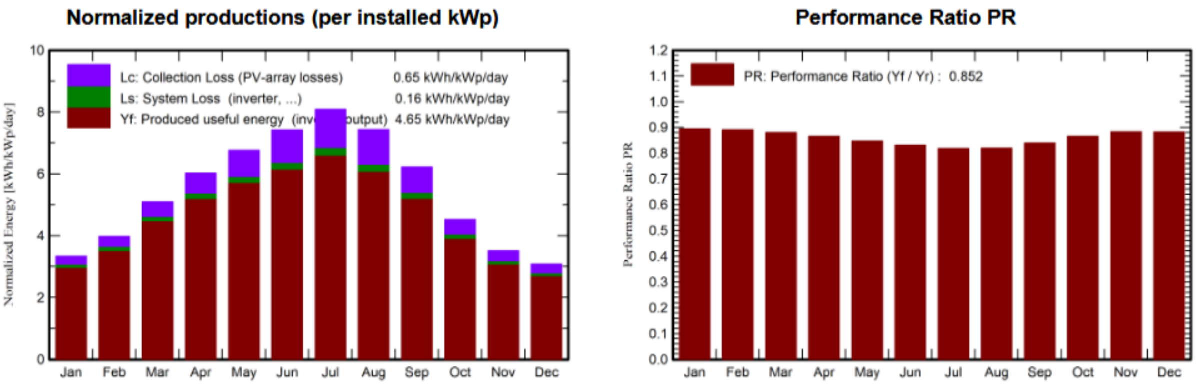

Figure IX.18 – Ortiga's PV Energy Production Data

Balances and main results

	GlobHor kWh/m²	DiffHor kWh/m²	T_Amb °C	GlobInc kWh/m²	GlobEff kWh/m²	EArray kWh	E_Grid kWh	PR ratio
January	69.9	28.98	7.87	103.4	98.5	1383512	1340867	0.894
February	83.4	32.14	9.25	111.0	106.9	1482782	1434947	0.891
March	132.7	55.05	11.69	157.7	152.2	2080241	2013024	0.880
April	166.6	66.49	12.51	180.5	173.9	2343970	2266838	0.866
May	207.9	70.54	16.68	209.6	201.8	2664512	2574236	0.847
June	225.7	64.08	21.84	222.4	214.4	2774368	2678429	0.830
July	250.1	52.30	23.63	250.6	241.9	3086235	2976175	0.819
August	217.1	49.13	24.32	230.3	222.3	2838345	2737611	0.820
September	161.2	50.28	20.94	186.6	180.4	2350127	2269757	0.839
October	109.0	41.04	16.16	140.4	135.4	1823743	1764006	0.866
November	74.0	29.34	10.65	105.1	100.6	1390560	1346027	0.883
December	61.1	21.23	8.25	95.5	90.2	1262700	1221948	0.882
Year	1759.0	560.62	15.35	1993.3	1918.5	25481093	24623863	0.852

Figure IX.19 – Ortiga's Summary of Monthly Irradiation, Temperature, Production and Performance

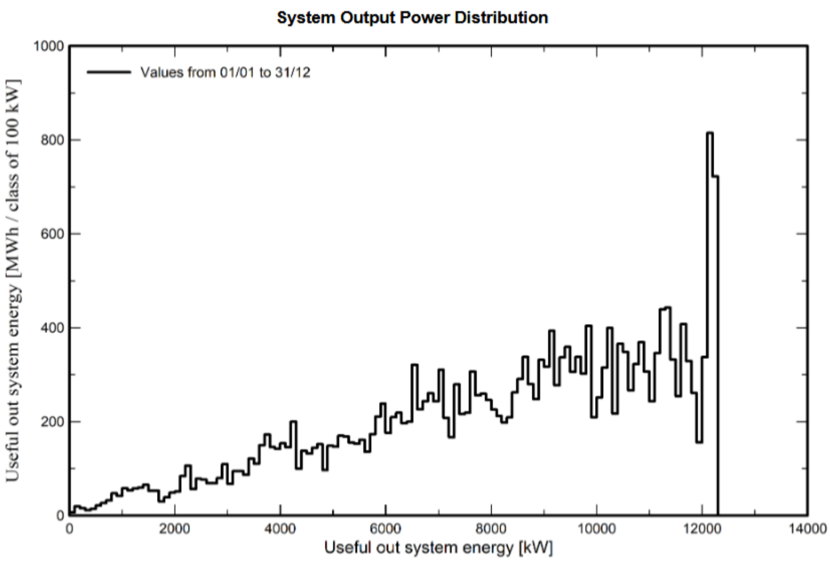

Figure IX.20 – Ortiga's System Output Power Distribution

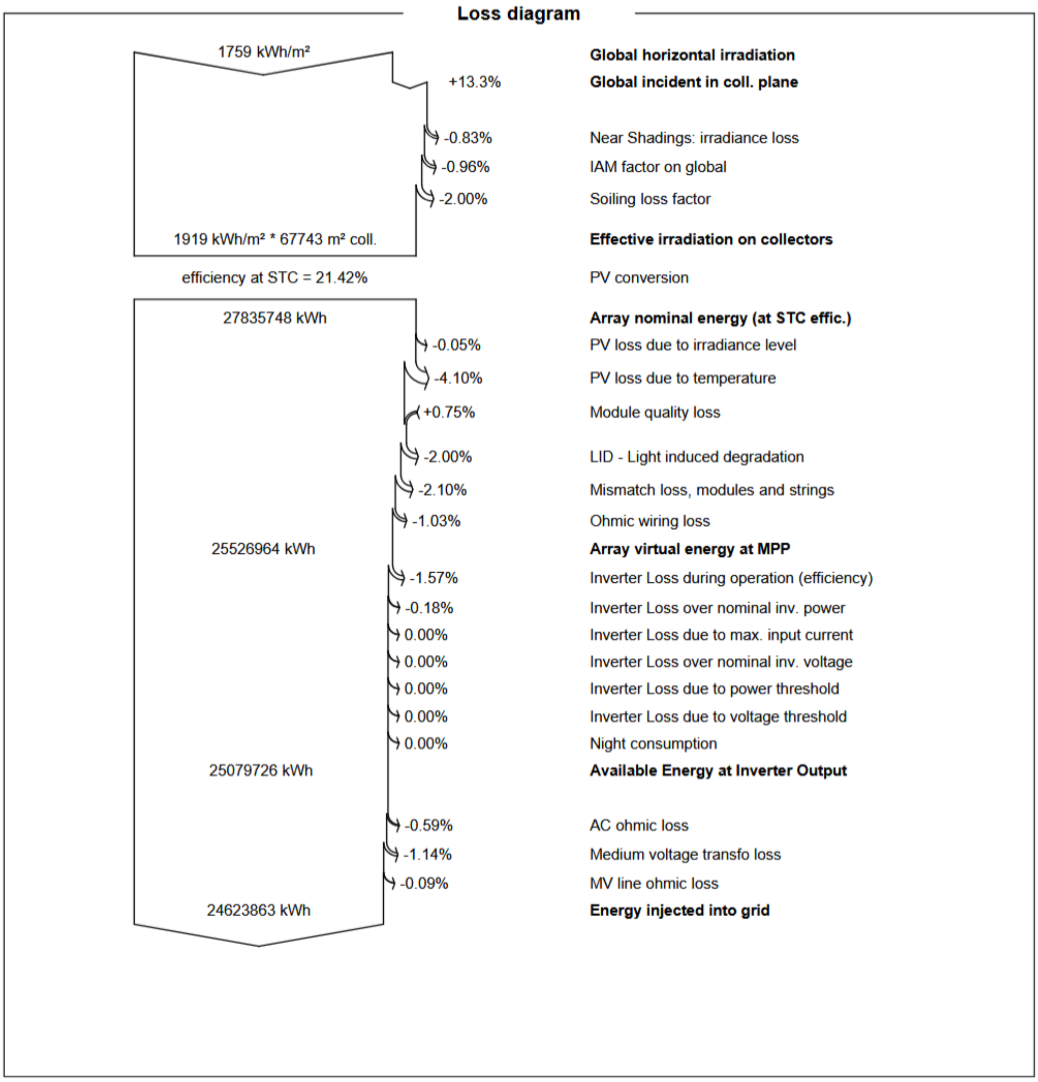

Figure IX.21 – Ortiga's Loss Diagram

Appendix IX.4: Cost Assessment

CASTELO JOINT PV SOLAR PLANT - EPC COST BREAKDOWN				
II.3	Design and engineering & Site studies	74,920.00	0.005	
II.4	Tests and Commissioning	149,840.00	0.010	
III	**BoP materials & equipment delivery & installation**	**5,079,576.00**	**0.209**	
III.1	Mounting structures & piles supply	1,273,640.00	0.085	
III.2	Inverters supply	299,680.00	0.020	
III.3	AC stations, including MV transformers supply	449,520.00	0.030	
III.4	SCADA including Remote Terminal Units	89,904.00	0.006	
III.5	Security & Control systems, Meteorological station	269,712.00	0.018	
III.6	Fiber optic & Comunication cables			
III.7	Other AC & Dc materials, Earthing supply	749,200.00	0.050	
III.8	Piles + foundations installation	674,280.00	0.045	
III.9	Mounting structures & modules installation	1,048,880.00	0.070	
III.10	Inverters & AC stations & MV Transf. & Other AC/DC installation Other equip. & materials & earthing installation	224,760.00	0.015	
IV	**Civil works**	**4,389,072.00**	**0.058**	
IV.1	Standard civil works	449,520.00	0.030	
IV.2	Fencing and gates	89,904.00	0.006	
IV.3	Roads & Earthworks	329,648.00	0.022	
IV.4	Connection to existing electrical facilities	3,520,000.00	0.000	
V	**Switching station & connection to electrical facilities**	**567,387.30**	**0.038**	
V.1	MV switchgear	409,252.93	0.027	
V.2	Prot. Equip., control, metering, auxil. telecommunication system	0.00		
V.3	Installation, Testing and Commissioning & Others	158,134.37	0.011	
VI	**Other costs and expenses**	**187,300.00**	**0.013**	
VI.1	Warranties	74,920.00	0.005	
VI.2	Others	112,380.00	0.008	
	TOTAL	**12,425,983.30**	**0.829**	
VII	**O&M Contract (Annual Fee)**		**7,000.00**	**€/MWp/year**

Figure IX.22 - Castelo's Engineering, Procurement and Construction Costs Summary

CASTELO JOINT PV SOLAR PLANT - OTHER COSTS

Country:	**Portugal**
Municipality:	**Mação**
Project:	**Castelo PV**
DC capacity [kWp]:	**14,984**
AC capacity [kVA]:	11,700
DC/AC ratio	1.18 - 1.25

Description	Total [€]	€/Wp	Comments
Lands (development phase)	222,500 €	0.015 €	
Studies (External consultants)	35,000 €	0.002 €	
Internal Development Costs	130,000 €	0.009 €	
Capitalized Interests		- €	
Costs for obtaining financing	225,000 €	0.015 €	
Legal & Other consultants (external)	25,000 €	0.002 €	
Interconnection Line Project+Land	30,000 €	0.002 €	
Interconnection Line Construction	600,000 €	0.040 €	
Metering systems	12,000 €	0.001 €	
Substation Adaptation	120,000 €	0.008 €	
ITC	7,300 €	0.000 €	
Supervision during construction	45,000 €	0.003 €	
Insurance during construction	25,000 €	0.002 €	
Compensations (counterparts)	- €	- €	
Contingencies (~2.5% BoP)	181,444 €	0.012 €	
Total	**1,658,244 €**	**0.111 €**	

Figure IX.23 - Castelo's Other Costs

Debt maturity	15 years
D/E ratio	65%
Debt amount	614,785.60 €/MW
Interest	4.5%

Investment	27.56 €/MWh
Variable costs	7.00 €/MWh
Fixed costs	3.63 €/MWh
TOTAL	38.00 €/MWh
TIR equity	0.0 %

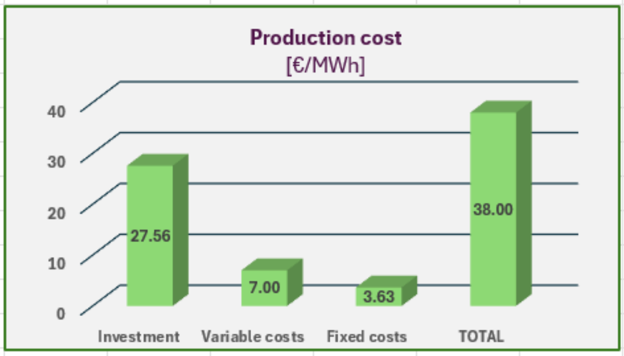

Figure IX.24 - Castelo's Debt, Investment and Cost at LCOE

Income statement	
Income	**[€/MW/year]**
Energy	62,223
Total income	**62,223**
Costs	**[€/year]**
Variable costs	11,578
Fixed costs	6,000
EBITDA	**44,645**
Fiscal amortization	37,833
Total costs	**55,411**
EBIT	**6,813**
Taxes	1,601
Net result	**5,212**

Figure IX.25 - Castelo's Income Statement at LCOE

ORTIGA PV SOLAR PLANT - EPC COST BREAKDOWN

Notes:	Country:	**Portugal**
	Municipality:	**Mação**
	Project:	**Ortiga PV**
	DC capacity [kWp]:	**14,502**
	AC capacity [kVA]:	11,400
	DC/AC ratio	1.18 - 1.25

#	Item	Total [€]	€/Wp	
I	**PV Modules supply**	**1,595,220.00**	**0.110**	
I.1	PV Modules supply	1,522,710.00	0.105	
I.2	PV modules unloading and handling	72,510.00	0.005	
II	**Studies, Design, Engineering and Project Management**	**536,574.00**	**0.037**	
II.1	Project and Construction Management	58,008.00	0.004	
II.2	Construction running costs, Temp. facilities, Site security	261,036.00	0.018	
Chart Area	esign and engineering & Site studies	72,510.00	0.005	
II.4	Tests and Commissioning	145,020.00	0.010	
III	**BoP materials & equipment delivery & installation**	**4,916,178.00**	**0.209**	
III.1	Mounting structures & piles supply	1,232,670.00	0.085	
III.2	Inverters supply	290,040.00	0.020	
III.3	AC stations, including MV transformers supply	435,060.00	0.030	
III.4	SCADA including Remote Terminal Units	87,012.00	0.006	
III.5	Security & Control systems, Meteorological station	261,036.00	0.018	
III.6	Fiber optic & Comunication cables			
III.7	Other AC & Dc materials, Earthing supply	725,100.00	0.050	
III.8	Piles + foundations installation	652,590.00	0.045	
III.9	Mounting structures & modules installation	1,015,140.00	0.070	
III.10	Inverters & AC stations & MV Transf. & Other AC/DC installation	217,530.00	0.015	
IV	**Civil works**	**1,501,116.00**	**0.058**	
IV.1	Standard civil works	435,060.00	0.030	
IV.2	Fencing and gates	87,012.00	0.006	
IV.3	Roads & Earthworks	319,044.00	0.022	
IV.4	Connection to existing electrical facilities	660,000.00	0.000	
V	**Switching station & connection to electrical facilities**	**549,135.79**	**0.038**	
V.1	MV switchgear	396,088.23	0.027	
V.2	Prot. Equip., control, metering, auxil. telecommunication system	0.00		
V.3	Installation, Testing and Commissioning & Others	153,047.56	0.011	
VI	**Other costs and expenses**	**181,275.00**	**0.013**	
VI.1	Warranties	72,510.00	0.005	
VI.2	Others	108,765.00	0.008	
	TOTAL	**9,279,498.79**	**0.640**	
VII	**O&M Contract (Annual Fee)**		**7,000.00**	**€/MWp/year**

Figure IX.26 – Ortiga's Engineering, Procurement and Construction Costs Summary

CASTELO JOINT PV SOLAR PLANT - OTHER COSTS

Country:	**Portugal**
Municipality:	**Mação**
Project:	**Ortiga PV**
DC capacity [kWp]:	**14,502**
AC capacity [kVA]:	11,400
DC/AC ratio	1.18 - 1.25

Description	Total [€]	€/Wp	Comments
Lands (development phase)	222,500 €	0.015 €	
Studies (External consultants)	35,000 €	0.002 €	
Internal Development Costs	130,000 €	0.009 €	
Capitalized Interests		- €	
Costs for obtaining financing	225,000 €	0.016 €	
Legal & Other consultants (external)	25,000 €	0.002 €	
Interconnection Line Project+Land	30,000 €	0.002 €	
Interconnection Line Construction	600,000 €	0.041 €	
Metering systems	12,000 €	0.001 €	
Substation Adaptation	120,000 €	0.008 €	
ITC	7,300 €	0.001 €	
Supervision during construction	45,000 €	0.003 €	
Insurance during construction	25,000 €	0.002 €	
Compensations (counterparts)	- €	- €	
Contingencies (~2.5% BoP)	181,444 €	0.013 €	
Total	**1,658,244 €**	**0.114 €**	

Figure IX.27 – Ortiga's Other Costs

Debt maturity	15 years
D/E ratio	65%
Debt amount	478,292.35 €/MW
Interest	4.5%

Investment	20.89 €/MWh
Variable costs	7.00 €/MWh
Fixed costs	3.53 €/MWh
TOTAL	31.30 €/MWh
TIR equity	0.0 %

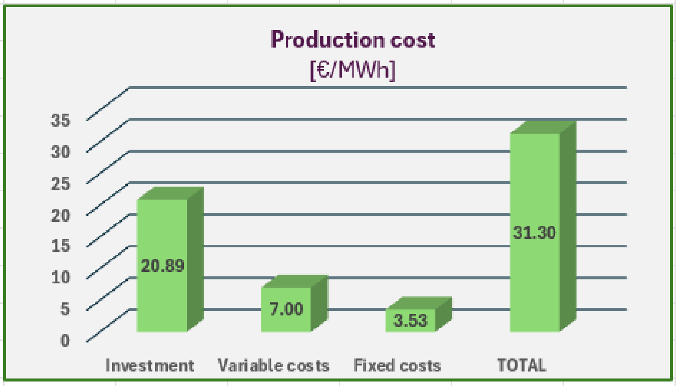

Figure IX.28 – Ortiga's Debt, Investment and cost at LCOE

Income statement		
Income	**[€/MW/year]**	
Energy	52,616	
Total income	**52,616**	
Costs	**[€/year]**	
Variable costs	11,886	
Fixed costs	6,000	
EBITDA	**34,730**	
Fiscal amortization	29,433	
Total costs	**47,319**	
EBIT	**5,297**	
Taxes	1,245	
Net result	**4,052**	

Figure IX.29 - Ortiga's Income Statement at LCOE

	Ortiga Park	Castelo Park
Output	14.5 MWp	14.98 MWp
Investment	€9.28M	€10.94M
LCOE	€31.3 MW/h	€38 MW/h
Return at 2024 Q4 Average PPA	6.70%	2.60%

Figure IX.30 - Project's Simple Overview